Příloha č. 1
Tvorba aduktů s DNA vzniklých aktivací ellipticinu potkaními jaterními (A), plicními (B) a ledvinnými (C) mikrosomy

A	RAL[a] (průměr/10^7 nukleotidů)				
	adukt 1	adukt 2	adukt 6	adukt 7	Total
nepremedikovaní potkani jaterní mikrosomy bez kofaktorů	n.d.	0.08±0.01	n.d.	n.d.	0.08±0.01
jaterní mikrosomy + NADPH	6.84±1.31	0.26±0.03	0.29±0.02	0.28±0.03	17.6±1.39
jaterní mikrosomy + NADPH + α-NF	6.19±0.45	0.13±0.02	0.10±0.01	0.05±0.01	6.47±0.48
jaterní mikrosomy + NADPH + furafylline	7.91±0.62	0.12±0.02	0.19±0.02	0.08±0.01	8.30±0.69
jaterní mikrosomy + NADPH + ketokonazol	1.00±0.1	0.15±0.01	0.08±0.01	0.02±0.01	1.25±0.11
jaterní mikrosomy + arachidonová kyselina	1.01±0.1	0.015±0.01	0.017±0.01	0.017±0.01	1.06±0.12
jaterní mikrosomy + arachidonová kyselina +IM	0.22±0.02	n.d.	n.d.	n.d.	0.22±0.02
jaterní mikrosomy + H_2O_2	1.10 ±0.1	0.02±0.01	0.02±0.01	0.02±0.01	1.16±0.12
potkani premedikovaní ellipticinem (40 mg/kg t.h.) jaterní mikrosomy bez kofaktorů	n.d.	0.11±0.01	n.d.	n.d.	0.11±0.01
jaterní mikrosomy + NADPH	33.03±2.52	0.42±0.03	0.40±0.03	0.48±0.03	34.39±2.87
jaterní mikrosomy + NADPH + a-NF	2.50±0.18	0.03±0.01	0.03±0.01	0.04±0.01	2.60±0.19
jaterní mikrosomy + NADPH + furafyllin	6.28±0.51	0.08±0.01	0.07±0.01	0.07±0.01	6.50±0.59
jaterní mikrosomy + NADPH + ketokonazol	6.50±0.58	0.20±0.02	0.40±0.03	0.40±0.03	7.50±0.61
jaterní mikrosomy + arachidonová kyselina	0.87±0.06	0.08±0.01	0.10±0.01	0.10±0.01	1.15±0.10
jaterní mikrosomy + arachidonová kyselina +IM	0.17±0.01	0.02±0.01	0.02±0.01	0.02±0.01	0.23±0.02
jaterní mikrosomy + H_2O_2	0.92±0.07	0.08±0.01	0.12±0.01	0.10±0.01	1.23±0.10

B	RAL[a] (průměr/10^7 nukleotidů)				
	adukt 1	adukt 2	adukt 6	adukt 7	Total
nepremedikovaní potkani plicní mikrosomy bez kofaktorů	0.03±0.01	0.03±0.01	0.03±0.01	0.02±0.01	0.11±0.01
plicní mikrosomy + NADPH	0.64±0.04	0.15±0.01	0.12±0.01	0.10±0.01	1.01±0.10
plicní mikrosomy + NADPH + α-NF	0.33±0.02	n.d.	n.d.	n.d.	0.33±0.027
plicní mikrosomy + NADPH + ketokonazol	0.52±0.041	0.10±0.01	0.09±0.01	0.08±0.01	0.79±0.08
plicní mikrosomy + arachidonová kyselina	0.03±001	0.03±0.01	0.30±0.03	0.14±0.01	0.50±0.05
plicní mikrosomy + arachidonová kyselina + IM	n.d.	n.d.	n.d.	n.d.	n.d.
potkani premedikovaní ellipticinem (40 mg/kg t.h.) plicní mikrosomy bez kofaktorů	0.60±0.04	0.03±0.01	0.20±0.02	0.10±0.01	0.93±0.11
plicní mikrosomy + NADPH	1.92±0.17	0.30±0.03	0.22±0.02	0.20±0.02	2.64±0.19
plicní mikrosomy + NADPH + α-NF	0.34±0.03	0.06±0.01	0.16±0.01	0.16±0.01	0.72±0.06
plicní mikrosomy + NADPH + ketokonazol	1.05±0.10	0.25±0.02	0.20±0.02	0.20±0.02	1.70±0.15
plicní mikrosomy + arachidonová kyselina	1.30±0.10	0.23±0.02	0.28±0.02	0.23±0.02	2.04±0.21
plicní mikrosomy + arachidonová kyselina + IM	0.60±0.05	0.03±0.01	0.10±0.01	0.05±0.01	1.15±0.10

C	RAL[a] (průměr/10^7 nukleotidů)				
	adukt 1	adukt 2	adukt 6	adukt 7	Total
nepremedikovaní potkani ledvinné mikrosomy bez kofaktorů	n.d.	n.d.	0.01±0.01	0.01±0.01	0.02±0.01
ledvinné mikrosomy + NADPH	0.21±0.02	0.03±0.01	0.08±0.01	0.03±0.01	0.35±0.04
ledvinné mikrosomy + NADPH + a-NF	0.04±0.01	n.d.	n.d.	n.d.	0.04±0.01
ledvinné mikrosomy + NADPH + ketokonazol	0.10±0.01	0.02±0.01	0.08±0.01	0.05±0.01	0.23±0.03
ledvinné mikrosomy+ arachidonová kyselina	n.d.	n.d.	0.02±0.01	0.02±0.01	0.04±0.01
ledvinné mikrosomy + arachidonová kyselina + IM	n.d.	n.d.	n.d.	n.d.	n.d.
potkani premedikovaní ellipticinem (40 mg/kg t.h.) ledvinné mikrosomy bez kofaktorů	0.12±0.01	0.03±0.01	0.05±0.01	0.03±0.01	0.33±0.04
ledvinné mikrosomy + NADPH	0.42±0.03	0.12±0.01	0.08±0.01	0.05±0.01	0.67±0.07
ledvinné mikrosomy + NADPH + a-NF	0.23±0.02	0.09±0.01	0.05±0.01	0.03±0.01	0.40±0.04
ledvinné mikrosomy + NADPH + ketokonazol	0.40±0.03	0.10±0.01	0.08±0.01	0.05±0.01	0.63±0.08
ledvinné mikrosomy + arachidonová kyselina	0.20±0.02	0.06±0.01	0.08±0.01	0.06±0.01	0.40±0.05
ledvinné mikrosomy + arachidonová kyselina + IM	0.10±0.01	0.04±0.01	0.04±0.01	0.02±0.01	0.20±0.03

[a] průměr RAL (relative adduct labeling) ze dvou nezávislých měření, n.d. - nedetekováno (detekční limit RAL byl $1/10^{10}$ nukleotidů).

Příloha 2

MARIE STIBOROVÁ, VOLKER M. ARLT, COLIN. J. HENDERSON, C. ROLAND WOLF, VĚRA KOTRBOVÁ, **MICHAELA MOSEROVÁ**, JIŘÍ HUDEČEK, DAVID H. PHILLIPS AND EVA FREI

ROLE OF HEPATIC CYTOCHROMES P450 IN BIOACTIVATION OF THE ANTICANCER DRUG ELLIPTICINE: STUDIES WITH THE HEPATIC NADPH: CYTOCHROME P450 REDUCTASE NULL MOUSE.

Toxicol. Appl. Pharmacol., 226: 318-327, 2008

Available online at www.sciencedirect.com
ScienceDirect
Toxicology and Applied Pharmacology 226 (2008) 318–327
Toxicology and Applied Pharmacology
www.elsevier.com/locate/ytaap

Role of hepatic cytochromes P450 in bioactivation of the anticancer drug ellipticine: Studies with the hepatic NADPH: Cytochrome P450 reductase null mouse

Marie Stiborová [a,*], Volker M. Arlt [b], Colin J. Henderson [c], C. Roland Wolf [c], Věra Kotrbová [a], Michaela Moserová [a], Jiří Hudeček [a], David H. Phillips [b], Eva Frei [d]

[a] Department of Biochemistry, Faculty of Science, Charles University, Albertov 2030, 128 40 Prague 2, Czech Republic
[b] Section of Molecular Carcinogenesis, Institute of Cancer Research, Brookes Lawley Building, Sutton, Surrey SM2 5NG, UK
[c] Cancer Research UK Molecular Pharmacology Unit, Biomedical Research Centre, Dundee DD1 9SY, UK
[d] Division of Molecular Toxicology, German Cancer Research Center, Im Neuenheimer Feld 280, 69120 Heidelberg, Germany

Received 24 August 2007; revised 14 September 2007; accepted 19 September 2007
Available online 26 September 2007

Abstract

Ellipticine is an antineoplastic agent, which forms covalent DNA adducts mediated by cytochromes P450 (CYP) and peroxidases. We evaluated the role of hepatic *versus* extra-hepatic metabolism of ellipticine, using the HRN (*H*epatic Cytochrome P450 *R*eductase *N*ull) mouse model, in which cytochrome P450 oxidoreductase (POR) is deleted in hepatocytes, resulting in the loss of essentially all hepatic CYP function. HRN and wild-type (WT) mice were treated i.p. with 1 and 10 mg/kg body weight of ellipticine. Multiple ellipticine–DNA adducts detected by ^{32}P-postlabelling were observed in organs from both mouse strains. Highest total DNA binding levels were found in liver, followed by lung, kidney, urinary bladder, colon and spleen. Ellipticine–DNA adduct levels in the liver of HRN mice were up to 65% lower relative to WT mice, confirming the importance of CYP enzymes for the activation of ellipticine in livers, recently shown *in vitro* with human and rat hepatic microsomes. When hepatic microsomes of both mouse strains were incubated with ellipticine, ellipticine–DNA adduct levels with WT microsomes were up to 2.9-fold higher than with those from HRN mice. The ratios of ellipticine–DNA adducts in extra-hepatic organs between HRN and WT mice of up to 4.7 suggest that these organs can activate ellipticine and that more ellipticine is available in the circulation. These results and the DNA adduct patterns found *in vitro* and *in vivo* demonstrate that both CYP1A or 3A and peroxidases participate in activation of ellipticine to reactive species forming DNA adducts in the mouse model used in this study.

Keywords: Anticancer drug; Ellipticine; Cytochrome P450; Peroxidase; DNA adducts; ^{32}P-postlabelling

Introduction

Ellipticine (5,11-dimethyl-6*H*-pyrido[4,3-*b*]carbazole, Fig. 1), an alkaloid isolated from *Apocyanaceae* plants, exhibit significant antitumor and anti-HIV activities (for a summary see Stiborová et al., 2001). The main reason for the interest in ellipticine and its derivatives for clinical purposes is their high efficiencies against several types of cancer, their rather limited toxic side effects, and their complete lack of haematological toxicity (Auclair, 1987). Nevertheless, ellipticine is a potent mutagen. Most ellipticine derivatives are mutagenic to *Salmonella typhimurium* Ames tester strains, bacteriophage T4, *Neurospora crassa*, and mammalian cells and induce prophage lambda in *Escherichia coli* (for an overview see Stiborová et al., 2001).

The prevalent mechanisms of ellipticine antitumour, mutagenic and cytotoxic activities have been suggested to be (i) intercalation into DNA (Auclair, 1987; Singh et al., 1994) and (ii) inhibition of DNA topoisomerase II activity (Auclair, 1987; Monnot et al., 1991; Fossé et al., 1992; Froelich-Ammon et al., 1995). We have demonstrated that ellipticine also covalently

Abbreviations: α-NF, α-naphthoflavone; COX, cyclooxygenase; CYP, cytochrome P450; HRN, hepatic cytochrome P450 reductase null; HPLC, high-performance liquid chromatography; i.p., intra-peritoneal; LPO, lactoperoxidase; MPO, myeloperoxidase; PEI-cellulose, polyethylenimine-cellulose; POR, cytochrome P450 oxidoreductase; RAL, relative adduct labeling; r.t., retention time; TLC, thin layer chromatography; WT, wild-type.

* Corresponding author. Fax: +420 221951283.
E-mail address: stiborov@natur.cuni.cz (M. Stiborová).

0041-008X/$ - see front matter © 2007 Elsevier Inc. All rights reserved.
doi:10.1016/j.taap.2007.09.017

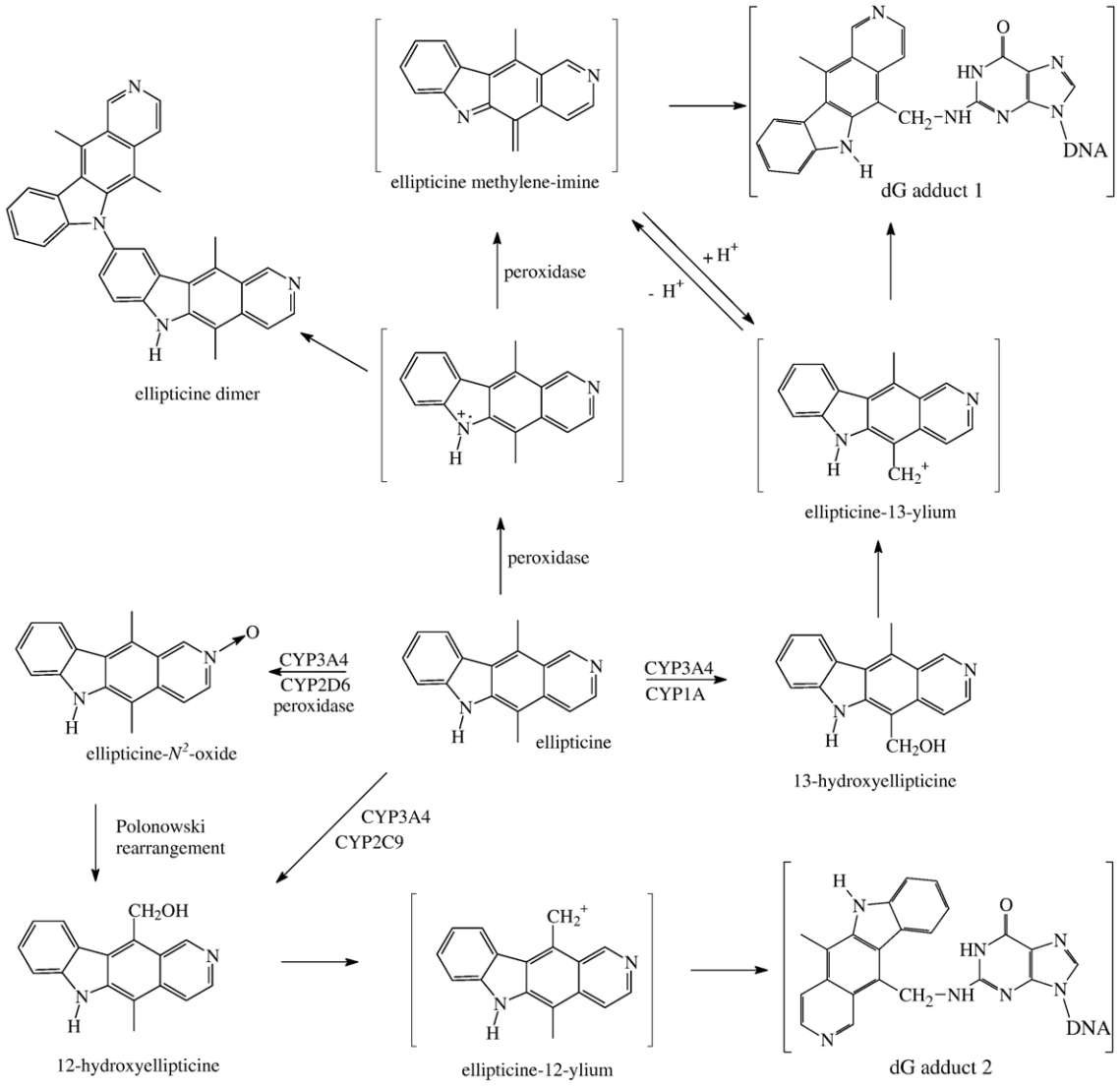

Fig. 1. Metabolism of ellipticine by peroxidases and human CYPs showing the characterized metabolites and those proposed to form DNA adducts. The compounds shown in brackets were not detected under the experimental conditions and are the electrophilic metabolites postulated as ultimate arylating species or the postulated N^2-deoxyguanosine adducts.

binds to DNA after being enzymatically activated with cytochromes P450 (CYP) or peroxidases (Stiborová et al., 2001; 2003a,b, 2004, 2006a, 2007a,b, Poljaková et al., 2006), suggesting a third possible mechanism of action.

Understanding which enzymes are involved in the metabolic activation of ellipticine is important in the assessment of susceptibility to this drug. Human and rat CYP1A and 3A are the predominant enzymes catalyzing oxidation of ellipticine *in vitro* either to metabolites that are excreted (7-hydroxy- and 9-hydroxyellipticine) or that form DNA adducts (12-hydroxy- and 13-hydroxyellipticine) (Stiborová et al., 2001, 2003a,b, 2004, 2006a). Of the peroxidases, human cyclooxygenase (COX)-2, ovine COX-1, bovine lactoperoxidase (LPO), human myeloperoxidase (MPO) and horseradish peroxidase efficiently generated ellipticine-derived DNA adducts (Fig. 1) (Poljaková et al., 2006; Stiborová et al., 2007a). The same DNA adducts were also detected in cells in culture expressing enzymes activating ellipticine (CYP1A1, COX-1 and MPO), such as human breast adenocarcinoma MCF-7 cells (Bořek-Dohalská et al., 2004), leukaemia HL-60 and CCRF-CEM cells (Poljaková et al., 2007) and V79 Chinese hamster lung fibroblasts transfected with human CYP3A4, 1A1 and 1A2 (Frei et al., 2002). On the basis of these data, ellipticine might be considered a drug, whose pharmacological efficiency and/or genotoxic side effects are dependent on its activation by CYPs and peroxidases in target tissues.

However, additional factors such as route of administration, absorption and renal clearance make it difficult to extrapolate from *in-vitro* data to the *in-vivo* situation. After i.p. administration of ellipticine to rats, the highest levels of DNA adducts were found in liver, followed by kidney and lung (Stiborová et al., 2003a, 2007b). Liver is a tissue rich in CYP enzymes, while kidney and lung contain high levels of peroxidases such as COX (Eling et al., 1990; Eling and Curtis, 1992; Stiborová et al., 1991, 2005; Culp et al., 1997). Knowledge about the participation of these enzymes in ellipticine activation in individual rat tissues is, however, scarce. Although previous

results indicate that CYP3A1 and 1A participate in formation of DNA adducts by ellipticine in rats *in vivo* (Stiborová et al., 2003a), it is unclear whether CYP or peroxidases are more important in ellipticine activation in different organs.

Gene knock-out and transgenic mice have been developed to study the role of specific enzymes in drug metabolism (Gonzalez and Kimura, 2001; Henderson and Wolf, 2003). Although CYP knock-out mouse models have yielded important data on the effect of single CYP enzymes on the metabolism of drugs and chemical carcinogens (Buters et al., 1999, 2002; Kimura et al., 1999, 2003; Tsuneoka et al., 2003; Uno et al., 2004), the functional redundancy inevitably found in the large CYP family of isoenzymes makes it difficult to determine the role of CYPs as a whole in metabolism of xenobiotics (Henderson et al., 2006). To overcome these limitations a mouse line, HRN (*H*epatic Cytochrome P450 *R*eductase *N*ull), has been developed in which cytochrome P450 oxidoreductase (POR), the unique electron donor to CYPs, is deleted specifically in hepatocytes, resulting in the loss of essentially all hepatic CYP function (Henderson et al., 2003). The HRN mouse as a model has been used to establish the role of hepatic *versus* extra-hepatic CYP-mediated metabolism and disposition of drugs such as cyclophosphamide (Pass et al., 2005; Henderson et al., 2006). With this model we found that the carcinogen 3-nitrobenzanthrone is predominantly activated *in vivo* by cytosolic nitroreductases rather than microsomal POR, whereas the oxidative activation of 3-aminobenzanthrone, the main metabolite of 3-nitrobenzanthrone, is CYP-dependent, both *in vitro* and *in vivo* (Arlt et al., 2003, 2004, 2005, 2006).

In this study, we have used the HRN mouse model to examine the hepatic CYP-dependent metabolism of ellipticine. DNA adduct formation *in vivo* in hepatic and extra-hepatic tissues was investigated using ^{32}P-postlabelling. In addition, we examined ellipticine metabolism and DNA adduct formation *in vitro* using hepatic microsomes.

Materials and methods

Animals. HRN ($Por^{lox/lox}$+Cre^{ALB}) mice on a C57BL/6 background used in this study were constructed as described previously (Henderson et al., 2003). Mice homozygous for loxP sites at the *Por* locus ($Por^{lox/lox}$) were used as wild-type (WT). All procedures were carried out under the Animal (Scientific Procedures) Act (1986) in accordance with UK law, and following local ethical review.

Treatment of HRN mice and WT mice with ellipticine. Male HRN (Henderson et al., 2003) and WT mice (25–30 g; n=3/group) were treated with a single intraperitoneal (i.p.) dose of 1 or 10 mg/kg body weight of ellipticine by intraperitoneal injection. Ellipticine was administered dissolved in 1% acetic acid at a concentration of 2.5 mg/ml. Control mice (n=3/group) received the solvent only. Animals were killed 24 h after treatment. Six organs (liver, lung, kidney, spleen, bladder and colon) were removed and stored at −80 °C until DNA isolation by standard phenol/chloroform extraction.

Measurement of ellipticine–DNA adducts. ^{32}P-postlabelling analysis with nuclease P1 enrichment, thin-layer chromatography (TLC) and high performance liquid chromatography (HPLC) of ^{32}P-labelled 3′5′-deoxyribonucleoside bisphosphate adducts were done as reported recently (Stiborová et al., 2003a, 2004, 2007a).

Preparation of microsomes and assays. Microsomes were isolated from the pooled livers of each strain as described (Stiborová et al., 2003b). Pooled microsomal fractions were used for further analyses.

Preparation of POR antibodies. Rabbit liver NADPH:CYP reductase was purified as described (Yasukochi et al., 1979). Leghorn chickens were immunised subcutaneously three times (with one-week intervals) with rabbit hepatic POR (0.1 mg/animal) emulsified in complete Freund's adjuvant for the first injection and in incomplete adjuvant for boosters. The immunoglobulin fraction was purified from pooled egg yolks using fractionation by polyethylene glycol 6000 (Stiborová et al., 2002).

Determination of POR protein levels in hepatic microsomes. Immunoquantitation of hepatic microsomal POR was done essentially as described previously using sodium dodecyl sulfate-polyacrylamide gel electrophoresis (Stiborová et al., 2002, 2006b). The POR protein was probed with the chicken polyclonal antibodies as reported (Stiborová et al., 2002, 2006b). The antigen–antibody complex was visualised with an alkaline phosphatase-conjugated rabbit anti-chicken IgG antibody and 5-bromo-4-chloro-3-indolylphosphate/nitrobluetetrazolium as the chromogenic substrate (Stiborová et al., 2002, 2006b).

Determination of POR enzymatic activity in hepatic microsomes. Hepatic microsomal samples were characterized for POR activity using cytochrome *c* as a substrate, by the procedure reported previously (Arlt et al., 2003).

Microsomal incubations. Incubation mixtures used to generate DNA adduct formation by ellipticine *in vitro* consisted of 50 mM potassium phosphate buffer (pH 7.4), 1 mM NADPH, pooled hepatic microsomal fraction (0.5 mg protein) from HRN or WT mice, 0.1 mM ellipticine (dissolved in 7.5 µl methanol) and 0.5 mg of calf thymus DNA in a final volume of 750 µl. Incubations were also carried out in the presence of a COX cofactor, arachidonic acid (Eling and Curtis, 1992; Stiborová et al., 2005). Mixtures then contained 0.1 mM arachidonic acid as cofactor instead of NADPH, and additionally 5 mM magnesium chloride. Incubations were carried out at 37 °C for 30 min; ellipticine–DNA adduct formation was found to be linear up to 30 min of incubation (Stiborová et al., 2001). Control incubations were carried out (*i*) without microsomes, (*ii*) without NADPH or arachidonic acid, (*iii*) without DNA and (*iv*) without ellipticine. After the incubation, DNA was isolated by a standard phenol–chloroform extraction method.

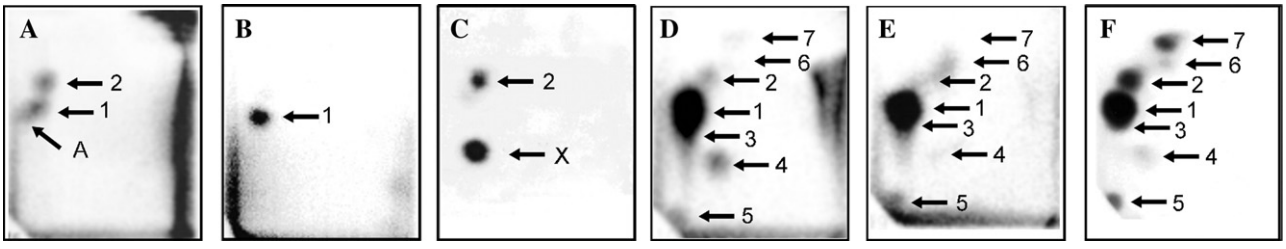

Fig. 2. Autoradiographs of TLC maps of ^{32}P-labelled digests of calf thymus DNA reacted with ellipticine and hepatic microsomes from WT mice (A), from calf thymus DNA reacted with 13-hydroxyellipticine (B) (Stiborová et al., 2004) and 12-hydroxyellipticine (C) (Stiborová et al., 2007a), of DNA from livers of WT (D) and HRN (E) mice treated with 10 mg ellipticine/kg body weight, from livers of rats treated with 40 mg ellipticine/kg body weight (F) (Stiborová et al., 2007b). Analyses were performed by the nuclease P1 version of the ^{32}P-postlabelling assay. Exposure times of the TLC plates in Instant Imager were 40 (A), 5 (B), 10 (C), 20 (D), 40 (E) and 10 min (F).

Table 1
DNA adduct formation by ellipticine activated by hepatic microsomes from HRN and WT mice

	RAL[a] (mean/10^8 nucleotides)			
	Spot 1	Spot 2	Spot A	Total
HRN mice hepatic microsomes+NADPH	5.9±0.3	2.3±0.2	6.7±0.3	14.9±0.8
HRN mice hepatic microsomes+NADPH+α-lipoic acid	1.2±0.1	1.7±0.1	0.9±0.1	3.8±0.3
HRN mice hepatic microsomes+NADPH+α-NF	2.8±0.2	2.2±0.2	1.0±0.1	6.0±0.5
HRN mice hepatic microsomes+NADPH+ketoconazole	2.5±0.2	2.0±0.2	1.0±0.1	5.5±0.4
HRN mice hepatic microsomes+arachidonic acid	2.9±0.2	2.4±0.2	ND	5.3±0.4
HRN mice hepatic microsomes without cofactor	0.2±0.04	1.9±0.2	ND	2.0±0.2
WT mice hepatic microsomes+NADPH	13.0±0.9	3.2±0.2	4.8±0.4	21.0±1.5
WT mice hepatic microsomes+NADPH+α-lipoic acid	7.6±0.6	2.7±0.2	0.7±0.1	11.0±0.9
WT mice hepatic microsomes+NADPH+α-NF	6.5±0.5	2.7±0.2	1.2±0.1	10.4±0.8
WT mice hepatic microsomes+NADPH+ketoconazole	6.0±0.5	2.1±0.2	1.0±0.1	8.1±0.7
WT mice hepatic microsomes+arachidonic acid	5.7±0.4	4.6±0.3	ND	10.3±0.8
WT mice hepatic microsomes without cofactor	0.3±0.02	2.0±0.2	ND	2.3±0.2

[a]Mean RAL (relative adduct labeling) of four determinations (duplicate analyses of two independent *in vitro* incubations). ND — not detected (the detection limit of RAL was $1/10^{10}$ nucleotides).

Incubation mixtures used to form the ellipticine metabolites contained 50 mM potassium phosphate buffer (pH 7.4), 1 mM $NADP^+$, 10 mM D-glucose 6-phosphate, 1 U/ml D-glucose 6-phosphate dehydrogenase (NADPH-generation system), 0.2 mg protein of pooled hepatic microsomal fraction and 10 μM ellipticine (dissolved in 5 μl methanol) in a final volume of 500 μl. The reaction was initiated by adding the substrate. In the control incubation, ellipticine was omitted from the incubation mixture. After incubation in open glass tubes (37 °C, 20 min) the reaction was stopped by adding 100 μl of 2 M NaOH. The oxidation of ellipticine is linear up to 30 min of incubation (Stiborová et al., 2006a). After incubation, 5 μl of 1 mM phenacetine in methanol was added as an internal standard and the ellipticine metabolites were extracted twice with ethyl acetate (2×1 ml). Analyses of ellipticine metabolites were performed by HPLC as described (Stiborová et al., 2004, 2006a). Recoveries of ellipticine metabolites were around 95% in the presence of microsomes without a CYP cofactor (NADPH-generation system).

Inhibition studies. The following chemicals were used to inhibit the activation of ellipticine to form DNA adducts in the presence of mouse hepatic microsomes: α-naphthoflavone (α-NF), which inhibits CYP1A1 and 1A2 (Arlt et al., 2004; Rendic and DiCarlo, 1997; Stiborová et al., 2005), ketoconazole, an inhibitor of CYP3A, and α-lipoic acid, which inhibits POR (Slepneva et al., 1995). Inhibitors were dissolved in 7.5 μl of methanol, to yield final concentrations of 0.1 mM in the incubation mixtures. Mixtures were then incubated at 37 °C for 10 min with NADPH prior to adding ellipticine, and then incubated for a further 30 min at 37 °C. After the incubation, DNA was isolated as described above.

Results

Hepatic microsomes of HRN mice are capable of activating ellipticine

In order to evaluate the role of the mouse hepatic POR-dependent CYP in the activation of ellipticine, we first performed

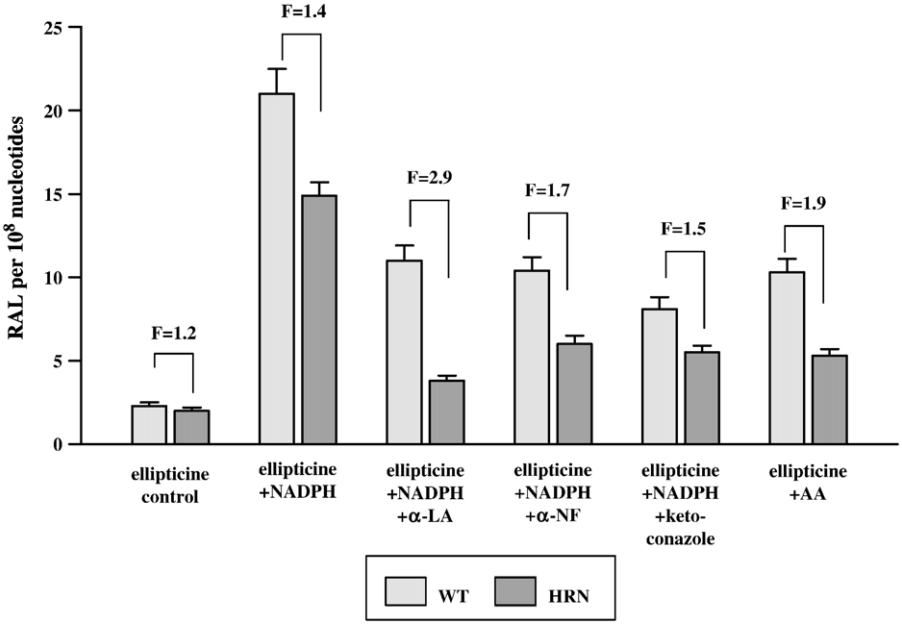

Fig. 3. DNA adduct formation by ellipticine activated with microsomes isolated from livers of HRN and WT mice as determined by TLC ^{32}P-postlabelling. *F*=fold higher DNA adducts levels in microsomes from WT mice compared to HRN mice. *Columns*: Mean RAL (relative adduct labelling)±standard deviations shown in the figure represent total levels of DNA adducts of four determinations (duplicate analyses of two independent *in vitro* incubations). Control=without cofactor; AA=arachidonic acid; α-NF=α-naphthoflavone; α-LA=α-lipoic acid. ND=not detected.

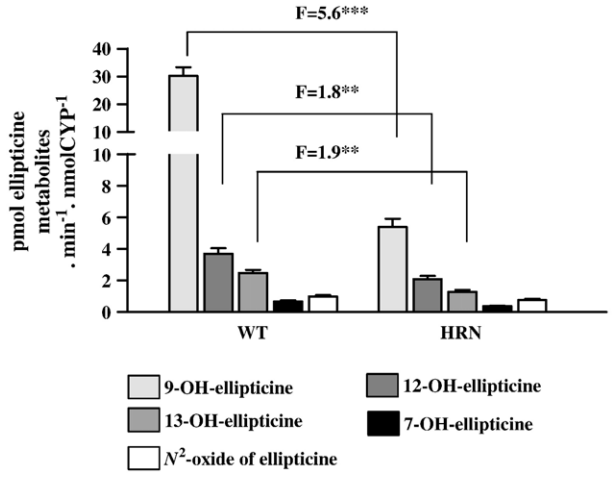

Fig. 4. Levels of ellipticine metabolites formed by hepatic microsomes (0.2 mg protein) of HRN and WT mice from 10 μM ellipticine. Levels of ellipticine metabolites were determined by HPLC (Stiborová et al., 2004, 2006a) and are averages ± standard deviations of triplicate incubations. Values significantly different from HRN mice: $^{**}P<0.01$, $^{***}P<0.001$.

in-vitro experiments. Microsomes isolated from livers of HRN and WT mice used for such experiments were characterized for POR expression by Western blotting. Hepatic POR expression was detected in WT mice, while as expected, its levels in HRN mice were very low, but still detectable, by immunostaining. Hepatic POR levels in HRN mice were estimated to be less than 1.5% of the levels in WT mice. POR activity measured with cytochrome *c* as a substrate was, however, not detectable in hepatic microsomes of HRN mice.

The activation of ellipticine by mouse hepatic microsomes was determined by ^{32}P-postlabeling. The adduct pattern obtained is shown in Fig. 2A. The DNA adduct pattern generated by ellipticine consisted of at least two adducts (spots 1 and 2), which were identical to those formed *in vivo* in rats treated with ellipticine (Fig. 2F), each a product of 13-hydroxyellipticine (Fig. 2B) or 12-hydroxyellipticine (Fig. 2C) metabolites, generated by CYP and peroxidase (see scheme in Fig. 1). Chromatographic analysis of spots 1 and 2 on HPLC confirmed that these adducts are derived from 13-hydroxy- and 12-hydroxyellipticine, respectively, by their coelution with prepared reference compounds (data not shown). An additional ellipticine-derived DNA adduct, spot A, was found in DNA that had been incubated with ellipticine and mouse hepatic microsomes (Fig. 2A), predominantly in microsomes isolated from HRN mice (Table 1). This ellipticine–DNA adduct was not formed by either human or rat hepatic microsomes (Stiborová et al., 2001, 2003b, 2004) or in rats (Stiborová et al., 2003a, 2007b) (Fig. 2F) or mice (Figs. 2D, E). Control incubations without microsomes were free of adduct spots 1 and A, but adduct spot 2 was always detected (data not shown). This finding is consistent with our previous results showing that this adduct is formed also non-enzymatically (Stiborová et al., 2001, 2003b, 2004, 2007a). In the presence of microsomes without NADPH, a low but detectable amount of adduct 1 was found (Table 1).

Because CYPs and peroxidases were found to activate ellipticine (Stiborová et al., 2001; 2003b, 2004, 2007a), we investigated the modulation of ellipticine–DNA adduct formation by cofactors and selective inhibitors of these enzymes using hepatic microsomes isolated both from HRN and WT mice. In the presence of NADPH, a cofactor of POR- and CYP-dependent enzyme systems, hepatic microsomal samples of both mice strains were capable of activating ellipticine to form DNA adducts (Fig. 3). Surprisingly, levels of DNA adducts 1 and 2 formed by hepatic microsomes from HRN mice were only one half of levels formed by this hepatic subcellular fraction from WT mice (Table 1), even though POR expression in livers of HRN mice was two orders of magnitude lower.

α-Lipoic acid, a selective inhibitor of POR (Slepneva et al., 1995), decreased ellipticine–DNA adduct formation by 50–75% with hepatic microsomes from both strains of mice, with a greater extent of inhibition with HRN microsomes than with those from WT livers. Therefore, some of the activity in HRN mice is POR-dependent. Likewise, α-NF, an inhibitor of CYP1A1 and 1A2 (Rendic and DiCarlo, 1997) and ketoconazole, a selective inhibitor of CYP3A enzymes (Rendic and DiCarlo, 1997; Ueng et al., 1997), decreased the levels of ellipticine–DNA adducts generated by hepatic microsomes of both mice strains to essentially equal extent (Fig. 3, Table 1). These results point additionally to CYP enzymes, namely of the 1A and 3A subfamilies, as having a role in ellipticine–DNA adduct formation in mouse livers. Arachidonic

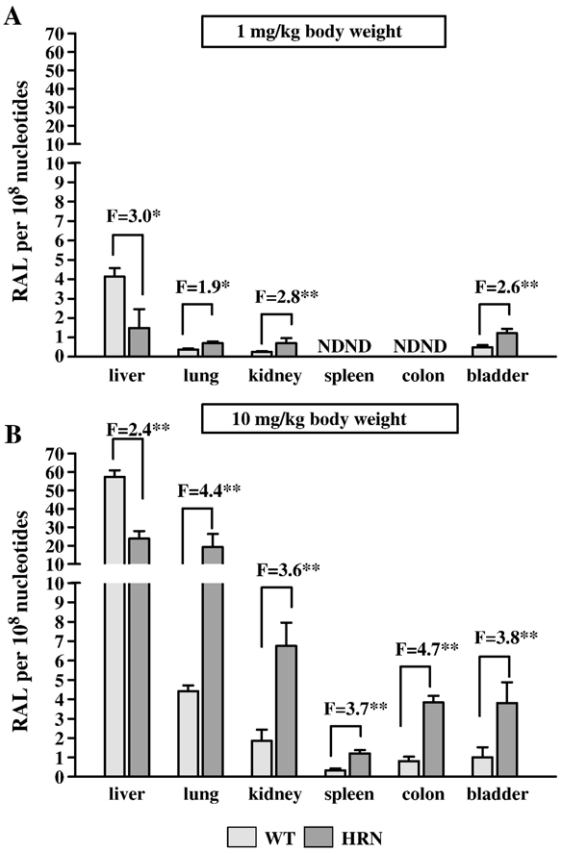

Fig. 5. Total levels of ellipticine–DNA adducts determined and quantified by ^{32}P-postlabelling analysis of DNA isolated from organs of HRN and WT mice treated i.p. with (A) 1 mg ellipticine/kg body weight or (B) 10 mg ellipticine/kg body weight. *F* = fold higher and/or lower DNA adducts in HRN than WT mice. *Columns*, mean; *bars*, S.D. ($n=3$); each DNA sample was analysed twice. $^{*}P<0.05$, $^{**}P<0.01$, $^{***}P<0.001$. RAL, relative adduct labelling. ND = not detected.

acid, a cofactor for COX-dependent oxidation (Eling et al., 1990; Eling and Curtis, 1992; Stiborová et al., 2004, 2005; Arlt et al., 2006), mediated formation of DNA adducts 1 and 2 by ellipticine in hepatic microsomes of both mice strains, but was less effective than NADPH (Fig. 3). The ratio of adduct levels between WT and HRN mice was similar to that observed with NADPH as cofactor.

The profile of ellipticine metabolites in hepatic microsomes from both mouse lines was similar (Fig. 4). The levels of individual metabolites were, however, different; 9-hydroxyellipticine levels were only one sixth, while the amounts of 13-hydroxy- and 12-hydroxyellipticine, were about one half in incubations with HRN microsomes compared with the levels in incubations with WT microsomes.

There might be at least two reasons for the above findings: (i) the low residual levels of POR are still sufficient to mediate CYP-catalyzed ellipticine oxidation or (ii) additional enzymes, besides CYPs, may be present in hepatic microsomes of HRN mice that activate ellipticine. Therefore, we also considered other ellipticine-activating enzymes such as COX (Stiborová et al., 2007a).

DNA adduct formation by ellipticine in HRN mice

To evaluate the importance of hepatic CYP enzymes in the oxidative activation of ellipticine to DNA adducts *in vivo* we treated HRN and WT mice i.p. with a single dose of 1 or 10 mg ellipticine/kg body weight. We chose i.p. injection as the route of administration to achieve high levels of ellipticine in the liver.

In both mouse lines treated with ellipticine essentially the same pattern of up to seven ellipticine-specific DNA adducts as that found *in vivo* in rats (Fig. 2F) (Stiborová et al., 2003a, 2007b) was observed in liver, lung, kidney and bladder (see Figs. 2D, E for liver). No ellipticine-derived DNA adducts were observed in spleen and colon at the lower dose (Fig. 5) or in any of the organs of control animals treated with vehicle only (data not shown). Adduct spots 1 and 2 (Fig. 2) were the predominant adducts in all the other tissues of mice exposed to 1 or 10 mg/kg ellipticine (Table 2). Co-chromatographic analyses of these adduct spots on HPLC confirmed that they were identical to adducts derived from 13-hydroxy- and 12-hydroxyellipticine, respectively, and deoxyguanosine.

Besides these adducts, up to five additional adducts were detected in DNA of liver, lung, kidney, colon and urinary bladder (see Fig. 2 and Table 2). The low levels of these adducts prevented HPLC co-chromatographic analysis or their further characterization.

Quantitative ^{32}P-postlabeling DNA adduct analysis is shown in Fig. 5 and Table 2. Even though the adducts 1, 2 and 3 were not well resolved on TLC plates (Fig. 2), their quantitation using different exposure times of the TLC plates on the Instant Imager allowed us to see these adducts as separated spots. DNA adduct formation was dose- and organ-specific (Fig. 5). The main target organ for DNA adduct formation was the liver in both mouse strains. The levels of three ellipticine–DNA adduct in the livers of HRN mice (adduct spots 1–3, Table 2) were substantially lower (by up to 65%) than in the livers of WT mice

Table 2
DNA adduct formation in various organs of HRN and WT mice treated with 1 or 10 mg ellipticine/kg body weight

Strain	Organ	Dose (mg/kg bw)	RAL[a] (mean/10^8 nucleotides)						
			Spot 1	Spot 2	Spot 3	Spot 4	Spot 5	Spot 6	Spot 7
WT	Liver	1	2.6±0.3	0.3±0.04	0.34±0.08	0.53±0.03	0.34±0.08	ND[b]	ND
HRN	Liver	1	1.0±0.7	0.03±0.05	0.13± 0.06	0.08±0.03	0.25±0.14	ND	ND
WT	Lung	1	0.19±0.04	0.05±0.01	ND	0.14±0.03	ND	ND	ND
HRN	Lung	1	0.47±0.09	0.06±0.01	ND	0.12±0.03	ND	ND	ND
WT	Kidney	1	0.21±0.04	0.04±0.02	ND	ND	ND	ND	ND
HRN	Kidney	1	0.65±0.24	0.05±0.03	ND	ND	ND	ND	ND
WT	Bladder	1	0.35±0.04	0.12±0.02	ND	ND	ND	ND	ND
HRN	Bladder	1	1.0±0.24	0.21±0.02	ND	ND	ND	ND	ND
WT	Spleen	1	ND	ND	ND	ND	ND	ND	ND
HRN	Spleen	1	ND	ND	ND	ND	ND	ND	ND
WT	Colon	1	ND	ND	ND	ND	ND	ND	ND
HRN	Colon	1	ND	ND	ND	ND	ND	ND	ND
WT	Liver	10	47.3±3.1	1.8±0.4	2.9±0.6	2.8±0.1	1.7±0.6	0.5±0.2	0.5±0.2
HRN	Liver	10	16.3±2.3	0.7±0.04	1.2±0.07	3.5±0.9	1.3±0.4	0.6±0.3	0.3±0.2
WT	Lung	10	3.4±0.3	0.2±0.04	0.31±0.02	0.32±0.06	0.15±0.03	ND	ND
HRN	Lung	10	15.0±5.6	0.9±0.03	0.8±0.03	1.3±0.6	0.7±0.5	0.3±0.1	0.2±0.03
WT	Kidney	10	1.51±0.45	0.23±0.09	ND	0.12±0.04	ND	ND	ND
HRN	Kidney	10	5.54±1.24	0.56±0.06	ND	0.34±0.03	ND	0.32±0.09	ND
WT	Bladder	10	0.67±0.3	0.34±0.15	ND	ND	ND	ND	ND
HRN	Bladder	10	2.4±0.6	0.88±0.4	ND	ND	ND	0.57±0.14	ND
WT	Spleen	10	0.24±0.07	0.1±0.04	ND	ND	ND	ND	ND
HR	Spleen	10	0.65±0.1	0.57±0.02	ND	ND	ND	ND	ND
WT	Colon	10	0.63±0.2	0.17±0.05	ND	ND	ND	ND	ND
HRN	Colon	10	3.0±0.4	0.5 0±0.08	ND	0.31±0.15	ND	ND	ND

[a]RAL, relative adduct labeling. All results are presented as the mean±S.D. from three mice; each DNA sample was determined by two postlabelling analyses.
[b]ND — not detected.

at both doses, indicating that CYP enzyme activity is important for the oxidative activation of ellipticine to metabolites generating these adducts. Significantly lower levels of adduct 4 were also found in livers of HRN mice treated with the lower ellipticine dose, but no significant differences in levels of adducts 4–7 were found in livers of the two mouse strains treated with the higher dose (Table 2).

Up to 4.7-fold higher levels of DNA adducts were found in extra-hepatic organs of HRN mice than of WT mice, suggesting that these tissues have the metabolic capacity to oxidize ellipticine and, more importantly, that the same reactive species forming DNA adducts are produced, probably independently of CYP-catalyzed ellipticine activation in the liver. Even though adducts 6 and 7, both known to be generated *in vitro* mainly by peroxidase-mediated oxidation (Poljaková et al., 2006; Stiborová et al., 2007a), were not found in any organ of HRN and WT mice treated with the lower dose, they were both detected in liver and lung and adduct 6 was detected in kidney and urinary bladder of HRN mice treated with 10 mg ellipticine/kg body weight. In WT mice, however, these adducts were only detected in liver (Table 2).

Discussion

Ellipticine is an anticancer agent, whose biological effects such as pharmacological efficiencies and its potential genotoxic side effects may depend on its CYP- and peroxidase mediated metabolism leading to formation of DNA adducts (Stiborová et al., 2001; 2003a,b, 2004, 2007a; Frei et al., 2002; Poljaková et al., 2006, 2007). Although the physiological disposition and DNA adduct formation by this anticancer prodrug have been studied in several animal models (Chadwick et al., 1978; Branfam et al., 1978; Stiborová et al., 2003a, 2007b), the balance between CYPs and peroxidases in the activation of ellipticine *in vivo* is not known. In order to evaluate the contribution and importance of hepatic CYP enzymes to the bioactivation of ellipticine *in vivo* we treated HRN mice with ellipticine. These mice carry a deletion of the *POR* gene in the liver (Henderson and Wolf, 2003; Henderson et al., 2003), and thus lack CYP function in hepatocytes.

We found that ellipticine is metabolized in this animal model, generating ellipticine–DNA adducts in several organs of both HRN and WT mice. Highest total DNA binding levels were always found in liver, followed by lung, kidney, urinary bladder, colon and spleen for both ellipticine doses tested. The pattern and levels of ellipticine–DNA adducts in the organs of WT mice were similar to those found in rats treated with this drug (Stiborová et al., 2003a, 2007b). These data indicate that rats and mice have a similar susceptibility to ellipticine. The adduct pattern consisted of at least two DNA adducts accounting for up to 82% of total levels in the liver of WT mice. These adducts are formed from two reactive species, ellipticine-13-ylium and ellipticine-12-ylium (Fig. 1), which we had suggested earlier to react with one of the nucleophilic centers in the deoxyguanosine residue in DNA (e.g. the exocyclic amino group of guanine, Fig. 1) (Stiborová et al., 2004, 2007a; Poljaková et al., 2006). The low amount of each DNA adduct recovered from digests of DNA treated with 13-hydroxyellipticine or 12-hydroxyellipticine (Fig. 2), however, prevented their further structural characterization. Synthetic approaches are currently being followed in our laboratory to prepare authentic ellipticine–DNA adduct standards. Besides these adducts, up to five additional adduct spots were found in some of the organs analysed.

The finding that ellipticine–DNA adducts are formed in all organs we tested in the study suggest that ellipticine or its metabolites are distributed via the blood stream to different organs and that these tissues have the metabolic capacity to oxidatively activate ellipticine. As found by Chadwick and coworkers (Chadwick et al., 1978; Branfam et al., 1978), ellipticine is very rapidly distributed from the blood, and its excretion is essentially complete by 24 h in several species including mice, rats, dogs and monkeys. The rate of ellipticine elimination from blood was found to reflect the rate of metabolism of this drug (Chadwick et al., 1978). The main organ responsible for its biotransformation was found to be the liver, forming predominantly 9-hydroxyellipticine, which is excreted mainly in bile as its glucuronide or sulfate conjugate (Chadwick et al., 1978; Branfam et al., 1978). Other *in-vivo* pathways involving hydroxylation at as yet unknown positions have also been found (Chadwick et al., 1978; Branfam et al., 1978). In *in-vitro* experiments, ellipticine was metabolized by CYP-mediated reactions by hepatic microsomes of a variety of species, such as humans, rats, rabbits (Stiborová et al., 2004; 2006a) and mice (this study) to several hydroxylated derivatives, with 9-hydroxy-, 12-hydroxy- and 13-hydroxyellipticine being the major metabolites in most species. However, because 13-hydroxy- and 12-hydroxyellipticine are reactive and have been found to form the two major ellipticine–DNA adducts (Stiborová et al., 2004, 2007a; Poljaková et al., 2006), they will not be easily detectable *in vivo*. In addition, radioactively labelled ellipticine was found to be deposited in a number of organs with the highest levels in the liver, followed by kidney, lung, intestine and spleen, and was located primarily in the nuclear fraction (Chadwick et al., 1978). One of the explanation for this may be the ellipticine–DNA binding we found in these tissues.

The levels of the two major ellipticine–DNA adducts were significantly lower in livers of HRN mice, confirming the importance of CYP enzymes in the ellipticine activation to species responsible for DNA adduct formation in this organ *in vivo*. It is remarkable from *in vitro* incubations with hepatic microsomes that the highest effect of the lack of hepatic POR was on the levels of the 9-hydroxyellipticine, the major detoxication product of ellipticine, while the metabolites which form DNA adducts were less affected. Inhibition of NADPH-dependent ellipticine activation to DNA binding species in hepatic microsomes of HRN and WT mice by α-NF and ketoconazole suggests that enzymes from the CYP1A and 3A subfamilies play a major role in this process in mouse liver, as it was found in human and rat liver (Stiborová et al., 2001, 2003b, 2004). The ratio of 13-hydroxyellipticine formed in hepatic microsomes from WT and HRN mice correlated well with the ratio of ellipticine–DNA adduct 1 formed not only *in vitro*, but also *in vivo*. A new ellipticine-derived DNA adduct (see adduct A in Fig. 2A), undetectable in incubations with hepatic microsomes from human or rat (Stiborová et al., 2001,

2003a, 2004) or *in vivo* in rats (Stiborová et al., 2003a, 2007b) or mice treated with ellipticine (present paper), was found in DNA incubated with ellipticine and mouse hepatic microsomes. The metabolite, as well as the enzymes responsible for its formation, remains to be investigated.

Although POR was deleted in hepatocytes of HRN mice the formation of DNA adducts in livers of these mice was not completely eliminated, but occurred at 35% of the level in WT mice. *In vitro* the ratio was somewhat higher with levels of the two major ellipticine–DNA adducts amounting to 50% of WT levels. In addition, inhibitors of POR and CYPs led to a decrease in levels of these two major DNA adducts in hepatic microsomes of both mouse lines of 40–65%. All these results suggest that either other enzymes also activate ellipticine in livers of the mouse model used or the substantial induction in the expression of CYP3A and CYP1A in the liver of HRN mice (Henderson et al., 2003), the enzymes that play a significant role in ellipticine activation, contributes to metabolic activation of this drug in the HRN liver. The results with added arachidonic acid confirm earlier results that *in vitro* COX might be another enzyme system capable of activating ellipticine (Poljaková et al., 2006; Stiborová et al., 2007a). It is however conspicuous that ellipticine activation with a cofactor of COX (arachidonic acid) in microsomes of HRN mice is not as high as in WT mice, on the contrary, the ratio of levels of DNA adducts was similar with arachidonic acid as with NADPH. *In vivo* a similar observation was made in that the levels of "peroxidase-catalysed" adducts 6 and 7 in livers of HRN mice were not higher than in WT mice, as might have been expected as a compensatory reaction of the organism to POR deletion. The reason for low arachidonic acid-dependent activity in hepatic POR knock-out mice is not known.

In contrast to the liver, up to 4.7-fold higher DNA adduct levels were observed in extra-hepatic tissues of HRN mice analysed in this study. Ellipticine delivered i.p. is absorbed via the mesenteric veins and lymphatic systems, and passes through the liver, where most of its metabolism occurs. In the absence of CYP-mediated oxidation in the liver, however, more ellipticine reaches the blood circulation and all distal tissues, where it is activated to DNA adducts, leading to higher levels in HRN than in WT mice. In a future study, the pharmacokinetic profiles of ellipticine in the two mouse lines shall be investigated to provide evidence of increased ellipticine plasma concentrations in HRN mice. An alternative explanation for higher DNA adduct levels in extra-hepatic tissues of HRN mice might be a possible induction of non-CYP/POR-dependent metabolic activities towards ellipticine in these tissues, such as peroxidases.

The question whether CYPs or peroxidases or both of these enzymes are responsible for ellipticine activation in extra-hepatic organs remains to be answered, but the pattern of the ellipticine–DNA adducts found in individual organs as well as knowledge on expression of CYPs and peroxidases in these tissues can help to evaluate their relative importance. In contrast to low constitutive expression of CYPs in extra-hepatic tissues, lung, kidney and urinary bladder are rich in peroxidases such as COX-1, COX-2 and LPO (Eling et al., 1990; Eling and Curtis, 1992). The role of peroxidases in ellipticine activation *in vitro* was studied by us recently, utilising both pure peroxidases (LPO, MPO, COX-1 and -2) (Poljaková et al., 2006; Stiborová et al., 2007a) and microsomes from human kidney, in which peroxidases such as COX are expressed (Stiborová et al., 2007a). All these systems activated ellipticine to ellipticine-13-ylium and ellipticine-12-ylium species generating the two major DNA adducts 1 and 2 (Fig. 1) (Poljaková et al., 2006; Stiborová et al., 2007a). Since these reactive species are the same as those formed by ellipticine oxidation by CYPs, the DNA adducts 1 and 2 cannot serve as markers for either enzyme. The formation of the two minor DNA adducts 6 and 7 (Fig. 2) *in vitro* is, however, mainly peroxidase-catalysed (Stiborová et al., 2007a). These adducts were detected in lung, kidney and urinary bladder of HRN mice treated with 10 mg ellipticine/kg body weight, but not in those of WT mice. These results suggest strongly that peroxidases such as COX and LPO might participate significantly in ellipticine activation in these organs. Therefore, the objective of our future work is to analyse the participation of peroxidases in the metabolic activation of ellipticine *in vivo*. For instance, MPO-knockout mice may help to evaluate the involvement of this enzyme in the bioactivation of ellipticine *in vivo* (Noguchi et al., 2000).

Although expression of CYP enzymes in extra-hepatic organs is much lower than in the liver (Rendic and DiCarlo, 1997), it can be induced by ellipticine not only in the liver, but also in extra-hepatic tissues such as lung and kidney, as we found in rats for CYP1A (Aimová et al., 2007). As a consequence, ellipticine oxidation both to metabolites generating DNA adducts (13-hydroxy- and 12-hydroxyellipticine) and to those leading to its excretion (9-hydroxy- and 7-hydroxyellipticine) is increased (Aimová et al., 2007). Therefore, participation of CYPs in ellipticine activation in extra-hepatic organs cannot be excluded, and awaits further investigation.

In conclusion, despite hepatic POR knock-out, ellipticine–DNA adducts are still detected *in vitro* with HRN hepatic microsomes and *in vivo* in HRN mice treated with single doses of ellipticine. The major difference between the HRN and WT lines is a considerable increase in levels of extra-hepatic DNA adducts in HRN mice. The reason for relatively high levels of liver DNA adducts could be residual POR, e.g. in non-parenchymal cells, or other enzymes like peroxidases. Furthermore, the major effect of POR is on ellipticine detoxication (formation of 9-hydroxyellipticine by microsomal CYPs), and less on its oxidative activation to 12-hydroxy and 13-hydroxyellipticine. Therefore, more unmetabolized ellipticine might be distributed among extra-hepatic tissues. Our results reveal that ellipticine metabolism and DNA adduct formation *in vitro* correspond well to levels of DNA adducts *in vivo* in the HRN mouse model used in the study.

Acknowledgments

This work was supported in part by Grant Agency of the Czech Republic, grant 203/06/0329, Ministry of Education of the Czech Republic, grants MSM0021620808 and 1M4635608802-Center of Targeted Therapeutics and by Cancer Research UK. V.M. Arlt, C.J. Henderson, C.R. Wolf and D.H. Phillips are partners of ECNIS (Environmental Cancer Risk, Nutrition and Individual

Susceptibility), a network of excellence operating within the European Union 6th Framework Program, Priority 5: "Food Quality and Safety" (Contract No. 513943).

References

Aimová, D., Svobodová, L., Kotrbová, V., Mrázová, B., Hodek, P., Hudeček, J., Václavíková, R., Frei, E., Stiborová, M., 2007. The anticancer drug ellipticine is a potent inducer of rat cytochromes P450 1A1 and 1A2, thereby modulating its own metabolism. Drug Metab. Dispos. 35, 1926–1934.

Arlt, V.M., Stiborová, M., Hewer, A., Schmeiser, H.H., Phillips, D.H., 2003. Human enzymes involved in the metabolic activation of the environmental contaminant 3-nitrobenzanthrone: evidence for reductive activation by human NADPH:cytochrome P450 reductase. Cancer Res. 63, 2752–2761.

Arlt, V.M., Hewer, A., Sorg, B.L., Schmeiser, H.H., Phillips, D.H., Stiborová, M., 2004. 3-Aminobenzanthrone, a human metabolite of the environmental pollutant 3-nitrobenzanthrone, forms DNA adducts after metabolic activation by human and rat liver microsomes: evidence for activation by cytochrome P450 1A1 and P450 1A2. Chem. Res. Toxicol. 17, 1092–1101.

Arlt, V.M., Stiborová, M., Henderson, C.J., Osborne, M.R., Bieler, C.A., Frei, E., Martinek, V., Sopko, B., Wolf, C.R., Schmeiser, H.H., Phillips, D.H., 2005. Environmental pollutant and potent mutagen 3-nitrobenzanthrone forms DNA adducts after reduction by NAD(P)H:quinone oxidoreductase and conjugation by acetyltransferases and sulfotransferases in human hepatic cytosols. Cancer Res. 65, 2644–2652.

Arlt, V.M., Henderson, C.J., Wolf, C.R., Schmeiser, H.H., Phillips, D.H., Stiborová, M., 2006. Bioactivation of 3-aminobenzanthrone, a human metabolite of the environmental pollutant 3-nitrobenzanthrone: evidence for DNA adduct formation mediated by cytochrome P450 enzymes and peroxidases. Cancer Lett. 234, 220–231.

Auclair, C., 1987. Multimodal action of antitumor agents on DNA: the ellipticine series. Arch. Biochem. Biophys. 259, 1–14.

Bořek-Dohalská, L., Frei, E., Stiborová, M., 2004. DNA adduct formation by the anticancer drug ellipticine and its hydroxy derivatives in human breast adenocarcinoma MCF-7 cells. Collect. Czech. Chem. Commun. 69, 603–615.

Branfam, A.R., Bruni, R.J., Reihold, V.N., Silveira, D.M., Chadwick, M., Yesair, D.W., 1978. Characterization of metabolites of ellipticine in rat bile. Drug Metab. Dispos. 6, 542–548.

Buters, J.T., Sakai, S., Richter, T., Pineau, T., Alexander, D.L., Savas, U., Doehmer, J., Ward, J.M., Jefcoate, C.R., Gonzalez, F.J., 1999. Cytochrome P450 CYP1B1 determines susceptibility to 7,12-dimethylbenz[*a*]anthracene-induced lymphomas. Proc. Natl. Acad. Sci. U. S. A. 96, 1977–1982.

Buters, J.T., Mahadevan, B., Quintanilla-Martinez, L., Gonzalez, F.J., Greim, H., Baird, W.M., Luch, A., 2002. Cytochrome P450 1B1 determines susceptibility to dibenzo[*a*,*l*]pyrene-induced tumor formation. Chem. Res. Toxicol. 15, 1127–1135.

Chadwick, M., Silveira, D.M., Platz, B.R., Hayes, D., 1978. Comparative physiological disposition of ellipticine in several animal species after intravenous administration. Drug Metab. Dispos. 6, 528–541.

Culp, S.J., Roberts, D.W., Talaska, G., Lang, N.P., Fu, P.P., Lay Jr., J.O., Teitel, C.H., Snawder, J.E., Von Tungeln, L.S., Kadlubar, F.F., 1997. Immunochemical, ^{32}P-postlaeling, and GC/MS detection of 4-aminobiphenyl–DANN adducts in human peripheral lung in relation to metabolic activation pathways involving pulmonary *N*-oxidation, conjugation, and peroxidation. Mutat. Res. 378, 97–112.

Eling, T.E., Curtis, J.F., 1992. Xenobiotic metabolism by prostaglandin H synthase. Pharm. Ther. 53, 261–273.

Eling, T.E., Thompson, D.C., Foureman, G.L., Curtis, J.F., Hughes, M.F., 1990. Prostaglandin H synthase and xenobiotic oxidation. Annu. Rev. Pharmacol. Toxicol. 30, 1–45.

Fossé, P., René, B., Charra, M., Paoletti, C., Saucier, J.M., 1992. Stimulation of topoisomerase II-mediated DNA cleavage by ellipticine derivatives: structure–activity relationships. Mol. Pharmacol. 42, 590–595.

Frei, E., Bieler, C.A., Arlt, V.M., Wiessler, M., Stiborová, M., 2002. Covalent binding of the anticancer drug ellipticine to DNA in V79 cells transfected with human cytochrome P450 enzymes. Biochem. Pharmacol. 64, 289–295.

Froelich-Ammon, S.J., Patchan, M.W., Osheroff, N., Thompson, R.B., 1995. Topoisomerase II binds to ellipticine in the absence or presence of DNA. Characterization of enzyme–drug interactions by fluorescence spectroscopy. J. Biol. Chem. 270, 14998–15004.

Gonzalez, F.J., Kimura, S., 2001. Understanding the role of xenobiotic-metabolism in chemical carcinogenesis using gene knockout mice. Mutat. Res. 477, 79–87.

Henderson, C.J., Wolf, C.R., 2003. Transgenic analysis of human drug-metabolizing enzymes: preclinical drug development and toxicology. Mol. Interv. 3, 331–343.

Henderson, C.J., Otto, D.M.E., Carrie, D., Magnuson, M.A., McLaren, A.W., Rosewell, I., Wolf, C.R., 2003. Inactivation of the hepatic cytochrome P450 system by conditional deletion of hepatic cytochrome P450 reductase. J. Biol. Chem. 278, 13480–13486.

Henderson, C.J., Pass, G.J., Wolf, C.R., 2006. The hepatic cytochrome P450 reductase null mouse as a tool to identify a successful candidate entity. Toxicol. Lett. 162, 111–117.

Kimura, S., Kawabe, M., Ward, J.M., Morishima, H., Kadlubar, F.F., Hammons, G.J., Fernandez-Salguero, P., Gonzalez, F.J., 1999. CYP1A2 is not the primary enzyme responsible for 4-aminobiphenyl-induced hepatocarcinogenesis in mice. Carcinogenesis 20, 1825–1830.

Kimura, S., Kawabe, M., Yu, A., Morishima, H., Fernandez-Salguero, P., Hammons, G.J., Ward, J.M., Kadlubar, F.F., Gonzalez, F.J., 2003. Carcinogenesis of the food mutagen PhIP in mice is independent of CYP1A2. Carcinogenesis 24, 583–587.

Monnot, M., Mauffret, O., Simon, V., Lescot, E., Psaume, B., Saucier, J.M., Charra, M., Belehradek Jr., J., Fermandjian, S., 1991. DNA–drug recognition and effects on topoisomerase II-mediated cytotoxicity. A three-mode binding model for ellipticine derivatives. J. Biol. Chem. 25, 1820–1829.

Noguchi, N., Nakano, K., Aratani, Y., Koyama, H., Kodama, T., Niki, E., 2000. Role of myeloperoxidase in the neutrophil-induced oxidation of low density lipoprotein as studied by myeloperoxidase-knockout mouse. J. Biochem. (Tokyo) 127, 971–976.

Pass, G.J., Carrie, D., Boylan, M., Lorimore, S., Wright, E., Houston, B., Henderson, C.J., Wolf, C.R., 2005. Role of hepatic cytochrome P450s in the pharmacokinetics and toxicity of cyclophosphamide: studies with the hepatic cytochrome P450 reductase null mouse. Cancer Res. 65, 4211–4217.

Poljaková, J., Dračínský, M., Frei, E., Hudeček, J., Stiborová, M., 2006. The effect of pH on peroxidase-mediated oxidation of and DNA-adduct formation by ellipticine. Collect. Czech. Chem. Commun. 71, 1169–1185.

Poljaková, J., Frei, E., Gomez, J.E., Aimová, D., Eckschlager, T., Hraběta, J., Stiborová, M., 2007. DNA adduct formation by the anticancer drug ellipticine in human leukemia HL-60 and CCRF-CEM cells. Cancer Lett. 252, 270–279.

Rendic, S., DiCarlo, F.J., 1997. Human cytochrome P450 enzymes: a status report summarizing their reactions, substrates, inducers, and inhibitors. Drug Metab. Rev. 29, 413–480.

Singh, M.P., Hill, G.C., Peoch, D., Rayner, B., Inabach, J.L., Lown, J.W., 1994. High-field NMR and restrained molecular modeling studies on a DNA heteroduplex containing a modified apurinic abasic site in the form of covalently linked 9-aminoellipticine. Biochemistry 33, 10271–10285.

Slepneva, I.A., Sergeeva, S.V., Khramtsov, V.V., 1995. Reversible inhibition of NADPH–cytochrome P450 reductase by alpha-lipoic acid. Biochem. Biophys. Res. Commun. 214, 1246–1253.

Stiborová, M., Frei, E., Schmeiser, H.H., Anzenbacher, P., 1991. The role of peroxidases in the activation of chemical carcinogens. Drug Metab. Interact. 9, 177–190.

Stiborová, M., Bieler, C.A., Wiessler, M., Frei, E., 2001. The anticancer agent ellipticine on activation by cytochrome P450 forms covalent DNA adducts. Biochem. Pharmacol. 62, 675–684.

Stiborová, M., Martínek, V., Rýdlová, H., Hodek, P., Frei, E., 2002. Sudan I is a potential carcinogen for humans: evidence for its metabolic activation and detoxication by human recombinant cytochrome P450 1A1 and liver microsomes. Cancer Res. 62, 5678–5684.

Stiborová, M., Breuer, A., Aimová, D., Stiborová-Rupertová, M., Wiessler, M., Frei, E., 2003a. DNA adduct formation by the anticancer drug ellipticine in rats determined by ^{32}P-postlabeling. Int. J. Cancer 107, 885–890.

Stiborová, M., Stiborová-Rupertová, M., Bořek-Dohalská, L., Wiessler, M., Frei, E., 2003b. Rat microsomes activating the anticancer drug ellipticine to species

covalently binding to deoxyguanosine in DNA are a suitable model mimicking ellipticine bioactivation in humans. Chem. Res. Toxicol. 16, 38–47.

Stiborová, M., Sejbal, J., Bořek-Dohalská, L., Aimová, D., Poljaková, J., Forsterová, K., Rupertová, M., Wiesner, J., Hudeček, J., Wiessler, M., Frei, E., 2004. The anticancer drug ellipticine forms covalent DNA adducts, mediated by human cytochromes P450, through metabolism to 13-hydroxyellipticine and ellipticine N^2-oxide. Cancer Res. 64, 8374–8380.

Stiborová, M., Frei, E., Hodek, P., Wiessler, M., Schmeiser, H.H., 2005. Human hepatic and renal microsomes, cytochromes P450 1A1/2, NADPH:cytochrome P450 reductase and prostaglandin H synthase mediate the formation of aristolochic acid–DNA adducts found in patients with urothelial cancer. Int. J. Cancer 113, 189–197.

Stiborová, M., Bořek-Dohalská, L., Aimová, D., Kotrbová, V., Kukačková, K., Janouchová, K., Rupertová, M., Ryšlavá, H., Hudeček, J., Frei, E., 2006a. Oxidation pattern of the anticancer drug ellipticine by hepatic microsomes — similarity between human and rat systems. Gen. Physiol. Biophys. 25, 245–261.

Stiborová, M., Dračínská, H., Hájková, J., Kadeřábková, P., Frei, E., Schmeiser, H.H., Souček, P., Phillips, D.H., Arlt, V.M., 2006b. The environmental pollutant and carcinogen 3-nitrobenzanthrone and its human metabolite 3-aminobenzanthrone are potent inducers of rat hepatic cytochromes P450 1A1 and -1A2 and NAD(P)H:quinone oxidoreductase. Drug Metab. Dispos. 34, 1398–1405.

Stiborová, M., Poljaková, J., Ryšlavá, H., Dračínský, M., Eckschlager, T., Frei, E., 2007a. Mammalian peroxidases activate anticancer drug ellipticine to intermediates forming deoxyguanosine adducts in DNA identical to those found *in vivo* and generated from 12-hydroxyellipticine and 13-hydroxyellipticine. Int. J. Cancer 120, 243–251.

Stiborová, M., Rupertová, M., Aimová, D., Ryšlavá, H., Frei, E., 2007b. Formation and persistence of DNA adducts of anticancer drug ellipticine in rats. Toxicology 236, 50–60.

Tsuneoka, Y., Dalton, T.P., Miller, M.L., Clay, C.D., Shertzer, H.G., Talaska, G., Medvedovic, M., Nebert, D.W., 2003. 4-Aminobiphenyl-induced liver and urinary bladder DNA adduct formation in Cyp1a2(−/−) and Cyp1a2(+/+) mice. J. Natl. Cancer Inst. 95, 1227–1237.

Ueng, Y.-F., Kuwabara, T., Chun, Y.-J., Guengerich, F.P., 1997. Cooperativity in oxidation catalyzed by cytochrome P450 3A4. Biochemistry 36, 370–381.

Uno, S., Dalton, T.P., Derkenne, S., Curran, C.P., Miller, M.L., Shertzer, H.G., Nebert, D.W., 2004. Oral exposure to benzo[*a*]pyrene in the mouse: detoxication by inducible cytochrome P450 is more important than metabolic activation. Mol. Pharmacol. 65, 1225–1237.

Yasukochi, Y., Peterson, J.A., Masters, B., 1979. NADPH-cytochrome *c* (P450) reductase: spectrophotometric and stopped flow kinetic studies on the formation of reduced flavoprotein intermediates. J. Biol. Chem. 254, 7097–7104.

Příloha 3

MICHAELA MOSEROVÁ, VĚRA KOTRBOVÁ, MARTINA RUPERTOVÁ, KAREL NAIMAN, JIŘÍ HUDEČEK, PETR HODEK, EVA FREI AND MARIE STIBOROVÁ

ISOLATION AND PARTIAL CHARACTERIZATION OF THE ADDUCT FORMED BY 13-HYDROXYELLIPTICINE WITH DEOXYGUANOSINE IN DNA.

Neuro Endocrinol. Letters, 29(5), 728-732,2008

ORIGINAL ARTICLE

Isolation and partial characterization of the adduct formed by 13-hydroxyellipticine with deoxyguanosine in DNA

Michaela Moserová [1], Věra Kotrbová [1], Martina Rupertová [1], Karel Naiman [1], Jiří Hudeček [1], Petr Hodek [1], Eva Frei [2], Marie Stiborová [1]

1. Department of Biochemistry, Faculty of Science, Charles University, Prague, Czech Republic
2. Division of Molecular Toxicology, German Cancer Research Center, Heidelberg, Germany

Correspondence to: Prof. Marie Stiborová, DSc.
Department of Biochemistry, Faculty of Science, Charles University,
Albertov 2030, 128 40 Prague 2, Czech Republic
TEL.: +420-2-2195 1285, FAX: +420-2-2195 1283
E-MAIL: stiborov@natur.cuni.cz

Submitted: 2008-06-30 Accepted: 2008-08-27

Key words: **anticancer drug; ellipticine; 13-hydroxyellipticine; DNA adducts; HPLC**

Neuroendocrinol Lett 2008; **29**(5):728–732 **PMID:** 18987592 NEL290508A19

Abstract

OBJECTIVES: Ellipticine is a potent antineoplastic agent exhibiting multiple mechanisms of its action. Recently, we have found that 13-hydroxyellipticine, formed from ellipticine as the predominant metabolite in human livers, is bound to deoxyguanosine in DNA, generating the major DNA adduct *in vivo* and *in vitro*. The development of the methods suitable for the preparation of this adduct in the amounts sufficient for identification of its structure and those for its isolation and partial characterization is the aim of this study.

METHODS: High performance liquid chromatography (HPLC) was employed for separation of 13-hydroxyellipticine-mediated deoxyguanosine adduct. The ^{32}P-postlabeling technique was utilized to detect this adduct in DNA.

RESULTS: The formation of the 13-hydroxyellipticine-derived deoxyguanosine adduct in DNA *in vitro* was increased under the alkaline pH of the incubations and by the formation of the sulfate and acetate conjugates of 13-hydroxyellipticine generated by reactions with 3'-phosphoadenosine-5'-phosphosulfate (PAPS) or acetyl-coenzyme A (acetyl-CoA) catalyzed by human sulfotransferases (SULTs) 1A1 and 1A2 and *N,O*-acetyltransferases (NATs) 1 and 2. The HPLC method suitable for separation the 13-hydroxyellipticine-derived deoxyguanosine adduct from other reactants, deoxyguanosine and 13-hydroxyellipticine, was developed. The structure of this adduct is proposed to correspond to the product formed from ellipticine-13-ylium with the exocyclic 2-NH_2 group of guanine in DNA.

CONCLUSIONS: The data are the first report on HPLC isolation of the deoxyguanosine adduct formed by 13-hydroxyellipticine in DNA and its partial characterization.

Abbreviations

Acetyl-CoA -acetyl-coenzyme A
CYP - cytochrome P450
HPLC - high performance liquid chromatography
NAT - *N,O*-acetyltransferase
PAPS - 3′-phosphoadenosine-5′-phosphosulfate
RAL - relative adduct labeling
r.t. - retention time
SULT - sulfotransferase

INTRODUCTION

Ellipticine (Figure 1), an alkaloid isolated from Apocynanacea plants, exhibits significant antitumor activities (for a summary, see [10]). Ellipticine has been reported to arrest cell cycle progression, to induce apoptotic cell death by the generation of cytotoxic free radicals, an increase of wild-type p53, the rescue of mutant p53 activity and the initiation of mitochondrial pathway (for a summary, see [15]). Chemotherapy-induced cell cycle arrest was shown to result from various DNA damages caused by a variety of chemotherapeutics. In the case of ellipticine, it was suggested that the prevalent DNA-mediated mechanisms of their antitumor, mutagenic and cytotoxic activities are (i) intercalation into DNA [1,15] and (ii) inhibition of DNA topoisomerase II activity [1,15]. We have demonstrated that ellipticine also covalently binds to DNA *in vitro* and *in vivo* after being enzymatically activated with cytochromes P450 (CYP) or peroxidases [7,9–11,13,14,16,17], suggesting a third possible mechanism of action.

Human and rat CYP1A, 1B1 and 3A are the predominant enzymes catalyzing oxidation of ellipticine *in vitro* either to metabolites that are excreted (7-hydroxy- and 9-hydroxyellipticine) or that form DNA adducts (12-hydroxy- and 13-hydroxyellipticine) [6,10,11,16,17]. Of the mammalian peroxidases, cyclooxygenase-1 and -2, lactoperoxidase and myeloperoxidase efficiently generated ellipticine-derived DNA adducts (Figure 1) [7,13]. The same DNA adducts were also detected in cells in culture expressing enzymes activating ellipticine (CYP1A1, cyclooxygenase-1 and myeloperoxidase), such as human breast adenocarcinoma MCF-7 cells [2], leukemia HL-60 and CCRF-CEM cells [8] and V79 Chinese hamster lung fibroblasts transfected with human CYP3A4, 1A1 and 1A2 [5]. On the basis of these data, ellipticine might be considered a drug, whose pharmacological efficiency and/or genotoxic side effects are dependent on its activation by CYPs and peroxidases in target tissues.

13-Hydroxyellipticine formed as the predominant metabolite by CYP3A4 in human livers was identified to bind to deoxyguanosine in DNA, generating the major DNA adduct *in vitro* and *in vivo* (Figure 1) [6,9,11,13,16,17]. We have suggested earlier that the reactive carbenium ion formed spontaneously from 13-hydroxyellipticine, ellipticine-13-ylium, might react with one of the nucleophilic centers in the deoxyguanosine residue in DNA (e.g. the exocyclic amino group of guanine, Figure 1) to form the adduct [7,9,13,16]. The low amount of this DNA adduct recovered from digests of DNA treated with 13-hydroxyellipticine, however, prevented its further structural characterization. Therefore, to prepare this adduct in amounts sufficient for its further characterization, we investigated how to increase its formation *in vitro*. To increase the levels of the 13-hydroxyellipticine-derived DNA adduct, we investigated the modulation of the reaction of 13-hydroxyellipticine with DNA (or deoxyguanosine) by pH and/or by its conjugation with PAPS or acetyl-CoA catalyzed by the phase II biotransformation enzymes, human SULT1A1/2 and NAT1 and NAT2. Moreover, the HPLC isolation procedure to obtain the adduct was developed.

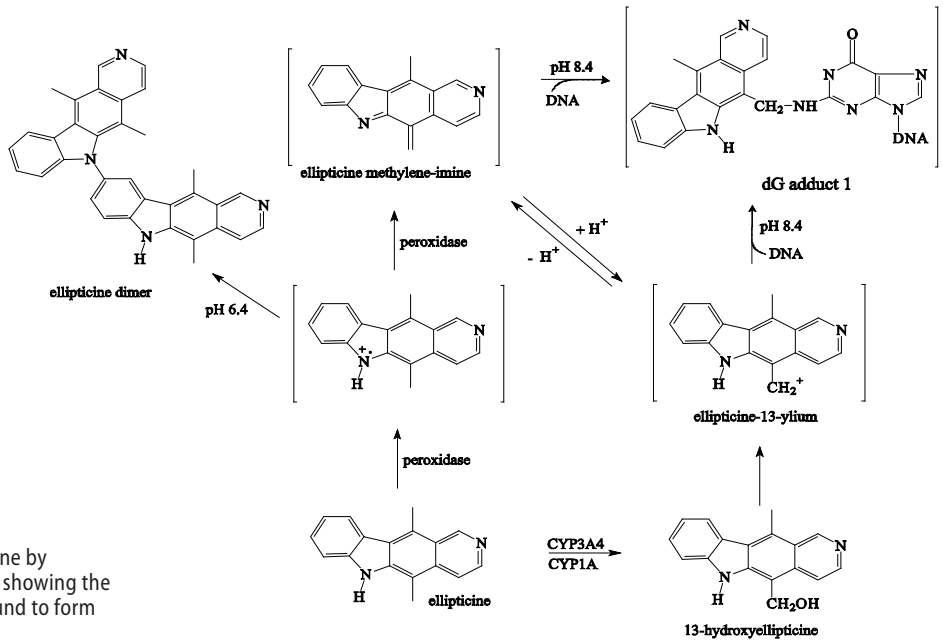

Figure 1. Metabolism of ellipticine by human CYPs and peroxidases showing the characterized metabolites found to form the major DNA adduct

MATERIAL AND METHODS

Ellipticine, deoxyguanosine, acetyl-CoA, PAPS and calf thymus DNA were from Sigma Chemical Co (St Louis, MO, USA). 13-Hydroxyellipticine was synthesized as described [4]. Cytosolic extracts, isolated from insect cells transfected with baculovirus constructs containing cDNA of human SULT1A1*2, -1A2*1 were obtained from Oxford Biomedical Research Inc. (Oxford, MA, USA), and those containing cDNA of human NAT1*4 or NAT2*4 from Gentest Corp. (Woburn, MA, USA). Enzymes and chemicals for the ^{32}P-postlabeling assay were obtained from sources described [10,12]. All these and other chemicals were reagent grade or better. The incubation mixtures in a final volume of 500 µl consisted of 0.1 mM phosphate buffer (pH 6.0, 7.4 or 8.4), 1 mg calf thymus DNA or 1 mM deoxyguanosine and 50 µM 13-hydroxyellipticine either in the presence or absence of 39 nmol human SULT1A1/2 or NAT1 or 2 and SULTs and NATs cofactors (2 mM acetyl-CoA or 100 µM PAPS). Mixtures were incubated at 37 °C for 1–24 h. Aliquots of the mixtures (50 µl) were applied onto a HPLC column, where components of the incubation mixtures were separated. The HPLC was performed with a reversed phase column (Ultrasphere, ODS, 250 × 4.6 mm, 5 µM; Beckman-Coulter, USA) using a linear methanol – acetic acid (32 mM in distilled water) gradient of 0% methanol rising to 100% in 70 min and isocratic elution of 100% methanol in 5 min (flow rate of 1 ml/min, detection at 250 and 318 nm). Deoxyguanosine, 13-hydroxyellipticine and the 13-hydroxyellipticine-derived deoxyguanosine adduct were eluted with retention times (r.t.) of 10.0, 42.2 and 23.8 min, respectively, and identified by mass spectroscopy. ^{32}P-postlabeling assays of the 13-hydroxyellipticine-mediated adduct were performed using nuclease P1 enrichment [10].

Table 1. The effect of pH on levels of the adduct formed by reaction of 13-hydroxyellipticine with DNA[a], detected by ^{32}P-postlabeling[b]

pH	RAL[c] (mean ± SD/10^7 nucleotides)
6.0	1.3 ± 0.3
7.4	23.3 ± 2.0
8.4	49.7 ± 3.2

[a]See adduct spot 1 in Figure 2. [b]Experimental conditions were as described in Material and methods excerpt that 50 µM 13-hydroxyellipticine and 1 mg calf thymus DNA (37 °C, 90 min) were used. [c]RAL, relative adduct labeling, and standard deviations were obtained from triplicate determinations.

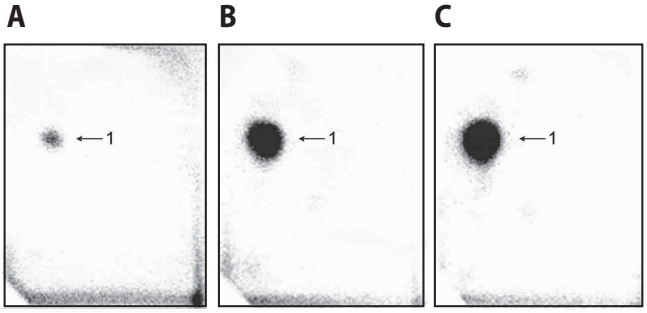

Figure 2. Autoradiographic profiles of 13-hydroxyellipticine-derived DNA adduct levels in relation to pH, analyzed with ^{32}P-postlabeling assay. (**A**) pH 6.0; (**B**) pH 7.4; (**C**) pH 8.4.

RESULTS

The effect of pH on formation of deoxyguanosine adduct from 13-hydroxyellipticine in DNA

13-Hydroxyellipticine incubated with DNA *in vitro* generates the major deoxyguanosine adduct, which was detected and quantified by the nuclease P1 version of the ^{32}P-postlabeling technique (see adduct spot 1 formed in DNA in Figure 2). The yield of formation of this ellipticine-DNA adduct is pH-dependent. Only low levels of this DNA adduct was detectable at pH 6.0, while increasing pH resulted in a pronounced increase in formation of this adduct (Figure 2, Table 1). The 13-hydroxyellipticine-derived adduct is also formed by incubation of 13-hydroxyellipticine with deoxyguanosine (Figure 3). In order to isolate the 13-hydroxyellipticine-derived deoxyguanosine adduct, a novel HPLC procedure was developed. The reversed-phase HPLC was found to be appropriate to isolate this adduct from residual deoxyguanosine and 13-hydroxyellipticine, the adduct eluted with r.t. of 23.8 min (Figure 3). An increase in pH of the incubation mixture leads again to an increase in formation of this adduct. Whereas adduct was formed at pH 8.4, no detectable levels of this adduct were found at pH 7.4 (Figure 3).

The effect of conjugation of 13-hydroxyellipticine with PAPS and acetyl-Co A catalyzed by SULT1A1/2 and NAT1/2 on formation of 13-hydroxyellipticine-derived DNAadduct

The levels of 13-hydroxyellipticine-derived DNA adduct were significantly increased by incubation of 13-hydroxyellipticine and DNA with the human SULT1A1 and 1A2 conjugation enzymes and their cofactor, PAPS, by 1.7- and 26-fold, respectively (Figure 4). Likewise, NAT1 and NAT2 in the presence of their cofactor, acetyl-CoA, stimulated the formation of the 13-hydroxyellipticine-derived DNA adduct, by 33- and 288-fold (Figure 4). An increase in its formation was detected both by the ^{32}P-postlabeling assay (Figure 4) and by HPLC (see the adduct peak eluted at 23.8 min in Figure 5).

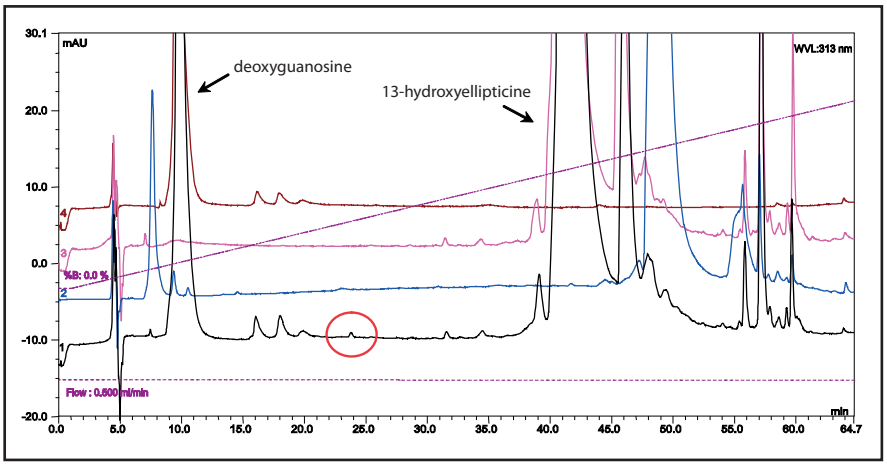

Figure 3. HPLC of 13-hydroxyellipticine-derivated DNA adduct formed by incubation of 13-hydroxyellipticine with deoxyguanosine at pH 7.4 and 8.4
1 – incubation of 13-hydroxyellipticine with deoxyguanosine at pH 8.4; **2** – incubation of 13-hydroxyellipticine with deoxyguanosine at pH 7.4; **3** – 13-hydroxyellipticine; **4** – deoxyguanosine.

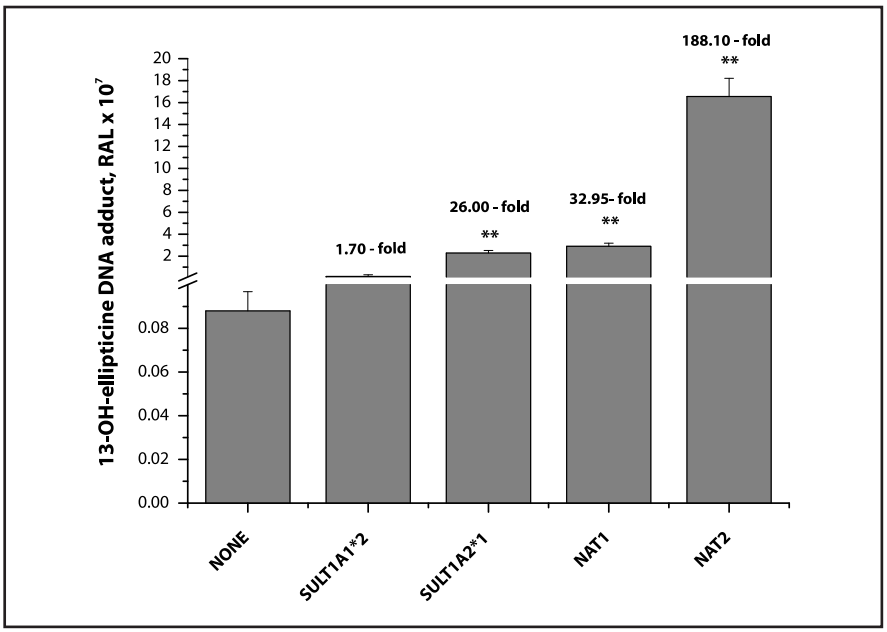

Figure 4. The effect of SULT1A1/2 and NAT1 and 2 on formation of deoxyguanosine adduct in DNA by its incubation with 13-hydroxyellipticine

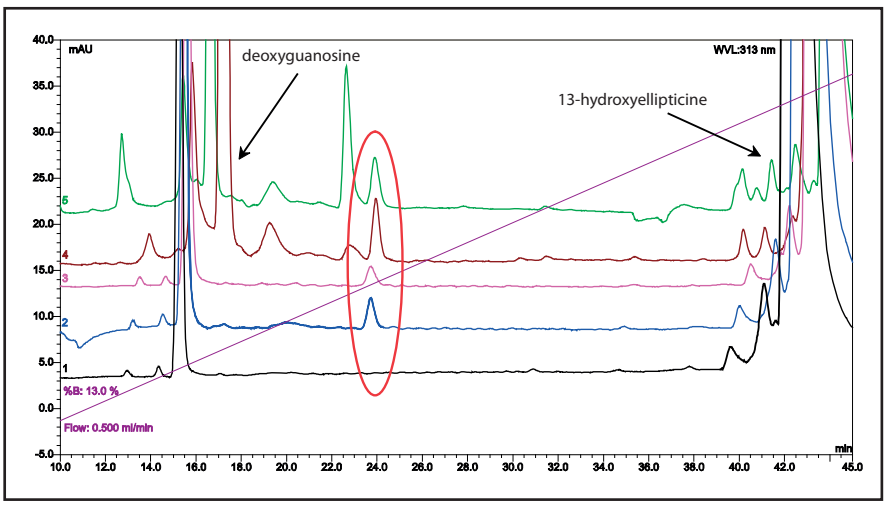

Figure 5. HPLC of 13-hydroxyellipticine-derivated DNA adduct formed by incubation of 13-hydroxyellipticine with deoxyguanosine at pH 7.4 in the presence of SULT 1A1/2 and NAT1 and NAT2 in the presence of their cofactors, PAPS and acetyl-CoA, respectively.
1 – incubation of 13-hydroxyellipticine with deoxyguanosine at pH 7.4; **2** – incubation of 13-hydroxyellipticine with deoxyguanosine at pH 7.4 with PAPS and SULT1A1;
3 – incubation of 13-hydroxyellipticine with deoxyguanosine at pH 7.4 with PAPS and SULT1A2; **4** – incubation of 13-hydroxyellipticine with deoxyguanosine at pH 7.4 with acetyl-CoA and NAT1;
5 – incubation of 13-hydroxyellipticine with deoxyguanosine at pH 7.4 with acetyl-CoA and NAT2.

DISCUSSION

The present paper shows the results which might increase our knowledge on the mechanism of DNA adduct formation by the anticancer drug ellipticine. Here, we demonstrate that the formation of the major DNA adduct by ellipticine *in vitro* and *in vivo*, 13-hydroxyellipticine-derived DNA adduct, is increased by an increase in pH of the incubation mixture. This adduct was proposed to be formed from the reactive species, carbenium ion (ellipticine-13-ylium), formed in the ellipticine oxidation with CYPs and peroxidases (through 13-hydroxyellipticine and/or ellipticine methylene-imine) [13] (Figure 1). Such a species was proposed to react with one of the nucleophilic centers in the deoxyguanosine residue (i.e. the 2-NH_2 group of guanine) in DNA [9,12]. The finding that the levels of this deoxyguanosine adduct significantly decreased under acidic conditions strongly supported the above suggestion. A decrease in pH leads to protonation of the NH_2 group of guanine in the DNA chain, causing a decrease in its nucleophilicity, essential for binding of ellipticine-13-ylium. The basic pH might also facilitate the second electron transfer to form the ellipticine methylene-imine (Figure 1).

The formation of the 13-hydroxyellipticine-derived DNA adduct was also significantly increased by conjugation of 13-hydroxyellipticine with PAPS or acetyl-CoA to the sulfate and acetate esters catalyzed by SULTs and NATs. This finding might have physiological significance. Some of these conjugation enzymes were found to be expressed in the target tumors for ellipticine action (e.g. human breast cancer) [18]. Therefore, by stimulation of the formation of the 13-hydroxyellipticine-derived DNA, by 13-hydroxyellipticine conjugation to sulfate and acetate esters, the pharmacological efficiency of ellipticine should be increased.

We can conclude that the results found in this work support the proposed mechanism of the reaction responsible for formation of the major deoxyguanosine adduct formed in DNA by ellipticine (Figure 1). Ellipticine is bound to deoxyguanosine by its 13-methyl group, which is activated after hydroxylation due to CYP-mediated oxidation to alcohol (13-hydroxyellipticine). Namely, this hydroxylated methyl group either alone or as the sulfate or acetate ester acts as the precursor of the vinylogous imine intermediate or the carbenium ion. Michael-type addition of the intermediates to external amino group of deoxyguanosine then leads to formation of the adduct found in DNA [3]. The study targeted to confirm this suggestion is under way in our laboratory.

ACKNOWLEDGMENT

Supported by grants 203/06/0329, MSM0021620808 and 1M0505.

REFERENCES

1 Auclair C. Multimodal action of antitumor agents on DNA: The ellipticine series. Arch Biochem Biophys 1985; **259**: 1–14.
2 Bořek-Dohalská L, Frei E., Stiborová M. DNA adduct formation by the anticancer drug ellipticine and its hydroxy derivatives in human breast adenocarcinoma MCF-7 cells. Collect Czech Chem Commun 2004; **69**: 603–615.
3 Donaghy M.J., Stanforch S.P. Nucleophilic addition of fused benzimidazole *N*-oxide. Tetrahedron 1999; **55**: 1441–1448.
4 Dračínský M., Sejbal J., Rygerová B., Stiborová M. An efficient modification of ellipticine synthesis and preparation of 13-hydroxyellipticine. Tetrahetron Lett 2007; **48**: 6893–6895.
5 Frei E, Bieler C, Arlt VM, Wiessler M, Stiborová M. Covalent binding of the anticancer drug ellipticine to DNA in V79 cells transfected with human cytochrome P450 enzymes. Biochem Pharmacol 2002; **64**: 289–295.
6 Kotrbová V., Aimová D., Březinová A., Janouchová K.., Poljaková J., Hodek P., Frei E., Stiborová M. Cytochromes P450 reconstituted with NADPH: P450 reductase mimic the activating and detoxicating metabolism of the anticancer drug ellipticine in microsomes. Neuro Endocrinol Lett 2006; **27** (Suppl. 2): 18–20.
7 Poljaková J, Dračínský M, Frei E, Hudeček J, Stiborová M. The effect of pH on peroxidase-mediated oxidation of and DNA adduct formation by ellipticine. Collect Czech Chem Commun 2006; **71:** 1169–1185.
8 Poljaková J., Frei E., Gomez J.E., Aimová D., Eckschlager T., Hraběta J., Stiborová M. DNA adduct formation by the anticancer drug ellipticine in human leukemia HL-60 and CCRF-CEM cells. Cancer Lett 2007; **252**: 270–279.
9 Stiborová M., Arlt V.M., Henderson C.J., Wolf C.R., Kotrbová V., Moserová M., Hudeček J., Phillips D.H., Frei E. Role of hepatic cytochromes P450 in bioactivation of the anticancer drug ellipticine: studies with the hepatic NADPH: cytochrome P450 reductase null mouse. Toxicol Appl Pharmacol 2008; **226:** 318–327.
10 Stiborová M, Bieler CA, Wiessler M, Frei E. The anticancer agent ellipticine on activation by cytochrome P450 forms covalent DNA adducts. Biochem Pharmacol 2001; **62**: 1675–1684.
11 Stiborová M, Breuer A, Aimová D, Stiborová-Rupertová M, Wiessler M, Frei E. DNA adduct formation by the anticancer drug ellipticine in rats determined by ^{32}P-postlabeling. Int J Cancer 2003; **107**: 885–890.
12 Stiborová M, Martínek V, Schmeiser HH, Frei E. Modulation of CYP1A1-mediated oxidation of carcinogenic azo dye Sudan I and its binding to DNA by cytochrome b_5. Neuro Endocrinol Lett 2006; **27**(Suppl. 2): 35–39.
13 Stiborová M, Poljaková J, Ryšlavá H, Dračínský M, Eckschlager T, Frei E. Mammalian peroxidases activate ellipticine to intermediates forming deoxyguanosine adducts in DNA identical to those found *in vivo* and generated from 12-hydroxyellipticine and 13-hydroxyellipticine. Int J Cancer 2007; **120**: 243–251.
14 Stiborová M., Rupertová M., Aimová D., Ryšlavá H., Frei E. Formation and persistence of DNA adducts of anticancer drug ellipticine in rats. Toxicology 2007; **236**: 50–60.
15 Stiborová M, Rupertová M, Schmeiser HH, Frei E. Molecular mechanism of antineoplastic action of an anticancer drug ellipticine. Biomed. Pap 2006; **150**: 13–23.
16 Stiborová M, Sejbal J, Bořek-Dohalská L, Aimová D, Poljaková J, Forsterová K, Rupertová M, Wiesner J, Hudeček J, Wiessler M, Frei E. The anticancer drug ellipticine forms covalent DNA adducts, mediated by human cytochromes P450, through metabolism to 13-hydroxyellipticine and ellipticine N^2-oxide. Cancer Res 2004; **64**: 8374–8380.
17 Stiborová M, Stiborová-Rupertová M, Bořek-Dohalská L, Wiessler M, Frei E. Rat microsomes activating the anticancer drug ellipticine to species covalently binding to deoxyguanosine in DNA are a suitable model mimicking ellipticine bioactivation in humans. Chem Res Toxicol 2003; **16**: 38–47.
18 Williams J.A., Phillips D.H. Mammary expression of xenobiotic metabolizing enzymes and their potential role in breast cancer. Cancer Res 2000; **60**: 4667–77.

Příloha 4

DAGMAR AIMOVÁ, JITKA POLJAKOVÁ, VĚRA KOTRBOVÁ, **MICHAELA MOSEROVÁ**, EVA FREI, VOLKER M. ARLT AND MARIE STIBOROVÁ

ELLIPTICINE AND BENZO(A)PYRENE INCREASE THEIR OWN METABOLIC ACTIVATION VIA MODULATION OF EXPRESSION AND ENZYMATIC ACTIVITY OF CYTOCHROMES P450 1A1 AND 1A2

Interdisc. Toxicol., 1(2): 160-168, 2008

Interdisc Toxicol. 2008; **Vol. 1**(2): 160–168.
Published online in SETOX (www.setox.eu/intertox)

interdisciplinary toxicology

A COMPARATIVE STUDY

Ellipticine and benzo(a)pyrene increase their own metabolic activation via modulation of expression and enzymatic activity of cytochromes P450 1A1 and 1A2

Dagmar AIMOVÁ [1], Jitka POLJAKOVÁ [1], Věra KOTRBOVÁ [1], Michaela MOSEROVÁ [1], Eva FREI [2], Volker M. ARLT [3], Marie STIBOROVÁ [1]

[1] Department of Biochemistry, Faculty of Science, Charles University, Prague, Albertov 2030, 128 40 Prague 2, CZECH REPUBLIC
[2] Division of Molecular Toxicology, German Cancer Research Center, Im Neuenheimer Feld 280, 69120 Heidelberg, GERMANY
[3] Section of Molecular Carcinogenesis, Institute of Cancer Research, Brookes Lawley Building, Sutton, Surrey SM2 5NG, UNITED KINGDOM

ITX010208A04 • Received: 4 July 2008 • Revised: 7 August 2008 • Accepted: 18 August 2008

ABSTRACT
Two compounds known to covalently bind to DNA after their activation with cytochromes P450 (CYPs), carcinogenic benzo(a)pyrene (BaP) and an antineoplastic agent ellipticine, were investigated for their potential to induce CYP and NADPH:CYP reductase (POR) enzymes in rodent livers, the main target organ for DNA adduct formation. Two animal models were used in the study: (i) rats as animals mimicking the fate of ellipticine in humans and (ii) mice, especially wild-type (WT) and hepatic POR null (HRN™) mouse lines. Ellipticine and BaP induce expression of CYP1A enzymes in livers of experimental models, which leads to increase in their enzymatic activity. In addition, both compounds are capable of generating DNA adducts, predominantly in livers of studied organisms. As determined by ^{32}P postlabelling analysis, levels of ellipticine-derived DNA adducts formed *in vivo* in the livers of HRN™ mice were reduced (by up to 65%) relative to levels in WT mice, indicating that POR mediated CYP enzyme activity is important for the activation of ellipticine. In contrast to these results, 6.4 fold higher DNA binding of BaP was observed in the livers of HRN™ mice than in WT mice. This finding suggests a detoxication role of CYP1A in BaP metabolism *in vivo*. In *in vitro* experiments, DNA adduct formation in calf thymus DNA was up to 25 fold higher in incubations of ellipticine or BaP with microsomes from pretreated animals than with controls. This stimulation effect was attributed to induction of CYP1A1/2 enzymes, which are responsible for oxidative activation of both compounds to the metabolites generating major DNA adducts *in vitro*. Taken together, these results demonstrate that by inducing CYP1A1/2, ellipticine and BaP modulate their own enzymatic metabolic activation and detoxication, thereby modulating their either pharmacological (ellipticine) and/or genotoxic potential (both compounds).

KEY WORDS: benzo(a)pyrene; ellipticine; induction; cytochromes P450; NADPH:cytochrome P450 reductase; HRN™ mice

Introduction

Ellipticine and benzo[*a*]pyrene (BaP) are compounds exhibiting significant biological activities. Ellipticine is an efficient anticancer agent (for a summary, see Stiborová *et al.*, 2006b), while BaP is a strong carcinogen (for a summary, see Arlt *et al.*, 2008). Therefore, both two compounds were employed by us for studies concerning their phatmacological and toxicological effects.

Ellipticine, an alkaloid isolated from *Apocyanaceae* plants, and its derivatives exhibits significant antitumor and anti-HIV activities, characterized by high efficiencies against several types of cancer and rather limited toxic side effects, including complete lack of hematological toxicity. Nevertheless, ellipticines are potent mutagens. Several mechanisms of their antitumor, mutagenic and cytotoxic activities have been hitherto suggested: (i) intercalation into DNA; (ii) inhibition of DNA topoisomerase II activity; (iii) selective inhibition of p53 protein phosphorylation; (iv) disruption of the energy balance of cells by uncoupling mitochondrial oxidative phosphorylation (for a summary, see Stiborová *et al.*, 2001; 2006b). Recently, we have shown that ellipticine also binds covalently to DNA *in vitro* and *in vivo,* after being enzymatically activated with cytochromes

Correspondence address:
Prof. Marie Stiborová, DrSc.
Department of Biochemistry, Faculty of Science, Charles University, Prague, Albertov 2030, 128 40 Prague 2, Czech Republic
E-MAIL: stiborov@natur.cuni.cz

P450 (CYP) (Figure 1) or peroxidases, suggesting a third possible mechanism of action (Stiborová *et al.*, 2001; 2003a,b; 2004; 2007a).

On the basis of *in vitro* studies, human and rat CYPs of 1A and 3A subfamilies seem to be the predominant enzymes oxidizing ellipticine either to metabolites that are excreted (7- or 9-hydroxyellipticine) or form DNA adducts (12- or 13-hydroxy-ellipticine) (Stiborová *et al.*, 2001; 2003b; 2004; 2006; Kotrbová *et al.*, 2006). Besides these CYPs, peroxidases such as mammalian cyclooxygenases (COX-1 and -2), lactoperoxidase and myeloperoxidase, efficiently generate the same ellipticine-derived DNA adducts *in vitro* (Stiborová *et al.*, 2007a; Poljaková *et al.*, 2006). Identical DNA adducts were also detected in cells in culture, in which both CYPs and peroxidases are expressed, such as human breast adenocarcinoma MCF-7 cells (Bořek-Dohalská *et al.*, 2004), leukemia HL-60 and CCRF-CEM cells (Poljaková *et al.*, 2007) and V79 Chinese hamster lung fibroblasts transfected with human CYP3A4, 1A1 and 1A2 (Frei *et al.*, 2002). After *i.p.* administration of ellipticine, the ellipticine-DNA adduct levels seem to be related to CYP3A1 and 1A content in different tissues of rat, but the real impact of CYPs or peroxidases in this process could not be still exactly evaluated (Stiborová *et al.*, 2003a, 2007b).

BaP, as the second model compound in this comparative study is, similarly to the other polycyclic aromatic hydrocarbons (PAHs), mutagenic and carcinogenic (IARC, 1983; Phillips 1999, 2002). PAHs are produced mainly by incomplete combustion or pyrolysis of organic matter and are ubiquitous in the environment, leading to measurable background levels of exposure in the general population (IARC, 1983). Beside the inhalation of polluted air, the main routes of exposure are through tobacco smoke, diet (Phillips 1999, 2002) and occupational exposition throughout e.g. coal, coke or coal-tar processing and use of coal-tar products (IARC, 1983). Prior to the reaction with DNA, BaP analogously to ellipticine requires metabolic activation (Figure 2), which is an essential step in the mechanism by which BaP exerts its genotoxic effects. CYP1A1 and CYP1B1 are widely accepted to be the most important enzymes in the metabolic activation of BaP (Baird *et al.*, 2005). However, current studies show that BaP-induced DNA damage was increased in mice lacking CYP1A1, indicating that *in vivo* the CYP1A1 enzyme plays a detoxification role, and protects mice against BaP toxicity (Uno *et al.*, 2004, 2006). PAHs affect the expression of numerous enzymes involved in metabolism of xenobiotics (including CYP1A1) mainly *via* the aromatic hydrocarbon receptor (AhR). AhR-dependent inducibility was correlated to the predisposion to some types of cancer (Kouri *et al.*, 1973).

The detailed knowledge on the role of CYP enzymes in activation and/or detoxication of BaP and ellipticine and that on their induction mediated by these xenobiotics, is crucial for the possibility to modify their carcinogenic and/or the therapeutic efficiency. Therefore, this field was extensively investigated in our laboratory. To investigate the real role of CYPs in metabolism of both compounds, we have used several animal models, such as rats, rabbits and/or mice in our previous studies (Stiborová *et al.*, 2001; 2003a; b; 2004; 2006; 2007b; 2008; Kotrbová *et al.*, 2006; Arlt *et al.*, 2008). In the case of mice, the HRN™ (Hepatic Cytochrome P450 Reductase Null) mice, the mouse line lacking the hepatic NADPH:CYP oxidoreductase (POR), the unique electron donor to CYPs, which results in the loss of essentially all hepatic CYP function (Henderson *et al.*, 2003, 2006), was utilized (Stiborová *et al.*, 2008; Arlt *et al.*, 2008).

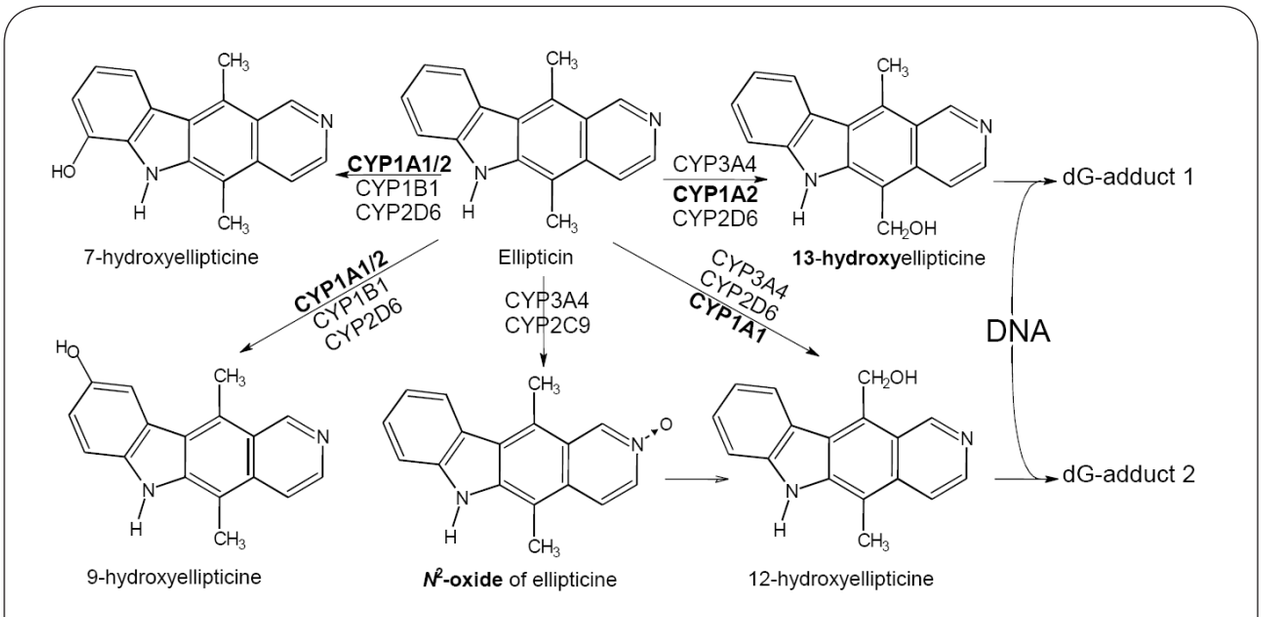

Figure 1. Metabolism and activation of ellipticine (5,11-dimethyl-6*H*-pyrido[4,3-*b*]carbazole) by cytochromes P450.

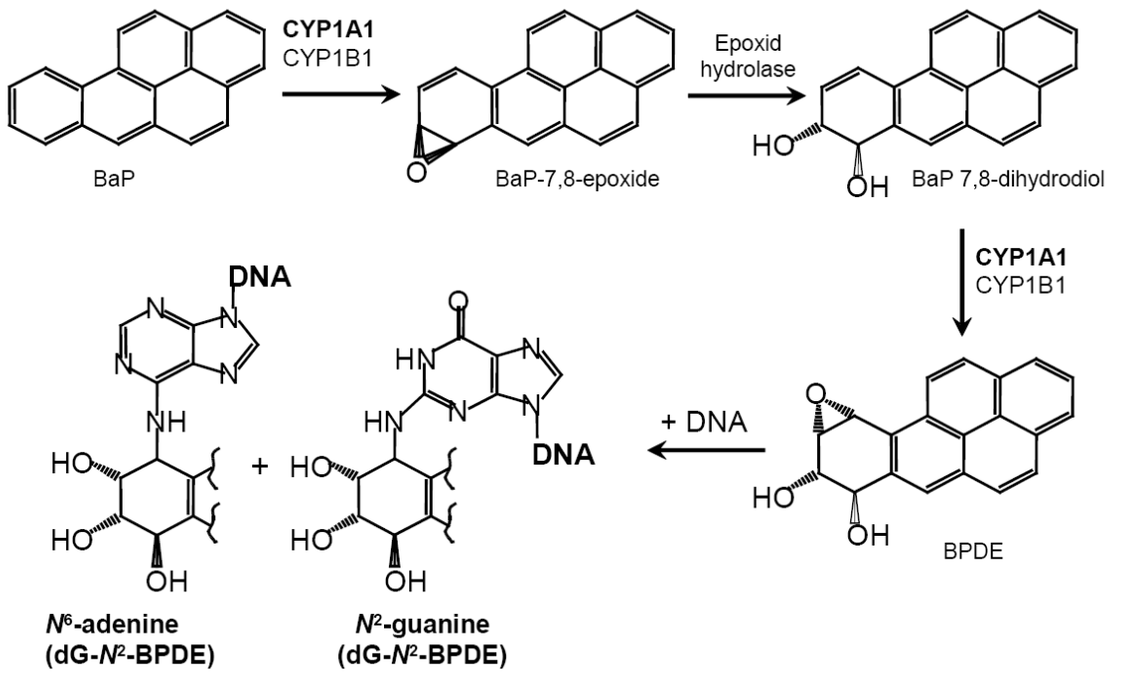

Figure 2. Metabolic activation and DNA adduct formation by benzo(a)pyrene: The typical 3-step activation process with contribution of CYP1A1 or CYP1B1 and epoxide hydrolase leads to the formation of the ultimately reactive species, benzo[a]pyrene-7,8-dihydrodiol-9,10-epoxide (BPDE) that can react with DNA, forming adducts preferentially at guanine residues.

Here, we summarize the results obtained with rats and mice previously, and present novel data obtained with these animal models. Such a study is necessary to evaluate results found till the present time and to suggest which further studies are necessary to improve our knowledge in this field.

Material and methods

Animal models

The study was conducted in accordance with the Regulations for the Care and Use of Laboratory Animals (311/1997, Ministry of Agriculture, Czech Republic), which complies with Declaration of Helsinki. Rats, the animal model found to be suitable to mimic the fate of ellipticine in humans (Stiborová *et al.*, 2003a; 2006), and two mouse lines, namely,.(i) „Hepatic Reductase Null" (HRN™) mice based on a C57BL/6 background (CXR Bioscience Ltd, Dundee, UK), in which NADPH:cytochrome P450 reductase (POR) is specifically deleted in the liver (*Por*$^{lox/lox}$ + *Cre*^{ALB}) (Henderson *et al.*, 2003, 2006) and (ii) mice homozygous for loxP sites at the Por locus (Por$^{lox/lox}$) as wild-type (WT) mice, were used in this study.

Treatment of animals with ellipticine and benzo(a)pyrene

Male and female Wistar rats (~100 g) were treated with a single dose of 4, 40 or 80 mg/kg body weight (n = 3) of ellipticine by intraperitoneal injection as described (Aimová *et al.*, 2007). Ellipticine was dissolved in sunflower oil/dimethyl sulphoxide (1:1, v/v) at a concentration of 6 mg/ml, control animals (n = 3) received solvent only. The doses of ellipticine used for the treatment of rats are in the range of dosage in human therapy (80–100 mg/m^2).

Groups (n = 3) of female HRN™ and WT mice (3 months old, 25–30 g) were treated intraperitoneally with a single dose of 10 mg ellipticine per kg body weight as described previously (Stiborová *et al.*, 2008). Ellipticine was administered as 10 mg/ml solution in distilled 1% acetic acid, control animals (n = 3) received solvent only.

To evaluate the BaP-mediated induction of CYP1A, groups (n = 3) of HRN™ and WT female mice were treated with 125 mg BaP per kg body weight once daily for five days by intraperitoneal injection. BaP was dissolved in corn-oil at a concentration of 12.5 mg/ml, control animals (n = 3) received solvent only (Arlt *et al.*, 2008).

Preparation of microsomes and assays

Microsomes were isolated from pooled rodent livers as described (Stiborová *et al.*, 2003b). Protein concentrations in the microsomal fractions (bicinchoninic acid protein assay with bovine serum albumin as a standard), the activities of hepatic microsomal CYP1A1/2 (7-ethoxyresorufin *O*-deethylation, EROD) and POR (using cytochrome c) as well as the protein levels of these enzymes (Western Blot) were determined as described previously (Stiborová *et al.*, 2003a,b, 2005).

Oxidation of ellipticine by hepatic microsomes. Incubation mixtures contained 50 mM potassium phosphate

buffer (*pH* 7.4), NADPH-generating system (1 mM $NADP^+$, 10 mM D-glucose 6-phosphate, 1 U/ml D-glucose 6-phosphate dehydrogenase), 0.2 mg microsomal protein, 10 μM ellipticine (dissolved in 5 μl methanol) in a final volume of 500 μl. The reaction was initiated by adding the substrate. After incubation in open glass tubes (37°C, 20 min) the reaction was stopped by adding 100 μl of 2 M NaOH, 5 μl of 1 mM phenacetine in methanol was added as an internal standard. Ellipticine metabolites were extracted twice with ethyl acetate (2 × 1 ml) and analyzed by HPLC as described (Stiborová *et al.*, 2006; 200ß).

Activation of ellipticine or BaP by hepatic microsomes

Incubation mixtures (final volume of 750 μl) used to asses DNA adduct formation consisted of 50 mM potassium phosphate buffer (pH 7.4), 1 mM NADPH, 0.5 mg of microsomal proteins and 0.5 mg of calf thymus DNA. Incubations were also carried out in the presence of a COX cofactor, 0.1 mM arachidonic acid instead of NADPH, and additionally 5 mM magnesium chloride. The reaction was initiated by adding 0.1 mM ellipticine (dissolved in 7.5 μl methanol) or 0.1 mM BaP (dissolved in 7.5 μl dimethyl sulphoxide). Incubations at 37°C were carried out for 30 or 90 min with ellipticine or BaP, respectivelly. DNA was isolated from the residual water phase by the phenol/chloroform extraction method as described (Stiborová *et al.*, 2001).

Inhibition studies

The following chemicals were used to inhibit the activation of ellipticine and BaP by mouse hepatic microsomes: α-naphthoflavone (α-NF), which inhibits CYP1A1 and 1A2; indomethacin, a selective inhibitor of COX; α-lipoic acid (α-LA), which inhibits POR; ellipticine, frequently utilized as competitive inhibitor of CYP1A1 enzyme. Inhibitors were added to incubation mixture in 7.5 μl of methanol to yield final concentrations of 0.1 mM and pre-incubated at 37 °C for 10 min with NAD*PH* prior to adding substrate (ellipticine or BaP) and then incubated for as described above. After the incubation, DNA was isolated as described above.

Measurement of DNA adducts

^{32}P-postlabeling analysis with nuclease P1 enrichment, thin-layer chromatography (TLC) and high performance liquid chromatography (HPLC) of ^{32}P-labelled 3'5'-deoxyribonucleoside bisphosphate adducts with ellipticine were done as reported recently (Stiborová *et al.*, 2001; 2003a; 2004; 2007a). DNA adducts formed by BaP were analyzed

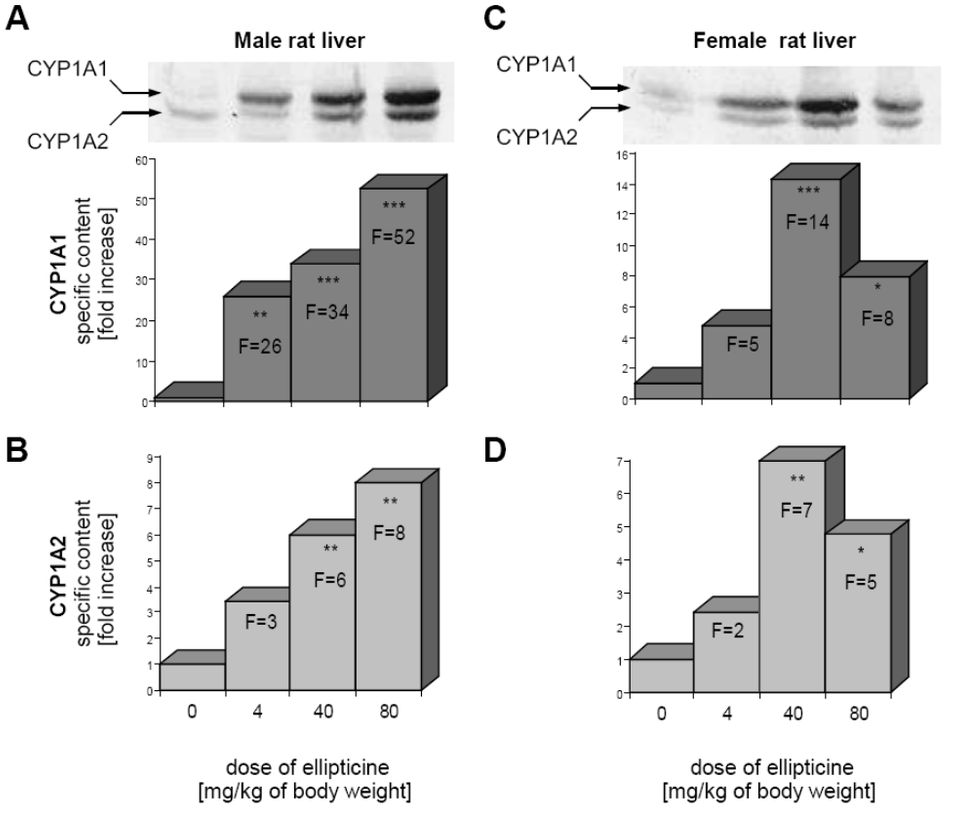

Figure 3. Induction of CYP1A1 (**A,C**) and 1A2 (**B,D**) proteins in livers of male (**A,B**) and female (**C,D**) rats, uninduced or treated with 4, 40 or 80 mg of ellipticine per kg of body weight. Inset in A and C: immunoblots of microsomal CYP1A1 and 1A2 from untreated and ellipticine-treated male and female rats, respectively, stained with antibody against rat CYP1A1. Mean values shown in figure represent results obtained from livers of three rats (n=3), SD < 15%. Values significantly different from the control: *p<0.05, **p<0.01, ***p<0.001.

analogously, using the ^{32}P-postlabeling technique as described previously (Arlt *et al*., 2008).

Results

Induction of hepatic CYP1A by ellipticine and BaP

Ellipticine and BaP induced expression of CYP1A1 and 1A2 proteins, which leads to an increase their enzymatic activities in livers of animal models used in the experiments (rats for ellipticine and mice for BaP) (Figures 3 and 4).

As shown in Figure 3, the induction of CYP1A by ellipticine was dose-dependent. The increase in expression of CYP1A proteins correlated with that in specific CYP1A-mediated activity, EROD (Table 1).

In the case of BaP, mouse models, HRN™ and its parental WT-line, were utilized for the induction experiments. HRN™ mice were found to be more susceptible to BaP-mediated CYP1A induction than the WT mouse line (Figure 4A). Using this model, lacking hepatic POR, we also evaluated whether expression of this enzyme is influenced by treating animals with BaP. Treatment of mice with BaP led to a moderate increase in expression of hepatic POR in both WT (1.2-fold increase) and HRN™ mice (1.4-fold increase). In spite of POR deficiency, CYP1A activity (EROD) was restored by BaP treatment in HRN™ mice, representing the 73-fold increase in EROD activity in microsomes of uninduced WT mice and 30 % of this activity in BaP-induced WT mice (Figure 4B).

DNA adduct formation *in vivo*

In further part of the study, we evaluated the potential of ellipticine and BaP to induce DNA adduct formation *in vivo*. Mice were used as models in these experiments. Treatment of individual mouse strains with ellipticine and BaP resulted in DNA adduct formation (Figure 5–7). The livers of all animal models were the major target organ for DNA adduct formation. Comparative analyses on TLC and HPLC have shown that DNA adduct formation *in vivo* proceeds *via* the reactive metabolite BPDE bound to the N^2 position of guanine (dG-N^2-BPDE) for BaP (Figures 2 and 6) and *via* 13-hydroxy- and 12-hydroxyellipticine in the case of the two major ellipticine-derived DNA adducts (spots 1 and 2 in Figures 1 and 5).

The experiments employing the mouse models helped us to improve our knowledge on the efficiency of CYPs to activate ellipticine and BaP. Levels of ellipticine-derived adducts in livers of HRN™ mice (Figure 5E) were reduced (by up to

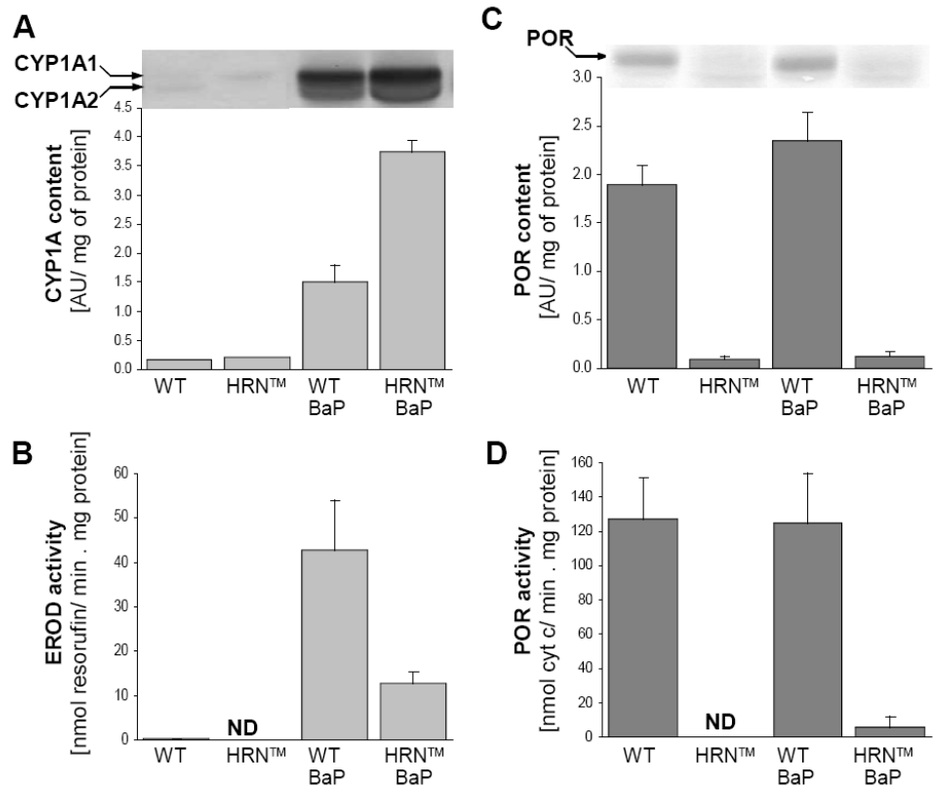

Figure 4. Induction of CYP1A (**A,B**) and POR (**C,D**) protein levels (**A,C**) and activities (**B,D**) in livers of female mice with deleted (HRN™) or intact (WT) liver POR, uninduced or treated (i.p.) with 5 × 125 mg of BaP per kg of body weight. Inset in A: immunoblots of microsomal CYP1A1/2 stained with chicken antibody against rat CYP1A1. Inset in C: immunoblots of microsomal POR stained with chicken antibody against rabbit POR. Microsomes were pooled from livers of 3 animals. Mean and SD evaluated from three separate experiments (n=3). ND = not detectable at used conditions.

65%) relative to levels in WT mice (Figure 5D), indicating that POR-mediated CYP enzyme activity is important for the oxidative activation of ellipticine to metabolites generating these adducts.

In contrast to these results, the highest DNA binding of BaP was observed in livers of HRN™ mice (Figure 6A) which was 6.4-fold ($p<0.01$) higher than DNA binding in WT mice (Figure 6B). This unexpectable finding indicates increasing the CYP-mediated activation of BaP by lack of POR in the liver.

Table 1. Specific CYP1A activity (EROD) in hepatic microsomes of control and ellipticine-treated rats.

CYP activity	Control rats		Ellipticine-treated rats	
	Male	Female	Male	Female
EROD	80.7 ± 2.0	225.8 ± 50.5	551.4 ± 92.2	1737.5 ± 161.3

[a] Each value (pmol of reaction product/min/nmol CYP) represents the mean ± standard deviation of data from two rats in two separate assays (n=4).

Activation of ellipticine and BaP by hepatic microsomes

In order to further investigate the participation of CYPs in activation of ellipticine and BaP and which of these enzymes play the major role, the *in vitro* experiments were carried out. First, incubations of DNA with BaP and/or ellipticine with microsomes isolated from livers of HRN™ and WT mice, untreated or treated with BaP, were performed. In all cases, the patterns of DNA adducts formed by ellipticine and BaP in these experiments were essentially the same as those found *in vivo* (Figures 5 and 6), generated by the pathways shown in Figures 1 and 2. The identity of adducts formed by both compounds *in vitro* with those formed *in vivo* was proved using the TLC and HPLC-cochromatography (data not shown).

Hepatic microsomes isolated from animals treated with ellipticine or BaP were always more effective to form ellipticine- and BaP-derived DNA adducts (Figures 5 and 7) than microsomes from untreated animals. A decrease in levels of ellipticine-derived adducts formed by microsomes from HRN™ mice compared with WT-mice (Figure 7C–D) correlated with almost 2-fold lower levels of 13-hydroxy- and 12-hydroxyellipticine, the metabolites generating the ellipticine-DNA adducts, formed by these microsomes (Stiborová *et al*., 2008).

NADPH-dependent activation of BaP was even 4- to 7-fold lower in HRN™ compared to WT mouse microsomes (Figure 7A–B). The study investigating the pattern of BaP metabolites formed by microsomes from livers of all mouse groups (control HRN™ and WT-mice as well as these mice treated with BaP), which might explain this feature is under way in our laboratory. Preliminary results suggest that the treatment of WT mice with BaP influenced only the relative metabolites ratio instead of the total efficiency of BaP metabolite formation.

In all model systems, the use of POR-inhibitor (α-lipoic acid), CYP1A-inhibitors (α-naphthoflavone, ellipticine) and a CYP3A-inhibitor (ketoconazole) decreased the DNA-adduct formation by both compounds (Figure 7). These results suggest that even very low levels of the POR enzyme in livers of HRN™ mice are still sufficient to mediate CYP-catalyzed activation reactions.

In order to determine which CYPs and/or other enzymes are responsible for DNA adduct formation by both compounds, modulation of microsome-mediated activation with cofactors and inhibitors of individual enzymes was utilized. Addition of NADH, a cofactor of microsomal NADH:cytochrome b_5 reductase, acting as second electron donor for CYP-dependent systems, lowered the difference between HRN™ and WT microsomal BaP-activation (Figure 7A–B). Arachidonic acid (AA), a cofactor of COX-dependent oxidation, was effective to activate ellipticine to species forming DNA adducts (Figure 7C–D), but not to mediate the BaP-DNA adduct formation (Figure 7A–B). On the contrary, an inhibitor of COX, indomethacin (IM) decreases BaP activation in incubations with hepatic microsomes from BaP-treated HRN™ mice, by 30–40% (Figure7B). These results may indicate the participation of COX in activation of both compounds, but with lower efficiency than CYPs.

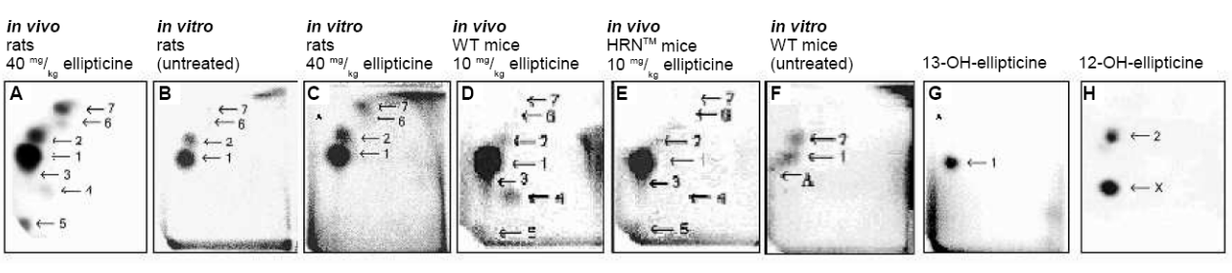

Figure 5. Autoradiographic profile of ellipticine-derived DNA adducts:
- *in vivo* in liver DNA of ellipticine-treated rats (**A**); HRN™ (**D**) and WT (**E**) mice.
- *in vitro* in calf thymus DNA after ellipticine activation with hepatic microsomes of untreated (**B**) and ellipticine-treated (**C**) male rats and wild-type mice (**F**)
- *in vitro* in calf thymus DNA reacted directly with ellipticine metabolites 13-hydroxyellipticine (**G**) or 12-hydroxyellipticine (**H**) (without enzymatic activation). Analyses were performed by the nuclease P1 version of the ^{32}P-postlabelling assay.

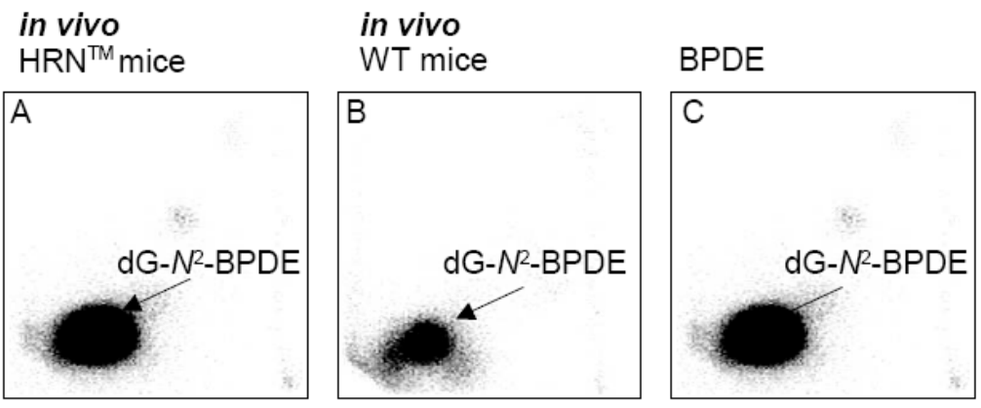

Figure 6. Autoradiographic profiles of BaP-derived DNA adducts *in vivo* in liver DNA of HRN™ (**A**) and WT (**B**) mice treated with 5 times 125 mg of BaP/kg body weight and *in vitro* in salmon testis DNA modified with BPDE (**C**) (without enzymatic activation). Analyses were performed by the nuclease P1 version of the ^{32}P-postlabelling assay.

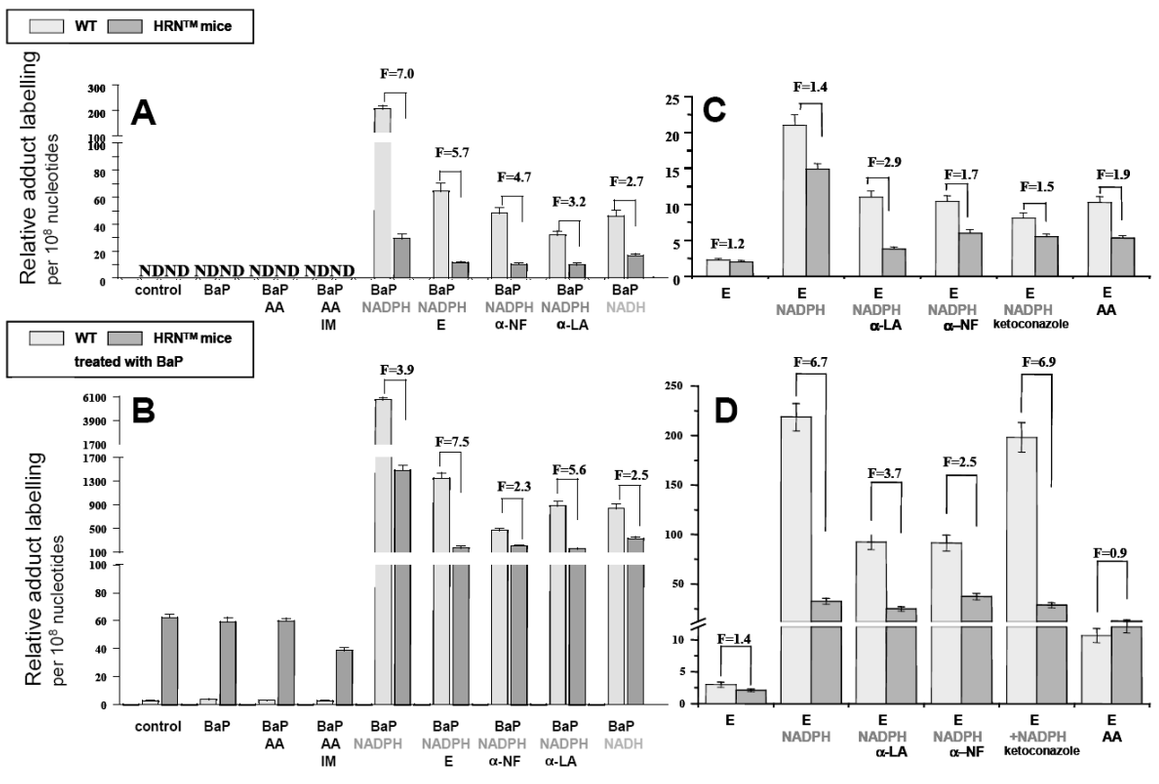

Figure 7. DNA adduct formation after activation of BaP (**A,B**) or ellipticine (**C,D**) with microsomes from livers of HRN™ and WT mice, untreated (**A,C**), or treated with 5×125 mg/kg BaP (**B,D**). Each value represents the mean of two separate analyses (n=2). F = fold increase, WT mice: HRN™ mice; ND = not detected. Control = microsomes + DNA without cofactor; AA = arachidonic acid; IM = indomethacin; E = ellipticine; α-NF = α-naphthoflavone; α-LA = α-lipoic acid.

Discussion

As shown in several studies published previously, ellipticine and BaP are two xenobiotics that react with DNA forming covalent DNA adducts (for a summary, see Stiborová *et al.*, 2006b; Arlt *et al.*, 2008). This genotoxic effect is mediated by their CYP-mediated metabolism. Although the CYP enzymes activating ellipticine and BaP to species binding to DNA *in vitro* have already been identified (Baird *et al.*, 2005; Stiborová *et al.*, 2001; 2003a; 2004; 2006a; 2008; Kotrbová *et al.*, 2006; Arlt *et al.*, 2008), the knowledge on the real impact of these CYPs on the activation of these compounds *in vivo* is limited. Likewise, the effects of repeated exposure of organisms to these compounds on enzyme-mediated activation process are scarce.

To evaluate the contribution and importance of hepatic CYP enzymes to the activation of ellipticine and BaP *in vivo,* we have used in our former and present studies the rats and especially the HRN™ mice, lacking POR and thus also POR-mediated CYP enzyme activity in the liver (Henderson *et al*., 2003; 2006), as model organisms. The use of the HRN™ mouse model has already contributed to resolve the *in vivo* enzymatic activation of several environmental toxicants, including carcinogenic 3-nitrobenzanthrone, activated by cytosolic nitroreductases rather than microsomal POR, and its reductive metabolite 3-aminobenzanthrone (Svobodová *et al*., 2007), whose activation is CYP-dependent (Arlt *et al*., 2003, 2004, 2005, 2006).

Ellipticine and BaP significantly induced expressions of CYP1A1 and 1A2 proteins as well as their enzymatic activity such as EROD in rodent livers. The CYP1A induction resulted in a significant increase in levels of ellipticine- and BaP-derived DNA adducts *in vitro*, in incubations of ellipticine or BaP with microsomes from rats treated with these compounds than in incubations with control microsomes. This is an important finding, because CYP1A enzymes are essential for ellipticine and BaP metabolism. Indeed, the importance of POR-mediated CYP1A1 activation of both compounds *in vitro* was confirmed by inhibition studies using a specific POR inhibitor, α-lipoic acid, and a CYP1A inhibitor, α-naphtoflavone.

Analogously to the results found *in vitro*, the levels of two major DNA adducts in animals treated with ellipticine were significantly decreased in liver DNA of HRN™ mice, confirming the importance of CYP enzymes in ellipticine activation in this organ *in vivo*. Inhibition of NADPH-dependent ellipticine activation in hepatic microsomes of HRN™ and WT mice by α-NF and ketoconazole suggests that CYPs of 1A and 3A subfamilies play a major role in this process in mice livers, analogously to human and rat livers (Stiborová *et al*., 2001; 2003a, b). Nevertheless, the reduction of DNA adduct formation in the liver of HRN™ mice was not absolute, being ~65%. Likewise, the decrease in levels of these two ellipticine-DNA adducts in hepatic microsomes of HRN™ mice caused by inhibitors of POR and CYPs was between 40–65%. These results suggest that other enzymes may also activate ellipticine in mice livers. A potential of arachidonic acid, a cofactor of COX enzymes, to increase the formation of these adducts in mice hepatic microsomes *in vitro* indicate that COX might be one of such enzymes.

On the contrary, BaP-induced DNA adduct formation *in vivo* was significantly increased in liver of HRN™ compared to WT mice, indicating that the real function of POR-mediated CYPs reactions is the BaP detoxification. Taken our results together with those from the CYP1-deletion studies (Uno *et al*., 2004, 2006), there is a remarkable discrepancy between the *in vivo* DNA adduct levels and *in vitro* BaP activation, which is still very difficult to explain. Although hepatic CYP enzyme activity has been essentially inactivated by the conditional deletion of hepatic POR, in non-parenchymal liver cells, the POR deletion may be incomplete. This residual POR activity, in combination with more pronounced induction of CYP enzymes (and probably also by induction of POR) in livers of HRN™ mice liver may explain these *in vitro* findings. Another explanation could be the induction of other metabolizing enzymes.

Taken together, these results show evidence of the crucial role of CYP1A enzymes in ellipticine and BaP genotoxic effect *in vivo.* By inducing CYP1A1/2, both compounds modulate their either pharmacological (ellipticine) and/or genotoxic potential (both chemicals); ellipticine increases its own metabolism leading to enhanced formation of reactive species forming DNA adducts and BaP enhances its detoxification process.

REFERENCES

Aimová D, Svobodová L, Kotrbová V, Mrázová B, Hodek P, Hudecek J, Václavíková R, Frei E, Stiborová M (2007) The anticancer drug ellipticine is a potent inducer of rat cytochromes P450 1A1 and 1A2, thereby modulating its own metabolism. *Drug Metab Dispos* **35**: 1926–34.

Arlt VM, Henderson CJ, Wolf CR, Schmeiser HH, Phillips DH, Stiborova M (2006) Bioactivation of 3-aminobenzanthrone, a human metabolite of the environmental pollutant 3-nitrobenzanthrone: evidence for DNA adduct formation mediated by cytochrome P450 enzymes and peroxidases. *Cancer Lett* **234**: 220–31.

Arlt VM, Hewer A, Sorg BL, Schmeiser HH, Phillips DH, Stiborova M (2004) 3-Aminobenzanthrone, a human metabolite of the environmental pollutant 3-nitrobenzanthrone, forms DNA adducts after metabolic activation by human and rat liver microsomes: evidence for activation by cytochrome P450 1A1 and P450 1A2. *Chem Res Toxicol* **17**: 1092–101.

Arlt VM, Stiborova M, Henderson CJ, Osborne MR, Bieler CA, Frei E, Martinek V, Sopko B, Wolf CR, Schmeiser HH, Phillips DH (2005) Environmental pollutant and potent mutagen 3-nitrobenzanthrone forms DNA adducts after reduction by NAD(P)H: quinone oxidoreductase and conjugation by acetyltransferases and sulfotransferases in human hepatic cytosols. *Cancer Res* **65**: 2644–52.

Arlt VM, Stiborová M, Henderson CJ, Thiemann M, Frei E, Aimová D, Singh R, Gamboa da Costa G, Schmitz OJ, Farmer PB, Wolf CR, Phillips DH (2008) Metabolic activation of benzo[a]pyrene in vitro by hepatic cytochrome P450 contrasts with detoxification in vivo: experiments with hepatic cytochrome P450 reductase null mice. *Carcinogenesis* **29**: 656–65.

Arlt VM, Stiborova M, Hewer A, Schmeiser HH, Phillips DH (2003) Human enzymes involved in the metabolic activation of the environmental contaminant 3-nitrobenzanthrone: evidence for reductive activation by human NADPH: cytochrome P450 reductase. *Cancer Res* **63**: 2752–61.

Baird WM, Hooven LA, Mahadevan B (2005) Carcinogenic polycyclic aromatic hydrocarbon-DNA adducts and mechanism of action. *Environ Mol Mutagen* **45**: 106–14.

Bořek-Dohalská L, Frei E, Stiborová M (2004) DNA adduct formation by the anticancer drug ellipticine and its hydroxy derivatives in human breast adenocarcinoma MCF-7 cells. *Collect Czech Chem Commun* **69**: 603–615.

Frei E, Bieler CA, Arlt VM, Wiessler M, Stiborová M (2002) Covalent binding of the anticancer drug ellipticine to DNA in V79 cells transfected with human cytochrome P450 enzymes. *Biochem Pharmacol* **64**: 289–95.

Henderson CJ, Otto DM, Carrie D, Magnuson MA, McLaren AW, Rosewell I, Wolf CR (2003) Inactivation of the hepatic cytochrome P450 system by conditional deletion of hepatic cytochrome P450 reductase. *J Biol Chem* **278**: 13480–6.

Henderson CJ, Pass GJ, Wolf CR (2006) The hepatic cytochrome P450 reductase null mouse as a tool to identify a successful candidate entity. *Toxicology letters* **162**: 111–7.

IARC Monogr Eval Carcinog Risk Chem Hum (1983) Polynuclear Aromatic Compounds **32**, 211.

Kotrbová V, Aimová D, Březinová A, Janouchová K, Poljaková J, Hodek P, Frei E, Stiborová M (2006) Cytochromes P450 reconstituted with NADPH: P450 reductase mimic the activating and detoxicating metabolism of the anticancer drug ellipticine in microsomes. *Neuro Endocrinol Lett* **27**(Suppl. 2): 18–20.

Kouri RE, Salerno RA, Whitmire CE (1973) Relationships between aryl hydrocarbon hydroxylase inducibility and sensitivity to chemically induced subcutaneous sarcomas in various strains of mice. *J Natl Cancer Inst* **50**: 363–8.

Phillips DH (1999) Polycyclic aromatic hydrocarbons in the diet. *Mutat Res* **443**: 139–47.

Phillips DH (2002) Smoking-related DNA and protein adducts in human tissues *Carcinogenesis* **23**: 1979–2004.

Poljaková J, Dračínský M, Frei E, Hudeček J Stiborová, M (2006) The effect of *pH* on peroxidase-mediated oxidation of and DNA-adduct formation by ellipticine. *Collect. Czech. Chem. Commun.* **71**: 1169–1185.

Poljaková J, Frei E, Gomez JE, Aimová D, Eckschlager T, Hraběta J, Stiborová M (2007) DNA adduct formation by the anticancer drug ellipticine in human leukemia HL-60 and CCRF-CEM cells. *Cancer Lett* **252**: 270–9.

Stiborová M, Arlt VM, Henderson CJ, Wolf CR, Kotrbová V, Moserová M, Hudecek J, Phillips DH, Frei E.(2008) Role of hepatic cytochromes P450 in bioactivation of the anticancer drug ellipticine: studies with the hepatic NADPH: cytochrome P450 reductase null mouse. *Toxicol Appl Pharmacol* **226**: 318–27.

Stiborová M, Bieler CA, Wiessler M, Frei E (2001) The anticancer agent ellipticine on activation by cytochrome P450 forms covalent DNA adducts. *Biochem Pharmacol* **62**: 675–84.

Stiborová M, Bořek-Dohalská L, Aimová D, Kotrbová V, Kukačková K, Janouchová K, Rupertová M, Ryšlavá H, Hudeček J, Frei E (2006a) Oxidation pattern of the anticancer drug ellipticine by hepatic microsomes – Similarity between human and rat systems. *Gen Physiol Biophys* **25**: 245–261.

Stiborová M, Breuer A, Aimová D, Stiborová-Rupertová M, Wiessler M, Frei E (2003a) DNA adduct formation by the anticancer drug ellipticine in rats determined by ^{32}P-postlabeling. *Int J Cancer* **107**: 885–890.

Stiborová M, Martínek V, Rýdlová H, Koblas T, Hodek P (2005) Expression of cytochrome P450 1A1 and its contribution to oxidation of a potential human carcinogen 1-phenylazo-2-naphthol (Sudan I) in human livers. *Cancer Lett* **220**: 145–154.

Stiborová M, Poljaková J, Ryšlavá H, Dračínský M, Eckschlager T, Frei E (2007a) Mammalian peroxidases activate anticancer drug ellipticine to intermediates forming deoxyguanosine adducts in DNA identical to those found *in vivo* and generated from 12-hydroxyellipticine and 13-hydroxyellipticine. *Int J Cancer* **120**: 243–251.

Stiborová M, Rupertová M, Aimová D, Ryšlavá H, Frei E (2007b) Formation and persistence of DNA adducts of anticancer drug ellipticine in rats. *Toxicology* **236**: 50–60.

Stiborová M, Rupertová M, Schmeiser HH, Frei E (2006b) Molecular mechanism of antineoplastic action of an anticancer drug ellipticine. *Biomed Pap* **150**: 13–23.

Stiborová M, Sejbal J, Bořek-Dohalská L, Aimová D, Poljaková J, Forsterová K, Rupertová M, Wiesner J, Hudeček J, Wiessler M, Frei E (2004) The anticancer drug ellipticine forms covalent DNA adducts, mediated by human cytochromes P450, through metabolism to 13-hydroxyellipticine and ellipticine N^2-oxide. *Cancer Res* **64**: 8374–8380.

Stiborová M, Stiborová-Rupertová M, Bořek-Dohalská L, Wiessler M, Frei E (2003b) Rat microsomes activating the anticancer drug ellipticine to species covalently binding to deoxyguanosine in DNA are a suitable model mimicking ellipticine bioactivation in humans. *Chem Res Toxicol* **16**: 38–47.

Svobodová M Šístková J, Dračínská H, Hudeček J, Hodek P, Schmeiser HH, Arlt VM, Frei E, Stiborová M (2007) Reductive activation of environmental pollutants 3-nitrobenzanthrone and 2-nitrobenzanthrone. *Che. Listy* **100**: s277–s279.

Uno S, Dalton TP, Derkenne S, Curran CP, Miller ML, Shertzer HG, Nebert DW (2004) Oral exposure to benzo[a]pyrene in the mouse: detoxication by inducible cytochrome P450 is more important than metabolic activation. *Mol Pharmacol* **65**: 1225–37.

Uno S, Dalton TP, Dragin N, Curran CP, Derkenne S, Miller ML, Shertzer HG, Gonzalez FJ, Nebert DW (2006) Oral benzo[a]pyrene in Cyp1 knockout mouse lines: CYP1A1 important in detoxication, CYP1B1 metabolism required for immune damage independent of total-body burden and clearance rate. *Mol Pharmacol* **69**: 1103–14.

Příloha 5

MICHAELA MOSEROVÁ, VĚRA KOTRBOVÁ, MIROSLAV ŠULC, EVA FREI, MARIE STIBOROVÁ

ANALYSIS OF BENZO[*A*]PYRENE METABOLITES FORMED BY RAT HEPATIC MICROSOMES USING HIGH PRESSURE LIQUID CHROMATOGRAPHY: OPTIMIZATION OF THE METHOD.

Interdisc. Toxicol., 2(4): 101-106, 2009

Interdisc Toxicol. 2009; **Vol. 2**(4): 101–106.
doi:

Published online in:
www.setox.eu/intertox & www.versita.com/science/medicine/it/

Interdisciplinary Toxicology

ORIGINAL ARTICLE

Analysis of benzo[*a*]pyrene metabolites formed by rat hepatic microsomes using high pressure liquid chromatography: optimization of the method

Michaela MOSEROVÁ [1], Věra KOTRBOVÁ [1], Dagmar AIMOVÁ [1], Miroslav ŠULC [1], Eva FREI [2], Marie STIBOROVÁ [1]

[1] *Department of Biochemistry, Faculty of Science, Charles University, Albertov 2030, 128 40 Prague 2, Czech Republic*
[2] *Department of Molecular Toxicology, German Cancer Research Center, 69 120 Heidelberg, Germany*

ITX020409A01 • Received: 07 August 2009 • Revised: 25 August 2009 • Accepted: 28 August 2009

ABSTRACT

A simple and sensitive method was developed to separate the carcinogenic polycyclic aromatic hydrocarbon (PAH), benzo[*a*]pyrene (BaP), and six of its oxidation metabolites generated by rat hepatic microsomes enriched with cytochrome P450 (CYP) 1A1, by high pressure liquid chromatography (HPLC). The HPLC method, using an acetonitrile/water gradient as mobile phase and UV detection, provided appropriate separation and detection of both mono- and di-hydroxylated metabolites of BaP as well as BaP diones formed by rat hepatic microsomes and the parental BaP. In this enzymatic system, 3-hydroxy BaP, 9-hydroxy BaP, BaP-4,5-dihydrodiol, BaP-7,8-dihydrodiol, BaP-9,10-dihydrodiol and BaP-dione were generated. Among them the mono-hydroxylated BaP metabolite, 3-hydroxy BaP followed by di-hydroxylated BaP products, BaP-7,8-dihydrodiol and BaP-9,10-dihydrodiol, predominated, while BaP-dione was a minor metabolite. This HPLC method will be useful for further defining the roles of the CYP1A1 enzyme with both *in vitro* and *in vivo* models in understanding its real role in activation and detoxification of BaP.

KEY WORDS: benzo[*a*]pyrene; metabolism; HPLC

Introduction

Benzo[*a*]pyrene (BaP) is the prototype compound of polycyclic aromatic hydrocarbons (PAH). BaP and other PAHs are produced mainly by incomplete combustion or pyrolysis of organic matter and are ubiquitous in the environment, leading to measurable background levels of exposure in the general population (IARC, 1983). Beside the inhalation of polluted air, the main routes of exposure are through tobacco smoke, diet (Phillips, 1999; 2002) and occupational exposition throughout, e.g. coal, coke or coal tar processing and use of coal tar products (IARC, 1983). BaP has been shown to cause cytotoxic, teratogenic, genotoxic, mutagenic, and carcinogenic effects in various tissues and cell types in organisms (Nebert, 1989; Ellard *et al.*, 1991). Chronic exposure of laboratory animals to BaP has been associated with developments of cancer, primarily in the skin, stomach, and lungs as target tissues (IARC, 1983). BaP requires metabolic activation (Figure 1) prior to reaction with DNA, which is an essential step in the mechanism, by which BaP exerts its genotoxic effects.

Cytochrome P450 (CYP) enzymes in a combination with epoxide hydrolase are the major enzymes activating BaP to species binding to DNA. First, the CYP enzymes oxidize BaP to form an epoxide that is additionally converted to a dihydrodiol by epoxide hydrolase (Baird *et al.*, 2005; Luch and Baird, 2005) (Figure 1). Further bioactivation step catalyzed by CYPs leads to the formation of the reactive species, benzo[a]pyrene-7,8-dihydrodiol-9,10-epoxide (BPDE) that can react with DNA, forming adducts preferentially at guanine residues. The 10-(deoxyguanosin-N^2-yl)-7,8,9-trihydroxy-7,8,9,10-tetrahydrobenzo[a]pyrene (dG-N^2-BPDE) adduct is the major adduct formed from BPDE in DNA *in vitro* and *in vivo* (Phillips, 2005) (Figure 1). Among CYP enzymes, CYP1A1 and 1B1 are widely accepted as the most important enzymes in such BaP metabolic activation (Baird *et al.*, 2005; Luch and Baird, 2005). Nevertheless, controversial results have been found recently in several laboratories, showing a more important role of CYP1A1 *in vivo* in BaP detoxification than in its activation (Uno *et al.*, 2004; 2006;

Correspondence address:
Prof. Marie Stiborová, DSc.
Department of Biochemistry, Faculty of Science, Charles University,
Albertov 2030, 128 40 Prague 2, Czech Republic
TEL: +420-221951285 • E-MAIL: stiborov@natur.cuni.cz

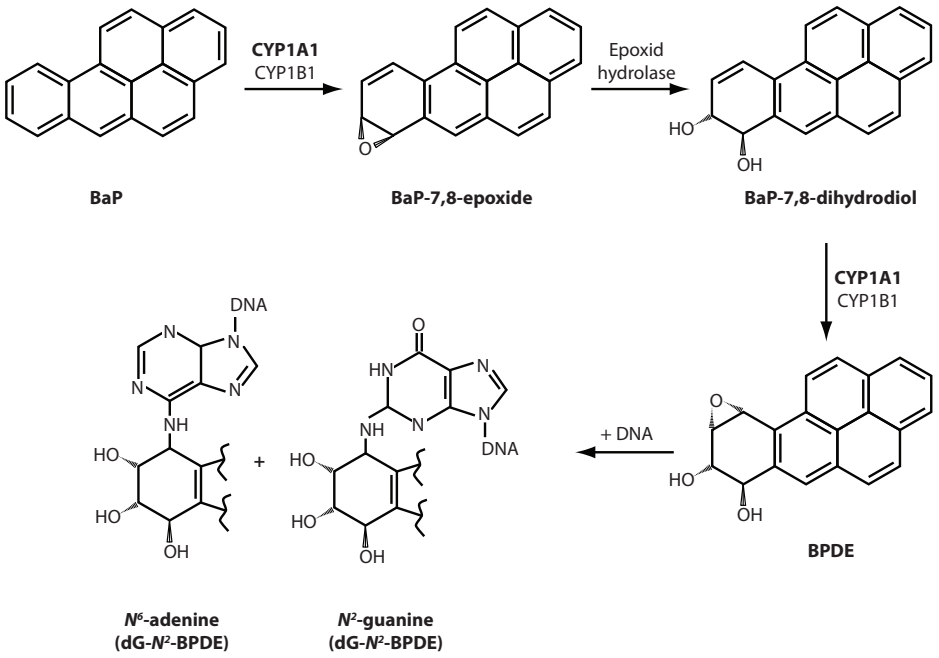

Figure 1. Metabolic activation and DNA adduct formation by benzo[*a*]pyrene. The typical three- step activation process with contribution of CYP1A1 or CYP1B1 and epoxide hydrolase leads to the formation of the ultimately reactive species, benzo[*a*]pyrene-7,8- dihydrodiol-9,10-epoxide (BPDE) that can react with DNA, forming adducts preferentially at guanine residues.

Arlt *et al.,* 2008). In order to explain such findings, activation and detoxification metabolism of BaP *in vitro* and *in vivo* should, therefore, be carefully re-evaluated. For such studies, appropriate methods separating and quantifying all BaP metabolites generated by CYPs in combination with epoxide hydrolase, besides methods evaluating the DNA adduct formation by this carcinogen, are necessary.

A variety of high pressure liquid chromatography (HPLC) procedures [reverse phase (RP)-HPLC] separating BaP metabolites was described by several authors for the last several decades (Selkirk *et al.*, 1974; Selkirk, 1977; Angener et al., 1997; Gündel and Angerer, 2000; Hecht, 2001; Sasaki *et al.,* 2002; Toriba *et al.,* 2003; Wang *et al.,* 2003; Sagredo *et al.,* 2006; Jiang *et al.,* 2007; Zhu *et al.,* 2008). In the 1970´s, HPLC was used for separating BaP metabolites combined with UV or scintillation counter detection. However, UV detection in these studies was not sufficient to detect all BaP metabolites (Selkirk, 1977). Therefore, quantitation by measuring fluorescence as detection method was developed (Krahn *et al.,* 1984). However, BaP diones, do not exhibit fluorescence, and the method does not quantitate individual metabolites prohibiting application of fluorescence detection for a detailed study of BaP metabolism. Thereafter, on-line or off-line radioactivity detection played a major role in the study of BaP metabolism (for summary see Zhu *et al.,* 2008). The disadvantages of the radioactive method include cost, radiolabeled individual metabolites are not available, and it cannot be used for the analysis of environmental samples. The improvement of chromatographic separation methods have allowed for significantly better separation of BaP metabolites during the 1990´s (James *et al.,* 1995; 1997; Kim *et al.,* 1998). From 2000, HPLC coupled with mass spectrometry was introduced in the study of BaP metabolism, though there were still problems associated with high detection limits for BaP diones (van Schanke *et al.,* 2001). Recently, ultra-performance liquid chromatography has been introduced with improved performance over traditional HPLC (Zhu *et al.,* 2008). However, there are still several disadvantages in all these methods, predominantly cost of analyses, which prohibit them to be suitable for general use in most of laboratories. Therefore, the aim of this study was to improve the HPLC procedure to be effective for separation of BaP metabolites generated by BaP oxidation with rat hepatic microsomes and sensitive enough to be able to detect BaP metabolites with UV detection.

Materials and methods

Chemicals

Chemicals were obtained from the following sources: methanol (MetOH; HPLC supergradient) from Lachner (Czech Republic); acetonitrile (HPLC grade) from Merck (Darmstadt, Germany); benzo[a]pyrene (≥ 96% based on HPLC), $NADP^+$, glucose-6-phosphate, phenacetine and bicinchoninic acid (2,2´-biquinoline-4,4´-dicarboxylic acid) from Sigma Chemical Co. (St. Louis, MO, USA) and glucose-6-phosphate dehydrogenase from Serva (Heidelberg, Germany). All these and other chemicals used in the experiments were of analytical purity or better.

Preparation and characterization of microsomes

The animal experiment was conducted in accordance with the Regulations for the Care and Use of Laboratory Animals (311/1997, Ministry of Agriculture, Czech Republic), which is in compliance with the Declaration of Helsinki. Microsomes from rats pretreated with Sudan I were isolated from pooled livers of ten rats as described previously (Stiborová *et al.*, 2003). Protein concentration in the microsomal fraction was measured using bicinchoninic acid protein assay (Wiechelman *et al.*, 1988) with bovine serum albumin as a standard. The content of CYPs was determined by differential spectroscopy based on utilizing a characteristic absorption of the complex of this hemthiolate protein in reduced state with carbon oxide at 450 nm (Omura and Sato, 1964).

Incubations

Incubation mixtures used for studying BaP metabolism contained 100 mM sodium phosphate buffer (pH 7.4), NADPH-generating system (1 mM $NADP^+$, 10 mM D-glucose-6-phosphate, 1 U/ml D-glucose-6-phosphate dehydrogenase), 0.5 mg of microsomal protein, 50 µM BaP (dissolved in 5 µl methanol) in a final volume of 500 µl. The reaction was initiated by adding 50 µl of the NADPH-generating system. Control incubations were carried out either without enzymatic system (microsomes) or without NADPH-generating system or without BaP. After incubation in open tubes (37 °C, 20 min), 5 µl of 1 mM phenacetine in methanol was added as an internal standard. BaP metabolites were extracted twice with ethyl acetate (2 × 1 ml) and evaporated to dryness. The samples were dissolved in 25 µl methanol and BaP metabolites formed in this system separated by HPLC.

HPLC instrument used for HPLC analysis of BaP metabolites

HPLC analyses of BaP metabolites were performed using a Dionex system consisting of a Dionex pump P580, a UV/VIS Detector UVD 170S/340S, an ASI-100 Automated Sample Injector, a termobox COLUMN OVEN LCO 101 and an In-Line Mobile Phase Degasser Degasys DG-1210 Dionex controlled with Chromeleon™ 6.11 build 490 software. Chromatographic separation was performed on two types of reversed phase columns, Ultrasphere® ODS, C18, 5 µm, 250 × 4.6 mm (Beckman-Coulter, USA) and Nucleosil® 100-5 C18, 5 µm, 250 × 4 mm (Macherey Nagel, Germany).

Chromatographic conditions

Four different conditions to separate BaP metabolites were used. The first one was analogous to that used by Selkirk *et al.*, 1974. Mobile phase A: 30% methanol (30:70 methanol: water, v/v), mobile phase B: 70% methanol (70:30 methanol: water, v/v), flow rate: 0.6 ml/min at operation temperature of 35 °C, detection at 254 nm. The 20 µl sample was injected for HPLC analysis. BaP metabolite separation was performed using a Nucleosil® C18 reverse phase column, (250 × 4 mm, 5 µm; Macherey Nagel). Linear gradient system started from 30% methanol to 70% methanol in 33 min and followed by isocratic elution of mobile phase B in 32 min (Procedure 1, Figure 2A).

In the second procedure (Procedure 2) the same conditions as in Procedure 1 were used except that separation of BaP metabolites was performed using an Ultrasphere®, ODS, C18 reverse phase column (250 × 4.6 mm, 5 µm) (Figure 2B).

In the Procedure 3 the experimental conditions were as follows: mobile phase: 85% acetonitrile (85:15 acetonitrile: water, v/v), flow rate: 0.6 ml/min at operation temperature of 35 °C, detection at 254 nm. The 20 µl sample was injected for HPLC analysis.

BaP metabolite separation was performed using the isocratic elution of mobile phase in 55 min, on a Nucleosil® C18 reverse phase column, (250 × 4 mm, 5 µm; Macherey Nagel) (Figure 3).

In the Procedure 4 the experimental conditions were as follows: mobile phase A: 50% acetonitrile (50:50 acetonitrile: water, v/v), mobile phase B: 85% acetonitrile (85:15 acetonitrile: water, v/v). Initial elution conditions were 50% acetonitrile with a linear gradient to 85% acetonitrile in 35 min, then an isocratic elution of 85% acetonitrile in 5 min, a linear gradient from 85% acetonitrile to 50% acetonitrile in 5 min, followed by an isocratic elution of 50% acetonitrile in 5 min. Total run time was 50 min. BaP metabolite separation was performed on a Nucleosil® C18 reverse phase column, (250 × 4 mm, 5 µm; Macherey Nagel). The used gradient program is shown in Table 1. The BaP metabolite peaks (Figure 4) were collected and analyzed by mass spectrometry.

Mass spectrometry

Mass spectra were measured on a matrix-assisted laser desorption/ionisation reflectron time-of-flight MALDITOF mass spectrometer ultraFLEX (Bruker-Daltonics, Bremen, Germany). Positive spectra were calibrated externally using the monoisotopic [M+H]+ ion of bradykinin 757.399 m/z and CCA matrix peaks 190.050, 379.092 m/z. A 10 mg/ml solution of α-cyano-4-hydroxy-cinnamic acid or 2,5-dihydrobenzoic acid in 50% acetonitrile/0.3% acetic acid was used as a MALDI matrix. A 0.5 µl of sample dissolved in acetonitrile was premixed with a 0.5 µl of the matrix solution on the target and allowed to dry at ambient temperature. The MALDI-TOF positive spectra were collected in reflectron mode.

Results and discussion

In order to receive the BaP metabolites, which are formed by a combination of CYP- and epoxide hydrolase-mediated reactions, rat hepatic microsomes used in the experiments. Because CYP1A1 is one of the most efficient enzymes metabolizing BaP *in vitro*, hepatic microsomes of rats treated with a CYP1A1 inducer, Sudan I (Lubet *et al.,* 1983; Martínek and Stiborová, 2002; Stiborová *et al.,* 2002), were employed. Using such microsomes, formation of a spectrum of mono- and di-hydroxylated BaP metabolites as well as quinones (diones) of BaP that were found to be formed by CYP1A1 with epoxide hydrolase (Baird *et al.*, 2005; Luch and Baird 2005) was expected.

To improve the existing HPLC chromatographic method analyzing BaP metabolites and to make them sensitive

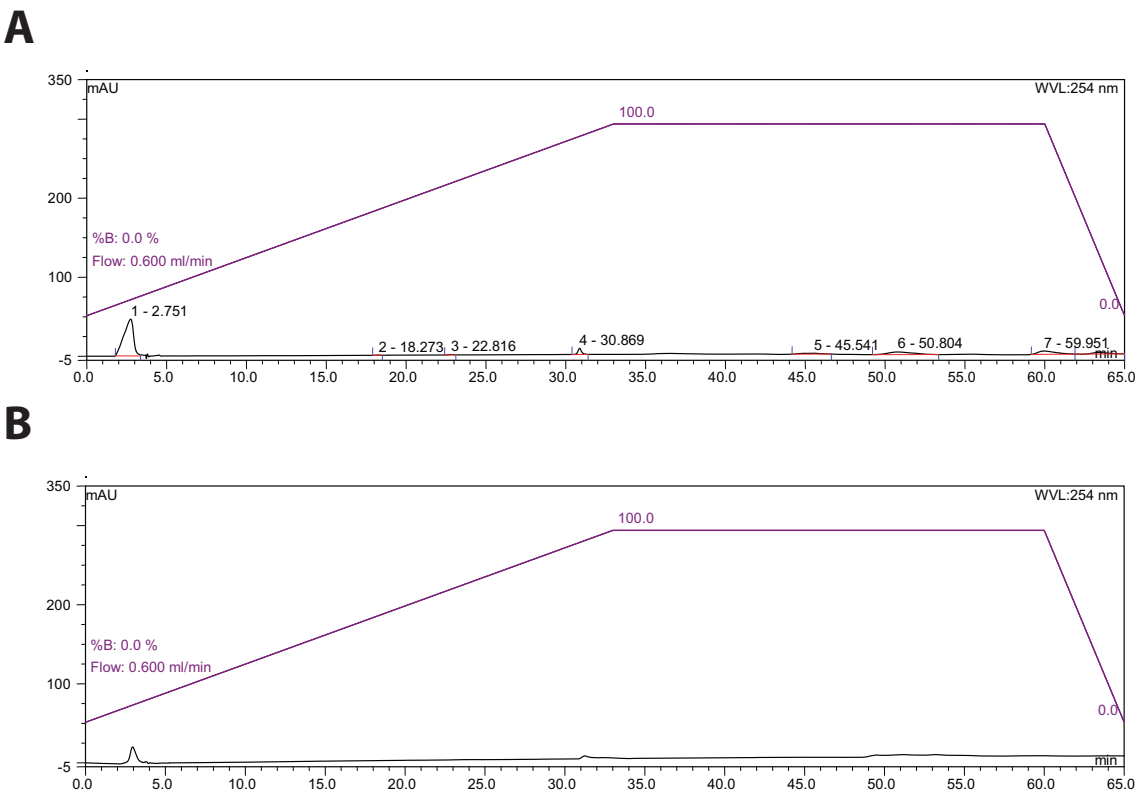

Figure 2. HPLC separation of the BaP metabolites generated by rat hepatic microsomes using Nucleosil® C18 (**A**) and Ultrasphere® C18 reverse phase columns (**B**). A linear gradient elution from 30% methanol to 70% methanol in 65 min. Flow rate 0.6 ml/min, UV detection at 254 nm.

enough to be detected with UV detection, we investigated various elution systems and chromatographic procedures. In addition, two different HPLC analytical columns were examined to evaluate their efficiencies to separate BaP metabolites. The columns Ultrasphere® and Nucleosil® obtained from Beckman-Coulter and Macherey-Nagel, respectively, were utilized for such a study. Constant flow rate of 0.6 ml/min under 35 °C was used. To detect BaP and its metabolites, a spectrum of different wavelengths were tested to detect BaP (data not shown). The highest sensitivity to detect BaP and its metabolites separated by HPLC was at 254 nm. Four procedures (Procedures 1, 2, 3 and 4, see the Materials and Methods section) were tested in this work.

Because several methods described in the former studies used methanol/water or acetonitrile/water as mobile phases in HPLC for separation of BaP metabolites, we tested both these mobile phases in different arrangements. First we tried methanol/water as mobile phase with gradient program (30% to 70% methanol), which was analogous to mobile phase used previously by Selkirk *et al.,* 1974, but even after optimization and using two chromatographic columns (Nucleosil® C18 and Ultrasphere® reverse phase columns), we were unable to detect any BaP metabolites or even BaP itself under these conditions (see Figure 2 showing the results found using the Procedures 1 and 2). Chromatographic profiles were as almost baseline without elution of BaP and metabolites (Figure 2), probably by retaining the BaP and its metabolites on the resin under such conditions.

Since the methanol/water mobile phase was found to be inappropriate for elution of BaP and its metabolites, we utilized acetonitrile/water as mobile phase in further studies. In this case, we first tried 85% acetonitrile in water (v/v) with an isocratic elution using the Nucleosil® C18 reverse phase column (Procedure 3), however, even after optimization, we did not achieve ideal separation of BaP metabolites formed by rat hepatic microsomes (Figure 3). BaP metabolites eluted between 4 to 11 min, while BaP at 18.6 min (Figure 3). When we changed the elution conditions with acetonitrile/water as mobile phase to the gradient program shown in Table 1 (Procedure 4), six BaP metabolites were almost perfectly separated using the same chromatographic column (a Nucleosil® C18 reverse phase column, Figure 4). The BaP

Table 1. HPLC conditions used for a step gradient elution of BaP metabolites on a Nucleosil® C18 reverse phase column

Time [min]	Mobile phase A 50% acetonitrile	Mobile Phase B 85% acetonitrile	Flow rate
0	100%	0%	
35	0%	100%	
40	0%	100%	0.6 ml/min
45	100%	0%	
50	100%	0%	

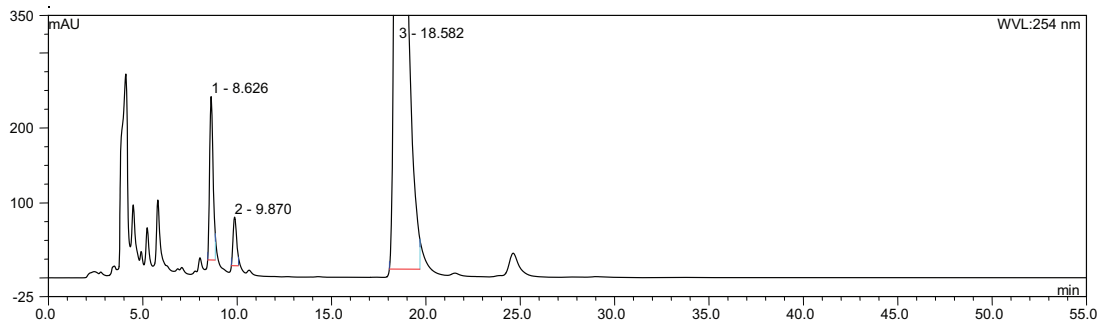

Figure 3. HPLC separation of the BaP metabolites generated by rat hepatic microsomes using a Nucleosil® C18 reverse phase column. An isocratic elution of 85% acetonitrile in 55 min. Flow rate 0.6 ml/min, UV detection at 254 nm.

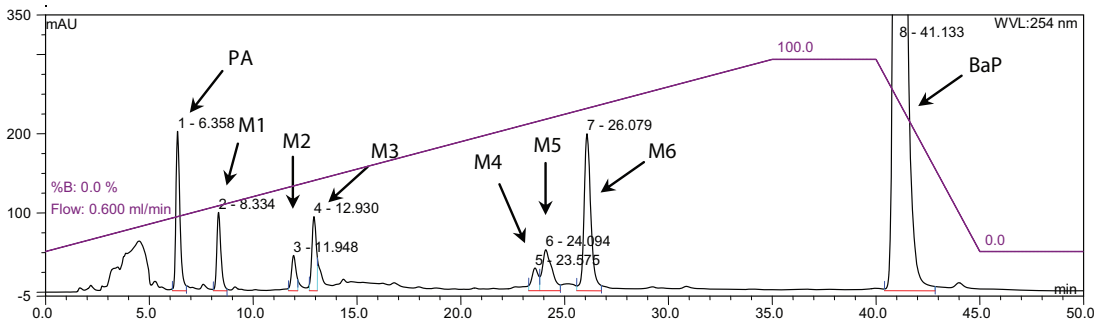

Figure 4. HPLC separation of the BaP metabolites generated by rat hepatic microsomes using a Nucleosil® C18 reverse phase column. A linear gradient elution from 50% methanol to 85% methanol in 50 min. Flow rate 0.6 ml/min, UV detection at 254 nm. PA, phenacetine, M1-M6, BaP metabolites [BaP-9,10-dihydrodiol (M1), BaP-4,5-dihydrodiol (M2), BaP-7,8-dihydrodiol (M3), one of the BaP diones (1,6 or 3,6 or 6,12-BaP-dione, M4), 9-hydroxy BaP (M5) and 3-hydroxy BaP (M6)].

metabolites formed by rat hepatic microsomes, assigned in Figure 4 as metabolites M1-M6 and eluted at retention times of 8.3 (M1), 11.9 (M2), 12.9 (M3), 23.6 (M4), 24.1 (M5) and 26.1 min (M6), were characterized by mass spectrometry and tentatively identified to be BaP-9,10-dihydrodiol (M1), BaP-4,5-dihydrodiol (M2), BaP-7,8-dihydrodiol (M3), one of the BaP diones (1,6 or 3,6 or 6,12-BaP-dione, M4), 9-hydroxy BaP (M5) and 3-hydroxy BaP (M6). Parental BaP was eluted at 41 min. The study resolving which of BaP diones is a metabolite M4 is under way in our laboratory.

Conclusion

The new HPLC method developed in this work allows for separation of BaP metabolites with increased resolution, simple procedure and high detection sensitivity. Because of controversial results suggesting a more important role of CYP1A1 *in vivo* in BaP detoxification than in its activation (Uno *et al.*, 2004; 2006; Arlt *et al.*, 2008), BaP metabolism and DNA adducts formation should be re-investigated in more details. The developed HPLC method will be useful for such additional studies, to further define the real roles of the CYP1A1 enzyme both *in vitro* and *in vivo* in activation and detoxification of BaP.

Acknowledgement

The research was supported in part Grant Agency of the Czech Republic (grants 303/09/0472 and 305/09/H008), the Grant Agency of Charles University (grant 127208) and the Ministry of Education of the Czech Republic (grant MSM0021620808, 1M0505 and RP MSMT 14/63).

REFERENCES

Angerer J, Mannschreck C, Gündel J. (1997). Biological monitoring and biochemical effect monitoring of exposure to polycyclic aromatic hydrocarbons. *Int Arch Occup Environ Health* **70**: 365–377.

Arlt VM, Stiborová M, Henderson CJ, Thiemann M, Frei E, Aimová D, Singhs R, da Costa GG, Schmitz OJ, Farmer PB, Wolf CR, Phillips DH. (2008). Metabolic activation of benzo[a]pyrene *in vitro* by hepatic cytochrome P450 contrasts with detoxification *in vivo*: experim ents with hepatic cytochrome P450 reductase null mice. *Carcinogenesis* **29**: 656–665.

Baird WM, Hooven LA, Mahadevan B. (2005). Carcinogenic polycyclic aromatic hydrocarbon-DNA adducts and mechanism of action. *Environ Mol Mutagen* **45**: 106–114.

Ellard S, Mohammed Y, Dogra S, Wolfel C, Doehmer J, Parry JM. (1991). Use of genetically engineered V79 Chinese hamster cultures expressing rat liver CYP1A1, 1A2 and 2B1 cDNAs in micronucleus assays. *Mutagenesis* **6**: 461–470

Gündel J, Angerer J. (2000). High-performance liquid chromatographic method with fluorescence detection for the determination of 3-hydroxybenzo[a]pyrene and 3-hydroxybenz[a]anthracene in the urine of polycyclic aromatic hydrocarbon-exposed workers. *J Chromatogr B Biomed Sci Appl* **738**: 47–55.

Hecht SS. (2001). Carcinogen biomarkers for lung or oral cancer chemoprevention trials. *IARC Sci Publ* **154**: 245–255.

IARC Monogr Eval Carcinog Risk Chem Hum. (1983). *Polynuclear Aromatic Compounds* **32**, 211.

James MO, Altman AH, Li CL, Schell JD Jr. (1995). Biotransformation, hepatopancreas DNA binding and pharmacokinetics of benzo[a]pyrene after oral and parenteral administration to the American lobster, Homarus americanus. *Chem Biol Interact* **95**: 141–160.

James MO, Altman AH, Morris K, Kleinow KM, Tong Z. (1997). Dietary modulation of phase 1 and phase 2 activities with benzo(a)pyrene and related compounds in the intestine but not the liver of the channel catfish, Ictalurus punctatus. *Drug Metab Dispos* **25**: 346–354.

Jiang H, Gelhaus SL, Mangal D, Harvey RG, Blair IA, Penning TM. (2007). Metabolism of benzo[a]pyrene in human bronchoalveolar H358 cells using liquid chromatography-mass spectrometry. *Chem Res Toxicol* **20**: 1331–1341.

Kim JH, Stansbury KH, Walker NJ, Trush MA, Strickland PT, Sutter TR. (1998). Metabolism of benzo[a]pyrene and benzo[a]pyrene-7,8-diol by human cytochrome P450 1B1. *Carcinogenesis* **19**: 1847–1853.

Krahn MM, Myers MS, Burrows DG, Malins DC. (1984). Determination of metabolites of xenobiotics in the bile of fish from polluted waterways. *Xenobiotica* **14**: 633–646.

Lubet RA, Connolly G, Kouri RE, Nebert DW, Bigelow SW. (1983). Biological effects of Sudan I dyes. Role of the cytosolic *Ah* receptor. *Biochem Pharmacol* **32**: 3053–3058.

Luch A, Baird WM. (2005). Metabolic activation and detoxification of polycyclic aromatic hydrocarbons. *The Carcinogenic Effects of Polycyclic Aromatic Hydrocarbons*. Imperial College Press, London, 19–96.

Martínek V, Stiborová M. (2002). Metabolism of carcinogenic azo dye Sudan I by rat, rabbit, minipig and human hepatic microsomes. *Collect Czech Chem Commun* **67**: 1883–1898.

Nebert DW. (1989). The Ah locus: genetic differences in toxicity, cancer, mutation and birth defects. *Crit Rev Toxicol* **20**: 153–174.

Omura T, Sato R. (1964). The carbon monoxide-binding pigment of liver microsomes. II. Solubilization, purification, and properties. *J Biol Chem* **239**: 2379–85

Phillips DH. (1999). Polycyclic aromatic hydrocarbons in the diet. *Mutat Res* **443**: 139–47.

Phillips DH. (2002). Smoking-related DNA and protein adducts in human tissues *Carcinogenesis* **23**: 1979–2004

Phillips DH. (2005). Macromolecular adducts as biomarkers of human exposure to polycyclic aromatic hydrocarbons. *The Carcinogenic Effects of Polycyclic Aromatic Hydrocarbons*. Imperial College Press, London, 137–169.

Sagredo C, Øvrebø S, Haugen A, Fujii-Kuriyama Y, Baera R, Botnen IV, Mollerup S. (2006). Quantitative analysis of benzo[a]pyrene biotransformation and adduct formation in Ahr knockout mice. *Toxicol Lett* **167**: 173–182.

Sasaki H, Yonekubo J, Kanai M, Toriba A, Kizu R, Hayakawa K. (2002). Simultaneous detection of monohydroxybenzo[a]pyrene positional isomers by reversed-phase liquid chromatography coupled to electrospray ionization mass spectrometry. *Biomed Chromatogr* **16**: 432–436.

Selkirk JK, Croy RG, Gelboin HV. (1974). Benzo[a]pyrene metabolites: efficient and rapid separation by high-pressure liquid chromatography. *Science* **184**: 169–171.

Selkirk JK. (1977). Benzo[a]pyrene carcinogenesis: a biochemical selection mechanism. *J Toxicol Environ Health* 2: 1245–1258.

Stiborová M, Martínek V, Rýdlová H, Hodek P, Frei E. (2002). Sudan I is a potential carcinogen for humans: Evidence for its metabolic activation and detoxication by human recombinant cytochrome P450 1A1 and liver microsomes. *Cancer Res* **62**: 5678–5684.

Stiborová M, Stiborová-Rupertová M, Bořek-Dohalská L, Wiessler M, Frei E. (2003). Rat microsomes activating the anticancer drug ellipticine to species covalently binding to deoxyguanosine in DNA are a suitable model mimicking ellipticine bioactivation in humans. *Chem Res Toxicol* **16**: 38–47.

Toriba A, Nakamura H, Chetiyanukornkul T, Kizu R, Makino T, Nakazawa H, Yokoi T, Hayakawa K. (2003). Method for determining monohydroxybenzo[a]pyrene isomers using column-switching high-performance liquid chromatography. *Anal Biochem* **312**: 14–22.

Uno S, Dalton TP, Derkenne S, Curran CP, Miller ML, Shertzer HG, Nebert DW. (2004). Oral exposure to benzo [a] pyrene in the mouse: detoxication by inducible cytochrome P450 is more important than metabolic activation. *Mol Pharmacol* **65**: 1225–37.

Uno S, Dalton TP, Dragin N, Curran CP, Derkenne S, Miller ML, Shertzer HG, Gonzalez FJ, Nebert DW. (2006). Oral benzo[a]pyrene in Cyp1 knockout mouse lines: CYP1A1 important in detoxication, CYP1B1 metabolism required for immune damage independent of total-body burden and clearance rate. *Mol Pharmacol* **69**: 1103–14.

van Schanke A, Holtz F, van der Meer JP, Boon JP, Ariese F, Stroomberg G, van den Berg M, Everaarts JM. (2001). Dose- and time-dependent formation of biliary benzo[a]pyrene metabolites in the marine flatfish dab (Limanda limanda). *Environ Toxicol Chem* **20**: 1641–1647.

Wang JJ, Frazer DG, Law B, Lewis DM. (2003). Identification and quantification of urinary benzo[a]pyrene and its metabolites from asphalt fume exposed mice by microflow LC coupled to hybrid quadrupole time-of-flight mass spectrometry. *Analyst* **128**: 864–870.

Wiechelman KJ, Braun RD, Fitzpatrick JD. (1988). Investigation of the bicinchoninic acid protein assay: identification of the groups responsible for color formation. *Anal Biochem* **175**: 231–237.

Zhu S, Li L, Thornton C, Carvalho P, Avery BA, Willett KL. (2008). Simultaneous determination of benzo[a]pyrene and eight of its metabolites in Fundulus heteroclitus bile using ultra-performance liquid chromatography with mass spectrometry. *J Chromatogr B Analyt Technol Biomed Life Sci* **863**: 141–149.

ISSN: 1337-6853 *(print version)* | 1337-9569 *(electronic version)*

Příloha 6

MARIE STIBOROVÁ, **MICHAELA MOSEROVÁ**, BARBORA MRÁZOVÁ, VĚRA KOTRBOVÁ, EVA FREI

ROLE OF CYTOCHROMES P450 AND PEROXIDASES IN METABOLISM OF THE ANTICANCER DRUG ELLIPTICINE: ADDITIONAL EVIDENCE OF THEIR CONTRIBUTION TO ELLIPTICINE ACTIVATION IN RAT LIVER, LUNG AND KIDNEY.

Neuro Endocrinol. Letters, 31(Suppl.2):101-110, 2010

Role of cytochromes P450 and peroxidases in metabolism of the anticancer drug ellipticine: additional evidence of their contribution to ellipticine activation in rat liver, lung and kidney

Marie Stiborova [1], Michaela Moserova [1], Barbora Mrazova [1], Vera Kotrbova [1], Eva Frei [2]

1 Department of Biochemistry, Faculty of Science, Charles University Prague, Czech Republic
2 Division of Preventive Oncology, National Center for Tumour Diseases, German Cancer Research Center, Germany

Correspondence to: Prof. RNDr. Marie Stiborova, DSc.
Department of Biochemistry, Faculty of Science, Charles University in Prague, Albertov 2030, 128 40 Prague 2, Czech Republic.
TEL: +420-221 951 285; FAX: +420-221 951 283; E-MAIL: stiborov@natur.cuni.cz

Submitted: 2010-09-03 Accepted: 2010-11-22 Published online: 2010-00-00

Key words: **Ellipticine; anticancer drug; DNA adduct; cytochrome P450; peroxidase**

Neuroendocrinol Lett 2010; **31**(Suppl.2):101–110 **PMID:** ----- NEL31S210AXX

Abstract

OBJECTIVE: Ellipticine is a potent antineoplastic agent exhibiting multiple mechanisms of action. This anticancer agent should be considered a pro-drug, whose pharmacological efficiency and/or genotoxic side effects are dependent on its cytochrome P450 (CYP)- and/or peroxidase-mediated activation to species forming covalent DNA adducts. The target of this study was to investigate a role of CYP and peroxidase enzymes in ellipticine oxidative activation in rats, a suitable model mimicking the fate of ellipticine in humans, in details. The contribution of pulmonary and renal CYP- and peroxidase enzymes to ellipticine metabolic activation is investigated and compared with that found in the liver. **METHODS:** Ellipticine oxidation and DNA adduct formation *in vitro* were investigated using microsomes isolated from liver, lung and kidney of rats, either control (untreated) or treated i.p. with a single dose of 40 mg of ellipticine per kg of body weight. HPLC with UV detection was employed for the separation and characterization of ellipticine metabolites. Inhibitors of CYPs and cyclooxygenase (prostaglandin H synthase, COX) were used to characterize the enzymes participating in ellipticine oxidative activation in rat liver, lung and kidney. Ellipticine-derived DNA adducts were detected by ^{32}P-postlabeling. **RESULTS:** Using α-naphthoflavone, furafylline and ketoconazole, inhibitors of CYP1A, 1A2 and 3A, respectively, we found that the CYP1A and 3A enzymes play a major role in ellipticine activation to species forming DNA adducts in liver microsomes. Because of lower expression of these enzymes in lungs and kidneys, even after their induction by ellipticine, they play a minor role in ellipticine activation in these extrahepatic tissues. Arachidonic acid, a cofactor of COX, increased ellipticine activation in the microsomes of extrahepatic tissues. In addition, indomethacin, an inhibitor of COX, efficiently inhibited formation of ellipticine-derived DNA adduct in these microsomes. Based on these results, we attribute the higher activation of ellipticine in lung and kidney microsomes to COX than to CYP enzymes. **CONCLUSION:** The results demonstrate that whereas CYP enzymes of 1A and 3A subfamilies are the major enzymes activating ellipticine in rat livers, peroxidase COX plays a significant role in this process in lungs and kidneys.

ORIGINAL ARTICLE

Abbreviations:

α-NF	- α-naphthoflavone
COX	- cyclooxygenase
CYP	- cytochrome P450
HPLC	- high performance liquid chromatography
LPO	- lactoperoxidase
MPO	- myeloperoxidase
S.E.M.	- standard error medium
NADPH	- nicotinamidadeninedinucleotide phosphate (reduced)
RAL	- relative adduct labeling
TLC	- thin-layer chromatography

INTRODUCTION

Ellipticine (5,11-dimethyl-6*H*-pyrido[4,3-*b*]carbazole, Figure 1), an alkaloid isolated from *Apocyanaceae* plants, exhibit significant antitumor and anti-HIV activities (for a summary see Stiborova *et al.* 2001). The main reason for the interest in ellipticine and its derivatives for clinical purposes is their high efficiencies against several types of cancer, their rather limited toxic side effects, and their complete lack of haematological toxicity (Auclair 1987). Nevertheless, ellipticine is a potent mutagen. Most ellipticine derivatives are mutagenic to *Salmonella typhimurium* Ames tester strains, bacteriophage T4, *Neurospora crassa*, and mammalian cells and induce prophage lambda in *Escherichia coli* (for an overview see Stiborova *et al.* 2001).

Ellipticine has been reported to arrest cell cycle progression by regulating the expression of cyclin B1 and Cdc2 as well as phosphorylation of Cdc2 (Kuo *et al.* 2005a,b), to induce apoptotic cell death by the generation of cytotoxic free radicals, the activation of Fas/Fas ligand system, the regulation of Bcl-2 family proteins (Kuo *et al.* 2005a,b; 2006), an increase of wild-type p53, the rescue of mutant p53 activity and the initiation of the mitochondrial apoptosis pathway (Garbett & Graves 2004; Kuo *et al.* 2005a,b; 2006). Ellipticine also activates the p53 pathway in glioblastoma cells; its impact on these cancer cells depends on the p53 status. In a U87MG glioblastoma cell line expressing p53wt, ellipticine provoked an early G0/G1 cell cycle arrest, whereas in a U373 cell line expressing p53mt it caused arrest in S and G2/M phase (Martinkova *et al.* 2010).

Ellipticine and 9-hydroxyellipticine also cause selective inhibition of p53 protein phosphorylation in several human cancer cell lines (Ohashi *et al.* 1995; Sugikawa *et al.* 1999), and this correlates with their cytotoxic activity. However, the precise molecular mechanism responsible for these effects has not been explained yet. Chemotherapy-induced cell cycle arrest was shown to result from DNA damage caused by a variety of chemotherapeutics. In the case of ellipticine, it was suggested that the prevalent DNA-mediated mechanisms of its antitumor, mutagenic and cytotoxic activities are (i) intercalation into DNA, and (ii) inhibition of DNA topoisomerase II activity (Auclair 1987; Garbett & Graves 2004; Stiborova *et al.* 2006c; 2010).

We have demonstrated that ellipticine also covalently binds to DNA after being enzymatically activated with cytochromes P450 (CYP) or peroxidases (Stiborova *et al.* 2001; 2003a,b; 2004; 2006a; 2007a,b; Poljakova *et al.* 2006), suggesting a third possible mechanism of action. Two major DNA adducts generated from 13-hydroxy- and 12-hydroxyellipticine during the ellipticine CYP- and peroxidase-mediated metabolism are formed *in vitro* and *in vivo* in rats and mice treated with this anticancer drug (Stiborova *et al.* 2001; 2003a,b; 2004; 2006a; 2007a,b; 2008, Frei *et al.* 2002; Poljakova *et al.* 2006). The same DNA adducts were also detected in cancer cells in culture, such as human breast adenocarcinoma MCF-7 cells (Borek-Dohalska *et al.* 2004), leukaemia HL-60 and CCRF-CEM cells (Poljakova *et al.* 2007), neuroblastoma cells (Poljakova *et al.* 2009) and glioblastoma cells (Martinkova *et al.* 2009) *in vitro*, and in rat breast adenocarcinoma *in vivo* (Stiborova *et al.* 2010). Toxic effects of ellipticine to these cancer cells correlate with levels of ellipticine-derived DNA adducts and are dependent on expression of CYP1A1, 1B1, 3A4 and peroxidases LPO, COX and MPO in these cells (Borek-Dohalska *et al.* 2004; Poljakova *et al.* 2007; 2009; Martinkova *et al.* 2009). On the basis of these data, ellipticine might be considered a drug, whose pharmacological efficiency and/or genotoxic side effects are dependent on its activation by CYPs and peroxidases in target tissues.

All these results indicate that understanding which enzymes are involved in the metabolic activation of ellipticine is important in the assessment of susceptibility to this drug. Human and rat CYP1A and 3A were found to be the predominant enzymes catalyzing oxidation of ellipticine *in vitro* either to metabolites that are excreted (7-hydroxy- and 9-hydroxyellipticine) or that form DNA adducts (12-hydroxy- and 13-hydroxyellipticine) (Stiborova *et al.* 2001; 2003a,b; 2004; 2006a; 2008; Moserova *et al.* 2008). Of the mammalian peroxidases, human cyclooxygenase (COX)-2, ovine COX-1, bovine lactoperoxidase (LPO) and human myeloperoxidase (MPO) efficiently generated ellipticine-derived DNA adducts (Figure 1) (Poljakova *et al.* 2006; Stiborova *et al.* 2007a). However, the actual impacts of these enzymes *in-vivo* depend on several additional factors (Stiborova *et al.* 2008). One of them might be the presence of various patterns of individual CYP and peroxidase enzymes and/or even the presence of other proteins influencing their activities in target and non-target tissues. The CYP and peroxidase enzyme patterns depend also on a known phenomenon that ellipticine is a strong inducer of CYP1A enzymes in several tissues including cancer cells, which catalyze its own metabolism (Gasiewicz *et al.* 1996; Aimova *et al.* 2007; Martinkova *et al.* 2009). This feature might finally dictate the pharmacological efficiencies of ellipticine.

After i.p. administration of ellipticine to rats and mice, the highest levels of DNA adducts were found

in liver, followed by kidney and lung (Stiborova *et al.* 2003a; 2007b; 2008). Liver is a tissue rich in CYP enzymes, while kidney and lung contain high levels of peroxidases such as COX (Eling *et al.* 1990; 1992; Stiborova *et al.* 1991; 2005a; Culp *et al.* 1997). Knowledge about contributions of these enzymes to ellipticine activation in individual rat tissues are, however, scarce. Although previous results indicate that CYP3A1 and 1A participate in formation of DNA adducts by ellipticine in rats *in vivo* (Stiborova *et al.* 2003a), the impact of these CYPs or that of peroxidases in ellipticine activation in individual organs is not known.

In this study, we have used the Wistar rat model, known to be suitable to mimic the fate of ellipticine in humans (Stiborova *et al.* 2003; 2006a), to examine actual contributions of CYPs and peroxidases to DNA adduct formation by ellipticine in liver, lung and kidney of these rats.

MATERIALS AND METHODS

Chemicals

$NADP^+$, NADPH, ellipticine, D-glucose 6-phosphate, D-glucose 6-phosphate dehydrogenase and calf thymus DNA were obtained from Sigma Chemical Co (St Louis, MO, USA); 9-hydroxyellipticine (5,11-dimethyl-9-hydroxy-6*H*-pyrido[4,3-*b*]carbazole) were from Calbiochem (San Diego, CA, USA). All these and other chemicals from commercial sources used in the experiments were reagent grade or better. 7-Hydroxyellipticine and the N^2-oxide of ellipticine were synthesized as described (Wijsmuller *et al.* 1986; Boogaard *et al.* 1994) by J. Kucka (Charles University, Prague, Czech Republic); their purity was >99.5% as estimated by high-performance liquid chromatography (HPLC). Enzymatically prepared 12-hydroxy- and 13-hydroxyellipticine were obtained from multiple HPLC runs of ethyl acetate extracts of incubations of ellipticine with human and/or rat hepatic microsomes as described (Stiborova *et al.* 2004).

Animal experiments

The study was conducted in accordance with the Regulations for the Care and Use of Laboratory Animals (311/1997, Ministry of Agriculture, Czech Republic), which is in compliance with the Declaration of Helsinki. Male Wistar rats (~100 g) were treated with a single dose of 40 mg/kg body weight (n=3) of ellipticine by intraperitoneal injection. Ellipticine was dissolved in sunflower oil/DMSO (1:1, v/v) to give a concentration of 6 mg/ml. Three control animals received an equal volume of solvent only. Rats were placed in cages in temperature and humidity controlled rooms. Standardized diet and water were provided *ad libitum*. The animals were killed 48 hours after treatment by cervical dislocation. Livers, lungs and kidneys were removed immediately after death and used for isolation of microsomal fractions.

Preparation of microsomes

Microsomes were isolated from the livers, kidneys and lungs of rats as described (Stiborova *et al.* 2003b). Protein concentrations in the microsomal fractions were assessed using the bicinchoninic acid protein assay with bovine serum albumin as a standard (Wichelman *et al.* 1988). The concentration of CYP was estimated according to Omura and Sato (1964) based on the absorption of the complex of reduced CYP with carbon monoxide. Specific content of CYP in hepatic, pulmonary and renal microsomes of control and ellipticine-treated rats (40 mg/kg) is shown in our former work (Aimova *et al.* 2007). Hepatic, renal and pulmonary microsomal preparations from rats that had been pre-treated with ellipticine were analyzed for the presence of ellipticine or its metabolites by HPLC as described (Stiborova *et al.* 2004). Neither ellipticine nor any of its metabolites were detectable in microsomal fractions from tissues of rats that had been pretreated with ellipticine.

Microsomal incubations

Incubation mixtures used to asses DNA adducts formed by ellipticine consisted of 50 mM potassium phosphate buffer (pH 7.4), 1 mM NADPH, pooled microsomal samples from liver, kidney and lung (0.5 mg protein) from 3 male rats, either control or treated with 40 mg/kg body weight of ellipticine, 100 μM ellipticine (dissolved in 7.5l methanol) and 0.5 mg of calf thymus DNA in a final volume of 750 μl. The reaction was initiated by adding ellipticine. Incubations were also carried out in the presence of COX cofactors, arachidonic acid and/or hydrogen peroxide (Eling *et al.* 1992; Stiborova *et al.* 2005a). Mixtures then contained 0.1 mM arachidonic acid and/or 0.1 mM hydrogen peroxide as cofactors instead of NADPH, and additionally 5 mM magnesium chloride. Incubations were carried out at 37 °C for 30 minutes; ellipticine-DNA adduct formation was found to be linear up to 30 min of incubation (Stiborova *et al.* 2001). Control incubations were carried out (*i*) without microsomes, (*ii*) without NADPH or arachidonic acid, (*iii*) without DNA and (*iv*) without ellipticine.

Incubation mixtures used to study the ellipticine metabolites contained 50 mM potassium phosphate buffer (pH 7.4), 1 mM $NADP^+$, 10 mM D-glucose 6-phosphate, 1 U/ml D-glucose 6-phosphate dehydrogenase (NADPH-generation system), 0.2 mg protein of pooled hepatic microsomal fraction from 3 male rats, either untreated or treated with 40 mg/kg body weight ellipticine and 10 μM ellipticine (dissolved in 5 μl methanol) in a final volume of 500 μl. The reaction was initiated by adding the substrate. In the control incubation, ellipticine was omitted from the incubation mixture. After incubation in open glass tubes (37 °C, 20 min) the reaction was stopped by adding 100 μl of 2 M NaOH. The oxidation of ellipticine is linear up to 30 min of incubation (Stiborová *et al.* 2004; 2006a). After incubation, 5 μl of 1 mM phenacetine in methanol was added as an internal standard and the ellipticine metabo-

lites were extracted twice with ethyl acetate (2 × 1 ml). Analyzes of ellipticine metabolites were performed by HPLC as described (Stiborova *et al.* 2004). Recoveries of ellipticine metabolites were around 95%.

Inhibition studies

The following chemicals were used to inhibit the activation of ellipticine in hepatic microsomes of male rats: α-naphthoflavone (α-NF), which inhibits CYP1A1 and 1A2, being more efficient to inhibit CYP1A1 (Rendic & DiCarlo 1997; Stiborova *et al.* 2005a,b), furafylline, which inhibits CYP1A2, ketoconazole, which inhibits CYP3A (Rendic & DiCarlo 1997; Ueng *et al.* 1997; Stiborova *et al.* 2005b) and indomethacin, which inhibits COX (Eling *et al.* 1992; Stiborova *et al.* 2005a). Inhibitors were dissolved in 7.5 µl of methanol, to yield final concentrations of 100 µM in the incubation mixtures used to asses DNA adducts formed by ellipticine (see above). Mixtures were then incubated at 37 °C for 10 min with NADPH prior to adding ellipticine, and then incubated for a further 30 min at 37 °C. After the incubation, DNA was isolated as mentioned above.

^{32}P-Postlabeling analysis and HPLC analysis of ^{32}P-labeled 3',5'-deoxyribonucleoside bisphosphate adducts

The ^{32}P-postlabeling of nucleotides using nuclease P1 enrichment procedure, found previously to be appropriate to detect and quantify ellipticine-derived DNA adducts formed *in vitro* (Stiborova *et al.* 2001, 2003c, 2004, 2007a, b) and *in vivo* (Stiborova *et al.* 2003a, 2007b, 2008), was employed in the experiments. The TLC and HPLC analyzes were done as reported recently (Stiborova *et al.* 2001, 2003a, c, 2004, 2007a, b).

RESULTS AND DISCUSSION

Hepatic, pulmonary and renal microsomes of rats are capable of activating ellipticine

To evaluate the role of the rat hepatic, pulmonary and renal CYPs and peroxidases in the activation of ellipticine, we performed *in vitro* experiments employing microsomes isolated from livers, lungs and kidneys of either control (untreated) rats or animals treated with 40 mg of ellipticine per kg of body weight.

The DNA adduct pattern generated by ellipticine activated with microsomes and NADPH, a cofactor of the NADPH:CYP reductase-dependent CYP enzyme system, consisted of one major and three minor adducts (see spots 1, 2, 6 and 7 in Figure 2), which were identical to those formed *in vivo* in rats treated with ellipticine (Figure 2C). Adducts spots 1 and 2 are products of 13-hydroxyellipticine (Figure 2D) and 12-hydroxyellipticine (Figure 2E) metabolites, respectively, generated by CYP and peroxidase (see scheme in Figure 1). Chromatographic analysis of spots 1 and 2 on

Tab. 1. DNA adduct formation by ellipticine activated with rat hepatic (A), pulmonary (B) and renal (C) microsomes

A	RAL[a] (mean/10^7 nucleotides)				
	Spot 1	Spot 2	Spot 6	Spot 7	Total
Untreated rats					
hepatic microsomes without cofactor	n.d.	0.08±0.01	n.d.	n.d.	0.08±0.01
hepatic microsomes + NADPH	6.84±1.31	0.26±0.03	0.29±0.02	0.28±0.03	17.6±1.39
hepatic microsomes + NADPH + a-NF	6.19±0.45	0.13±0.02	0.10±0.01	0.05±0.01	6.47±0.48
hepatic microsomes + NADPH + furafylline	7.91±0.62	0.12±0.02	0.19±0.02	0.08±0.01	8.30±0.69
hepatic microsomes + NADPH + ketoconazole	1.00±0.1	0.15±0.01	0.08±0.01	0.02±0.01	1.25±0.11
hepatic microsomes + arachidonic acid	1.01±0.1	0.015±0.01	0.017±0.01	0.017±0.01	1.06±0.12
hepatic microsomes + arachidonic acid + IM	0.22±0.02	n.d.	n.d.	n.d.	0.22±0.02
hepatic microsomes + H_2O_2	1.10 ±0.1	0.02±0.01	0.02±0.01	0.02±0.01	1.16±0.12
Rats treated with ellipticine (40 mg/kg b.w.)					
hepatic microsomes without cofactor	n.d.	0.11±0.01	n.d.	n.d.	0.11±0.01
hepatic microsomes + NADPH	33.03±2.52	0.42±0.03	0.40±0.03	0.48±0.03	34.4±2.87
hepatic microsomes + NADPH + a-NF	2.50±0.18	0.03±0.01	0.03±0.01	0.04±0.01	2.60±0.19
hepatic microsomes + NADPH + furafylline	6.28±0.51	0.08±0.01	0.07±0.01	0.07±0.01	6.50±0.59
hepatic microsomes + NADPH + ketoconazole	6.50±0.58	0.20±0.02	0.40±0.03	0.40±0.03	7.50±0.61
hepatic microsomes + arachidonic acid	0.87±0.06	0.08±0.01	0.10±0.01	0.10±0.01	1.15±0.10
hepatic microsomes + arachidonic acid + IM	0.17±0.01	0.02±0.01	0.02±0.01	0.02±0.01	0.23±0.02
hepatic microsomes + H_2O_2	0.92±0.07	0.08±0.01	0.12±0.01	0.10±0.01	1.23±0.10

B	RAL[a] (mean/10^7 nucleotides)				
	Spot 1	Spot 2	Spot 6	Spot 7	Total
Untreated rats					
lung microsomes without cofactor	0.03±0.01	0.03±0.01	0.03±0.01	0.02±0.01	0.11±0.01
lung microsomes + NADPH	0.64±0.04	0.15±0.01	0.12±0.01	0.10±0.01	1.01±0.10
lung microsomes + NADPH + a-NF	0.33±0.02	n.d.	n.d.	n.d.	0.33±0.03
lung microsomes + NADPH + ketoconazole	0.52±0.041	0.10±0.01	0.09±0.01	0.08±0.01	0.79±0.08
lung microsomes + arachidonic acid	0.03±001	0.03±0.01	0.30±0.03	0.14±0.01	0.50±0.05
lung microsomes + arachidonic acid + indomethacin	n.d.	n.d.	n.d.	n.d.	n.d.
Rats treated with ellipticine (40 mg/kg b.w.)					
lung microsomes without cofactor	0.60±0.04	0.03±0.01	0.20±0.02	0.10±0.01	0.93±0.11
lung microsomes + NADPH	1.92±0.17	0.30±0.03	0.22±0.02	0.20±0.02	2.64±0.19
lung microsomes + NADPH + a-NF	0.34±0.03	0.06±0.01	0.16±0.01	0.16±0.01	0.72±0.06
lung microsomes + NADPH + ketoconazole	1.05±0.10	0.25±0.02	0.20±0.02	0.20±0.02	1.70±0.15
lung microsomes + arachidonic acid	1.30±0.10	0.23±0.02	0.28±0.02	0.23±0.02	2.04±0.21
lung microsomes + arachidonic acid + indomethacin	0.60±0.05	0.03±0.01	0.10±0.01	0.05±0.01	1.15±0.10

C	RAL[a] (mean/10^7 nucleotides)				
	Spot 1	Spot 2	Spot 6	Spot 7	Total
Untreated rats					
kidney microsomes without cofactor	n.d.	0.004±0.001	0.01±0.01	0.01±0.01	0.02±0.01
kidney microsomes + NADPH	0.21±0.02	0.03±0.01	0.08±0.01	0.03±0.01	0.35±0.04
kidney microsomes + NADPH + a-NF	0.04±0.01	n.d.	n.d.	n.d.	0.04±0.01
kidney microsomes + NADPH + ketoconazole	0.10±0.01	0.02±0.01	0.08±0.01	0.05±0.01	0.23±0.03
kidney microsomes + arachidonic acid	n.d.	n.d.	0.02±0.01	0.02±0.01	0.04±0.01
kidney microsomes + arachidonic acid + indomethacin	n.d.	n.d.	n.d.	n.d.	n.d..
Rats treated with ellipticine (40 mg/kg b.w.)					
kidney microsomes without cofactor	0.12±0.01	0.03±0.01	0.05±0.01	0.03±0.01	0.33±0.04
kidney microsomes + NADPH	0.42±0.03	0.12±0.01	0.08±0.01	0.05±0.01	0.67±0.07
kidney microsomes + NADPH + a-NF	0.23±0.02	0.09±0.01	0.05±0.01	0.03±0.01	0.40±0.04
kidney microsomes + NADPH + ketoconazole	0.40±0.03	0.10±0.01	0.08±0.01	0.05±0.01	0.63±0.08
kidney microsomes + arachidonic acid	0.20±0.02	0.06±0.01	0.08±0.01	0.06±0.01	0.40±0.05
kidney microsomes + arachidonic acid + indomethacin	0.10±0.01	0.04±0.01	0.04±0.01	0.02±0.01	0.20±0.03

Experimental conditions are described in Materials and methods. Mean RAL ± standard deviations shown in the figure represent DNA adducts of three parallel *in vitro* incubations. ND, not detectable (the detection limit of RAL was 1 adducts/10^{10} nucleotides).

HPLC confirmed that these adducts are derived from 13-hydroxy- and 12-hydroxyellipticine, respectively, by their coelution with prepared reference compounds (data not shown). Additional minor DNA adducts formed by ellipticine are adducts 6 and 7 (Figure 2). The low levels of these adducts prevented HPLC co-chromatographic analysis or their further characterization. Control incubations without enzyme cofactors, but in the presence of hepatic microsomes, were free of adduct spots 1, 6 and 7, but adduct spot 2 was always detected (Table 1). However, in control incubations containing renal and pulmonary microsomes without enzyme cofactors, ellipticine-derived DNA adducts 1, 2, 6 and 7 were found (Table 1B,C). This finding indicates that other enzymes than only CYPs dependent on NADPH:CYP reductase might activate ellipticine in lung and kidney. This is consistent with results found in our former study with the HRN (Hepatic Cyto-

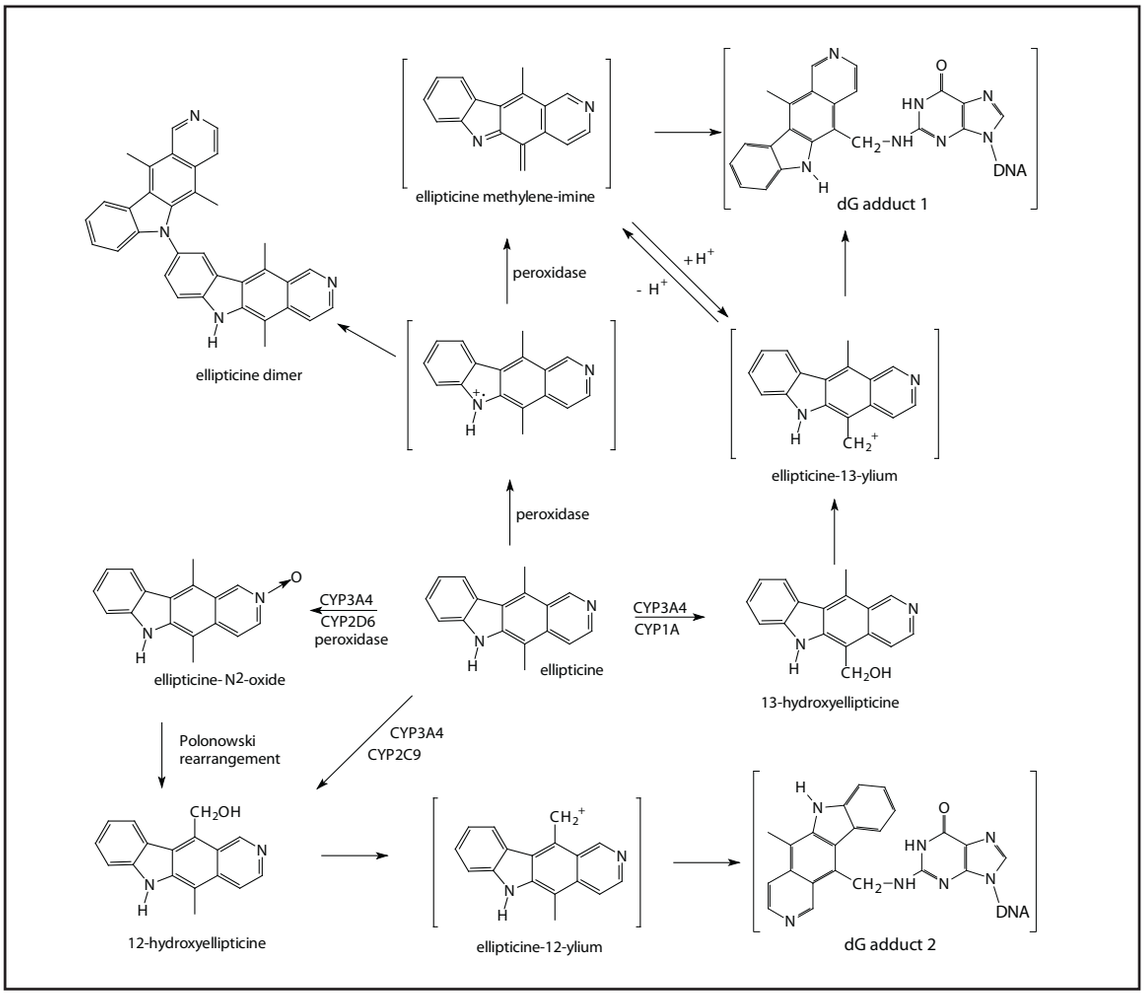

Fig. 1. Metabolism of ellipticine by peroxidases and human CYPs showing the characterized metabolites and those proposed to form DNA adducts. The compounds shown in brackets were not detected under the experimental conditions and are the electrophilic metabolites postulated as ultimate arylating species or the postulated N^2-deoxyguanosine adducts.

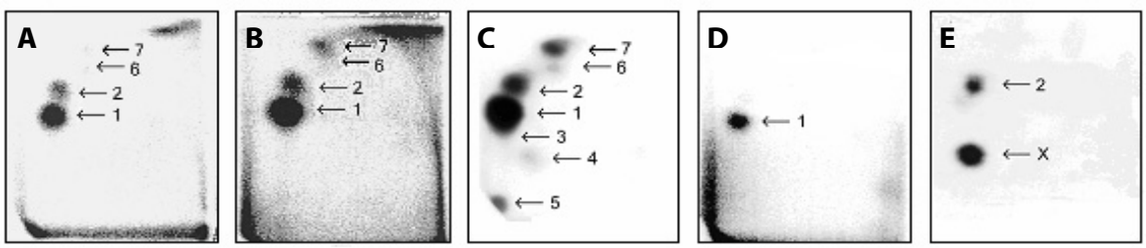

Figure 2. Autoradiographic profile of DNA adducts generated in calf thymus DNA by ellipticine after its activation with hepatic microsomes of untreated (A) and ellipticine-treated (40 mg/kg) male rats (B), of ^{32}P-labeled digests of DNA from liver of male rats treated with the same dose of ellipticine (C), from calf thymus DNA reacted with 13-hydroxyellipticine (D) or 12-hydroxyelipticine (E). Analyses were performed by the nuclease P1 version of the ^{32}P-postlabeling assay.

chrome P450 Reductase Null) mouse model, in which NADPH:CYP reductase is deleted specifically in hepatocytes, resulting in the loss of essentially all hepatic CYP function (Stiborova *et al.* 2008), which indicate that ellipticine activation should, at least partially, be catalyzed also by enzymes, whose activities are not dependent on NADPH:CYP reductase (Stiborova *et al.* 2008). Besides peroxidases that were found to activate ellipticine (Stiborova *et al.* 2007a), the CYP2S1 enzyme, which is abundantly expressed in several tissues (Saarikoski *et al.* 2005; Downie *et al.* 2005; Bui *et al.* 2009a) might be such an enzyme. Namely, it was shown that it catalyzes the oxidation of compounds having polycyclic aromatic structures similar to ellipticine without participation of NADPH:CYP reductase (Bui *et al.* 2009a,b). While a role of peroxidases is investigated in this study, the participation of CYP2S1 in ellipticine activation still awaits further examination. Therefore, the efficiency of

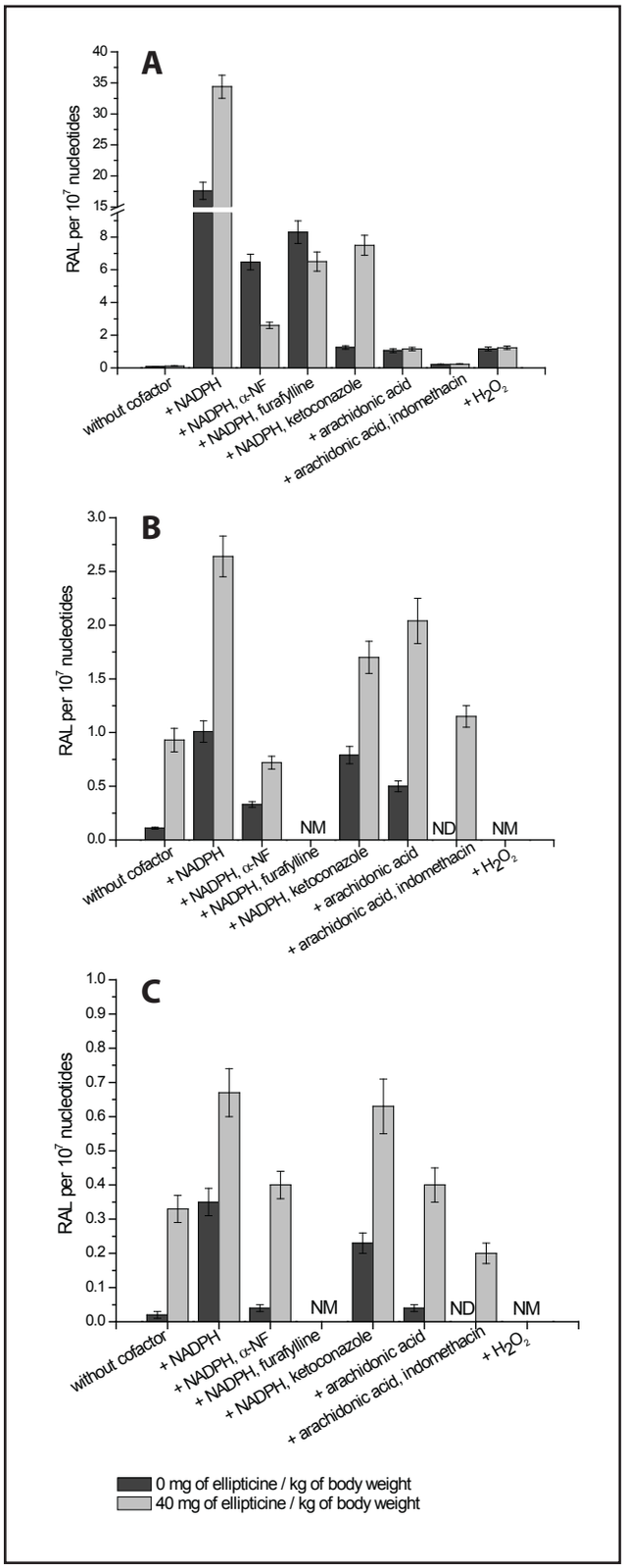

Fig. 3. DNA adduct formation by ellipticine activated with microsomes isolated from livers (**A**), lungs (**B**) and kidneys (**C**) of rats, control (uninduced) or pretreated with 40 mg/kg ellipticine and the effect of inhibitors of CYP1A, 3A and COX on ellipticine-DNA adduct formation in these microsomes. Mean RAL ± standard deviations shown in the figure represent total levels of DNA adducts of three parallel *in vitro* incubations. ND, not detectable (the detection limit of RAL was 1 adducts/10^{10} nucleotides). NM, not measured.

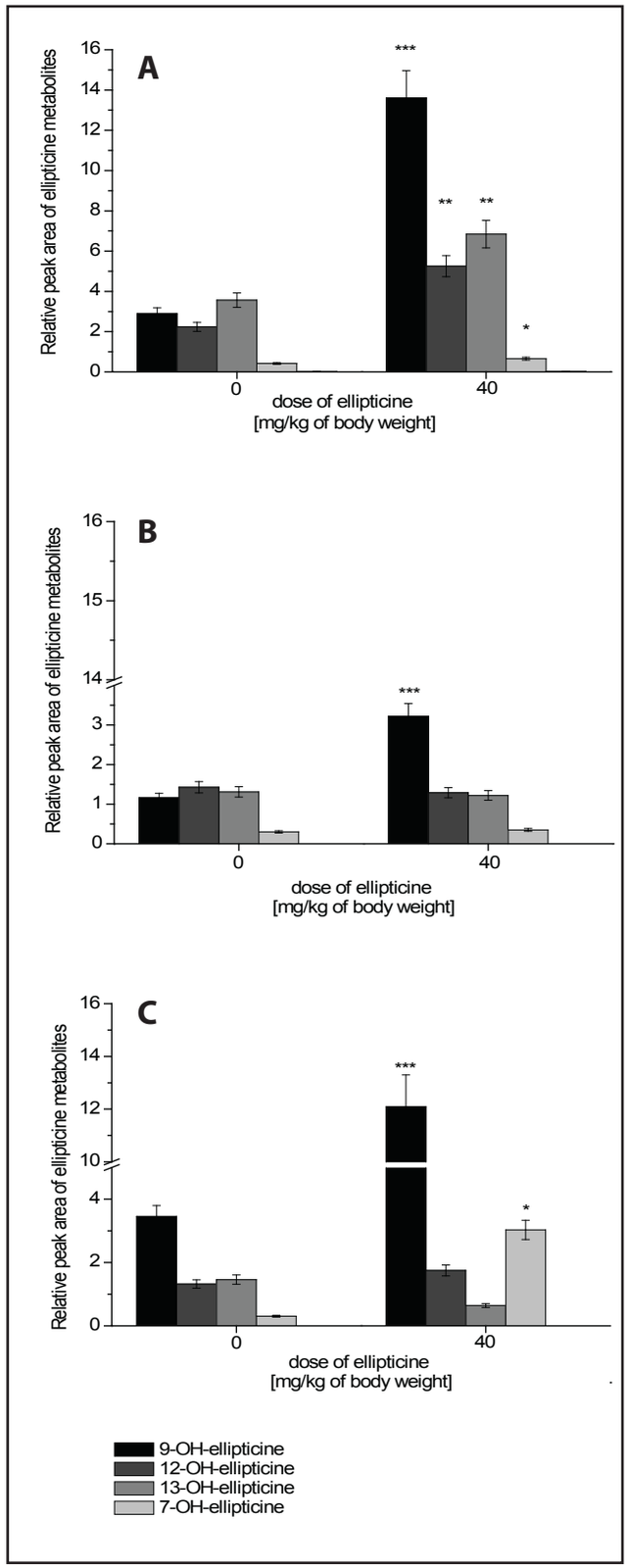

Fig 4. Ellipticine metabolism in rat liver (**A**), lung (**B**) and kidney microsomes (**C**) of control animals and those treated with 40 mg/kg ellipticine. Microsomes containing 0.2 mg microsomal protein, and 10 μM ellipticine were used in all experiments. Levels of ellipticine metabolites are averages ± standard deviations of triplicate incubations. Values significantly different from control: *$p<0.05$, **$p<0.01$, ***$p<0.001$ (Student's t-test).

CYP2S1 to oxidize ellipticine is planned to be investigated in our future work.

In order to evaluate the contribution of CYP1A, 3A and peroxidases, found previously to activate ellipticine *in vitro* (Stiborova *et al.* 2001, 2003b, 2004, 2008), to ellipticine activation in liver, lung and kidney, we investigated the modulation of ellipticine-DNA adduct formation by cofactors and selective inhibitors of these enzymes. Among microsomes of control (untreated) rats and those of rats pre-treated with ellipticine tested in this study, hepatic microsomes in the presence of NADPH were the most effective in activation of ellipticine. Pulmonary and renal microsomes also activated ellipticine to species forming DNA adducts, but they were more than 17- and 50-fold less efficient than microsomes isolated from livers (Figure 3, Table 1).

In the presence of NADPH, hepatic, pulmonary and renal microsomes isolated from rats treated with ellipticine were up to 2.6-fold more effective to form ellipticine-derived DNA adducts than microsomes of control (untreated) rats (Figure 3, Table 1).

In hepatic, pulmonary and renal microsomes of control (untreated) rats, ketoconazole, a selective inhibitor of CYP3A enzymes (Rendic & DiCarlo 1997; Ueng *et al.* 1997; Stiborova *et al.* 2005b), inhibited formation of ellipticine-DNA adducts mediated by the NADPH-dependent enzymatic system, by 93, 22 and 34 %, respectively (Figure 3, Table 1). However, in microsomes of rats treated with ellipticine, the impact of this inhibitor to decrease ellipticine activation to species forming DNA adducts was lower in liver and kidney. In this case, ketoconazole inhibited formation of ellipticine-derived DNA adducts by 78 and 6 % in liver and kidney, respectively (Table 1). Such findings indicate that treating rats with ellipticine shifts the CYP enzyme expression in livers and kidney to another pattern where CYP3A enzymes have lower impact on activation of this drug. Indeed, CYP1A enzymes are induced by ellipticine on mRNA and protein levels in all these tissues (Aimova *et al.* 2007), thereby increasing their own participation in ellipticine metabolism (see below).

α-Naphthoflavone (α-NF), an inhibitor of CYP1A1 and 1A2 (Rendic & DiCarlo 1997), decreased the levels of ellipticine-DNA adducts generated by hepatic, pulmonary and renal microsomes of both control and ellipticine-treated rats, but also to a different extent (Figure 3, Table 1). In hepatic and pulmonary microsomes of rats treated with ellipticine, α-NF was much more efficient to inhibit ellipticine-DNA adduct formation than in those of control rats (Table 1). Microsomes of rat kidneys were, however, the exception; α-NF was efficient inhibitor of DNA adduct formation by ellipticine also in control rats (Figure 3, Table 1). Furafylline, an inhibitor of CYP1A2 (Rendic & DiCarlo 1997), was also efficient compound decreasing activation of ellipticine by hepatic microsomes (Figure 3, Table 1). This inhibitor was, however, not tested using pulmonary and renal microsomes, because of low expression of CYP1A2 in these organs. The results found using the CYP1A inhibitors point to CYP1A enzymes as having a role in ellipticine-DNA adduct formation in rat livers, lungs and kidneys. Depending on their expression levels, they activate ellipticine to species binding to DNA. In addition, all these results indicate that in organisms treated with ellipticine, these CYP enzymes might play, because of CYP1A induction, the predominant role in the ellipticine anticancer activity based on covalent modification of DNA in target tissues.

Arachidonic acid and/or hydrogen peroxide, cofactors for peroxidase (COX)-dependent oxidation (Eling *et al.* 1990; 1992; Stiborova *et al.* 2004; 2005a; Arlt *et al.* 2006), mediated formation of DNA adducts by ellipticine in hepatic, pulmonary and renal microsomes, being increased by treating rats with ellipticine, mainly in lung (Table 1). Since COX cofactors were much less effective than NADPH in livers (Figure 3, Table 1), contribution of this enzyme to ellipticine activation in this organ is lower than that of CYPs. On the contrary, the results showing the effect of arachidonic acid and a COX inhibitor, indomethacin, on ellipticine-derived DNA adduct formation in microsomes of extrahepatic tissues indicate that COX is capable of effective ellipticine activation in these organs. It even more efficiently contributes to activation of ellipticine in these tissues of rats treated with ellipticine than in those of control (untreated) rats. Levels of adducts formed by microsomes of lung and kidney of rats treated with ellipticine in the presence of arachidonic acid were high; they represented 77 and 59 % of adduct levels formed by lung and kidnay microsomes in the presence of NADPH, respectively (Table 1). Therefore, this finding suggests a relatively high contribution COX to ellipticine activation in lung and kidney of organisms treated with this anticancer drug.

Ellipticine as a CYP inducer increases efficiencies of rat hepatic, pulmonary and renal microsomes to oxidize ellipticine to its hydroxylated metabolites

Ellipticine is oxidized by hepatic, pulmonary and renal microsomes to four metabolites, 7-hydroxy-, 9-hydroxy-, 12-hydroxy and 13-hydroxyellipticine (Figure 4). Ellipticine N^2-oxide was also produced, but this metabolite was not quantitated because of its spontaneous rearrangement to 12-hydroxyellipticine.

The increase in levels of ellipticine-DNA adducts (Figure 3, Table 1) correlates with an increase in ellipticine oxidation by hepatic microsomes isolated from rats treated with ellipticine (Figure 4). Besides an increase in oxidation of ellipticine to 9-hydroxyellipticine and 7-hydroxyellipticine, which was expected, because these metabolites are predominantly formed by CYP1A1/2 (Stiborova *et al.* 2004; Kotrbova *et al.* 2006), an up to 2-fold increase in formation of 13-hydroxy- and 12-hydroxyellipticine, the metabolites generating DNA adducts 1 and 2, was found in hepatic microsomes (Figure 4). This finding can be

caused by a strong induction not only of CYP1A1/2 (Aimova *et al.* 2007), but also of CYP3A in livers of rats treated with ellipticine. Indeed, induction of CYP3A4 by ellipticine has recently been found in glioblastoma U87MG cells (Martinkova *et al.* 2009). In addition, ellipticine might also influence expression of another protein, cytochrome b_5 (Stiborova *et al.* unpublished results), which is a component of the CYP microsomal system modulating the enzymatic activities of several CYPs, including CYP3A4 (for a summary see Schenkman *et al.* 2003) and CYP1A1 (Stiborova *et al.* 2006b). Hence, its expression might also cause higher formation of 13-hydroxy- and 12-hydroxyellipticine, thereby increasing the formation of ellipticine-DNA adducts.

In contrast to liver microsomes, no increase in formation of 13-hydroxy- and 12-hydroxyellipticine was found during oxidation of ellipticine catalyzed by lung and kidney nicrosomes of rats treated with ellipticine (Figure 4). Only an increase in oxidation of ellipticine to 9-hydroxyellipticine and/or 7-hydroxyellipticine was found in lung and kidney (Figure 4). Because a more than 4- and 10-fold increase in arachidonic acid (COX)-mediated activation of ellipticine was found in lung and kidney microsomes, respectively, as compared to activation of ellipticine by liver microsomes (Table 1), the peroxidase activity of COX might be responsible for increased formation of ellipticine metabolites generating DNA adducts in these extrahepatic tissues. The question whether ellipticine might also act as an inducer of COX enzymes such as an inducible COX-2 enzyme (Soslow *et al.* 2000; Matsuo *et al.* 2001; Shono *et al.* 2001), remains to be answered.

CONCLUSIONS

The results found in this study shed more light on our previous data, showing the importance of CYP and peroxidase enzymes in ellipticine activation *in vivo* (Stiborova *et al.* 2003c; 2007a,b; 2008). The importance of CYP1A and 3A enzymes in ellipticine-derived DNA adduct formation *in vitro* and *in vivo* has already been demonstrated previously (Stiborova *et al.* 2001; 2003a; 2004; 2007a,b; 2008). Here, we show that these enzymes play a major role in ellipticine activation in the liver. However, because of their lower expression in extrahepatic organs such as lung and kidney, even after their induction by ellipticine (Aimova *et al.* 2007), they play a minor role in ellipticine activation in these extrahepatic tissues. Arachidonic acid (COX)-mediated ellipticine activation has the higher impact in this process in rat lung and kidney, predominantly after treatment of rats with ellipticine. The results also show that enzymatic activity of COX to catalyze ellipticine activation was increased in extrahepatic organs by treating rats with ellipticine. One of the COX enzymes, COX-2, was demonstrated in multiple cancer types (i.e. carcinomas and brain tumors) known to be the targets for ellipticine treatment and is even inducible by carcinogenic processes and/or by several compounds, including anticancer drugs (Soslow *et al.* 2000; Matsuo *et al.* 2001; Shono *et al.* 2001). Because of efficiency of COX-2 to mediate formation of ellipticine-derived DNA adducts *in vitro* (Stiborova *et al.* 2007a) and the results found in this work (Table 1), its participation in ellipticine activation in cells of the extrahepatic tissues, including cancer cells should be taken into account. The study of the effect of ellipticine on COX-2 expression in healthy and cancer tissues of animal models and/or cancer cells in culture is therefore under way in our laboratory.

ACKNOWLEDGEMENTS

This work was supported in part by the Grant Agency of the Czech Republic, grants P301/10/0356 and 305/09/H008, the Ministry of Education of the Czech Republic, grants MSM0021620808 and 1M0505, Grant Agency of Charles University, grants 258188, 127208 and the German Cancer Research Center.

REFERENCES

1 Aimova D, Svobodova L, Kotrbova V, Mrazova B, Hodek P, Hudecek J, *et al.* (2007). The anticancer drug ellipticine is a potent inducer of rat cytochromes P450 1A1 and 1A2, thereby modulating its own metabolism. Drug Metab Dispos. 35: 1926–1934.
2 Arlt VM, Henderson CJ, Wolf CR, Schmeiser HH, Phillips DH and Stiborova M (2006). Bioactivation of 3-aminobenzanthrone, a human metabolite of the environmental pollutant 3-nitrobenzanthrone: evidence for DNA adduct formation mediated by cytochrome P450 enzymes and peroxidases. Cancer Lett. 234: 220–231.
3 Auclair C (1987). Multimodal action of antitumor agents on DNA: The ellipticine series. Arch Biochem Biophys. **259**: 1–14.
4 Boogaard AT, Pandit UK and Koomen GJ (1994). Ring-D modifications of ellipticine. 2. Chlorination of ellipticine via its *N*-oxide and synthesis and selective acetylation of 5,6,11-trimethyl-5*H* benzo[*B*]carbazole. Tetrahedron 50: 4811–4828.
5 Borek-Dohalska L, Frei E and Stiborova M (2004). DNA adduct formation by the anticancer drug ellipticine and its hydroxy derivatives in human breast adenocarcinoma MCF-7 cells. Collect Czech Chem Commun. **69**: 603–615.
6 Bui PH and Hankinson O (2009a). Functional characterization of human cytochrome P450 2S1 using a synthetic gene-expressed protein in *Escherichia coli*. Mol Pharmacol. **76**: 1031–1043.
7 Bui PH, Hsu EL and Hankinson O (2009b). Fatty acid hydroperoxides support cytochrome P450 2S1-mediated bioactivation of benzo[a]pyrene-7,8-dihydrodiol, Mol Pharmacol. **76**: 1044–1052.
8 Culp SJ, Roberts DW, Talaska G, Lang NP, Fu PP, Lay JO Jr, *et al.* (1997). Immunochemical, ^{32}P-postlaeling, and GC/MS detection of 4-aminobiphenyl-DANN adducts in human peripheral lung in relation to metabolic activation pathways involving pulmonary *N*-oxidation, conjugation, and peroxidation. Mutat Res. **378**: 97–112.
9 Downie SD, McFadyen MC, PH Rooney PH, Cruickshank ME, Parkin DE, Miller ID, *et al.* (2005). Profiling cytochrome P450 expression in ovarian cancer: identification of prognostic markers. Clin Cancer Res. **11**: 7369–7735.
10 Eling TE, Thompson DC, Foureman GL, Curtis JF and Hughes MF (1990). Prostaglandin H synthase and xenobiotic oxidation. Annu Rev Pharmacol Toxicol. **30**: 1–45.
11 Eling TE and Curtis JF (1992). Xenobiotic metabolism by prostaglandin H synthase. Pharm Ther. **53**: 261–273.

12 Frei E, Bieler CA, Arlt VM, Wiessler M and Stiborova M (2002). Covalent binding of the anticancer drug ellipticine to DNA in V79 cells transfected with human cytochrome P450 enzymes. Biochem Pharmacol. **64**: 289–295.
13 Garbett NC and Graves DE (2004). Extenting nature's leads: the anticancer agent ellipticine. Curr Med Chem Anti-Cancer Agents **4**: 149–72.
14 Gasiewicz TA, Kende RS, Rucci G, Whitney B and Willey JJ (1996). Analysis of structural requirements for Ah receptor antagonist activity: Ellipticines, flavones, and related compounds. Biochem Pharmacol. **52**: 1787–830.
15 Kotrbova V., Aimova D., Brezinova A., Janouchova K.., Poljakova J., Hodek P., *et al.* (2006). Cytochromes P450 reconstituted with NADPH:P450 reductase mimic the activating and detoxicating metabolism of the anticancer drug ellipticine in microsomes. Neuro Endocrinol Lett., **27** (Suppl. 2): 18–20.
16 Kuo PL, Hsu YL, Chang CH and Lin CC (2005a). The mechanism of ellipticine-induced apoptosis and cell cycle arrest in human breast MCF-7 cancer cells. Cancer Lett. **223**: 293–301.
17 Kuo PL, Hsu YL, Kuo YC, Chang CH and Lin CC (2005b). The antiproliferative inhibition of ellipticine in human breast mda-mb-231 cancer cells is through cell cycle arrest and apoptosis induction. Anti-Cancer Drugs **16**: 789–795.
18 Kuo PL, Kuo YC, Hsu YL, Cho CY and Lin CC (2006). Ellipticine induced apoptosis through p53-dependent pathway in human hepatocellular carcinoma HepG2 cells. Life Sci. **78**: 2550–2557.
19 Martinkova E, Dontenwill M, Frei E and Stiborova M (2009). Cytotoxicity of and DNA adduct formation by ellipticine in human U87MG glioblastoma cancer cells. Neuro Endocrinol Lett. **30** (Suppl): 60–66.
20 Martinkova E, Maglott A, Leger, DY, Bonnet D, Stiborova M, Takeda K, *et al.* (2010). α5β1 integrin antagonists reduce chemotherapy-induced premature senescence and facilitate apoptosis in human glioblastoma cells. Int J Cancer **127**: 1240–1248.
21 Matsuo M, Yonemitsu N, Zaitsu M, Ishii K, Hamasaki Y, Fukuyama K, *et al.* (2001). Expression of prostaglandin H synthase-2 in human brain tumors. Acta Neuropathol. **102**: 181–187.
22 Moserova M, Kotrbova V, Rupertova M, Naiman K, Hudecek J, Hodek P, *et al.* (2008). Isolation and partial characterization of the adduct formed by 13-hydroxyellipticine with deoxyguanosine in DNA. Neuro Endocrinol Lett. **29**: 728–732.
23 Ohashi M, Sugikawa E and Nakanishi N (1995). Inhibition of p53 protein phosphorylation by 9-hydroxyellipticine: A possible anticancer mechanism. Jpn J Cancer Res. **86**: 819–829.
24 Omura T and Sato R (1964). The carbon monoxide-binding pigment of liver microsomes. I. Evidence for its hemoprotein nature. J Biol Chem. **239**: 2370–2378.
25 Poljakova J, Dracinsky M, Frei E., Hudecek J and Stiborova M (2006). The effect of pH on peroxidase-mediated oxidation of and DNA-adduct formation by ellipticine. Collect Czech Chem Commun. **71**: 1169–1185.
26 Poljakova J, Frei E, Gomez JE, Aimova D, Eckschlager T, Hrabeta J, *et al.* (2007). DNA adduct formation by the anticancer drug ellipticine in human leukemia HL-60 and CCRF-CEM cells. Cancer Lett. **252**: 270–279.
27 Poljakova J, Eckschlager T, Hrabeta J, Hrebackova J, Smutny S, Frei E, *et al.* (2009). The mechanism of cytotoxicity and DNA adduct formation by the anticancer drug ellipticine in human neuroblastoma cells. Biochem Pharmacol. **77**: 1466–1479.
28 Rendic S and DiCarlo FJ (1997). Human cytochrome P450 enzymes: A status report summarizing their reactions, substrates, inducers, and inhibitors. Drug Metab Rev. **29**: 413–480.
29 Saarikoski T, Rivera SP, Hankinson O and Husgafvel-Pursiainen K (2005). CYP2S1: a short review, Toxicol Appl Pharmacol. **207** (Suppl. 2): 62–69.
30 Schenkman JB and Jansson I (2003). The many roles of cytochrome b_5, Pharmacol Ther. **97**: 139–152.
31 Shono T, Tofilon PJ, Bruner JM, Owolabi O and Lang FF (2001). Cyclooxygenase-2 expression in human gliomas: Prognostic significance and molecular correlations. Cancer Res. **61**: 4375–4381.
32 Soslow RA, Dannenberg AJ, Rush D, Woemer BM, Khan KM, Masferrerer J, *et al.* (2000). COX-2 is expressed in human pulmonary, colonic, and mammary tumors. Cancer **89**: 2637–2645.
33 Stiborova M, Frei E, Schmeiser HH and Anzenbacher P (1991). The role of peroxidases in the activation of chemical carcinogens. Drug Metabol Interact. **9**: 177–190.
34 Stiborova M, Bieler CA, Wiessler M and Frei E (2001). The anticancer agent ellipticine on activation by cytochrome P450 forms covalent DNA adducts. Biochem Pharmacol. **62**: 675–684.
35 Stiborova M, Breuer A, Aimova D, Stiborova-Rupertova M, Wiessler M and Frei E (2003a). DNA adduct formation by the anticancer drug ellipticine in rats determined by ^{32}P-postlabeling. Int J Cancer **107**: 885–890.
36 Stiborova M, Stiborova-Rupertova M, Borek-Dohalska L, Wiessler M and Frei E (2003b). Rat microsomes activating the anticancer drug ellipticine to species covalently binding to deoxyguanosine in DNA are a suitable model mimicking ellipticine bioactivation in humans. Chem Res Toxicol. **16**: 38–47.
37 Stiborova M, Sejbal J, Borek-Dohalska L, Poljakova J, Forsterova K, Rupertova M *et al.* (2004). The anticancer drug ellipticine forms covalent DNA adducts, mediated by human cytochromes P450, through metabolism to 13-hydroxyellipticine and ellipticine N^2-oxide. Cancer Res. **64**: 8374–8380.
38 Stiborova M, Frei E, Hodek P, Wiessler M and Schmeiser HH (2005a). Human hepatic and renal microsomes, cytochromes P450 1A1/2, NADPH:cytochrome P450 reductase and prostaglandin H synthase mediate the formation of aristolochic acid-DNA adducts found in patients with urothelial cancer. Int J Cancer **113**: 189–197.
39 Stiborova M, Martinek V, Rydlova H, Koblas T and Hodek P (2005b). Expression of cytochrome P450 1A1 and its contribution to oxidation of a potential human carcinogen 1-phenylazo-2-naphthol (Sudan I) in human livers. Cancer Lett. 220: 145–154.
40 Stiborova M, Borek-Dohalska L, Kotrbova V, Kukackova K, Janouchova K, Rupertova M, *et al.* (2006a). Oxidation pattern of the anticancer drug ellipticine by hepatic microsomes – Similarity between human and rat systems. Gen Physiol Biophys. **25**: 245–61.
41 Stiborova M, Martinek V, Schmeiser HH and Frei E (2006b). Modulation of CYP1A1-mediated oxidation of carcinogenic azo dye Sudan I and its binding to DNA by cytochrome b_5. Neuro Endocrinol Lett. **27** (Suppl 2): 35–39.
42 Stiborova M, Rupertova M, Schmeiser HH and Frei E (2006c). Molecular mechanism of antineoplastic action of an anticancer drug ellipticine. Biomed Pap Med Fac Univ Palacky Olomouc Czech Repub. **150**: 13–23.
43 Stiborova M, Poljakova J, Ryslava H, Dracinsky M, Eckschlager T and Frei E (2007a). Mammalian peroxidases activate anticancer drug ellipticine to intermediates forming deoxyguanosine adducts in DNA identical to those found *in vivo* and generated from 12-hydroxyellipticine and 13-hydroxyellipticine. Int J Cancer **120**: 243–251.
44 Stiborova M, Rupertova M, Aimova D, Ryslava H and Frei E (2007b). Formation and persistence of DNA adducts of anticancer drug ellipticine in rats. Toxicology **236**: 50–60.
45 Stiborova M, Arlt VM, Henderson CJ, Wolf CR, Kotrbova V, Moserova M, *et al.* (2008). Role of hepatic cytochromes P450 in bioactivation of the anticancer drug ellipticine: studies with the hepatic NADPH:cytochrome P450 reductase null mouse. Toxicol Appl Pharmacol. **226**: 318–27.
46 Stiborova M, Rupertova M and Frei E (2010). Cytochrome P450- and peroxidase-mediated oxidation of anticancer alkaloid ellipticine dictates its anti-tumor efficiency. Biochim Biophys Acta, in press.
47 Sugikawa E, Hosoi T, Yazaki N, Gamanuma N, Nakanishi N and Ohashi M (1999). Mutant p53 mediated induction of cell cycle arrest and apoptosis at G1 phase by 9-hydroxyellipticine. Anticancer Res. **19**: 3099–3108.
48 Ueng Y-F, Kuwabara T, Chun Y-J and Guengerich FP (1997). Cooperativity in oxidation catalyzed by cytochrome P450 3A4. Biochemistry **36**: 370–381.
49 Wiechelman KJ, Braun RD and Fitzpatrick JD (1988). Investigation of the bicinchoninic acid protein assay: identification of the groups responsible for color formation. Anal Biochem **175:** 231–237.
50 Wijsmuller WFA, Warner MJ, Koonen GI, and Pandit UK (1986). Pyridocarbazole alkaloids. Synthesis of olivacine and ellipticine analogues. Heterocycles **24**: 1795–1797.

Příloha 7

KATEŘINA LEVOVÁ, **MICHAELA MOSEROVÁ,** VĚRA KOTRBOVÁ, MIROSLAV ŠULC, COLIN J. HENDERSON, ROLAND C. WOLF, DAVID H. PHILLIPS, EVA FREI, HEINZ H. SCHMEISER, JAN MAREŠ, MARIE STIBOROVÁ:

ROLE OF CYTOCHROMES P450 1A1/2 IN DETOXICATION AND ACTIVATION OFCARCINOGENIC ARISTOLOCHIC ACID I: STUDIES WITH THE NADPH:CYTOCHROMO P450 REDUCTASE NULL (HRN) MOUSE MODEL.

Toxicol Sci., 121(1):43-56, 2011

TOXICOLOGICAL SCIENCES **121(1)**, 43–56 (2011)
doi:10.1093/toxsci/kfr050
Advance Access publication February 28, 2011

Role of Cytochromes P450 1A1/2 in Detoxication and Activation of Carcinogenic Aristolochic Acid I: Studies with the Hepatic NADPH:Cytochrome P450 Reductase Null (HRN) Mouse Model

Kateřina Levová,* Michaela Moserová,* Věra Kotrbová,* Miroslav Šulc,* Colin J. Henderson,† C. Roland Wolf,† David H. Phillips,‡ Eva Frei§ Heinz H. Schmeiser,¶ Jaroslav Mareš,‖ Volker M. Arlt,‡ and Marie Stiborová*,[1]

*Department of Biochemistry, Faculty of Science, Charles University, Albertov 2030, 12840 Prague 2, Czech Republic; †Cancer Research UK Molecular Pharmacology Unit, Biomedical Research Institute, Dundee DD1 9SY, UK; ‡Section of Molecular Carcinogenesis, Institute of Cancer Research, Sutton, Surrey SM2 5NG, UK; §Division of Preventive Oncology, National Center for Tumour Diseases, German Cancer Research Center, 69120 Heidelberg, Germany; ¶Research Group Genetic Alterations in Carcinogenesis, German Cancer Research Center, 69120 Heidelberg, Germany; and; and ‖Institute of Biology and Medical Genetics, 2nd Medical School, Charles University and University Hospital Motol, V Úvalu 84, 150 06 Prague 5, Czech Republic

[1]To whom correspondence should be addressed. Fax: +420-2-21951283. E-mail: stiborov@natur.cuni.cz.

Received January 13, 2011; accepted February 18, 2011

Aristolochic acid (AA) causes aristolochic acid nephropathy, Balkan endemic nephropathy, and their urothelial malignancies. To identify enzymes involved in the metabolism of aristolochic acid I (AAI), the major toxic component of AA we used HRN (hepatic cytochrome P450 [Cyp] reductase null) mice, in which NADPH:Cyp oxidoreductase (Por) is deleted in hepatocytes. AAI was demethylated by hepatic Cyps *in vitro* to 8-hydroxy-aristolochic acid I (AAIa), indicating that less AAI is distributed to extrahepatic organs in wild-type (WT) mice. Indeed, AAI-DNA-adduct levels were significantly higher in organs of HRN mice, having low hepatic AAI demethylation capacity, than in WT mice. Absence of AAI demethylation in HRN mouse liver was confirmed *in vitro*; hepatic microsomes from WT, but not from HRN mice, oxidized AAI to AAIa. To define the role of hepatic Cyps in AAI demethylation, modulation of AAIa formation by CYP inducers was investigated. We conclude that AAI demethylation is attributable mainly to Cyp1a1/2. The higher AAI-DNA adduct levels in HRN than WT mice were the result of the lack of hepatic AAI demethylation concomitant with a higher activity of cytosolic NAD(P)H:quinone oxidoreductase (Nqo1), which activates AAI. Mouse hepatic Cyp1a1/2 also activated AAI to DNA adducts under hypoxic conditions *in vitro*, but in renal microsomes, Por and Cyp3a are more important than Cyp1a for AAI-DNA adduct formation. We propose that AAI activation and detoxication in mice are dictated mainly by AAI binding affinity to Cyp1a1/2 or Nqo1, by their turnover, and by the balance between oxidation and reduction of AAI by Cyp1a.

Key Words: **aristolochic acid; cytochrome P450; metabolism; DNA adducts; ^{32}P-postlabeling.**

The cytochrome P450 (CYP) superfamily consists of a large number of haem-containing mono-oxygenases that play a pivotal role in the metabolism of many drugs and carcinogens (Nebert and Dalton, 2006). Vital information on CYP regulation and function has been obtained by *in vitro* studies, however, for extrapolation from *in vitro* data to *in vivo* pharmacokinetics, additional factors such as route of administration, absorption, renal clearance, and tissue-specific CYP expression need to be considered (Nebert, 2006). Gene knockout and transgenic mice have been developed to study the role of specific enzymes in drug metabolism (Henderson *et al.*, 2003b). Although knockout mouse models have yielded important data on the effect of single Cyp enzymes on the metabolism of drugs and chemical carcinogens (Buters *et al.*, 1999; Kimura *et al.*, 2003; Tsuneoka *et al.*, 2003; Uno *et al.*, 2004), the functional redundancy inevitably found in the large CYP family of isoenzymes make it difficult to determine the role of CYPs as a whole in the metabolism of xenobiotics (Henderson *et al.*, 2006). To overcome these limitations a mouse line, HRN (hepatic cytochrome P450 reductase null), has been developed in which Cyp oxidoreductase (Por), the important electron donor to Cyps, is deleted specifically in hepatocytes, resulting in the loss of essentially all hepatic Cyp function (Henderson *et al.*, 2003a). The HRN mouse model has been used successfully to establish the role of hepatic versus extrahepatic Cyp-mediated xenobiotic metabolism and disposition (Arlt *et al.*, 2005, 2006, 2008; Pass *et al.*, 2005; Stiborová *et al.*, 2008a).

The herbal drug aristolochic acid (AA) derived from Aristolochia species has been shown to be the cause of so-called Chinese herbs nephropathy (CHN), now termed aristolochic acid nephropathy (AAN) (Debelle *et al.*, 2008; Schmeiser *et al.*, 2009). The plant extract AA is a mixture of structurally related nitrophenanthrene carboxylic acids, the major components being aristolochic acid I (AAI; Fig. 1) and aristolochic acid II. AAN is a rapidly progressive renal fibrosis

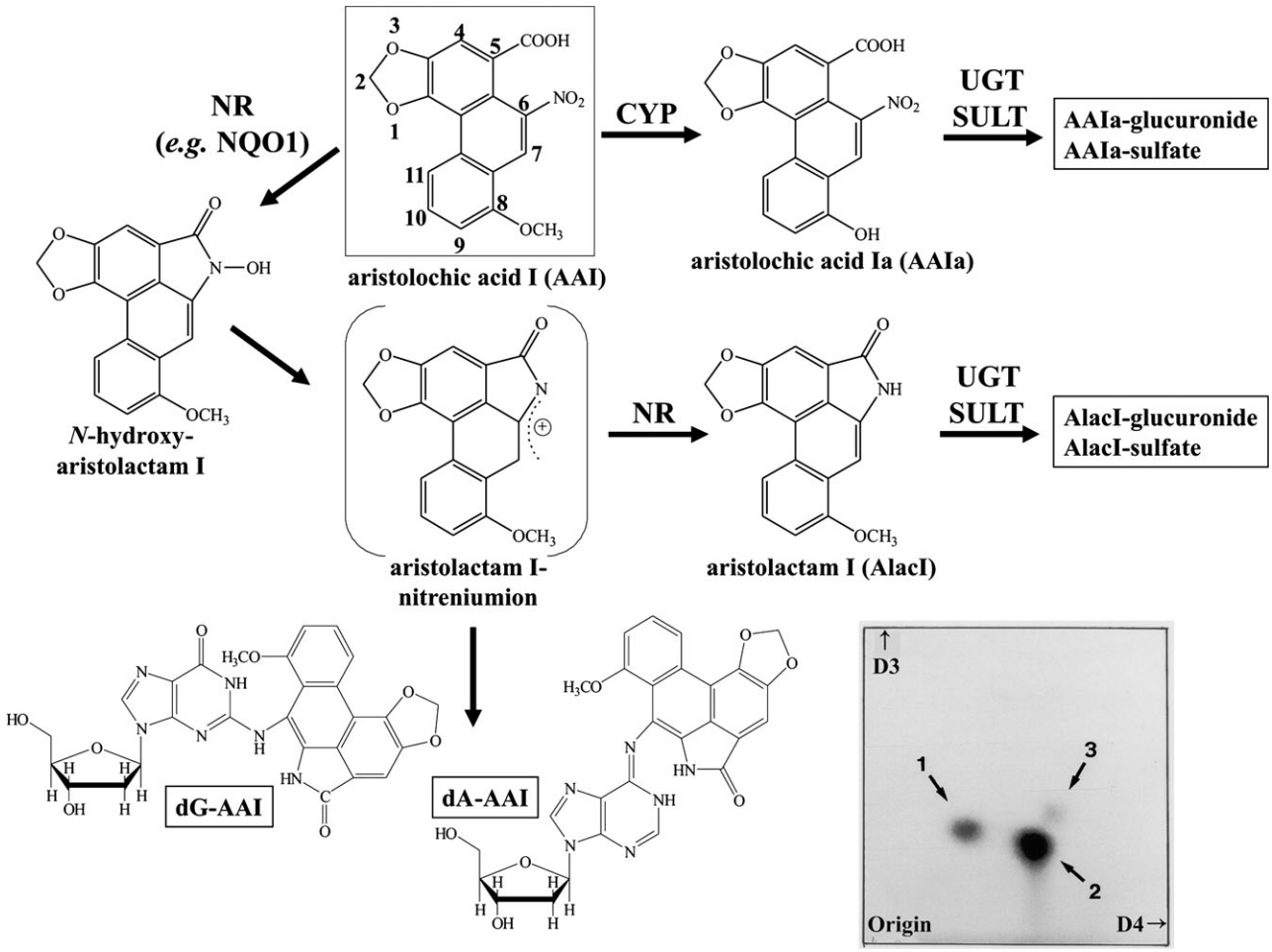

FIG. 1. Pathways of biotransformation and DNA adduct formation of AAI. dA-AAI, 7-(deoxyadenosin-N^6-yl)aristolactam I; dG-AAI, 7-(deoxyguanosin-N^2-yl)aristolactam I; NR, nitroreduction; UGT, UDP glucuronyl transferase; SULT, sulfotransferase. Inset: autoradiographic profile of AA-DNA adducts in kidney of HRN mice treated with 50 mg/kg bw of AAI by using the nuclease P1 enrichment version of the ^{32}P-postlabeling assay. The origin, in the bottom left-hand corner, was cut off before exposure. Spot 1, dG-AAI; spot 2, dA-AAI; spot 3, 7-(deoxyadenosin-N^6-yl)aristolactam II (dA-AAII).

that was observed initially in a group of Belgian women, who had ingested weight loss pills containing *Aristolochia fangchi* (Vanherweghem *et al*., 1993). Within a few years of taking the pills, AAN patients also developed a high risk of upper urothelial tract carcinoma (about 50%) and, subsequently, bladder urothelial carcinoma (Lemy *et al*., 2008; Nortier *et al*., 2000). Subsequently, similar cases have been reported elsewhere in Europe and Asia (Debelle *et al*., 2008; Lai *et al*., 2010; Lord *et al*., 2001). More recently, exposure to AA has been linked to Balkan endemic nephropathy (BEN) and its associated urothelial cancer (Arlt *et al*., 2007; Grollman *et al*., 2007; Nedelko *et al*., 2009). This nephropathy is endemic in certain rural areas of Serbia, Bosnia, Croatia, Bulgaria, and Romania. Exposure to AA was demonstrated by the identification of specific AA-DNA adducts in urothelial tissue of AAN and BEN patients (Arlt *et al*., 2002; Bieler *et al*., 1997; Grollman *et al*., 2007; Lord *et al*., 2001; Nortier *et al*., 2000; Schmeiser *et al*., 1996). The most abundant DNA adduct detected in patients exposed to AA is 7-(deoxyadenosin-N^6-yl)-aristolactam I (dA-AAI), which leads to characteristic AT→TA transversion mutations. Such AT→TA mutations have been observed in the *TP53* tumor suppressor gene in tumors from AAN and BEN patients (Arlt *et al*., 2007; Grollman *et al*., 2007; Lord *et al*., 2004; Nedelko *et al*., 2009), indicating the probable molecular mechanism of AA carcinogenesis in humans (Arlt *et al*., 2011; Simoes *et al*., 2008). As a consequence, AA was recently classified as carcinogenic to humans (Group 1) by the International Agency for Research on Cancer (Grosse *et al*., 2009).

In common with other nitroaromatics, the major activation pathway for AA is nitroreduction catalyzed by both cytosolic and microsomal enzymes, cytosolic NAD(P)H:quinone oxidoreductase (NQO1) being the most efficient (Stiborová *et al*., 2002a, 2003a, 2008b, 2011) (Fig. 1). The activation of AAI in human hepatic microsomes is mediated by CYP1A2 and to a lesser extent by CYP1A1; POR also plays a minor role

(Stiborová *et al.*, 2001b, 2001c, 2005a, 2005c). Prostaglandin H synthase (cyclooxygenase, COX) in human renal microsomes has also been shown to activate AAI (Stiborová *et al.*, 2001a, 2005a). Although the enzymes catalyzing the reductive activation of AAI leading to covalent DNA adducts have been widely investigated, those participating in its detoxication have not been extensively studied so far. Several studies have indicated that induction of Cyp1a (e.g., by 3-methylcholanthrene and ß-naphthoflavone) protect mice from AAI-induced acute renal injury (Xiao *et al.*, 2008, 2009; Xue *et al.*, 2008). One detoxication metabolite identified is 8-hydroxy-aristolochic acid I (aristolochic acid Ia, AAIa; Fig. 1) that is formed after demethylation of AAI and is, in turn, subject to conjugation, forming glucuronide or sulfate esters (Chan *et al.*, 2007; Krumbiegel *et al.*, 1987; Shibutani *et al.*, 2010). Human CYP1A1 and -1A2 can demethylate AAI to AAIa *in vitro* (Rosenquist *et al.*, 2010; Šístková *et al.*, 2008), and Cyp1a2 in mice appears to mediate this reaction *in vivo* (Rosenquist *et al.*, 2010). Nevertheless, because CYP1A1/2 also activate AAI in human and rat livers (Stiborová *et al.*, 2001a, 2005a, 2005c, 2008b), detailed knowledge of the catalytic specificities of CYP1A and other CYP enzymes in the detoxication and activation of AAI *in vitro* and *in vivo* is still lacking.

The aim of the present study was to evaluate the CYP-mediated oxidative detoxication of AAI. We have used the HRN mouse model to examine the hepatic Cyp-dependent metabolism of AAI. DNA adduct formation *in vivo* and *in vitro* was measured by ^{32}P-postlabelling. In addition, the formation of AAIa by human, rat and rabbit hepatic microsomes, and by rat recombinant CYPs was determined by high-performance liquid chromatography (HPLC).

MATERIALS AND METHODS

Animal treatment. HRN ($Por^{lox/lox}$ + Cre^{ALB}) mice on a C57BL/6 background (CXR Bioscience Ltd, Dundee, UK) used in this study were derived as described previously (Henderson *et al.*, 2003a). Mice homozygous for loxP sites at the *Por* locus ($Por^{lox/lox}$) were used as wild type (WT). Groups of male HRN and WT mice (3 months old; 25–30 g; $n = 3$/group) were treated orally with a single dose of 10 or 50 mg/kg body weight (bw) of AAI (as sodium salt isolated from the natural mixture of AA [38% AAI, 58% AAII; Sigma Chemical Co, St Louis, MO] by preparative HPLC [Schmeiser *et al.*, 1984]) at a concentration of 1 or 5 mg/ml, respectively. Control mice received solvent, water, only. Animals were killed 24 h after treatment. Liver, lung, kidney, spleen, colon, small intestine, and bladder were removed, snap frozen and stored at −80°C until analysis. All procedures were carried out under the Animal (Scientific Procedures) Act (1986) in accordance with UK law and following local ethical review.

DNA adduct analysis by ^{32}P-postlabeling. DNA from tissues was isolated by standard phenol/chloroform extraction. ^{32}P-Postlabelling analysis (Phillips and Arlt, 2007), using the nuclease P1 enrichment version, and thin layer chromatography (TLC) and HPLC were performed as described (Bieler *et al.*, 1997; Schmeiser *et al.*, 1996). TLC sheets were scanned using a Packard Instant Imager (Dowers Grove), and DNA adduct levels (relative adduct labeling) were calculated as described (Bieler *et al.*, 1997; Schmeiser *et al.*, 1996). Results were expressed as DNA adducts/10^8 nucleotides.

Preparation of microsomes and cytosols. Hepatic and renal microsomes and cytosols from HRN and WT mice were isolated as described (Stiborová *et al.*, 2003b, 2005a). Hepatic and renal microsomes and cytosols from HRN and WT mice pretreated (i.p.) with 125 mg/kg bw benzo[*a*]pyrene (BaP) daily for 5 days were obtained from a previous study (Arlt *et al.*, 2008). Pooled microsomal and cytosolic fractions were used for further analysis. Male human (pooled sample; catalog no. 452172) and human female hepatic microsomes (pooled sample; catalog no. 452183) were from Gentest Corp. (Woburn, MI). Microsomes were prepared from livers of ten untreated Wistar rats and three Chinchilla rabbits by the procedure described previously (Stiborová *et al.*, 1995, 2002b). Microsomes were also prepared from livers of groups of ten Wistar male rats pretreated with Sudan I, phenobarbital (PB), ethanol (EtOH), or pregnenolone-16α-carbonitrile (PCN) as described previously (Stiborová *et al.*, 2002b, 2003b).

Microsomal incubations used for AAI-DNA adduct analysis. The deaerated and argon-purged incubation mixtures, in a final volume of 750 µl, consisted of 50mM potassium phosphate buffer (pH 7.4), 1mM NADPH, 1 mg mouse hepatic or renal microsomal protein, 0.5 mg calf thymus DNA (2mM dNp), and 0.5mM AAI as described previously (Stiborová *et al.*, 2005a). Incubations with microsomes were carried out at 37°C for 60 min, and AAI-derived DNA adduct formation was found to be linear up to 2 h (Stiborová *et al.*, 2005a).

Microsomal incubations used for AAI demethylation. Incubation mixtures, in a final volume of 250 µl, consisted of 100mM potassium phosphate buffer (pH 7.4), 1mM NADPH, 1 mg human, rat, mouse, or rabbit hepatic, or mouse renal microsomal protein and 10µM AAI. Incubations with microsomes were carried out at 37°C for 20 min, and AAI oxidation (demethylation) to AAIa was linear up to 25 min. Control incubations were carried out (1) without microsomes, (2) without NADPH, or (3) without AAI. Supersomes, microsomes isolated from insect cells transfected with baculovirus constructs containing cDNA of single rat CYPs (CYP1A1, CYP1A2, CYP2A1, CYP2A2, CYP2B1, CYP2C6, CYP2C11, CYP2C12, CYP2C13, CYP2D1, CYP2D2, CYP2E1, CYP3A1, and CYP3A2), and expressing POR and/or cytochrome b_5 were obtained from Gentest Corp and tested for their efficiencies to oxidize AAI. Incubation mixtures, in a final volume of 250 µl, consisted of 100mM potassium phosphate buffer (pH 7.4), 1mM $NADP^+$, 10mM $MgCl_2$, 10mM D-glucose 6-phosphate, 1 U/ml D-glucose 6-phosphate dehydrogenase, to generate NADPH, 50nM CYPs in Supersomes, and 10µM AAI. Supersomes containing POR alone were used for control.

Determination of AAIa by HPLC. AAI and its metabolites (i.e., AAIa) were extracted from incubation mixtures twice into ethyl acetate (2 × 1 ml), the extracts were evaporated to dryness and the residues redissolved in 30 µl of methanol and subjected to reverse-phase HPLC. HPLC was performed with a reversed phase column (Nucleosil 100-5 C_{18}, 25 × 4.0 mm, 5 mm; Macherey-Nagel) preceded by a C-18 guard column, using a linear gradient of acetonitrile (20–60% acetonitrile in 55 min) in 100mM triethylamonium acetate with a flow rate of 0.6 ml/min. HPLC was carried out with a Dionex HPLC pump P580 with UV/VIS UVD 170S/340S spectrophotometer detector set at 254 nm, and peaks were integrated with CHROMELEON 6.01 integrator. A product of AAI metabolism and AAI itself eluted with retention times (r.t.) of 28.3 and 36 min, respectively. The product eluting at 28.3 min was identified as AAIa using mass-spectroscopy analyses. Mass spectra were measured on MALDI-TOF/TOF ultraFLEX III mass spectrometers (Bruker-Daltonics, Bremen, Germany). Positive spectra were calibrated externally using the monoisotopic $[M+H]^+$ ions of PepMixII calibrant (Bruker-Daltonics) or matrix peaks. A 10 mg/ml solution of α-cyano-4-hydroxy-cinnamic acid or 50 mg/ml solution of 2,5-dihydrobenzoic acid in 50% MeCN/0.1% TFA were used as MALDI matrix. A 0.5-µl sample dissolved in MeCN was directly mixed with 0.5-µl of the matrix solution and allowed to dry at ambient temperature on the target. For NALDI experiments, a 1-µl sample dissolved in MeCN was allowed to dry at ambient temperature on NALDI target. The MALDI- or NALDI-TOF positive spectra were collected in reflector mode.

Cytosolic incubations used for AAI-DNA adduct analysis. The deaerated and argon-purged incubation mixtures, in a final volume of 750 µl, consisted of 50mM Tris-HCl buffer (pH 7.4), containing 0.2% Tween 20, 1mM NADPH, 1 mg murine hepatic, or renal cytosolic protein, 0.5 mg calf thymus DNA (2mM dNp) and 0.5mM AAI as described previously (Stiborová *et al*., 2003a). Incubations with human cytosols were carried out at 37°C for 60 min, and AAI-derived DNA adduct formation was found to be linear up to 2 h (Stiborová *et al*., 2003a).

Inhibition studies. α-Naphthoflavone (α-NF), which inhibits Cyp1a1 and -1a2 (Stiborová *et al*., 2001b, 2005c); ellipticine (E), which competes with Cyp1a1 substrates, thus inhibiting Cyp1a1-mediated oxidation of other substrates (Stiborová *et al*., 2003b, 2004); furafylline (FF), which inhibits Cyp1a2 (Stiborová *et al*., 2001b); ketoconazole (KC), which inhibits Cyp3a4 (Stiborová *et al*., 2001b); and α-lipoic acid (α-LA), which inhibits Por (Arlt *et al*., 2003; Stiborová *et al*., 2005b) were used to inhibit the activation of AAI in murine microsomes. Dicoumarol was used to inhibit the activation of AAI by Nqo1 in mouse hepatic cytosols. The inhibition studies were performed as described (Arlt *et al*., 2005; Stiborová *et al*., 2001b, 2003a).

Determination of NQO1 activity and protein levels by Western blotting. NQO1 antibodies were prepared as described previously (Stiborová *et al*., 2002b, 2005b, 2006). Immunoquantitation of cytosolic NQO1 was carried out by SDS-polyacrylamide gel electrophoresis (Stiborová, 2006). Human recombinant NQO1 (Sigma) was used to identify the band Nqo1 in murine cytosols. NQO1 activity was measured essentially as described by Ernster (1967), but the method was improved by addition of cytochrome *c* (Mizerovská *et al*., 2011).

RESULTS

DNA Adduct Formation by AAI in HRN Mice

In order to evaluate the role of hepatic Por-dependent Cyp enzymes in the detoxication of AAI *in vivo*, we treated HRN and WT mice with a single dose of 10 or 50 mg/kg bw of AAI by oral gavage. The formation of AAI-DNA adducts in various organs (liver, lung, kidney, spleen, colon, small intestine, and urinary bladder) was determined by ^{32}P-postlabeling. Essentially, the same DNA adduct pattern as that found *in vivo* in humans (Bieler *et al*., 1997; Schmeiser *et al*., 1996) and rats (Schmeiser *et al*., 1988; Stiborová *et al*., 1994), in incubations using rat and human hepatic microsomes (Stiborová *et al*., 2001b, 2005a), and human hepatic and renal cytosols (Stiborová *et al*., 2003a) was observed in all tissues analyzed (see Fig. 1 inset for kidney of mice treated with 50 mg/kg bw AAI). Adducts were indentified to be 3′,5′-bisphospho-7-(deoxyguanosin-N^2-yl)-aristolactam I (dG-AAI, spot 1), 3′,5′-bisphospho-7-(deoxyadenosin-N^6-yl)-aristolactam I (dA-AAI, spot 2), and 3′,5′-bisphospho-7-(deoxyadenosin-N^6-yl)-aristolactam II (dA-AAII, spot 3) (Pfau *et al*., 1990; Schmeiser *et al*., 1996; Stiborová *et al*., 1994; Fig. 1). The identities of the individual AAI-derived DNA adducts were confirmed by cochromatographic analysis on TLC and HPLC as described previously (Schmeiser *et al*., 1996) (data not shown). No DNA adducts were observed in DNA isolated from the tissues of control animals (data not shown).

AAI-DNA adduct formation was concentration dependent and organ specific (Fig. 2 and Supplementary table S1). Adduct

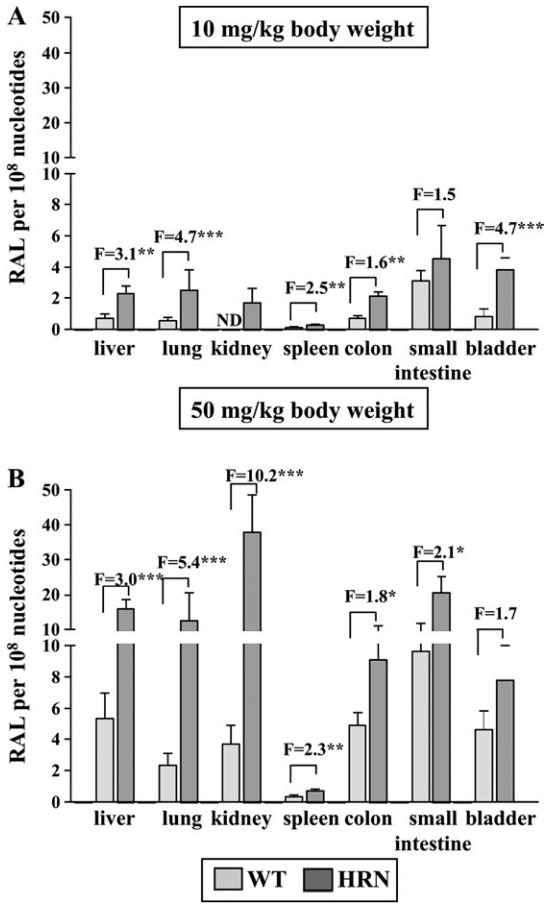

FIG. 2. Quantitative TLC^{32}P-postlabeling analysis of DNA adducts formed by AAI in organs of HRN and WT mice treated orally with 10 (A) or 50 mg AAI/kg bw for 24 h (B). F, fold increase in DNA adducts in HRN mice compared with WT mice. RAL, relative adduct labeling; ND, not detected. Values are given as means ± SD ($n = 3$). Values significantly different from WT mice: *$p < 0.05$, **$p < 0.01$, ***$p < 0.001$ (Student's *t*-test).

levels in WT mice were highest in the small intestine, followed by liver, colon, bladder, lung, spleen, and kidney, where adducts were only observed after 50 mg/kg (Fig. 2B). In HRN mice treated with either AAI dose, higher levels of AAI-DNA adducts were found than in WT mice in all organs analyzed, with the highest levels and largest differences in kidney (Fig. 2B). The latter finding indicates that the lack of Por-dependent Cyp-mediated detoxication of AAI in liver of HRN mice increased the effective concentration of AAI in this organ and in extrahepatic tissues.

Human, Mouse, Rat, and Rabbit Hepatic Microsomes Oxidize AAI to AAIa

In vitro experiments were performed to further examine the role of the mouse hepatic Cyps in the detoxication of AAI. Microsomes were isolated from livers of HRN and WT mice, either untreated or pretreated with BaP (i.e., HRN-BaP and

WT-BaP mice, Arlt *et al.*, 2008). For comparison, human, rabbit, and rat hepatic microsomes were utilized.

Hepatic microsomes of WT, WT-BaP, and HRN-BaP mice were capable of metabolizing AAI to one metabolite detectable by HPLC analysis (see peak with r.t. of 28.3 min in Fig. 3 for microsomes of WT mice). MS (NALDI- and MALDI-TOF-TOF, Fig. 4) was used to identify the structure of this metabolite. Negative NALDI-TOF-TOF MS detected a peak at *m/z* 325.803 (Fig. 4A), representing the molecular ion $[M\text{-}H]^-$ of 8-hydroxy-aristolochic acid (AAIa) (for structure, see Fig. 1). Positive MALDI-TOF-TOF detected peaks at *m/z* 328.043 and 327.029, representing the molecular ions $[M\text{-}H]^+$ and $[M]^+$ of AAIa, respectively (Fig. 4B). The peaks at *m/z* 283.021 and 311.031, representing ions of AAIa fragments, were also found (Fig. 4B). These results show that the detected metabolite is the demethylation product of AAI, 8-hydroxy-aristolochic acid (AAIa) (for structure, see Fig. 1), which was found to be a detoxication metabolite of AAI (Shibutani *et al.*, 2010). In contrast to hepatic microsomes of WT, WT-BaP and HRN-BaP mice, microsomes of HRN mice did not oxidize AAI (Figs. 3C and 5A). Pretreatment of mice with BaP, a potent CYP1A1/2 inducer (Arlt *et al.*, 2008) greatly stimulated AAI demethylation to AAIa. Even hepatic microsomes of HRN mice treated with BaP were capable of demethylating AAI

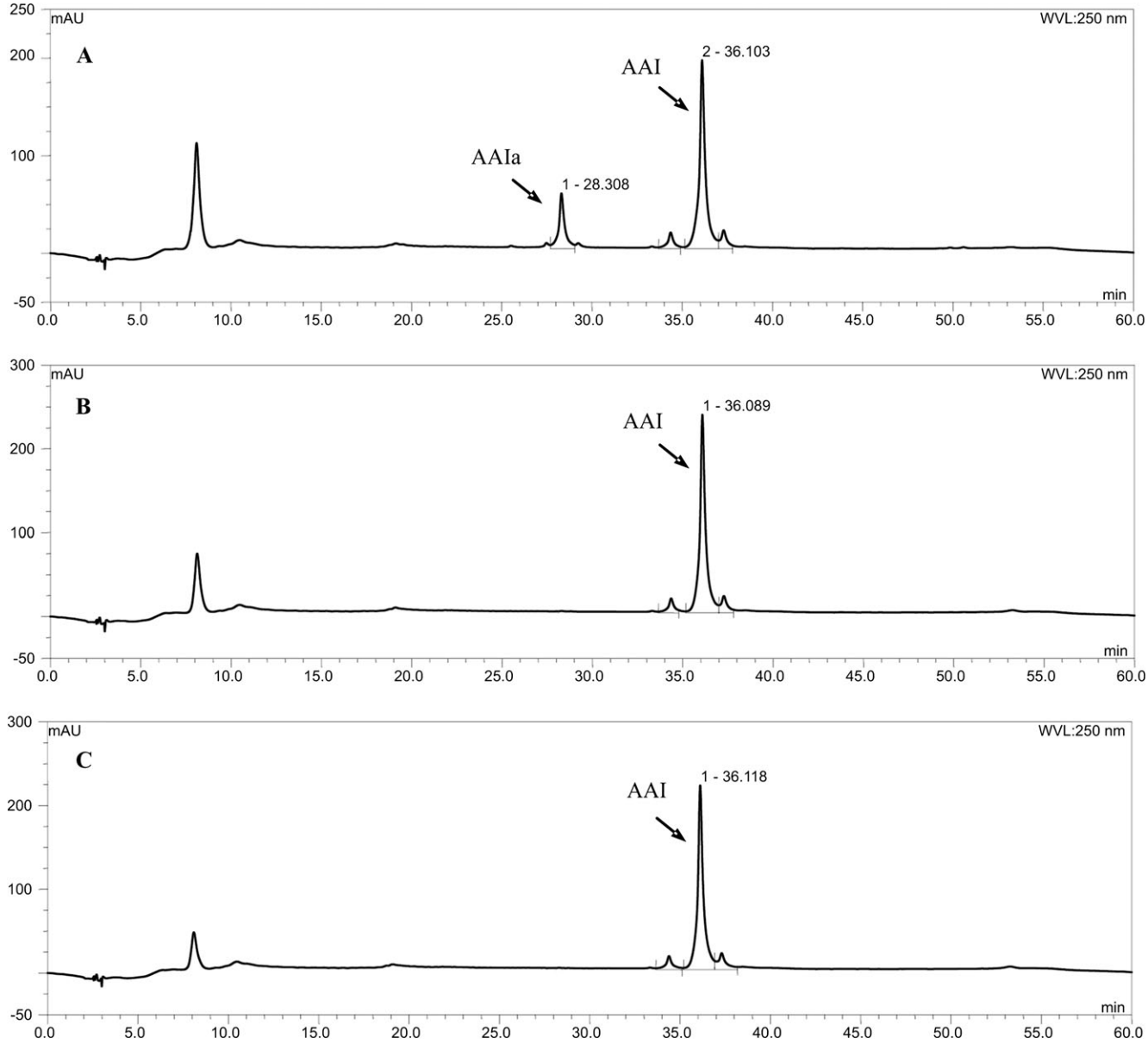

FIG. 3. HPLC chromatograph of AAIa metabolite (peak r.t. at 28.3 min) and AAI (peak r.t. at 36 min) produced by hepatic microsomes of WT mice incubated with AAI and NADPH (A), by hepatic microsomes of WT mice incubated with AAI without NADPH (B), and by hepatic microsomes of HRN mice incubated with AAI and NADPH (C). The peaks with the characterized AAI metabolite (AAIa) and the parent AAI are indicated in the chromatograms.

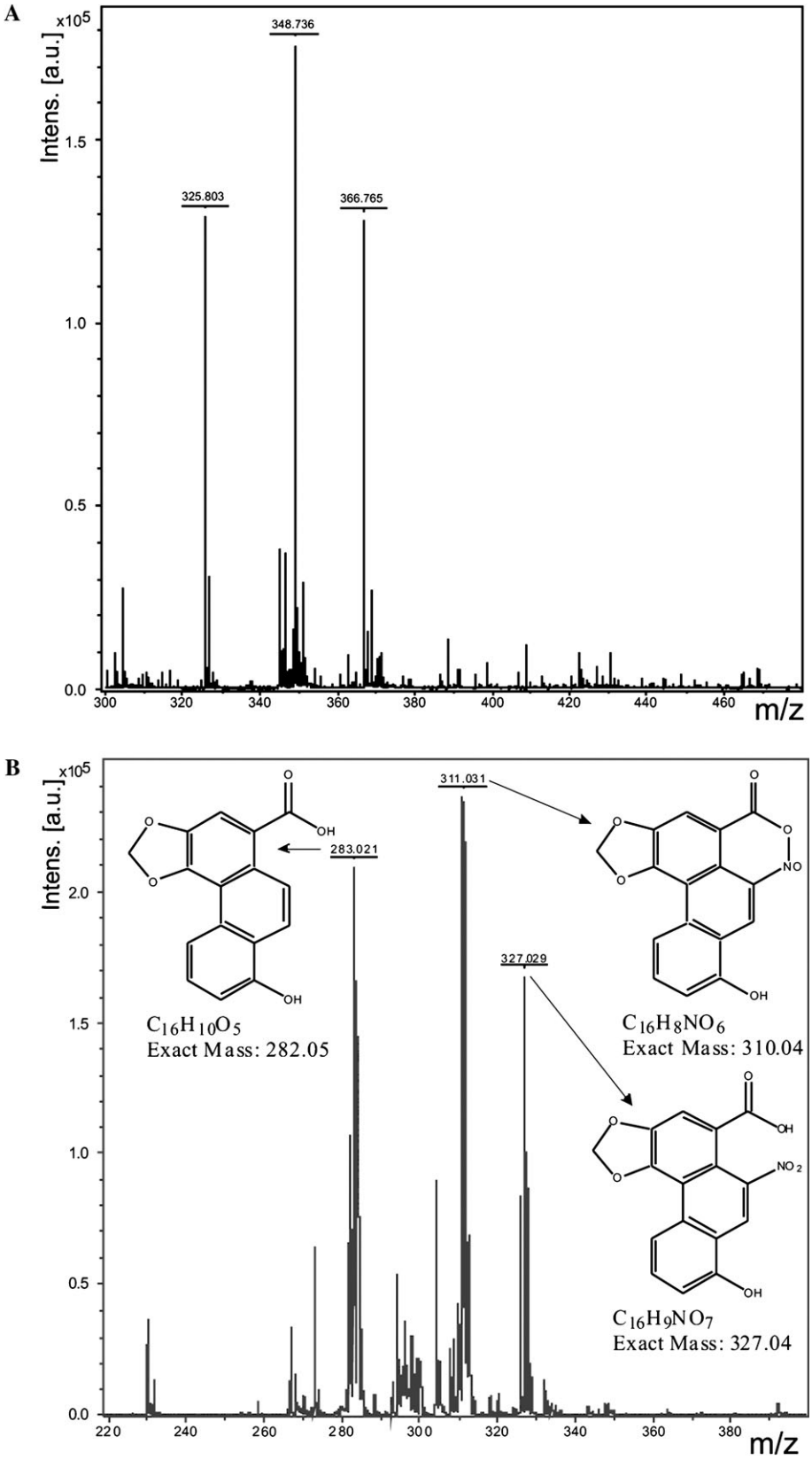

FIG. 4. Identification of AAI metabolite as AAIa. Negative NALDI-TOF/TOF (A) and positive MALDI-TOF/TOF (B) of AAIa. The peaks at *m/z* 348.736 and 366.765 in panel A are matrix peaks.

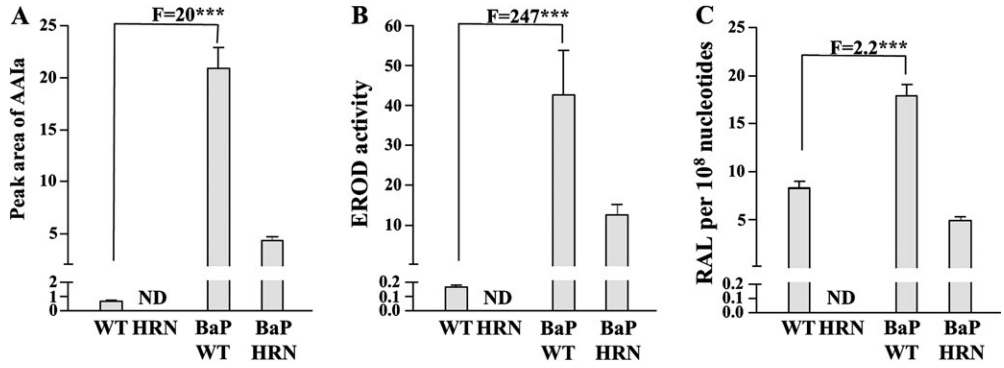

FIG. 5. Oxidation of AAI to AAIa by murine hepatic microsomes isolated from livers of HRN and WT mice, control mice (untreated) or mice pretreated (i.p.) with 125 mg BaP/kg bw daily for 5 days (Arlt *et al*., 2008) (A); Cyp1a enzymatic activity (EROD activity) in hepatic microsomes (B). DNA adduct formation by AAI activated with hepatic microsomes as determined by TLC ^{32}P-postlabeling (C). RAL, relative adduct labeling; ND, not detected. All values are given as means ± SD ($n = 3$). Values significantly different from control (untreated) WT mice: ***$p < 0.001$ (Student's *t*-test).

(Fig. 5A). These results correlated well with the protein expression of Cyp1a1/2 and the EROD activity in the hepatic microsomes (Arlt *et al*., 2008; compare Fig. 5B).

In contrast to mouse hepatic microsomes, renal microsomes from WT and HRN mice did not oxidize AAI to AAIa under the same experimental conditions (data not shown).

The efficiency of hepatic microsomes from WT mice to form AAIa was compared with that of human, rat, and rabbit hepatic microsomes (Supplementary fig. S1). Hepatic microsomes from all these species oxidized AAI to AAIa. Whereas human and rat hepatic microsomes oxidized AAI with similar efficiency, a 1.3-fold lower oxidation of AAI was found in mouse hepatic microsomes compared with human microsomes and even lower activity in microsomes of rabbits (Supplementary fig. S1).

The capacity of different CYPs to demethylate AAI to AAIa was studied using hepatic microsomes of rats treated with CYP inducers. As shown in Figure 6A, hepatic microsomes of rats treated with Sudan I (which induces CYP1A) and PB (which induces CYP2B and -2C) were 1.3 and 1.1 times more efficient to oxidize AAI to AAIa than uninduced microsomes. In contrast, other CYP inducers such as ethanol (which induces CYP2E1) and PCN (which induces CYP3A) decreased AAIa formation. Collectively, these findings strongly suggest that CYP1A1/2 enzymes are predominantly responsible for AAI demethylation to AAIa in mouse and rat liver microsomes.

Oxidation of AAI to AAIa by Rat Recombinant CYPs in Supersomes

Further experiments were conducted using microsomes of Baculovirus transfected insect cells (Supersomes) containing recombinantly expressed rat CYPs, POR, and/or cytochrome b_5 (Fig. 6B). Only rat CYPs could be utilized as Supersomes containing individual mouse Cyps are not available. Rat CYP1A2 was the most efficient enzyme at demethylating AAI to AAIa, followed by CYP1A1 (Fig. 6B). Rat recombinant CYP2C enzymes were also capable of demethylating AAI but to a lesser extent (Fig. 6B). No AAIa formation occurred in control incubations with Supersomes containing POR alone.

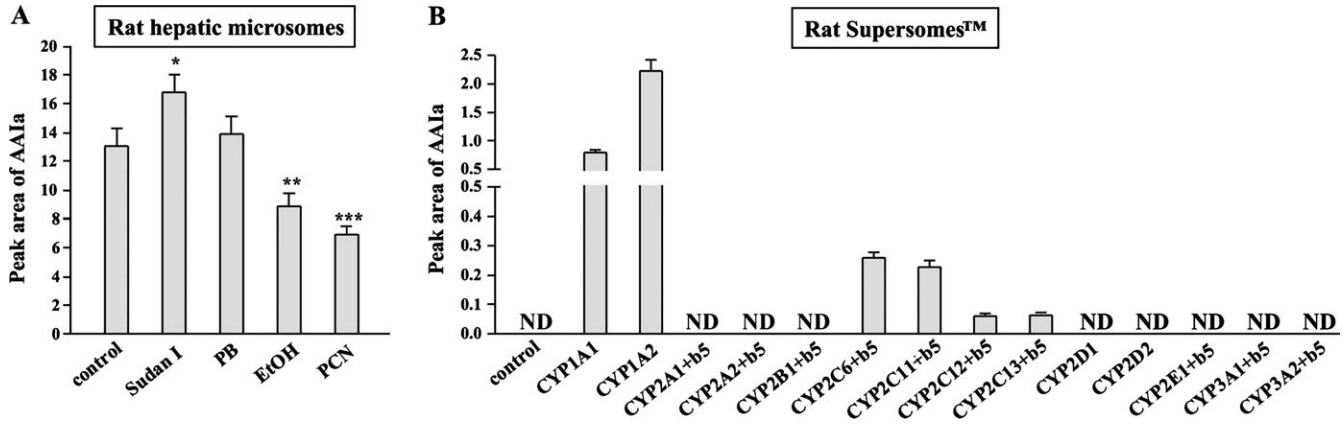

FIG. 6. Oxidation of AAI by rat hepatic microsomes (A) or recombinant CYPs of rat (B). Values are given as means ± SD ($n = 3$). Values significantly different from hepatic microsomes of control (untreated) rats: *$p < 0.05$, **$p < 0.01$, ***$p < 0.001$ (Student's *t*-test). Sudan I, phenobarbital (PB), ethanol (EtOH), and pregnenolone-16α-carbonitrile (PCN) were used as inducers of rat CYPs. One milligram microsomal protein or 50μM rat recombinant CYPs and 10μM AAI were used in incubations (see Materials and Methods). Control, control Supersomes containing POR alone (50nM). ND, not detected.

Hepatic Microsomes of WT, WT-BaP, and HRN-BaP but Not of HRN Mice Activate AAI to Species Forming DNA Adducts

In order to evaluate the role of Por-dependent Cyp-mediated activation of AAI in DNA adduct formation, we carried out *in vitro* incubations using the same hepatic mouse microsomes as those used in the experiments above, except that incubations were performed under hypoxic conditions. Incubation mixtures were purged with a stream of argon for 3 min before the addition of AAI. Although most of the oxygen was removed, we cannot exclude its presence in the membranes and lumen of microsomes present in the mixtures. AAI was activated by hepatic microsomes of WT, WT-BaP, and HRN-BaP mice, generating the same cluster of three DNA adducts as those obtained *in vivo* in mice (spots 1, 2, and 3 shown in Fig. 1), identified to be dG-AAI (spot 1), dA-AAI (spot 2), and dA-AAII (spot 3). Pretreatment of mice with BaP increased the levels of AAI-DNA adducts catalyzed by hepatic microsomes of both WT and HRN mice (Figs. 5C and 7C and Supplementary table S2). Because this increase corresponded to an increase in Cyp1a1/2 protein expression and their enzymatic activities (Arlt *et al.*, 2008; compare Fig. 5B), our findings indicate that mouse Cyp1a1/2 participate in the metabolic activation of AAI to form DNA adducts. Control incubations carried out in parallel without microsomes, or without DNA, or without AAI, were free of adduct spots in the region of interest (data not shown). Renal microsomes of both mouse strains (WT and HRN) also activated AAI to form the same AAI-DNA adducts, both with similar efficiencies. However, renal microsomes of WT mice were less effective than hepatic microsomes (Figs. 7A and 7B and Supplementary tables S2 and S3).

Whereas hepatic microsomes of WT, WT-BaP, and HRN-BaP mice activate AAI to species forming DNA adducts, those of HRN mice were not active (Figs. 5C and 7). This finding that again parallels Cyp1a1/2 enzyme activity (EROD) (Fig. 5B) might be caused either by the lack of Por-mediated or Por-dependent Cyp1a1/2-mediated activation of AAI.

To further investigate the role of Por-dependent-Cyp-mediated DNA adduct formation by AAI in mouse hepatic microsomes, inhibitors of several Cyps and Por were utilized. In hepatic microsomes, AAI-DNA adduct formation was inhibited with α-NF (which inhibits Cyp1a1/2), ellipticine (which inhibits Cyp1a1), and furafylline (which inhibits Cyp1a2) but not with ketoconazole (which inhibits Cyp3a) and α-lipoic acid (which inhibits Por) (Figs. 7A and 7C and Supplementary table S4). These results corroborate the suggestion that Cyp1a enzymes play an important role in AAI-DNA adduct formation in mouse liver, whereas participation of Por or other Cyps such as Cyp3a is negligible in this process. The major role of mouse hepatic microsomal Cyp1a1/2 in AAI activation is in accordance with former findings showing participation of these enzymes in this process in human and rat hepatic microsomes (Stiborová *et al.*, 2001b, 2005a, 2005c).

In contrast to hepatic microsomes, AAI-DNA adduct formation catalyzed by renal microsomes was inhibited by ketoconazole and α-lipoic acid but not by α-NF, ellipticine, or furafylline (Fig. 7B and Supplementary table S5). An increase in AAI-DNA adduct levels was even produced by α-NF, the compound known to stimulate oxidation of several substrates catalyzed by Cyps of the 3a subfamily (Bořek-Dohalská *et al.*, 2001; Bořek-Dohalská and Stiborová, 2010; Rendic and DiCarlo, 1997; Ueng *et al.*, 1997). Moreover, α-NF was also found to stimulate reduction of some substrates by POR including AAI, thereby increasing levels of AAI-DNA adducts (Hodek *et al.*, 2009; Stiborová *et al.*, 2001b, 2005a). Therefore, these results indicate that Cyp3a and Por might participate in AAI-DNA adduct formation in mouse kidney.

Whereas POR was found to catalyze AAI-DNA adduct formation in human kidney microsomes (Stiborová *et al.*, 2005a), human CYP3A4, the most abundant CYP enzyme in human livers (Rendic and diCarlo, 1997), was inactive (Stiborová *et al.*, 2001b, 2005a, 2005c). Human recombinant CYP3A5, the enzyme that is expressed in human kidney, was tested in this work to investigate its potential to activate AAI. As shown in Supplementary figure 2 and table S6, CYP3A5 expressed in Supersomes increases levels of AAI-derived DNA adducts when incubated with DNA *in vitro*, indicating its role in the activation process. This conclusion was also supported by the inhibition of AAI-DNA adduct formation in this system by ketoconazole.

Metabolic Activation of AAI Mediated by Mouse Hepatic and Renal Cytosols In Vitro

In initial experiments, we investigated the efficiency of hepatic and renal cytosolic samples of WT and HRN mice to generate adduct forming species from AAI. Incubations were carried out in the presence of NADPH, a cofactor of Nqo1, the enzyme shown to be most efficient in AAI activation (Stiborová *et al.*, 2002a, 2003a, 2011). Similarly, to human hepatic and renal cytosols (Stiborová *et al.*, 2003a, 2011), cytosols of both organs and of both mouse strains were capable of activating AAI to form DNA adducts (see Fig. 8A and Supplementary table S7 for hepatic cytosols and Supplementary table S8 for renal cytosols), but mouse renal cytosols were less effective than hepatic cytosols (Supplementary tables S7 and S8). Interestingly, hepatic cytosolic samples of HRN mice were more than 3-fold more efficient in activating AAI to DNA adducts than those of WT mice (Fig. 8A and Supplementary table S7).

In hepatic cytosols, we also tested whether pretreatment of WT and HRN mice with BaP, a Nqo1 inducer (Elovaara *et al.*, 2007; Hockley *et al.*, 2007; Vondráček *et al.*, 2009), influences the formation of AAI-DNA adducts. Indeed, more than 3- and 6-fold higher levels of AAI-DNA adducts catalyzed by hepatic cytosols of HRN-BaP and WT-BaP mice than untreated mice were determined, respectively (Fig. 8A and Supplementary

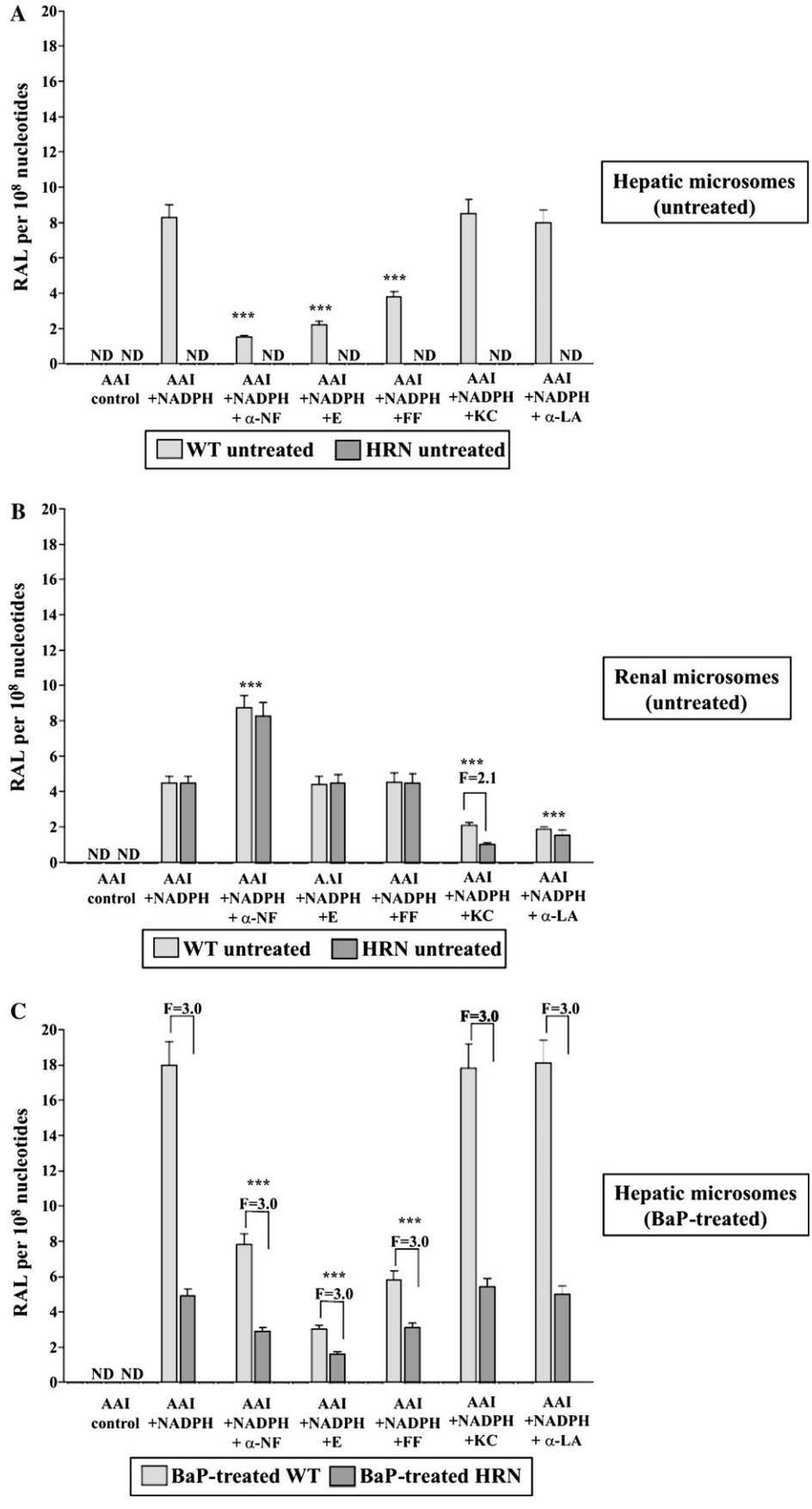

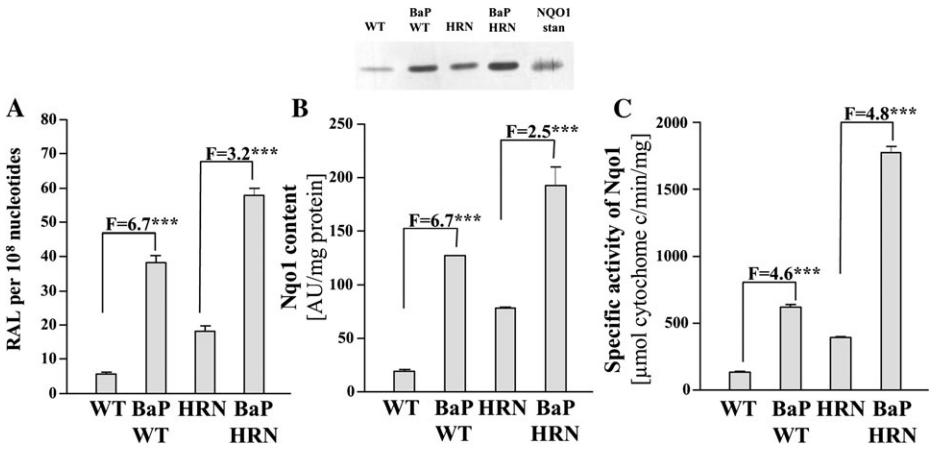

FIG. 8. DNA adduct formation by AAI activated with hepatic cytosols isolated from livers of HRN and WT mice, control mice (untreated), or mice pretreated (i.p.) with 125 mg/kg bw BaP daily for 5 days (Arlt *et al*., 2008) as determined by TLC^{32}P-postlabeling (A). RAL, relative adduct labeling. Nqo1 protein expression in hepatic cytosols as determined by Western blotting (see insert) (B). Nqo1 enzymatic activity in hepatic cytosols (C). Human recombinant NQO1 (Sigma; NQO1 stan, see insert B) was used to identify the Nqo1 band in murine cytosols. All values are given as means ± SD ($n = 3$). Values significantly different from control (untreated) mice: ***$p < 0.001$ (Student's *t*-test).

table S7). This was paralleled by an increase in Nqo1 protein expression and enzyme activity in these samples (Figs. 8B and 8C). These results demonstrate that Nqo1 plays an important role in livers of both WT and HRN mice, analogous to its role in human and rat liver cytosols (Stiborová *et al*., 2002a, 2003a, 2011). Indeed, participation of Nqo1 in AAI-DNA adduct formation with mouse hepatic cytosols was confirmed by the effect of dicoumarol, an Nqo1 inhibitor, in reducing DNA binding (Supplementary fig. 3 and Supplementary table S9).

DISCUSSION

A large body of evidence indicates that metabolic activation and detoxication of AAI influences its nephrotoxic and carcinogenic effects. Demethylation of AAI to AAIa is believed to be detoxication reaction because AAIa was found to be much less toxic than AAI (Shibutani *et al*., 2010). In addition, AAIa or its conjugates, the glucuronide, the acetate, and the sulfate esters, are readily excreted in urine (Chan *et al*., 2006, 2007).

Formation of AAIa was recently found to be catalyzed mainly by human CYP1A1 and -1A2 *in vitro* (Rosenquist *et al*., 2010; Šístková *et al*., 2008) and by mouse Cyp1a2 *in vivo* (Rosenquist *et al*., 2010). However, CYP1A1 and -1A2 are the enzymes that also activate AAI (Stiborová *et al*., 2001b, 2005a, 2005c). We therefore investigated participation of these and other CYPs both in detoxication and in activation of AAI in detail.

HRN mice carry a deletion of the *Por* gene in hepatocytes (Henderson and Wolf, 2003; Henderson *et al*., 2003b) and thus lack Cyp activity in the liver. AAI-DNA adducts were formed in all organs of both WT and HRN mice treated with AAI. These findings suggest that AAI is distributed via the blood stream to other organs and that these tissues have the metabolic capacity to reductively activate this carcinogen. Moreover, our results demonstrate that Por-dependent, Cyp-mediated metabolism of AAI in the liver dictates the formation of DNA adducts by this compound also in extrahepatic organs in mice *in vivo*. Besides such an *in vivo* study, we performed *in vitro* experiments utilizing subcellular systems (i.e., microsomes and cytosols) of the liver, the organ that is predominantly responsible for the biotransformation of many xenobiotics, as well as the kidney, the target organ for AAI toxicity. We demonstrated that hepatic Cyps oxidize AAI, thereby decreasing its concentrations in liver of WT mice, and lower amounts of AAI are distributed to extrahepatic organs than in HRN mice. Indeed, lower levels of AAI-DNA adducts were found in tissues of WT mice relative to HRN mice. Absence of AAI demethylation activity (i.e., detoxication) in livers of HRN mice was also shown by *in vitro* experiments. Whereas hepatic microsomes isolated from WT mice oxidized AAI to AAIa, those from HRN mice were not capable of catalyzing this reaction. These results fit well with the proposed scheme of

FIG. 7. Effect of different inhibitors on DNA adduct formation by AAI activated with hepatic or renal microsomes isolated from HRN and WT mice as determined by TLC^{32}P-postlabeling. Hepatic (A) and renal microsomes of control mice (untreated) (B). (C) Hepatic microsomes of mice pretreated (i.p) with 125 mg/kg bw BaP daily for 5 days (Arlt *et al*., 2008). Inhibitors α-NF, α-naphthoflavone; E, ellipticine; FF, furafylline; KC, ketoconazole; α-LA, lipoic acid were used in the experiments. F, fold increase in DNA binding in hepatic or renal microsomes from WT mice compared with HRN mice. RAL, relative adduct labeling. Control, without cofactor. ND, not detected. Values are given as means ± SD ($n = 3$). Values significantly different from incubations without inhibitors: ***$p <$ 0.001 (Student's *t*-test).

AAI metabolism (see Fig. 1). If AAI is not oxidized to AAIa in the liver, it is activated by several enzymes with nitroreductase activity (for a review, see Stiborová *et al*., 2008b, 2008c) to form a cyclic acylnitrenium ion generating DNA adducts (Fig. 1). Our results are in accordance with another study showing that mice that lack hepatic Por-dependent Cyp activity (also HRN mice but a different strain) are extremely sensitive to AA toxicity (Xiao *et al*., 2008). Together with the present study, these results demonstrate that the HRN mouse model used in the study is an excellent model not only to further investigate the toxic effects of AAI but also of other toxic agents.

We found that the hepatic CYP enzymes of the 1A subfamily of mice and rats are crucial for *in vitro d*emethylation of AAI in rodents, similar to its role in human systems (Rosenquist *et al*., 2010; Šístková *et al*., 2008). Inducers of these enzymes such as BaP (Arlt *et al*., 2008) and Sudan I (Stiborová *et al*., 2002b) increased demethylation of AAI catalyzed by mouse and rat hepatic microsomes. The results found in *in vitro* experiments using mouse hepatic microsomes correspond well to the situation *in vivo*; as shown by Rosenquist *et al*. (2010), treatment of mice lacking Cyp1a2 protein expression (Cyp1a2 knockout mice) with AAI led to elevated levels of AAI-DNA adducts in the renal cortex and to an increase in microalbuminuria, an indicator of renal tubule dysfunction, relative to WT mice. A major role of CYP1A in AAI demethylation was also confirmed in the present work by utilizing rat recombinant CYP enzymes; rat CYP1A2, followed by CYP1A1, were the most efficient in AAI demethylation to AAIa. In addition to rat CYP1A1/2, rat CYP enzymes of the 2C subfamily were also capable of demethylating AAI but with much lower efficiencies than CYP1A. But because CYP2C enzymes in rat hepatic microsomes constitute 55% of all CYP, whereas CYP1A only 2% (Nedelcheva and Gut, 1994; Rolsted and Kissmeyer, 2008), the contributions of CYP2C enzymes to AAI demethylation in rat livers might be important.

The increase in AAI-DNA adduct formation found in HRN mice is the combined result of the lack of AAI detoxication by demethylation catalyzed by hepatic Cyps and the reductive activation of AAI by Nqo1, the most effective activating enzyme in human and rat liver and kidney (Stiborová *et al*., 2002a, 2003a, 2011). Expression and activity of this enzyme in the liver of HRN mice were higher than in the liver of WT mice. This higher Nqo1 activity results in better activation of AAI to DNA adduct formation with hepatic cytosol of HRN mice. Likewise, increased AAI-DNA adduct formation was found with renal cytosol of HRN mice as compared with WT mice. Of note, it was reported that polymorphisms in the human NQO1 gene are important in AAI-induced nephropathy (i.e., BEN, a disease that is associated with dietary exposure to AA [Arlt *et al*., 2007; Grollman *et al*., 2007]) and/or carcinogenicity (Atanasova *et al*., 2005; Toncheva *et al*., 2004). Indeed, one of the NQO1 polymorphisms, the genotype NQO1*2/*2, was shown to predispose patients suffering from BEN to develop urothelial cancer (OR = 13.75, 95% CI 1.17–166.21) (Toncheva *et al*., 2004). This finding together with the demonstration of the importance of NQO1 in AAI activation could be an explanation for cancer induction by AAI in only some of the AAN and BEN patients. The results found in this and former (Stiborová *et al*., 2002a, 2003a, 2011) studies strongly support the hypothesis (Stiborová *et al*., 2008c) that a key point determining the carcinogenic and nephrotoxic effects of AAI lies in the balance of activities of reductases such as NQO1, catalyzing AAI-DNA adduct formation, and enzymes such as CYPs, which detoxify AAI to AAIa.

It should be emphasized, however, that under the hypoxic (anaerobic) conditions, mouse hepatic Cyp1a enzymes were also capable of reducing AAI to adduct forming species *in vitro*. Whereas hepatic microsomes of WT mice catalyzed activation of AAI to form AAI-DNA adducts, only hepatic microsomes of HRN mice pretreated with BaP, an inducer of Cyp1a, were able to catalyze this reaction but not microsomes from untreated HRN mice. The major role of Cyp1a in AAI-DNA adduct formation by hepatic microsomes was also demonstrated using selective inhibitors. Inhibitors of Cyp1a1 and -1a2, but not of Por and Cyp3a, decreased levels of AAI-DNA adducts formed by hepatic microsomes. These findings demonstrate that besides the levels of Cyp1a expression in the liver, the *in vivo* oxygen concentration in tissues will affect the balance between nitroreduction and demethylation of AAI, thereby influencing its toxicity and carcinogenicity. Taking into account all available data, we propose that the pathways of AAI metabolism are mainly dictated by the binding affinities of AAI to CYP1A or NQO1, and their enzymatic turnover as well as by the balance between the efficiency of CYP1A to oxidize and reduce AAI.

In contrast to mouse hepatic microsomes, Por and Cyp3a enzymes seem to be more important in AAI-DNA adduct formation in renal microsomes. Previously, POR was found to be an efficient enzyme catalyzing activation of AAI in human kidney (Stiborová *et al*., 2005a). However, the participation of renal mouse Cyp3a in AAI-DNA adduct formation was initially rather surprising because human CYP3A4 that was tested previously for its efficiency to activate AAI was found to be ineffective (Stiborová *et al*., 2005a). CYP3A5, another human enzyme of the CYP3A subfamily, predominantly expressed in human kidney, was herein found to activate AAI. This finding might explain the results of a pilot genetic study (Atanasova *et al*., 2005), which found a weak association between human CYP3A5*1 allele and BEN.

In conclusion, although the impact of individual metabolic enzymes on the nephrotoxicity and carcinogenicity of AAI is still not entirely resolved, one question was unambiguously answered by our present work and other recent studies (Rosenquist *et al*. 2010; Xiao *et al*., 2008), namely that hepatic Cyp1a enzymes detoxify AAI in mice, thus decreasing its renal toxicity. The evaluation of interindividual variations in the human enzymes that play a major role in AAI activation and

detoxication, including their genetic polymorphisms, remain a major challenge to explain human individual susceptibility to AAI and to predict the risk of cancer among the AAN and BEN patients.

SUPPLEMENTARY DATA

Supplementary data are available online at http://toxsci.oxfordjournals.org/.

FUNDING

The authors would like to thank to Grant Agency of Czech Republic (grants 303/09/0472, and 305/09/H008) and to the Ministry of Education of Czech Republic (grants MSM0021620808 and 1M0505). Work at the Biomedical Research Centre and Institute of Cancer Research is supported by Cancer Research UK.

REFERENCES

Arlt, V. M., Ferluga, D., Stiborova, M., Pfohl-Leszkowicz, A., Vukelic, M., Ceovic, S., Schmeiser, H. H., and Cosyns, J. P. (2002). Is aristolochic acid a risk factor for Balkan endemic nephropathy-associated urothelial cancer? *Int. J. Cancer.* **101,** 500–502.

Arlt, V. M., Henderson, C. J., Wolf, C. R., Schmeiser, H. H., Phillips, D. H., and Stiborova, M. (2006). Bioactivation of 3-aminobenzanthrone, a human metabolite of the environmental pollutant 3-nitrobenzanthrone: evidence for DNA adduct formation mediated by cytochrome P450 enzymes and peroxidases. *Cancer Lett.* **234,** 220–231.

Arlt, V. M., Stiborova, M., Henderson, C. J., Osborne, M. R., Bieler, C. A., Frei, E., Martinek, V., Sopko, B., Wolf, C. R., Schmeiser, H. H., *et al.* (2005). Environmental pollutant and potent mutagen 3-nitrobenzanthrone forms DNA adducts after reduction by NAD(P)H:quinone oxidoreductase and conjugation by acetyltransferases and sulfotransferases in human hepatic cytosols. *Cancer Res.* **65,** 2644–2652.

Arlt, V. M., Stiborova, M., Henderson, C. J., Thiemann, M., Frei, E., Aimova, D., Singh, R., Gamboa da Costa, G., Schmitz, O. J., Farmer, P. B., *et al.* (2008). Metabolic activation of benzo[a]pyrene in vitro by hepatic cytochrome P450 contrasts with detoxification in vivo: experiments with hepatic cytochrome P450 reductase null mice. *Carcinogenesis* **29,** 656–665.

Arlt, V. M., Stiborova, M., Hewer, A., Schmeiser, H. H., and Phillips, D. H. (2003). Human enzymes involved in the metabolic activation of the environmental contaminant 3-nitrobenzanthrone: evidence for reductive activation by human NADPH:cytochrome p450 reductase. *Cancer Res.* **63,** 2752–2761.

Arlt, V. M., Stiborova, M., vom Brocke, J., Simoes, M. L., Lord, G. M., Nortier, J. L., Hollstein, M., Phillips, D. H., and Schmeiser, H. H. (2007). Aristolochic acid mutagenesis: molecular clues to the aetiology of Balkan endemic nephropathy-associated urothelial cancer. *Carcinogenesis* **28,** 2253–2261.

Arlt, V. M., Zuo, J., Trenz, K., Roufosse, C. A., Lord, G. M., Nortier, J. L., Schmeiser, H. H., Hollstein, M., and Phillips, D. H. (2011). Gene expression changes induced by the human carcinogen aristolochic acid I in renal and hepatic tissue of mice. *Int. J. Cancer.* **128,** 21–32.

Atanasova, S., von Ahsen, N., Toncheva, D. I., Dimitrov, T. G., Oellerich, M., and Amstrong, V. M. (2005). Genetic polymorphism of cytochrome P450 among patients with Balkan endemic nephropathy (BEN). *Clin. Biochem.* **38,** 223–228.

Bieler, C. A., Stiborová, M., Wiessler, M., Cosyns, J. P., van Ypersele de Strihou, C., and Schmeiser, H. H. (1997). ^{32}P-post-labelling analysis of DNA adducts formed by aristolochic acid in tissues from patients with Chinese herbs nephropathy. *Carcinogenesis* **18,** 1063–1067.

Bořek-Dohalská, L., Hodek, P., Šulc, M., and Stiborová, M. (2001). α-Naphthoflavone acts as activator and reversible or irreversible inhibitor of rabbit microsomal CYP3A6. *Chem. Biol. Interact.* **138,** 85–106.

Bořek-Dohalská, L., and Stiborová, M. (2010). Cytochrome P450 3A activities and their modulation by α-naphthoflavone *in vitro* are dictated by the efficiencies of model experimental systems. *Collect. Czech. Chem. Commun.* **75,** 201–220.

Buters, J. T., Sakai, S., Richter, T., Pineau, T., Alexander, D. L., Savas, U., Doehmer, J., Ward, J. M., Jefcoate, C. R., and Gonzalez, F. J. (1999). Cytochrome P450 CYP1B1 determines susceptibility to 7, 12-dimethylbenz[a]anthracene-induced lymphomas. *Proc. Natl. Acad. Sci. U.S.A.* **96,** 1977–1982.

Chan, W., Cu, L., Xu, G., and Cai, Z. (2006). Study of the phase I and phase II metabolism of nephrotoxin aristolochic acid by liquid chromatography/tandem mass spectrometry. *Rapid Commun. Mass Spectrom.* **20,** 1755–1760.

Chan, W., Luo, H. B., Zheng, Y., Cheng, Y. K., and Cai, Z. (2007). Investigation of the metabolism and reductive activation of carcinogenic aristolochic acids in rats. *Drug Metab. Dispos.* **35,** 866–874.

Debelle, F. D., Vanherweghem, J. L., and Nortier, J. L. (2008). Aristolochic acid nephropathy: a worldwide problem. *Kidney Int.* **74,** 158–169.

Elovaara, E., Mikkola, J., Stockmann-Juvala, H., Luukkanen, L., Keski-Hynnilä, H., Kostiainen, R., Pasanen, M., Pelkonen, O., and Vainio, H. (2007). Polycyclic aromatic hydrocarbon (PAH) metabolizing enzyme activities in human lung, and their inducibility by exposure to naphthalene, phenanthrene, pyrene, chrysene, and benzo(a)pyrene as shown in the rat lung and liver. *Arch. Toxicol.* **81,** 169–182.

Ernster, L. (1967). DT-Diaphorase. *Methods Enzymol.* **10,** 309–317.

Grollman, A. P., Shibutani, S., Moriya, M., Miller, F., Wu, L., Moll, U., Suzuki, N., Fernandes, A., Rosenquist, T., Medverec, Z., *et al.* (2007). Aristolochic acid and the etiology of endemic (Balkan) nephropathy. *Proc. Natl. Acad. Sci. U.S.A.* **104,** 12129–12134.

Grosse, Y., Baan, R., Straif, K., Secretan, B., El Ghissassi, F., Bouvard, V., Benbrahim-Tallaa, L., Guha, N., Galichet, L., and Cogliano, V. (2009). A review of human carcinogens-Part A: pharmaceuticals. *Lancet Oncol.* **10,** 13–14.

Henderson, C. J., Otto, D. M., Carrie, D., Magnuson, M. A., McLaren, A. W., Rosewell, I., and Wolf, C. R. (2003a). Inactivation of the hepatic cytochrome P450 system by conditional deletion of hepatic cytochrome P450 reductase. *J. Biol. Chem.* **278,** 13480–13486.

Henderson, C. J., Otto, D. M., McLaren, A. W., Carrie, D., and Wolf, C. R. (2003b). Knockout mice in xenobiotic metabolism. *Drug Metab. Rev.* **35,** 385–392.

Henderson, C. J., Pass, G. J., and Wolf, C. R. (2006). The hepatic cytochrome P450 reductase null mouse as a tool to identify a successful candidate entity. *Toxicol. Lett.* **162,** 111–117.

Henderson, C. J., and Wolf, C. R. (2003). Transgenic analysis of human drug-metabolizing enzymes: preclinical drug development and toxicology. *Mol. Interv.* **3,** 331–343.

Hockley, S. L., Arlt, V. M., Brewer, D., Te Poele, R., Workman, P., Giddings, I., and Phillips, D. H. (2007). AHR- and DNA-damage-mediated gene expression responses induced by benzo(a)pyrene in human cell lines. *Chem. Res. Toxicol.* **20,** 1797–1810.

Hodek, P., Teplá, M., Křížková, J., and Stiborová, M. (2009). Modulation of cytochrome P450 enzyme system by flavonoid compounds. *Neuro Endocrinol. Lett.* **30**(Suppl. 1), 67–71.

Kimura, S., Kawabe, M., Yu, A., Morishima, H., Fernandez-Salguero, P., Hammons, G. J., Ward, J. M., Kadlubar, F. F., and Gonzalez, F. J. (2003). Carcinogenesis of the food mutagen PhIP in mice is independent of CYP1A2. *Carcinogenesis* **24,** 583–587.

Krumbiegel, G., Hallensleben, J., Mennicke, W. H., Rittmann, N., and Roth, H. J. (1987). Studies on the metabolism of aristolochic acids I and II. *Xenobiotica* **17,** 981–991.

Lai, M. N., Wang, S. M., Chen, P. C., Chen, Y. Y., and Wang, J. D. (2010). Population-based case-control study of Chinese herbal products containing aristolochic acid and urinary tract cancer risk. *J. Natl. Cancer Inst.* **102,** 179–186.

Lemy, A., Wissing, K. M., Rorive, S., Zlotta, A., Roumeguere, T., Muniz Martinez, M. C., Decaestecker, C., Salmon, I., Abramowicz, D., Vanherweghem, J. L., *et al.* (2008). Late onset of bladder urothelial carcinoma after kidney transplantation for end-stage aristolochic acid nephropathy: a case series with 15-year follow-up. *Am. J. Kidney Dis.* **51,** 471–477.

Lord, G. M., Cook, T., Arlt, V. M., Schmeiser, H. H., Williams, G., and Pusey, C. D. (2001). Urothelial malignant disease and Chinese herbal nephropathy. *Lancet* **358,** 1515–1516.

Lord, G. M., Hollstein, M., Arlt, V. M., Roufosse, C., Pusey, C. D., Cook, T., and Schmeiser, H. H. (2004). DNA adducts and p53 mutations in a patient with aristolochic acid-associated nephropathy. *Am. J. Kidney Dis.* **43,** e11–e17.

Mizerovská, J., Dračínská, H., Frei, E., Schmeiser, H. H., Arlt, V. M., and Stiborová, M. (2011). Induction of biotransformation enzymes by the carcinogenic air-pollutant 3-nitrobenzanthrone in liver; kidney and lung; after intra-tracheal instillation in rats. *Mutat. Res.* **720,** 34–41.

Nebert, D. W. (2006). Comparison of gene expression in cell culture to that in the intact animal: relevance to drugs and environmental toxicants. Focus on "development of a transactivator in hepatoma cells that allows expression of phase I, phase II, and chemical defense genes". *Am. J. Physiol.* **290,** C37–C41.

Nebert, D. W., and Dalton, T. P. (2006). The role of cytochrome P450 enzymes in endogenous signalling pathways and environmental carcinogenesis. *Nat. Rev. Cancer.* **6,** 947–960.

Nedelcheva, V., and Gut, I. (1994). P450 in the rat and man: methods of investigation, substrate specificities and relevance to cancer. *Xenobiotica* **24,** 1151–1175.

Nedelko, T., Arlt, V. M., Phillips, D. H., and Hollstein, M. (2009). TP53 mutation signature supports involvement of aristolochic acid in the aetiology of endemic nephropathy-associated tumours. *Int. J. Cancer.* **124,** 987–990.

Nortier, J. L., Martinez, M. C., Schmeiser, H. H., Arlt, V. M., Bieler, C. A., Petein, M., Depierreux, M. F., De Pauw, L., Abramowicz, D., Vereerstraeten, P., *et al.* (2000). Urothelial carcinoma associated with the use of a Chinese herb (*Aristolochia fangchi*). *N. Engl. J. Med.* **342,** 1686–1692.

Pass, G. J., Carrie, D., Boylan, M., Lorimore, S., Wright, E., Houston, B., Henderson, C. J., and Wolf, C. R. (2005). Role of hepatic cytochrome P450s in the pharmacokinetics and toxicity of cyclophosphamide: studies with the hepatic cytochrome P450 reductase null mouse. *Cancer Res.* **65,** 4211–4217.

Pfau, W., Schmeiser, H. H., and Wiessler, M. (1990). Aristolochic acid binds covalently to the exocyclic amino group of purine nucleotides in DNA. *Carcinogenesis* **1,** 313–319.

Phillips, D. H., and Arlt, V. M. (2007). The ^{32}P-postlabeling assay for DNA adducts. *Nature Protoc.* **2,** 2772–2781.

Rendic, S., and DiCarlo, F. J. (1997). Human cytochrome P450 enzymes: a status report summarizing their reactions, substrates, inducers, and inhibitors. *Drug Metab. Rev.* **29,** 413–480.

Rolsted, K., and Kissmeyer, A. M. (2008). Evaluation of cytochrome P450 activity in vitro, using dermal and hepatic microsomes from four species and two keratinocyte cell lines in culture. *Arch. Dermatol. Res.* **300,** 11–18.

Rosenquist, T. A., Einolf, H. J., Dickman, K. G., Wang, L., Smith, A., and Grollman, A. P. (2010). Cytochrome P450 1A2 detoxicates aristolochic acid in the mouse. *Drug Metab. Dispos.* **38,** 761–768.

Schmeiser, H. H., Bieler, C. A., Wiessler, M., van Ypersele de Strihou, C., and Cosyns, J. P. (1996). Detection of DNA adducts formed by aristolochic acid in renal tissue from patients with Chinese herbs nephropathy. *Cancer Res.* **56,** 2025–2028.

Schmeiser, H. H., Pool, B. L., and Wiessler, M. (1984). Mutagenicity of the two main components of commercially available carcinogenic aristolochic acid in Salmonella typhimurium. *Cancer Lett.* **23,** 97–101.

Schmeiser, H. H., Schoepe, K. B., and Wiessler, M. (1988). DNA adduct formation of aristolochic acid I and II in vitro and in vivo. *Carcinogenesis* **9,** 297–303.

Schmeiser, H. H., Stiborova, M., and Arlt, V. M. (2009). Chemical and molecular basis of the carcinogenicity of Aristolochia plants. *Curr. Opin. Drug Discov. Devel.* **12,** 141–148.

Shibutani, S., Bonala, R. R., Rosenquist, T., Rieger, R., Suzuki, N., Johnson, F., Miller, F., and Grollman, A. P. (2010). Detoxification of aristolochic acid I by *O*-demethylation: less nephrotoxicity and genotoxicity of aristolochic acid Ia in rodents. *Int. J. Cancer.* **127,** 1021–1027.

Simoes, M. L., Hockley, S. L., Schwerdtle, T., da Costa, G. G., Schmeiser, H. H., Phillips, D. H., and Arlt, V. M. (2008). Gene expression profiles modulated by the human carcinogen aristolochic acid I in human cancer cells and their dependence on TP53. *Toxicol. Appl. Pharmacol.* **232,** 86–98.

Šístková, J., Hudecek, J., Hodek, P., Frei, E., Schmeiser, H. H., and Stiborová, M. (2008). Human cytochromes P450 1A1 and 1A2 participate in detoxication of carcinogenic aristolochic acid. *Neuro Endocrinol. Lett.* **29,** 733–737.

Stiborová, M., Arlt, V. M., Henderson, C. J., Wolf, C. R., Kotrbova, V., Moserova, M., Hudecek, J., Phillips, D. H., and Frei, E. (2008a). Role of hepatic cytochromes P450 in bioactivation of the anticancer drug ellipticine: studies with the hepatic NADPH: cytochrome P450 reductase null mouse. *Toxicol. Appl. Pharmacol.* **226,** 318–327.

Stiborová, M., Asfaw, B., Frei, E., Schmeiser, H. H., and Wiessler, M. (1995). Benzenediazonium ion derived from Sudan I forms an 8-(phenylazo)guanine adduct in DNA. *Chem. Res. Toxicol.* **8,** 489–498.

Stiborová, M., Dračínská, H., Hájková, J., Kadeřábková, P., Frei, E., Schmeiser, H. H., Souček, P., Phillips, D. H., and Arlt, V. M. (2006). The environmental pollutant and carcinogen 3-nitrobenzanthrone and its human metabolite 3-aminobenzanthrone are potent inducers of rat hepatic cytochromes P450 1A1 and -1A2 and NAD(P)H:quinone oxidoreductase. *Drug Metab. Dispos.* **34,** 1398–1405.

Stiborová, M., Fernando, R. C., Schmeiser, H. H., Frei, E., Pfau, W., and Wiessler, M. (1994). Characterization of DNA adducts formed by aristolochic acids in the target organ (forestomach) of rats by ^{32}P-postlabelling analysis using different chromatographic procedures. *Carcinogenesis* **15,** 1187–1192.

Stiborová, M., Frei, E., Arlt, V. M., and Schmeiser, H. H. (2008b). Metabolic activation of carcinogenic aristolochic acid, a risk factor for Balkan endemic nephropathy. *Mutat. Res.* **658,** 55–67.

Stiborová, M., Frei, E., Breuer, A., Wiessler, M., and Schmeiser, H. H. (2001a). Evidence for reductive activation of carcinogenic aristolochic acids by prostaglandin H synthase—^{32}P-postlabeling analysis of DNA adduct formation. *Mutat. Res.* **493,** 149–160.

Stiborová, M., Frei, E., Hodek, P., Wiessler, M., and Schmeiser, H. H. (2005a). Human hepatic and renal microsomes, cytochromes P450 1A1/2, NADPH:-cytochrome P450 reductase and prostaglandin H synthase mediate the formation of aristolochic acid-DNA adducts found in patients with urothelial cancer. *Int. J. Cancer.* **113,** 189–197.

Stiborová, M., Frei, E., and Schmeiser, H. H. (2008c). Biotransformation enzymes in development of renal injury and urothelial cancer caused by aristolochic acid. *Kidney Int.* **73,** 1209–1211.

Stiborová, M., Frei, E., Sopko, B., Sopkova, K., Markova, V., Lankova, M., Kumstyrova, T., Wiessler, M., and Schmeiser, H. H. (2003a). Human cytosolic enzymes involved in the metabolic activation of carcinogenic aristolochic acid: evidence for reductive activation by human NAD(P)H: quinone oxidoreductase. *Carcinogenesis* **24,** 1695–1703.

Stiborová, M., Frei, E., Sopko, B., Wiessler, M., and Schmeiser, H. H. (2002a). Carcinogenic aristolochic acids upon activation by DT-diaphorase form adducts found in DNA of patients with Chinese herbs nephropathy. *Carcinogenesis* **23,** 617–625.

Stiborová, M., Frei, E., Wiessler, M., and Schmeiser, H. H. (2001b). Human enzymes involved in the metabolic activation of carcinogenic aristolochic acids: evidence for reductive activation by cytochromes P450 1A1 and 1A2. *Chem. Res. Toxicol.* **14,** 1128–1137.

Stiborová, M., Hájek, M., Frei, E., and Schmeiser, H. H. (2001c). Carcinogenic and nephrotoxic alkaloids aristolochic acids upon activation by NADPH: cytochrome P450 reductase form adducts found in DNA of patients with Chinese herbs nephropathy. *Gen. Physiol. Biophys.* **20,** 375–392.

Stiborová, M., Mareš, J., Frei, E., Arlt, V. M., Martínek, V., and Schmeiser, H. H. (2011). The human carcinogen aristolochic acid I is activated to form DNA adducts by human NAD(P)H:quinone oxidoreductase without the contribution of acetyltransferases or sulfotransferases. *Environ. Mol. Mutagen.*

Stiborová, M., Martinek, V., Rydlova, H., Hodek, P., and Frei, E. (2002b). Sudan I is a potential carcinogen for humans: evidence for its metabolic activation and detoxication by human recombinant cytochrome P450 1A1 and liver microsomes. *Cancer Res.* **62,** 5678–5684.

Stiborová, M., Martínek, V., Rýdlová, H., Koblas, T., and Hodek, P. (2005b). Expression of cytochrome P450 1A1 and its contribution to oxidation of a potential human carcinogen 1-phenylazo-2-naphthol (Sudan I) in human livers. *Cancer Lett.* **220,** 145–154.

Stiborová, M., Sejbal, J., Borek-Dohalska, L., Aimova, D., Poljakova, J., Forsterova, K., Rupertova, M., Wiesner, J., Hudecek, J., Wiessler, M., *et al.* (2004). The anticancer drug ellipticine forms covalent DNA adducts, mediated by human cytochromes P450, through metabolism to 13-hydroxyellipticine and ellipticine N^2-oxide. *Cancer Res.* **64,** 8374–8380.

Stiborová, M., Sopko, B., Hodek, P., Frei, E., Schmeiser, H. H., and Hudeček, J. (2005c). The binding of aristolochic acid I to the active site of human cytochromes P450 1A1 and 1A2 explains their potential to reductively activate this human carcinogen. *Cancer Lett.* **229,** 193–204.

Stiborová, M., Stiborová-Rupertová, M., Borek-Dohalská, L., Wiessler, M., and Frei, E. (2003b). Rat microsomes activating the anticancer drug ellipticine to species covalently binding to deoxyguanosine in DNA are a suitable model mimicking ellipticine bioactivation in humans. *Chem. Res. Toxicol.* **16,** 38–47.

Toncheva, D. I., von Ahsen, N., Atanasova, S. Y., Dimitrov, T. G., and Amstrong, V. M. (2004). Identification of NQO1 and GSTs genotype frequencies in Bulgarian patients with Balkan endemic nephropathy. *J. Nephrol.* **17,** 384–389.

Tsuneoka, Y., Dalton, T. P., Miller, M. L., Clay, C. D., Shertzer, H. G., Talaska, G., Medvedovic, M., and Nebert, D. W. (2003). 4-aminobiphenyl-induced liver and urinary bladder DNA adduct formation in Cyp1a2(-/-) and Cyp1a2(+/+) mice. *J. Natl. Cancer Inst.* **95,** 1227–1237.

Ueng, Y.-F., Kuwabara, T., Chun, Y.-J., and Guengerich, F. P. (1997). Cooperativity in oxidation catalyzed by cytochrome P450 3A4. *Biochemistry* **36,** 370–381.

Uno, S., Dalton, T. P., Derkenne, S., Curran, C. P., Miller, M. L., Shertzer, H. G., and Nebert, D. W. (2004). Oral exposure to benzo[a]pyrene in the mouse: detoxication by inducible cytochrome P450 is more important than metabolic activation. *Mol. Pharmacol.* **65,** 1225–1237.

Vanherweghem, J. L., Depierreux, M., Tielemans, C., Abramowicz, D., Dratwa, M., Jadoul, M., Richard, C., Vandervelde, D., Verbeelen, D., Vanhaelen-Fastre, R., *et al.* (1993). Rapidly progressive interstitial renal fibrosis in young women: association with slimming regimen including Chinese herbs. *Lancet* **341,** 387–391.

Vondráček, J., Krcmár, P., Procházková, J., Trilecová, L., Gavelová, M., Skálová, L., Szotáková, B., Buncek, M., Radilová, H., Kozubík, A., *et al.* (2009). The role of aryl hydrocarbon receptor in regulation of enzymes involved in metabolic activation of polycyclic aromatic hydrocarbons in a model of rat liver progenitor cells. *Chem. Biol. Interact.* **180,** 226–237.

Xiao, Y., Ge, M., Xue, X., Wang, C., Wang, H., Wu, X., Li, L., Liu, L., Qi, X., Zhang, Y., *et al.* (2008). Hepatic cytochrome P450s metabolize aristolochic acid and reduce its kidney toxicity. *Kidney Int.* **73,** 1231–1239.

Xiao, Y., Xue, X., Wu, Y. F., Xin, G. Z., Qian, Y., Xie, T. P., Gong, L. K., and Ren, J. (2009). beta-Naphthoflavone protects mice from aristolochic acid-I-induced acute kidney injury in a CYP1A dependent mechanism. *Acta Pharmacol. Sin.* **30,** 1559–1565.

Xue, X., Xiao, Y., Zhu, H., Wang, H., Liu, Y., Xie, T., and Ren, J. (2008). Induction of P450 1A by 3-methylcholanthrene protects mice from aristolochic acid-I-induced acute renal injury. *Nephrol. Dial. Transplant.* **23,** 3074–3081.

Příloha 8

VĚRA KOTRBOVÁ, BARBORA MRÁZOVÁ, **MICHAELA MOSEROVÁ**, VÁCLAV MARTÍNEK, PETR HODEK, JIŘÍ HUDEČEK, EVA FREI, MARIE STIBOROVÁ:

CYTOCHROME B_5 SHIFTS OXIDATION OF THE ANTICANCER DRUG ELLIPTICINE BY CYTOCHROMES P450 1A1 AND 1A2 FROM ITS DETOXICATION TO ACTIVATION, THEREBY MODULATING ITS PHARMACOLOGICAL EFFICACY

Biochem Pharmacol., 2011 v tisku.

Biochemical Pharmacology xxx (2011) xxx–xxx

Contents lists available at ScienceDirect

Biochemical Pharmacology

journal homepage: www.elsevier.com/locate/biochempharm

Cytochrome b_5 shifts oxidation of the anticancer drug ellipticine by cytochromes P450 1A1 and 1A2 from its detoxication to activation, thereby modulating its pharmacological efficacy

Věra Kotrbová [a], Barbora Mrázová [a], Michaela Moserová [a], Václav Martínek [a], Petr Hodek [a], Jiří Hudeček [a], Eva Frei [b], Marie Stiborová [a,*]

[a] Department of Biochemistry, Faculty of Science, Charles University, Albertov 2030, 128 40 Prague 2, Czech Republic
[b] Division of Preventive Oncology, National Center for Tumor Diseases, German Cancer Research Center, Im Neuenheimer Feld 280, 69120 Heidelberg, Germany

ARTICLE INFO

Article history:
Received 26 April 2011
Accepted 3 June 2011
Available online xxx

Keywords:
CYP1A1/2
Cytochrome b_5
Ellipticine
Modulation
Activation

ABSTRACT

Ellipticine is a pro-drug, whose activation is dependent on its oxidation by cytochromes P450 (CYP) and peroxidases. Cytochrome b_5 alters the ratio of ellipticine metabolites formed by isolated reconstituted CYP1A1 and 1A2, favoring formation of 12-hydroxy- and 13-hydroxyellipticine metabolites implicated in ellipticine–DNA adduct formation, at the expense of 9-hydroxy- and 7-hydroxyellipticine that are detoxication products. Cytochrome b_5 enhances the production of 12-hydroxy and 13-hydroxyellipticine. The change in metabolite ratio results in an increased formation of covalent ellipticine–DNA adducts, one of the DNA-damaging mechanisms of ellipticine antitumor action. This finding explains previous apparent discrepancies found with isolated enzymes and *in vivo*, where CYP1A enzymatic activation correlated with ellipticine–DNA-adduct levels while isolated CYP1A1 or 1A2 in reconstituted systems were much less effective than CYP3A4. The effect of cytochrome b_5 might be even more pronounced *in vivo*, since, as we show here, ellipticine increases levels of cytochrome b_5 in rat liver. Our results demonstrate that both the native 3D structure of cytochrome b_5 and the presence of the heme as an electron transfer agent in this protein enable a shift in ellipticine metabolites formed by CYP1A1/2.

1. Introduction

Ellipticine (5,11-dimethyl-6*H*-pyrido[4,3-*b*]carbazole, Fig. 1), an alkaloid isolated from Apocynaceae plants, exhibits significant antitumor and anti-HIV activities (for a summary see [1–3])]. The main reasons for the interest in ellipticine and its derivatives for clinical purposes are their high efficiencies against several types of cancer, their limited toxic side effects, and their lack of haematological toxicity [4]. Nevertheless, ellipticine is a potent mutagen. Many ellipticine derivatives are mutagenic to *Salmonella typhimurium* Ames tester strains, bacteriophage T4, *Neurospora crassa*, and mammalian cells and induce prophage lambda in *Escherichia coli* for overview (for overview, see [1–3]).

The precise molecular mechanism responsible for anticancer effects of ellipticine has not yet been explained. It was suggested that the major mechanisms of its antitumor, mutagenic and cytotoxic activities are (i) intercalation into DNA [4,5], and (ii) inhibition of DNA topoisomerase II activity [2–7].

We have demonstrated that ellipticine also covalently binds to DNA after being enzymatically activated by cytochromes P450 (CYP) or peroxidases [1–3,8–13], suggesting a third DNA-damaging mechanism of action. Two major DNA adducts generated from 13-hydroxy- and 12-hydroxyellipticine (Fig. 1) during the CYP- and peroxidase-mediated ellipticine metabolism are formed *in vitro* and *in vivo* in DNA of healthy organs of rats and mice treated with this anticancer drug [1,3,8–13]. Human CYP3A4 and rat CYP3A1 are the major enzymes oxidizing ellipticine to the reactive metabolites binding to DNA (13-hydroxy- and 12-hydroxyellipticine) *in vitro* [3,9,10]. The same DNA adducts were also detected in human cancer cells in culture, such as breast adenocarcinoma MCF-7 [14], the leukaemias HL-60 and CCRF-CEM [15], neuroblastoma [16] and glioblastoma cells [17], and in rat mammary adenocarcinoma *in vivo* [3]. Toxic effects of ellipticine in these cancer cells correlated with levels of ellipticine-derived DNA adducts and were dependent on expression of CYP1A1, 1B1, 3A4 and lactoperoxidase (LPO), cyclooxygenase (COX) and myeloperoxidase (MPO) in these cells

Abbreviations: COX, cyclooxygenase; CYP, cytochrome P450; HRN, hepatic cytochrome P450 reductase null; GAPDH, glyceraldehyde phosphate dehydrogenase; HPLC, high-performance liquid chromatography; i.p., intra-peritoneal; LPO, lactoperoxidase; MPO, myeloperoxidase; PEI-cellulose, polyethylenimine-cellulose; RAL, relative adduct labeling; r.t., retention time; TLC, thin layer chromatography.

* Corresponding author. Tel.: +420 221951285; fax: +420 221951283.
E-mail address: stiborov@natur.cuni.cz (M. Stiborová).

0006-2952/$ – see front matter © 2011 Published by Elsevier Inc.
doi:10.1016/j.bcp.2011.06.003

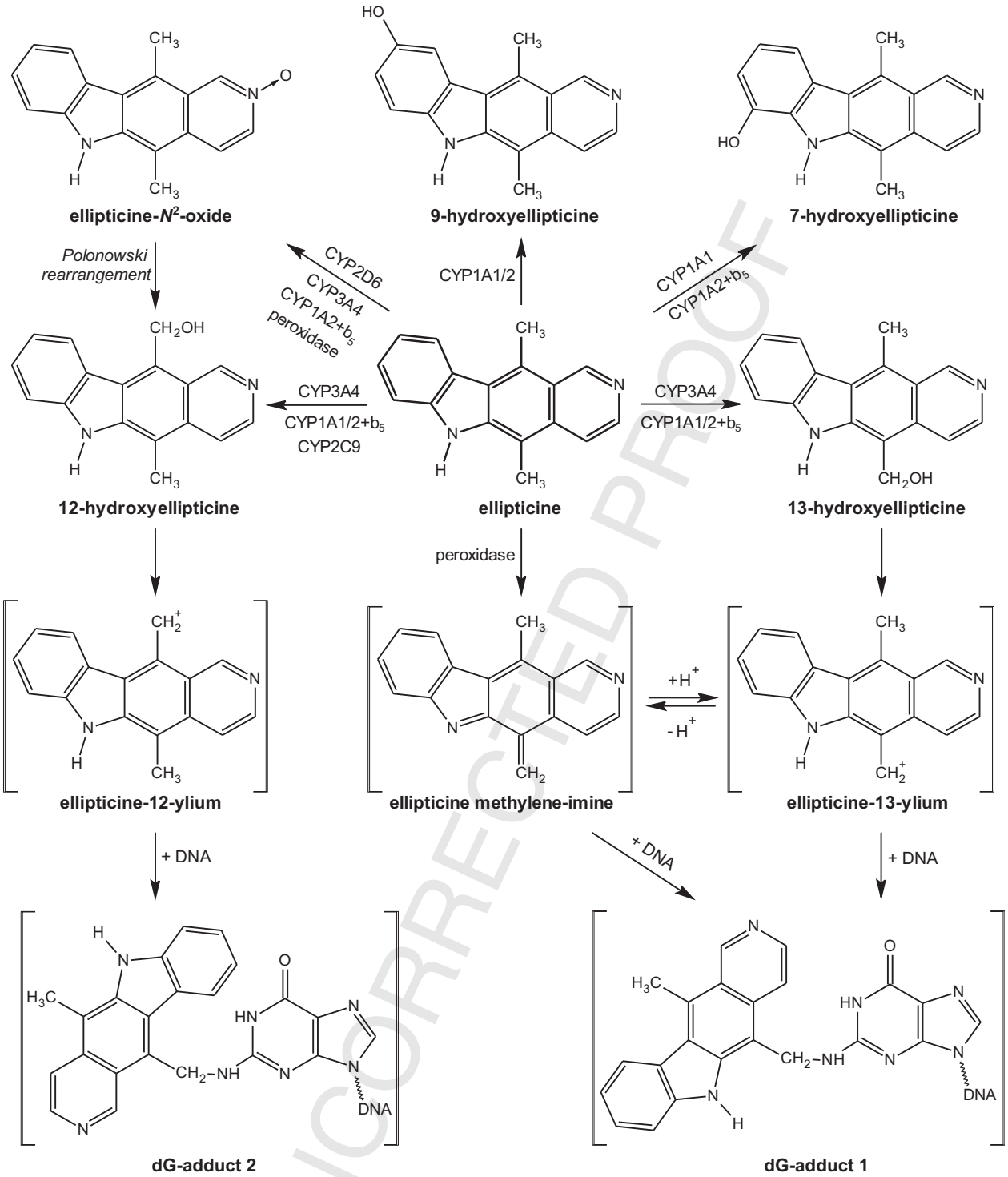

Fig. 1. Scheme of ellipticine metabolism by CYPs and peroxidases showing the identified metabolites and those proposed to form DNA adducts. The compounds shown in brackets were not detected under the experimental conditions and/or not structurally characterized. The CYP enzymes predominantly oxidizing ellipticine shown in the figure were identified in this work and/or in our previous studies [9,10,18].

[14–17]. Based on these data, ellipticine might be considered a drug, whose pharmacological efficiency and/or genotoxic side effects are dependent on its activation by CYPs and peroxidases in target tissues.

Concerning formation of ellipticine-derived DNA adducts in healthy organs, the risk of treating patients with this compound might be considered. Nevertheless, our *in vivo* studies using the rat experimental model mimicking the fate of ellipticine in human [8,12] demonstrated that ellipticine–DNA adducts did not persist in healthy tissues of rats treated with ellipticine [12]. Therefore, these results suggest a relatively low risk of the genotoxic side effects of ellipticine during the cancer treatment in human.

Studies correlating levels of individual ellipticine–DNA adducts to CYP enzyme expression determined in organs of rats treated with ellipticine showed good correlations of major adduct levels with CYP1A1/2 and CYP3A1 levels [8]. This finding is in contrast to

the metabolite patterns and DNA adduct levels seen with pure CYP enzymes of rat and human origin reconstituted with NADPH:CYP reductase [3,10,18]. Here CYP1A isoforms did not activate ellipticine, but 9-hydroxy- and 7-hydroxyellipticine, the detoxication products (Fig. 1), were the major metabolites, and as a consequence ellipticine–DNA adduct levels were very low.

In isolated microsomes, in cells and in intact organs cytochrome b_5 might influence CYP-catalyzed reactions [19]. The lack of cytochrome b_5 in our reconstituted systems could therefore be a reason for the low activating capacity of isolated CYP1A1/2. We therefore investigated the role of cytochrome b_5 on CYP catalyzed oxidation of ellipticine. A reconstituted system consisting of pure CYP1A1 or 1A2 enzymes with NADPH:CYP reductase in liposomes with or without cytochrome b_5 was used.

Many studies have investigated whether cytochrome b_5 can change the rates of CYP-mediated oxidation of substrates. Depending on the individual CYP involved, the experimental conditions and the substrate utilized, cytochrome b_5 has been shown to stimulate, inhibit or have no effect on CYP mediated reactions (for a summary, see [19–22]). This work is, to our knowledge, the first study showing that cytochrome b_5 can alter not only the amounts but also the types of metabolites produced from a single substrate by one CYP.

Mechanistic studies of the action of cytochrome b_5 on the catalysis of CYP1A1/2 were also performed using the holoprotein of cytochrome b_5, its apo-form (devoid of heme) or apo-cytochrome b_5 reconstituted with manganese protoporphyrin IX (Mn-cytochrome b_5).

2. Materials and methods

2.1. Chemicals

$NADP^+$, NADPH, ellipticine, D-glucose 6-phosphate, D-glucose 6-phosphate dehydrogenase, β-naphthoflavone (β-NF), dilauroyl phosphatidylcholine, dioleyl phosphatidylcholine, and dilauroyl-phosphatidylserine, lysozyme, hemin, cytochrome c, horse heart myoglobin, human serum albumin and calf thymus DNA were obtained from Sigma Chemical Co. (St. Louis, MO, USA); Sudan I from BDH (Poole, UK); 7-ethoxyresorufin and 7-methoxyresorufin from Fluka Chemie AG (Buchs, Switzerland); superoxide dismutase from Roche Diagnostics (Mannheim, Germany); 9-hydroxyellipticine (5,11-dimethyl-9-hydroxy-6*H*-pyrido[4,3-*b*]carbazole) were from Calbiochem (San Diego, CA, USA). All these and other chemicals from commercial sources used in the experiments were reagent grade or better. 7-Hydroxyellipticine and the N^2-oxide of ellipticine were synthesized as described [10] by Kučka (Charles University, Prague, Czech Republic); their purity was >99.5% as estimated by high-performance liquid chromatography (HPLC). Enzymatically prepared 12-hydroxy- and 13-hydroxyellipticine were obtained from multiple HPLC runs of ethyl acetate extracts of incubations of ellipticine with human and/or rat hepatic microsomes as described [10].

2.2. Animal experiments

The study was conducted in accordance with the Regulations for the Care and Use of Laboratory Animals (311/1997, Ministry of Agriculture, Czech Republic), in compliance with the Declaration of Helsinki. Male Wistar rats (~100 g) were treated with a single dose of 4 or 40 mg/kg body weight ($N = 3$) of ellipticine by intraperitoneal injection. Ellipticine was dissolved in sunflower oil/DMSO (1:1, v/v) to give a concentration of 6 mg/ml. Three control animals received an equal volume of solvent only. Rats were placed in cages in temperature and humidity controlled rooms. Standardized diet and water were provided *ad libitum*. The animals were killed 48 h after treatment by cervical dislocation. Livers were removed immediately after death and immediately used for preparation of microsomal fractions.

2.3. Preparation of microsomes

Microsomes were isolated from fresh livers of rats as described [9]. Protein concentrations in the microsomal fractions were assessed using the bicinchoninic acid protein assay with bovine serum albumin as a standard [23]. Hepatic microsomal preparations from rats that had been pre-treated with ellipticine were analyzed for the presence of ellipticine or its metabolites by HPLC as described [10]. Neither ellipticine nor any of its metabolites were detectable in microsomal fractions from tissues of rats that had been pretreated with ellipticine. Microsomes from the livers of three male rabbits pretreated with 80 mg/kg day of β-NF i.p. for four consecutive days were isolated as described [9].

2.4. Isolation of CYPs, NADPH:CYP reductase, cytochrome b_5 and apo-cytochrome b_5

Recombinant rat CYP1A1 protein was purified to homogeneity from membranes of *E. coli* transfected with a modified *CYP1A1* cDNA [24], in the laboratory of H.W. Strobel (University of Texas, Medical School of Houston, Texas, USA) by P. Hodek (Charles University, Prague, Czech Republic). CYP1A2 was isolated from liver microsomes of rabbits induced with β-NF by procedures described by Haugen and Coon [25]. Rabbit liver NADPH:CYP reductase was purified as described [26]. Cytochrome b_5 was isolated from rabbit liver microsomes by the procedure described by Roos [27]. The apo-cytochrome b_5 protein was prepared using heterologous expression in *E. coli* as described in our earlier work [28]. Briefly, the gene for rabbit cytochrome b_5 was constructed from synthetic oligonucleotides using polymerase chain reaction (PCR), cloned into pUC19 plasmid and amplified in DH5α cells. The gene sequence was verified by DNA sequencing. The sequence coding cytochrome b_5 was cleaved from pUC19 by NdeI and XhoI restriction endonucleases and subcloned into the expression vector pET22b. This vector was used to transform *E. coli* BL-21 (DE3) Gold cells by heat shock. Expression of cytochrome b_5 was induced with isopropyl β-D-1-thiogalactopyranoside (0.05 mM for 4 h). The cytochrome b_5 protein, produced predominantly in its apo-form, was purified to homogeneity from isolated membranes of *E. coli* cells by chromatography on a DEAE-Sepharose column [28].

2.5. Incorporation of heme into apo-cytochrome b_5

The preparation of hemin chloride solution and its incorporation into apo-cytochrome b_5 were performed by the procedure described elsewhere [29]. Solutions of heme were prepared by adding 2.6 mg of hemin chloride to a solution of 50% ethanol in water (4 ml) to give a final concentration of 1 mM. A small increment (10 μl) of 1 M NaOH was added and mixed to dissolve the hemin. The solution was then allowed to stand for several minutes so particulates could settle. A 10-μl aliquot was removed and diluted into 990 μl of 20 mM Tris, 1 mM EDTA, pH 8.0, at 25 °C and the absorbance of the Tris-ligated heme was measured at 385 nm. The process was repeated five-times, always by adding 10 μl of 1 M NaOH, until NaOH addition caused no further increase in absorbance at 385 nm. The hemin solution was further filtered through 0.2 μm Membrane MF Millipore filter (Millipore, Billerica, USA). Purified apo-cytochrome b_5 was diluted with 20 mM Tris, pH 8.0, containing 1 mM EDTA and 0.4% sodium cholate, to a protein concentration of 0.25 mg/ml. Aliquots of hemin chloride were added into the apo-cytochrome b_5 sample (1 ml) and the reconstitution of apo-cytochrome b_5 with heme was monitored

Please cite this article in press as: Kotrbová V, et al. Cytochrome b_5 shifts oxidation of the anticancer drug ellipticine by cytochromes P450 1A1 and 1A2 from its detoxication to activation, thereby modulating its pharmacological efficacy. Biochem Pharmacol (2011), doi:10.1016/j.bcp.2011.06.003

by absorbance spectroscopy. Absorbance spectra (from 350 to 500 nm) were recorded on Hewlett Packard 8453 UV spectrophotometer. The reconstitution was considered to be complete when the Soret peak of cytochrome b_5 shifted from 413 to 409 nm and an increase in absorbance at 385 nm, caused by excess of free Tris-ligated hemin, was observed in the spectrum.

Analogous procedures were utilized to incorporate manganese protoporphyrin IX (Frontier Scientific, USA) into apo-cytochrome b_5 (Mn-cytochrome b_5) [30].

2.6. Determination of reconstituted cytochrome b_5 content

The concentration of apo-cytochrome b_5 reconstituted with heme was determined spectrophotometrically (the absolute absorbance spectrum) using the molar extinction coefficient $\varepsilon_{413} = 117\ mM^{-1}\ cm^{-1}$ [31,32] or from the difference spectrum of reduced minus oxidized form, using molar extinction coefficient $\varepsilon_{424-409} = 185\ mM^{-1}\ cm^{-1}$, respectively [32]. The concentration of Mn-cytochrome b_5 was determined using an extinction coefficient of $57\ mM^{-1}\ cm^{-1}$ at 469 nm [33].

2.7. Determination of cytochrome b_5 protein levels in rat liver microsomes

Immunoquantitation of rat liver microsomal cytochrome b_5 was done by sodium dodecyl sulfate (SDS)-polyacrylamide gel electrophoresis [24,34]. Samples containing 75 μg microsomal proteins were subjected to electrophoresis on SDS/15% polyacrylamide gels. After migration, proteins were transferred onto polyvinylidene difluoride (PVDF) membranes. Cytochrome b_5 protein was probed with a rabbit polyclonal anti-cytochrome b_5 antibody (1:750, AbCam, MA, USA) overnight at 4 °C. Antibody against glyceraldehyde phosphate dehydrogenase (GAPDH) (1:750, Millipore, MA, USA) was used as loading control. The antigen–antibody complex was visualized with an alkaline phosphatase-conjugated goat anti-rabbit IgG antibody and 5-bromo-4-chloro-3-indolylphosphate/nitrobluetetrazolium as chromogenic substrate [24,34] and scanned with a computerized image-analyzing system (ElfoMan 2.0, Ing. Semecký, Prague, Czech Republic).

2.8. Incubations

Unless stated otherwise, incubation mixtures used to study ellipticine metabolism contained the following in a final volume of 500 μl: 100 mM potassium phosphate buffer (pH 7.4), 1 mM $NADP^+$, 10 mM D-glucose 6-phosphate, 1 U/ml D-glucose 6-phosphate dehydrogenase, to generate NADPH, CYP1A1 or CYP1A2 (100 pmol) reconstituted with NADPH:CYP reductase (5–150 pmol) without or with rabbit hepatic cytochrome b_5 (0–1000 pmol) and 20 μM ellipticine dissolved in 5 μl methanol. The enzyme reconstitution was performed as described [1,9,18,24,35], using different molar ratios of CYP1A1/2 to NADPH:CYP reductase and cytochrome b_5 (see Section 3). Briefly, recombinant rat CYP1A1 and rabbit CYP1A2 were reconstituted with rabbit NADPH:CYP reductase as follows (2 μM CYPs, 0.1–3 μM NADPH:CYP reductase, 0.5 μg/μl CHAPS, 0.1 μg/μl liposomes [dilauroyl phosphatidylcholine, dioleyl phosphatidylcholine, and dilauroylphosphatidylserine (1:1:1)], 3 mM reduced glutathione, and 50 mM HEPES/KOH, pH 7.4). An aliquot containing 100 pmol of reconstituted CYP enzyme was used to oxidize ellipticine. In the control incubation, either CYP or ellipticine were omitted. The reaction was initiated by adding ellipticine. After incubation at 37 °C for 20 min in open glass tubes (ellipticine oxidation was linear up to 30 min of incubation [18,36]), the reaction was stopped by adding 100 μl 2 M NaOH, then 5 μl of 1 mM phenacetine in methanol was added as an internal standard, and the ellipticine metabolites were extracted twice with ethyl acetate (2× 1 ml). The extracts were evaporated under a stream of nitrogen, dissolved in 50 μl of methanol and separated by HPLC (5 μm Ultrasphere ODS Beckman, 4.6 mm × 250 mm preceded by a C-18 guard column), the eluent was 64% methanol plus 36% of 5 mM heptane sulfonic acid in 32 mM acetic acid in water with a flow rate of 0.8 ml/min, detection was at 296 nm. Five ellipticine metabolites with the retention times of 6.3, 6.9, 7.8, 8.5 and 11.2 min, were separated [10,18]. Recoveries of ellipticine metabolites were approximately 95%. To characterize ellipticine metabolites, fractions containing the metabolites were collected from multiple HPLC runs, concentrated on a SpeedVac concentrator and analyzed by mass spectroscopy and/or NMR as described [10,37]. For kinetic studies 1–20 μM ellipticine was incubated with a complete reconstituted system containing CYP1A1 or CYP1A2, NADPH:CYP reductase and cytochrome b_5 (1:1:5), the metabolites analyzed as above and the kinetic parameters were determined (see Section 3).

Incubation mixtures used to analyze DNA-adduct formation by ellipticine were as described above, but contained 1 mM NADPH instead of the NADPH generating system plus 1 mg calf thymus DNA in a final volume of 750 μl. The reaction was initiated by adding ellipticine. Incubations were carried out at 37 °C for 30 min; ellipticine–DNA adduct formation was linear up to 30 min [1]. Control incubations were carried out either without (i) CYP or (ii) NADPH, or (iii) DNA, or (iv) ellipticine. After the incubation, DNA was isolated from the residual water phase by the phenol/chloroform extraction method as described [1].

2.9. CYP1A enzyme activity assays

The samples containing CYP1A1 or 1A2 reconstituted with NADPH:CYP reductase (see the procedure described above) were characterized for CYP1A1 activity using the oxidation of Sudan I for CYP1A1 [24,34] and 7-methoxyresorufin *O*-demethylation (MROD) for CYP1A2 [38,39].

2.10. ^{32}P-Postlabeling analysis and HPLC analysis of ^{32}P-labeled 3′,5′-deoxyribonucleoside bisphosphate adducts

The ^{32}P-postlabeling of nucleotides using nuclease P1 enrichment procedure, found previously to be appropriate to detect and quantify ellipticine-derived DNA adducts formed *in vitro* and *in vivo* [1,3,8–13], was employed in the experiments. The TLC and HPLC analyzes were done as reported recently [1,3,8–13].

2.11. Molecular modeling and visualization

Model of cytochrome b_5 holo-protein was based on coordinates of soluble domain of rat microsomal cytochrome b_5 obtained by three-dimensional NMR of ^{15}N labeled protein (PDB code 1BFX) [40]. The model of apo-cytochrome b_5 was based on coordinates of water-soluble domain of rat microsomal apo-cytochrome b_5 obtained by three-dimensional NMR of ^{13}C and ^{15}N labeled protein (PDB code 1I8C) [41]. The models were aligned and visualized in software package Discovery Studio Visualizer v2.5. Solvent accessible surface of both proteins was calculated with probe radius 1.4 Å and colored by mapping the interpolated partial atom charges to the surface.

3. Results

3.1. Cytochrome b_5 modulates ellipticine oxidation catalyzed by cytochromes P450 1A1 and 1A2

The CYP1A1 and CYP1A2 enzymes oxidize ellipticine to five metabolites, 7-hydroxy-, 9-hydroxy-, 12-hydroxy-, 13-hydroxyel-

Please cite this article in press as: Kotrbová V, et al. Cytochrome b_5 shifts oxidation of the anticancer drug ellipticine by cytochromes P450 1A1 and 1A2 from its detoxication to activation, thereby modulating its pharmacological efficacy. Biochem Pharmacol (2011), doi:10.1016/j.bcp.2011.06.003

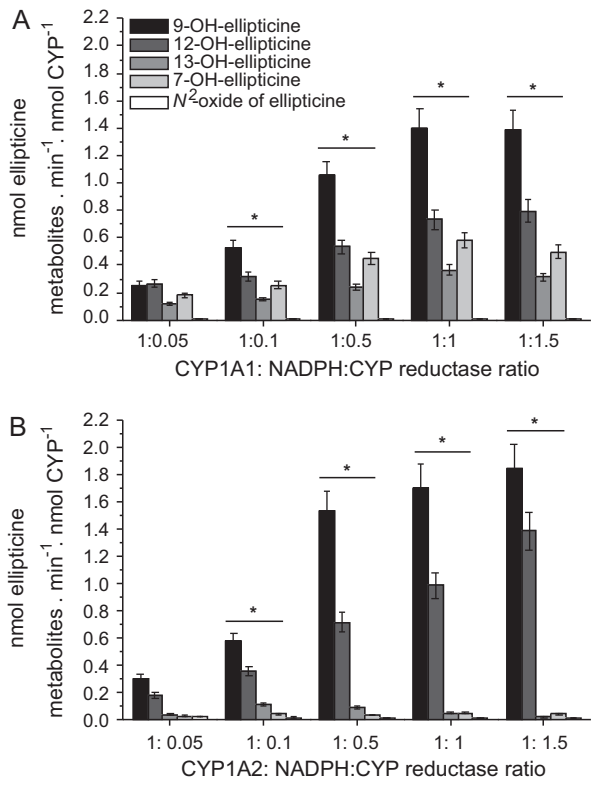

Fig. 2. The effect of increasing NADPH:CYP reductase amounts reconstituted with CYP in liposomes as described in the Materials and Methods section on rates of ellipticine oxidation (20 μM) by CYP1A1 (A) and CYP1A2 (B). Incubation time was 20 min at 37 °C, the metabolites were determined after ethyl acetate extraction of the incubations by HPLC as described. The values are averages and standard deviations of triplicate incubations. Values significantly different from incubations containing CYP1A1/2 and NADPH:CYP reductase in a ratio of 1:0.05: $^{*}p < 0.001$ (Student's *t*-test).

lipticine and N^2-oxide of ellipticine (Figs. 2 and 3), found previously to be formed by human, rat, rabbit and mouse hepatic microsomes [10,13,18,37]. Rates of ellipticine oxidation by isolated CYP1A1/2 reconstituted with NADPH:CYP reductase depend on molar ratios of CYP to NADPH:CYP reductase in the reconstituted systems. An increase in the NADPH:CYP reductase content resulted in an increased oxidation of ellipticine to all metabolites up to a molar ratio of CYP1A1/2:reductase of 1:1, with negligible changes in their yields at a ratio of 1:1.5 (Fig. 2). The yield in ellipticine metabolites was linear with increasing CYP1A1 or 1A2 concentrations up to 0.5 μM. We therefore used 0.2 μM CYP1A1/2 and reductase in further experiments.

With both CYP1A1 and 1A2, 9-hydroxyellipticine, a detoxication product of ellipticine [10,18], was the predominant metabolite (Figs. 2 and 3 and supplemental Tables 1 and 2). The other metabolites, 12-hydroxy-, 13-hydroxyellipticine and ellipticine N^2-oxide, which are responsible for formation of the major ellipticine-derived DNA adducts [10,11], and a further detoxication product, 7-hydroxyellipticine, were formed to a lower extent (Figs. 2 and 3). The levels of ellipticine N^2-oxide were slightly decreased with increasing ratios of CYP1A2:reductase, probably because of its spontaneous rearrangement to 12-hydroxyellipticine [10,11,37]. Indeed, the levels of 12-hydroxyellipticine increased accordingly (Fig. 2, supplemental Table 2).

The patterns and amounts of ellipticine metabolites generated by CYP1A1 and 1A2 changed significantly when cytochrome b_5 was present in the reconstituted system of either CYP1A1 or 1A2 with NADPH:CYP reductase under the optimal molar ratio of one. Changes in pattern of ellipticine metabolites were dependent on the molar ratios of CYP and cytochrome b_5. If CYP1A1 was used, the detoxication products of ellipticine (7-hydroxy- and 9-hydroxyellipticine) decreased with more added cytochrome b_5, while ellipticine N^2-oxide, 12-hydroxy- and 13-hydroxyellipticine increased considerably (Fig. 3A and supplemental Table 2). In the case of CYP1A2 again 12-hydroxyellipticine became the most prominent metabolite with increasing cytochrome b_5 amounts, while 9-hydroxyellipticine levels decreased. Here 7-hydroxyellipticine increased concomitant with 12-hydroxy-, 13-hydroxyellipticine and the ellipticine N^2-oxide (Fig. 3C and supplemental Table 2).

If the amount of NADPH:CYP reductase in the incubation was reduced to one tenth, the effect of cytochrome b_5 added into the reconstituted system containing CYP1A1 or 1A2 was even more dramatic, with yields of 12-hydroxyellipticine increasing 5–7-fold (Fig. 3B and D and supplemental Table 3).

Table 1
Effect of cytochrome b_5 on kinetic parameters of ellipticine oxidation by CYP1A1 and 1A2.

Ellipticine metabolites	K_m ($K_{0.5}$)[a] (μM)	V_{max} (μM/min^{-1})	k_{cat} (min^{-1})	k_{cat}/K_m (min^{-1} μM^{-1})	*n*
CYP1A1 without b_5					
9-Hydroxyellipticine	0.49 ± 0.06	0.264 ± 0.004	1.32 ± 0.02	2.7 ± 0.3	1
12-Hydroxyellipticine	0.8 ± 0.1	0.102 ± 0.002	0.51 ± 0.01	0.6 ± 0.1	1
13-Hydroxyellipticine	5 ± 2	0.057 ± 0.009	0.29 ± 0.05	0.05 ± 0.03	1
7-Hydroxyellipticine	0.50 ± 0.02	0.0649 ± 0.0004	0.325 ± 0.002	0.64 ± 0.03	1
CYP1A1 with b_5					
9-Hydroxyellipticine	0.5 ± 0.1	0.100 ± 0.003	0.50 ± 0.01	1.0 ± 0.2	1
12-Hydroxyellipticine	15 ± 1[a]	3.0 ± 0.4	15 ± 2	1.0 ± 0.1	4.5 ± 0.7[a]
13-Hydroxyellipticine	13.2 ± 0.4[a]	1.8 ± 0.1	9.0 ± 0.5	0.68 ± 0.05	6.3 ± 0.9[a]
7-Hydroxyellipticine	0.4 ± 0.2	0.020 ± 0.001	0.099 ± 0.007	0.3 ± 0.2	1
CYP1A2 without b_5					
9-Hydroxyellipticine	0.24 ± 0.04	0.191 ± 0.003	0.93 ± 0.04	3.9 ± 0.7	1
12-Hydroxyellipticine	4 ± 1	0.087 ± 0.009	0.44 ± 0.02	0.12 ± 0.04	1
13-Hydroxyellipticine	8 ± 2	0.087 ± 0.009	0.43 ± 0.05	0.06 ± 0.02	1
7-Hydroxyellipticine	7 ± 1	0.0058 ± 0.0004	0.029 ± 0.002	0.0044 ± 0.0008	1
CYP1A2 with b_5					
9-Hydroxyellipticine	0.22 ± 0.09	0.115 ± 0.004	0.58 ± 0.02	3 ± 1	1
12-Hydroxyellipticine	13 ± 1	0.49 ± 0.03	2.5 ± 0.1	0.19 ± 0.02	1
13-Hydroxyellipticine	4.1 ± 0.6	0.168 ± 0.008	0.84 ± 0.04	0.21 ± 0.03	1
7-Hydroxyellipticine	4.3 ± 0.8	0.0067 ± 0.0002	0.032 ± 0.001	0.008 ± 0.002	1

Assays were performed as described under Section 2. Kinetic parameters were determined from initial velocity data as described for $N = 3$. Average values ± SE are shown. b_5, cytochrome b_5; *n*, Hill coefficient.
[a] Sigmoidal data curves were fitted using Hill equation.

Please cite this article in press as: Kotrbová V, et al. Cytochrome b_5 shifts oxidation of the anticancer drug ellipticine by cytochromes P450 1A1 and 1A2 from its detoxication to activation, thereby modulating its pharmacological efficacy. Biochem Pharmacol (2011), doi:10.1016/j.bcp.2011.06.003

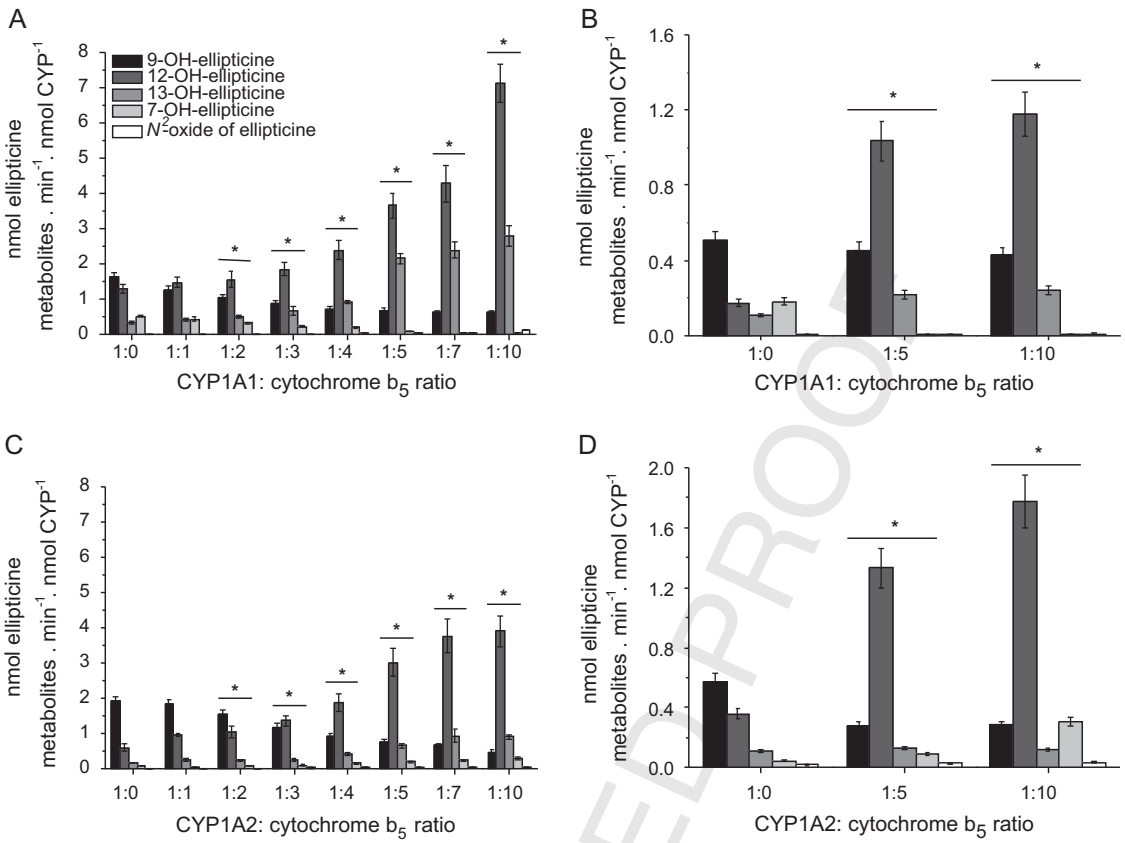

Fig. 3. Cytochrome b_5 alters patterns of ellipticine metabolites formed by its oxidation with CYP1A1 (A, B) and 1A2 (C, D) under the 1:1 (A, C) and the 1:0.1 molar ratio of CYP1A1/2:NADPH:CYP reductase (B, D). The molar ratio of CYP1A1/1A2 to cytochrome b_5 was 1:5. Conditions were as described in Fig. 2. The values are averages and standard deviations of triplicate incubations. Values significantly different from control (without cytochrome b_5); $^*p < 0.001$ (Student's *t*-test).

3.2. Cytochrome b_5 affects the kinetics of ellipticine oxidation by cytochromes P450 1A1/2

Further experiments were conducted to investigate the effects of cytochrome b_5 on kinetics of 1–20 μM ellipticine oxidation by CYP1A1 and 1A2 to its individual metabolites (Fig. 4, Table 1). The ratio of CYP to NADPH:CYP reductase used was 1:1 and the ratio of CYP to cytochrome b_5 was 1:5. Because of instability of ellipticine N^2-oxide, kinetics of its formation was not evaluated.

The presence of cytochrome b_5 increased the values of k_{cat} and the efficiencies (k_{cat}/K_m) of ellipticine oxidation to 12-hydroxy- and 13-hydroxyellipticine catalyzed by both CYP enzymes (Table 1). In addition, kinetics of ellipticine oxidation by CYP1A1, reconstituted with NADPH:CYP reductase and cytochrome b_5 changed completely from a Michaelis–Menten type saturation curve to a sigmoidal curve for 12-hydroxy- and 13-hydroxyellipticine. Indeed, Hill coefficients of 4.6 and 6.3 were determined for formation of 12-hydroxy- and 13-hydroxyellipticine, respectively (Fig. 4, Table 1). On the contrary, the kinetics of ellipticine oxidation by CYP1A2 in presence of cytochrome b_5 to these metabolites exhibited Michaelis–Menten kinetics (Fig. 4, Table 1).

3.3. Cytochrome b_5 increases the ellipticine-derived DNA adduct formation mediated by cytochromes P450 1A1 and 1A2

Using the nuclease P1 version of the ^{32}P-postlabeling assay, which was suitable to detect and quantify DNA adducts formed by ellipticine [1,8–12], two ellipticine-derived DNA adducts (see Fig. 1 for the structures of two deoxyguanosine adducts 1 and 2) were detected in the calf thymus DNA incubated with this drug and CYP1A1 or 1A2 reconstituted with NADPH:CYP reductase (Fig. 5A and B). The two adducts are identical to those found previously after *in vitro* incubation of calf thymus DNA with ellipticine, human, rat, rabbit and mouse hepatic microsomes or human and rat CYPs [1,9,10], or peroxidases [11] or after treatment of cells in culture with this anticancer drug [14–17,42] or *in vivo* (Fig. 5C), in several organs of rats including mammary adenocarcinoma [3,8,12] and mice [13] exposed to this agent. These adducts are generated from ellipticine-13-ylium and ellipticine-12-ylium (Fig. 1), the reactive species formed from the corresponding hydroxyellipticines (Fig. 5D and E) as confirmed by co-chromatographic analysis using TLC and HPLC [10,11,43]. The increased levels of 12-hydroxy- and 13-hydroxyellipticine formed by the reconstituted system containing cytochrome b_5 resulted in corresponding higher levels of these two ellipticine-derived DNA adducts (Table 2). In the case of CYP1A1, the presence of cytochrome b_5 resulted in 6.2-fold higher levels of the ellipticine–DNA adduct 1, which correlated with a 6.3-fold increased formation of 13-hydroxyellipticine, the metabolite generating this adduct (Table 2, Fig. 3). Likewise, CYP1A2 activation of ellipticine in presence of cytochrome b_5 resulted in 3.9-fold higher levels of DNA adduct 1 (Table 2) which was consistent with a similar increase (more than 3.8-fold) in 13-hydroxyellipticine metabolite formation by this system (Fig. 3). The same was true for the parallel effects of cytochrome b_5 on ellipticine–DNA-adduct 2 levels and 12-hydroxyellipticine yields in incubations with reconstituted CYP1A1 or 1A2 (Table 2, Fig. 3 and supplemental Table 2).

Please cite this article in press as: Kotrbová V, et al. Cytochrome b_5 shifts oxidation of the anticancer drug ellipticine by cytochromes P450 1A1 and 1A2 from its detoxication to activation, thereby modulating its pharmacological efficacy. Biochem Pharmacol (2011), doi:10.1016/j.bcp.2011.06.003

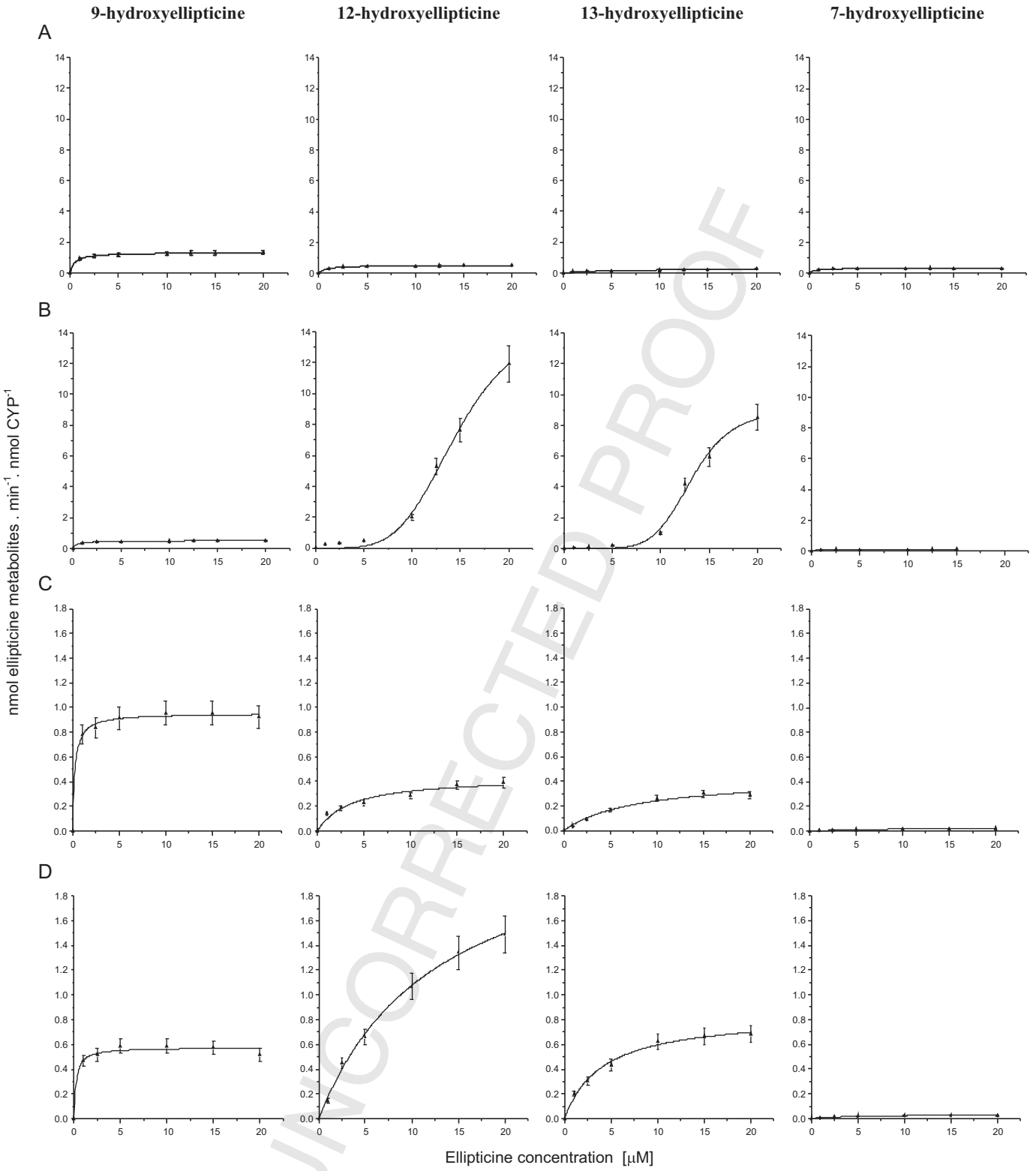

Fig. 4. Kinetics of ellipticine oxidation by CYP1A1 (A, B) and 1A2 (C, D) without (A, C) or with (B, D) cytochrome b_5. Ellipticine concentrations between 1 and 20 μM were incubated with the reconstituted liposomes containing CYP and reductase at a molar ratio of 1:1 in all incubations plus cytochrome b_5 at 5-fold higher concentrations than CYP in (B) and (D). The other conditions were as described in Fig. 2. The values are averages and standard deviations of triplicate incubations.

3.4. Modulation of ellipticine oxidation by cytochromes P450 1A1 and 1A2 is dependent on holo-cytochrome b_5

In order to investigate the mechanism of cytochrome b_5 mediated-modulation of ellipticine oxidation by CYP1A1 and 1A2, we also examined the influence of apo-cytochrome b_5 and Mn-cytochrome b_5. As shown in Fig. 6, the CYP1A1/2-mediated oxidation of ellipticine was significantly changed only by holo-cytochrome b_5 or apo-cytochrome b_5 reconstituted with heme, while apo-cytochrome b_5 without heme cofactor (see Fig. 7B

Please cite this article in press as: Kotrbová V, et al. Cytochrome b_5 shifts oxidation of the anticancer drug ellipticine by cytochromes P450 1A1 and 1A2 from its detoxication to activation, thereby modulating its pharmacological efficacy. Biochem Pharmacol (2011), doi:10.1016/j.bcp.2011.06.003

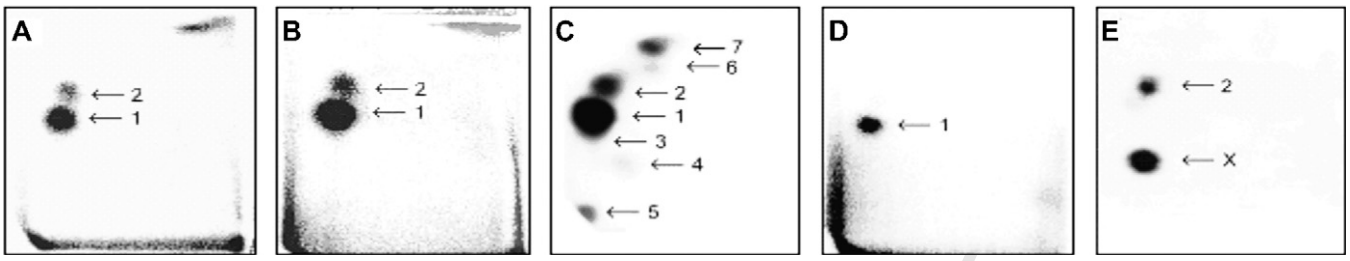

Fig. 5. Autoradiographic profile of ^{32}P-labeled DNA adducts generated in calf thymus DNA by ellipticine after its activation with reconstituted CYP1A1 without (A) and with cytochrome b_5 (CYP1A1:cytochrome b_5 1:5) (B): of ^{32}P-labeled digests of DNA from liver of a male rat treated with 40 mg ellipticine per kg body weight (C): from calf thymus DNA reacted with 13-hydroxyellipticine (D) or 12-hydroxyelipticine (E). Analyses were performed by the nuclease P1 version of the ^{32}P-postlabeling assay. Adduct spots 1–7 correspond to the ellipticine-derived DNA adducts. Besides adduct 2 formed by 12-hydroxyellipticine, another strong adduct (spot × in panel E), which was not found in any other activation systems or *in vivo* was generated.

Table 2
The effect of cytochrome b_5 on DNA adduct formation by ellipticine oxidized with CYP1A1 and 1A2.

Activating system	RAL (mean ± SD/10^7 nucleotides)		
	Adduct 1	Adduct 2	Total
CYP1A1 + NADPH:CYP reductase (1:1)	1.6 ± 0.2	0.8 ± 0.1	2.4 ± 0.3
CYP1A1 + NADPH:CYP reductase + cytochrome b_5 (1:1:5)	9.9 ± 0.6*	1.8 ± 0.3*	11.7 ± 0.9*
CYP1A2 + NADPH:CYP reductase (1:1)	0.9 ± 0.1	0.3 ± 0.1	1.2 ± 0.2
CYP1A2 + NADPH:CYP reductase + cytochrome b_5 (1:1:5)	3.5 ± 0.2*	0.8 ± 0.2	4.3 ± 0.3*

Values are given as means ± SD ($N = 6$). RAL, relative adduct labeling. The total RAL represents sum of RAL values of adducts 1 and 2.
* Values significantly different from control (without cytochrome b_5): $p < 0.001$ (Student's *t*-test).

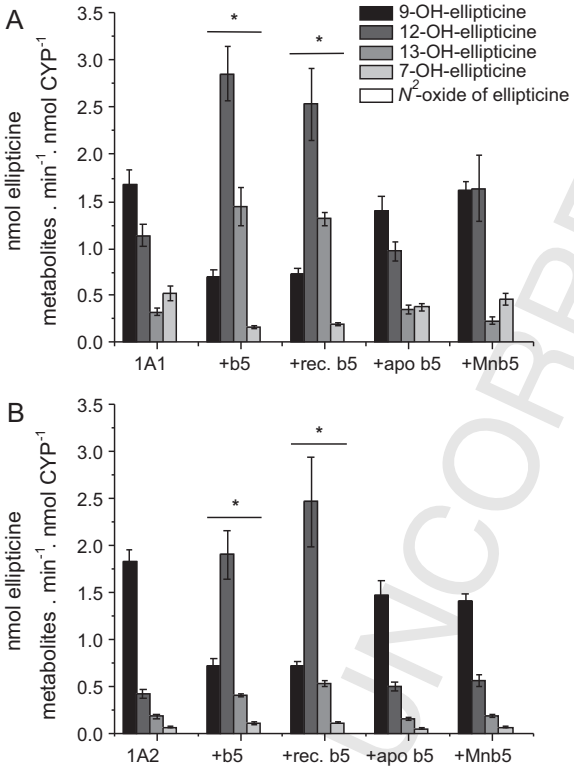

Fig. 6. The effect of cytochrome b_5, apo-cytochrome b_5 and Mn-cytochrome b_5 on rates of ellipticine oxidation by CYP1A1 (A) and 1A2 (B). Conditions were as described in Fig. 2 except that cytochrome b_5 (b_5), recombinant apo-cytochrome b_5 reconstituted with heme (rec. b_5), recombinant apo-cytochrome b_5 (apo-b_5) and recombinant apo-cytochrome b_5 reconstituted with Mn-protoporphyrin IX (Mnb_5) were added at 5-fold higher concentrations than CYP into the incubation mixtures. The values are averages and standard deviations of triplicate incubations. Values significantly different from control (without cytochrome b_5); $^*p < 0.001$ (Student's *t*-test).

and D) was essentially without such effects (Fig. 6). We also employed a structurally similar analogue of cytochrome b_5, known to have limited capability of the electron transfer, Mn-cytochrome b_5 [30,42]. The apo-cytochrome b_5 reconstituted with Mn-protoporphyrin IX should adopt the same 3D conformation as the native cytochrome b_5, but it lacks the electron transfer capability [19,30,44]. Also in the case of Mn-cytochrome b_5, essentially no changes in ellipticine oxidation were found (Fig. 6).

3.5. Ellipticine increases levels of cytochrome b_5 protein in rat livers

Western blots with rabbit polyclonal antibodies raised against cytochrome b_5 were used to investigate the effect of ellipticine on cytochrome b_5 levels *in vivo*. The levels of hepatic cytochrome b_5 protein were increased 4–5-fold in male rats treated with 4 or 40 mg/kg body weight ellipticine (Fig. 8). The mechanism of this increase in cytochrome b_5 levels (*i.e.* transcriptional or translational influences, or ellipticine-induced stabilization of cytochrome b_5) was, however, not evaluated in this work and awaits further investigation.

4. Discussion

The results of this study demonstrate for the first time that cytochrome b_5 alters the ratio of ellipticine metabolites formed by CYP1A1 and 1A2, "switching" oxidation of this anticancer agent from detoxication (9-hydroxy- and/or 7-hydroxyellipticine) to DNA-forming metabolites (12-hydroxy- and 13-hydroxyellipticine). These changes resulted in higher covalent DNA adduct levels by ellipticine, one of the DNA-damaging mechanisms of ellipticine antitumor action. Therefore, besides stimulating effect of cytochrome b_5 on CYP3A4-mediated oxidation of ellipticine to 13-hydroxyellipticine that was found previously to lead to an increase in ellipticine–DNA adduct formation [3,10], this heme protein might play a key role also in the CYP1A1/2-mediated DNA-damage induced by ellipticine. To further confirm these *in vitro* results, a cytochrome b_5-knockout cell model is planned to be used to

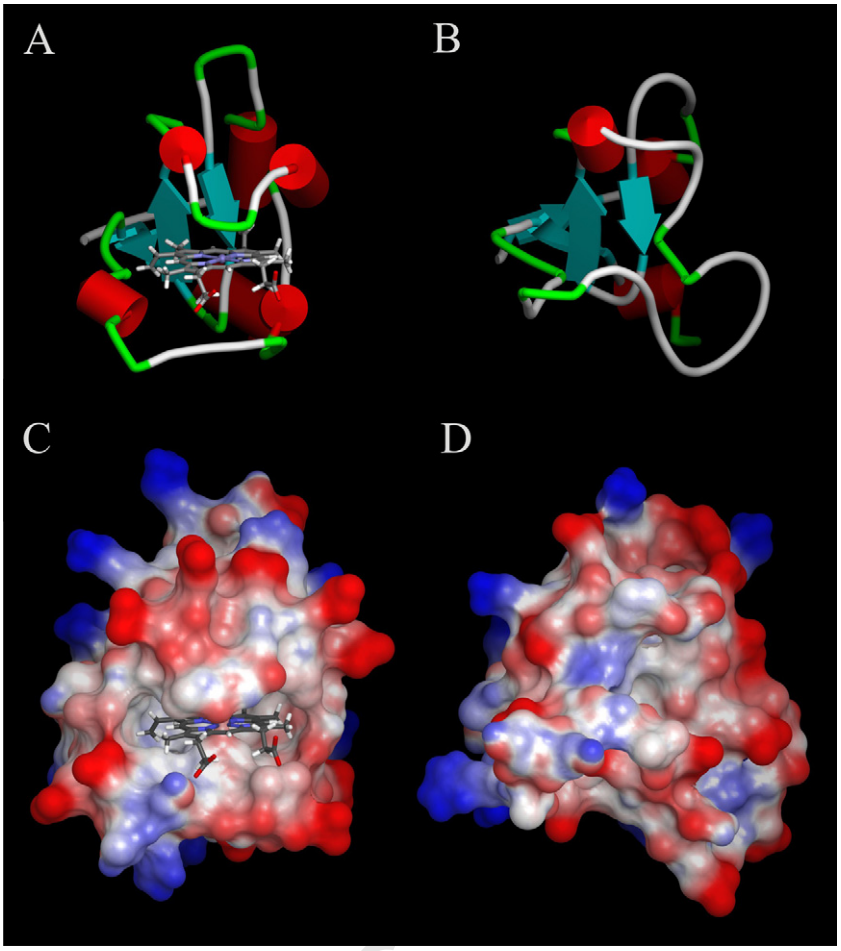

Fig. 7. Comparison of 3D structures of cytochrome b_5 (A, C) and apo-cytochrome b_5 (B, D) (based on PDB coordinates 1BFX [40] and 1I8C [41]). Heme loss results in substantial alteration of cytochrome b_5 secondary structure elements (A and B), for instance three alpha helices of apo-cytochrome b_5 are unfolded and the shape of apo-cytochrome b_5 polypeptide backbone altered (B). Colored surfaces (C and D) demonstrate the large differences in physico-chemical properties, *i.e.* surface shape and charge distribution between the holo- and apo-form of cytochrome b_5.

analyze the oxidation products of ellipticine and ellipticine-derived DNA adducts.

The findings described herein offer an explanation for previous discrepancies found in experiments with isolated CYP1A of rat and human origin reconstituted with NADPH:CYP reductase and *in vivo*. The efficiency of CYP1A in activating ellipticine to metabolites forming DNA adducts *in vivo* contrasted with the low yield of these metabolites *in vitro* [8–10]. The effect of cytochrome b_5, causing a shift in oxidation of ellipticine by CYP1A1/2 from detoxication to activation may be even more pronounced *in vivo*, because ellipticine increases levels of cytochrome b_5. Moreover, ellipticine as a ligand of aryl hydrocarbon receptor [45] also induces expression of CYP1A1/2, increasing their enzymatic activities [17,36]. Hence, both these ellipticine-mediated induction effects produce concerted regulatory effects of this drug on its own metabolism. Indeed, we have found recently that in hepatic microsomes of rats treated with ellipticine, contribution of the CYP1A enzymes to ellipticine–DNA adduct formation is higher than that of CYP3A [46]. To quantify the involvement of cytochrome b_5 in ellipticine metabolism *in vivo* we plan to use cytochrome b_5-knockout mice [47,48].

It should be noted that expression levels and activities of CYP1A1, 1A2 and 3A4 that metabolize ellipticine differ considerably among individuals, because the enzymes are influenced by several factors, including smoking, drugs and environmental chemicals [24,39,49]. Furthermore, besides induction of these enzymes by several compounds including ellipticine [17,36], different activities of CYP1A1 and 1A2 are also determined by genetic polymorphisms, which subsequently might modulate cancer development and treatment. The polymorphic expression of CYP1A1 has been attributed to altered expression of the aryl hydrocarbon (Ah) receptor, the transcription factor that modulates its regulation, or the Ah receptor nuclear translocator (Arnt) protein, its associated transcription factor [50,51]. Moreover, the *CYP1A1* and *CYP1A2* genes are polymorphic [39,49,52,53]. CYP1A1*2A, CYP1A1*2B and CYP1A1*4 polymorphisms have been found that might be associated with cancers of lung, esophagus or breast and with acute myeloid leukemia [54–57], while the CYP1A2*1F polymorphism might be associated with an increased risk of colorectal cancer [52]. In addition, the *CYP1A2*1C* allele has been associated with decreased caffeine 3-demethylation [58], and the *CYP1A2*1F* allele was correlated to increased activity [59,60]. The *CYP1A2*1F* allele has also been shown to influence the inducibility of the gene and affect the magnitude of increase of *in vivo* caffeine metabolism after both smoking [59,60] and omeprazole treatment [61,62]. Thus, genetic polymorphisms in CYP1A1 and 1A2 enzymes could be important determinants of pharmacological efficiencies of ellipticine. In contrast to CYP1A1 and 1A2, there is currently little evidence for a significant contribution of *CYP3A4* gene polymorphisms in determining CYP3A4 activity. Besides a number of rare amino acid variants [63], no polymorphisms with

Please cite this article in press as: Kotrbová V, et al. Cytochrome b_5 shifts oxidation of the anticancer drug ellipticine by cytochromes P450 1A1 and 1A2 from its detoxication to activation, thereby modulating its pharmacological efficacy. Biochem Pharmacol (2011), doi:10.1016/j.bcp.2011.06.003

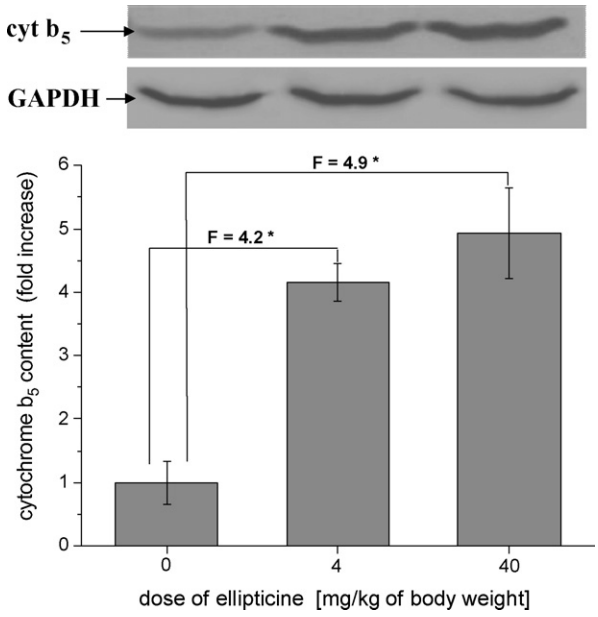

Fig. 8. Induction of cytochrome b_5 in livers of rats treated with 4 or 40 mg ellipticine per kg body weight. Liver microsomes were isolated 48 h after treatment. Mean values ± standard deviations shown in figure represent results obtained from livers of three rats ($N = 3$). Values significantly different from the control (untreated rats): $^*p < 0.001$ (Student's *t*-test). Inset: immunoblots of cytochrome b_5 from untreated and ellipticine-treated rats, respectively, stained with antibody against rat cytochrome b_5. Microsomes isolated from rat livers were subjected to SDS-PAGE, proteins transferred to PVDF membranes and probed with antibody as described in Material and Methods. Glyceraldehyde phosphate dehydrogenase (GAPDH) was used as loading control. *F*, fold increase in cytochrome b_5 expression in rats treated with ellipticine compared to control (uninduced) rats.

a clear genotype–phenotype relationship have so far been described for the CYP3A4 gene [64,65].

It should be emphasized that the effect of cytochrome b_5 upon CYP1A1/2 catalyzed metabolism resulting in the increase of certain metabolites at the expense of others of the same substrate has to our knowledge not been reported yet. This finding indicates that cytochrome b_5 effects show specificity for different hydroxylation sites in the ellipticine molecule. Cytochrome b_5-mediated specificity for different sites of substrate oxidation seems to occur also for testosterone hydroxylation by CYP2B6; a 4- and 2.25-fold increase in 6β- and 16α-hydroxylation of testosterone was produced by cytochrome b_5, respectively [66,67]. However, in the case of this substrate, both hydroxylation reactions were stimulated by cytochrome b_5. A similar effect of cytochrome b_5 was also found for metabolism of midazolam (1- and 4-hydroxylation) and metoprolol (formation of α-hydroxymetoprolol and *O*-desmethylmetoprolol) in hepatic microsomes isolated from "hepatic cytochrome b_5 null mice"(HBN) compared to wild-type controls [47]. In such an *ex vivo* system in which several CYPs are expressed in the hepatic microsomes it is not possible to determine if cytochrome b_5 affects different CYP to different extents.

Generally, two mechanisms of cytochrome b_5-mediated modulation of CYP catalysis have been suggested by several authors; it can affect the CYP catalytic activities by donating the second electron to CYP in a CYP catalytic cycle and/or by acting as an allosteric modifier of the oxygenase (for reviews see [19–22]). The mechanism(s) underlying such allosteric effects, based on reports that apo-cytochrome b_5 can stimulate CYP catalysis, remains uncertain. It does seem clear, however, that cytochrome b_5 binding can cause conformational changes to the substrate access channel and binding pocket in the CYP enzyme [19–22,67,68].

Here, we show that addition of cytochrome b_5 to CYP1A1 alters the kinetics of ellipticine oxidation by this enzyme. For all ellipticine metabolites, with the exception of 12-hydroxy- and 13-hydroxyellipticine, the data followed Michaelis–Menten kinetics, and K_m values were essentially unchanged by the presence of cytochrome b_5 (Table 1). In contrast, the data for formation of 12-hydroxy- and 13-hydroxyellipticine did not fit Michaelis–Menten kinetics, exhibiting positively cooperative binding. These findings indicate that the presence of cytochrome b_5 can cause a conformational change in the CYP1A1 structure affecting ellipticine binding. The effect of cytochrome b_5 upon CYP1A2 catalysis was not as pronounced as the kinetics still showed Michaelis–Menten characteristics, but also here the shift to ellipticine activation from detoxication was prominent.

The results found in this study also show that modulation of ellipticine oxidation by CYP1A1/2 is induced only by the holo-cytochrome b_5. These findings indicate a high specificity of interaction of CYP1A1/2 with holo-cytochrome b_5 containing heme, which is necessary not only for electron transfer, but also for the natural conformation of the cytochrome b_5 protein. The lack of effect of apo-cytochrome b_5 on CYP1A1/2 catalysis might hence be the result of not only the loss of the electron transfer activity, but may also result from changes in 3D structure of its protein. While the holo-cytochrome b_5 contains four helixes and three loops, forming the heme binding pocket, apo-cytochrome b_5 has only one structural element, a helix of amino acids 39-42 (Fig. 7B). This structural change results in significant alterations in surface geometry and electrostatic properties of apo-cytochrome b_5 (Fig. 7) preventing adequate protein–protein interactions of cytochrome b_5 with CYP1A enzymes. Moreover, essentially no changes in ellipticine oxidation were also produced by cytochrome b_5 containing manganese protoporphyrin IX (Mn-cytochrome b_5), a structural analogue of cytochrome b_5 absenting electron transfer ability. All these results demonstrate that both the natural 3D structure of the cytochrome b_5 protein, dictating optimal conformational states of CYP1A1–cytochrome b_5 complexes, and the presence of the protoporphyrin IX bonded-Fe ion as an electron transfer agent are necessary for the observed effects.

However, it is still questionable whether Mn-cytochrome b_5, we used as a structural analogue of cytochrome b_5, is really a suitable model for mechanistic studies. It was found that affinity of Mn-protoporphyrin IX toward apo-cytochrome b_5 is substantially lower than the affinity of heme to apo-cytochrome b_5 [33]. Under the conditions typically used in a reconstituted CYP system, free Mn-protoporphyrin IX and apo-cytochrome b_5 co-exist in solution [33]. Therefore, apo-cytochrome b_5 might be present in incubations instead of Mn-cytochrome b_5. Additional studies utilizing other structural analogues of cytochrome b_5 might explain this feature. The apo-cytochrome b_5 reconstituted with porphyrins containing other metal ions with potentially higher affinity to cytochrome b_5 than Mn-protoporphyrin IX will shed further light on this question.

In conclusion, the results of this study show for the first time that cytochrome b_5 alters the CYP1A1/2-catalyzed oxidation of the antitumor agent ellipticine *in vitro*, favoring formation of the metabolites producing the reactive species generating DNA adducts and that this phenomenon leads to similar results as those seen *in vivo*. Ellipticine also induces cytochrome b_5 (present work) and CYP1A1/2 enzyme expression [17,36], thereby increasing the contribution of these enzymes to form the DNA adducts found *in vivo* [8,46]. Therefore, cytochrome b_5 in combination with CYP1A1/2 can, together with other enzymes known to activate ellipticine such as CYP3A and/or peroxidases, play a crucial role in determining the pharmacological and/or genotoxic potential of this drug.

Please cite this article in press as: Kotrbová V, et al. Cytochrome b_5 shifts oxidation of the anticancer drug ellipticine by cytochromes P450 1A1 and 1A2 from its detoxication to activation, thereby modulating its pharmacological efficacy. Biochem Pharmacol (2011), doi:10.1016/j.bcp.2011.06.003

Conflict of interest

All authors have no conflict of interest.

Acknowledgements

This work was supported in part by the Grant Agency of the Czech Republic (grants P301/10/0356, 203/09/0812, 305/09/H008) and Ministry of Education of the Czech Republic (grants MSM0021620808 and 1M0505).

Appendix A. Supplementary data

Supplementary data associated with this article can be found, in the online version, at doi:10.1016/j.bcp.2011.06.003.

References

[1] Stiborová M, Bieler CA, Wiessler M, Frei E. The anticancer agent ellipticine on activation by cytochrome P450 forms covalent DNA adducts. Biochem Pharmacol 2001;62:1675–84.
[2] Stiborová M, Rupertová M, Schmeiser HH, Frei E. Molecular mechanism of antineoplastic action of an anticancer drug ellipticine. Biomed Pap Med Fac Univ Palacky Olomouc Czech Repub 2006;150:13–23.
[3] Stiborová M, Rupertová M, Frei E. Cytochrome P450- and peroxidase-mediated oxidation of anticancer alkaloid ellipticine dictates its anti-tumor efficiency. Biochim Biophys Acta 2011;1814:175–85.
[4] Auclair C. Multimodal action of antitumor agents on DNA: the ellipticine series. Arch Biochem Biophys 1987;259:1–14.
[5] Garbett NC, Graves DE. Extenting nature's leads: the anticancer agent ellipticine. Curr Med Chem Anti-Cancer Agents 2004;4:149–72.
[6] Fossé P, René B, Charra M, Paoletti C, Saucier JM. Stimulation of topoisomerase II-mediated DNA cleavage by ellipticine derivatives: structure–activity relationships. Mol Pharmacol 1992;42:590–5.
[7] Froelich-Ammon SJ, Patchan MW, Osheroff N, Thompson RB. Topoisomerase II binds to ellipticine in the absence or presence of DNA. Characterization of enzyme–drug interactions by fluorescence spectroscopy. J Biol Chem 1995; 270:14998–5004.
[8] Stiborová M, Breuer A, Aimová D, Stiborová-Rupertová M, Wiessler M, Frei E. DNA adduct formation by the anticancer drug ellipticine in rats determined by ^{32}P-postlabeling. Int J Cancer 2003;107:885–90.
[9] Stiborová M, Stiborová-Rupertová M, Bořek-Dohalská L, Wiessler M, Frei E. Rat microsomes activating the anticancer drug ellipticine to species covalently binding to deoxyguanosine in DNA are a suitable model mimicking ellipticine bioactivation in humans. Chem Res Toxicol 2003;16:38–47.
[10] Stiborová M, Sejbal J, Bořek-Dohalská L, Aimová D, Poljaková J, Forsterová K, et al. The anticancer drug ellipticine forms covalent DNA adducts, mediated by human cytochromes P450, through metabolism to 13-hydroxyellipticine and ellipticine N^2-oxide. Cancer Res 2004;64:8374–80.
[11] Stiborová M, Poljaková J, Ryšlavá H, Dračínský M, Eckschlager T, Frei E. Mammalian peroxidases activate anticancer drug ellipticine to intermediates forming deoxyguanosine adducts in DNA identical to those found *in vivo* and generated from 12-hydroxyellipticine and 13-hydroxyellipticine. Int J Cancer 2007;120:243–51.
[12] Stiborová M, Rupertová M, Aimová D, Ryšlavá H, Frei E. Formation and persistence of DNA adducts of anticancer drug ellipticine in rats. Toxicology 2007;236:50–60.
[13] Stiborová M, Arlt VM, Henderson CJ, Wolf CR, Kotrbová V, Moserová M, et al. Role of hepatic cytochromes P450 in bioactivation of the anticancer drug ellipticine: studies with the hepatic NADPH:cytochrome P450 reductase null mouse. Toxicol Appl Pharmacol 2008;226:318–27.
[14] Bořek-Dohalská L, Frei E, Stiborová M. DNA adduct formation by the anticancer drug ellipticine and its hydroxy derivatives in human breast adenocarcinoma MCF-7 cells. Collect Czech Chem Commun 2004;69:603–15.
[15] Poljaková J, Frei E, Gomez JE, Aimová D, Eckschlager T, Hraběta J, et al. DNA adduct formation by the anticancer drug ellipticine in human leukemia HL-60 and CCRF-CEM cells. Cancer Lett 2007;252:270–9.
[16] Poljaková J, Eckschlager T, Hraběta J, Hřebačková J, Smutný S, Frei E, et al. The mechanism of cytotoxicity and DNA adduct formation by the anticancer drug ellipticine in human neuroblastoma cells. Biochem Pharmacol 2009;77:1466–79.
[17] Martínková E, Dontenwill M, Frei E, Stiborová M. Cytotoxicity of and DNA adduct formation by ellipticine in human U87MG glioblastoma cancer cells. Neuro Endocrinol Lett 2009;30(Suppl. 1):60–6.
[18] Kotrbová V, Aimová D, Březinová A, Janouchová K, Poljaková J, Hodek P, et al. Cytochromes P450 reconstituted with NADPH:P450 reductase mimic the activating and detoxicating metabolism of the anticancer drug ellipticine in microsomes. Neuro Endocrinol Lett 2006;27(Suppl. 2):18–20.
[19] Schenkman JB, Jansson I. The many roles of cytochrome b_5. Pharmacol Ther 2003;9:139–52.
[20] Yamazaki H, Gillam EM, Dong MS, Johnson WW, Guengerich FP, Shimada T. Reconstitution of recombinant cytochrome P450 2C10(2C9) and comparison with cytochrome P450 3A4 and other forms: effects of cytochrome P450–P450 and cytochrome P450–b_5 interactions. Arch Biochem Biophys 1997;342: 329–37.
[21] Yamazaki H, Shimada T, Martin MV, Guengerich FP. Stimulation of cytochrome P450 reactions by apo-cytochrome b_5: evidence against transfer of heme from cytochrome P450 3A4 to apo-cytochrome b_5 or heme oxygenase. J Biol Chem 2001;276:30885–91.
[22] Zhang H, Myshkin E, Waskell L. Role of cytochrome b_5 in catalysis by cytochrome P450 2B4. Biochem Biophys Res Commun 2005;338:499–506.
[23] Wiechelman KJ, Braun RD, Fitzpatrick JD. Investigation of the bicinchoninic acid protein assay: identification of the groups responsible for color formation. Anal Biochem 1988;175:231–7.
[24] Stiborová M, Martínek V, Rýdlová H, Hodek P, Frei E. Sudan I is a potential carcinogen for humans: evidence for its metabolic activation and detoxication by human recombinant cytochrome P450 1A1 and liver microsomes. Cancer Res 2002;62:5678–84.
[25] Haugen DA, Coon MJ. Properties of electrophoretically homogeneous phenobarbital-inducible and beta-naphthoflavone-inducible forms of liver microsomal cytochrome P-450. J Biol Chem 1976;251:7929–39.
[26] Dignam JD, Strobel HW. NADPH-cytochrome P-450 reductase from rat liver: purification by affinity chromatography and characterization. Biochemistry 1977;6:1116–23.
[27] Roos PH. Chromatographic separation and behavior of microsomal cytochrome P450 and cytochrome b_5. J Chromatogr B Biomed Appl 1996;684: 107–31.
[28] Kotrbová V, Aimová D, Ingr M, Bořek-Dohalská L, Martínek V, Stiborová M. Preparation of a biologically active apo-cytochrome b_5 *via* heterologous expression in *Escherichia coli*. Protein Expr Purif 2009;66:203–9.
[29] Mulrooney SB, Waskell L. High-level expression in *Escherichia coli* and purification of the membrane-bound form of cytochrome b_5. Protein Expr Purif 2000;19:173–8.
[30] Zhang H, Hamdane D, Im SC, Waskell L. Cytochrome b_5 inhibits electron transfer from NADPH-cytochrome P450 reductase to ferric cytochrome P450 2B4. J Biol Chem 2008;283:5217–25.
[31] Strittmatter P, Velick SF. The isolation and properties of microsomal cytochrome. J Biol Chem 1956;221:253–64.
[32] Estabrook RW, Werringloer J. The measurement of difference spectra: application to the cytochromes of microsomes. Methods Enzymol 1978;52:212–20.
[33] Gruenke LD, Sun J, Loehr TM, Waskell L. Resonance Raman spectral properties and stability of manganese protoporphyrin IX cytochrome b_5. Biochemistry 1997;36:7114–25.
[34] Stiborová M, Martínek V, Rýdlová H, Koblas T, Hodek P. Expression of cytochrome P450 1A1 and its contribution to oxidation of a potential human carcinogen 1-phenylazo-2-naphthol (Sudan I) in human livers. Cancer Lett 2005;220:145–54.
[35] Farooq Y, Gordon GCK. Kinetics of electron transfer between NADPH-cytochrome P450 reductase and cytochrome P450 3A4. Biochem J 2010;432:485–93.
[36] Aimová D, Svobodová L, Kotrbová V, Mrazová B, Hodek P, Hudeček J, et al. The anticancer drug ellipticine is a potent inducer of rat cytochromes P450 1A1 and 1A2, thereby modulating its own metabolism. Drug Metab Dispos 2007;35:1926–34.
[37] Stiborová M, Bořek-Dohalská L, Aimová D, Kotrbová V, Kukacková K, Janouchová K, et al. Oxidation pattern of the anticancer drug ellipticine by hepatic microsomes—similarity between human and rat systems. Gen Physiol Biophys 2006;25:245–61.
[38] Guengerich FP, Shimada T. Oxidation of toxic and carcinogenic chemicals by human cytochrome P450 enzymes. Chem Res Toxicol 1991;4:391–407.
[39] Rendic S, DiCarlo FJ. Human cytochrome P450 enzymes: a status report summarizing their reactions, substrates, inducers, and inhibitors. Drug Metab Rev 1997;29:413–80.
[40] Arnesano F, Banci L, Bertini I, Felli IC, Koulougliotis D. Solution structure of the B form of oxidized rat microsomal cytochrome b_5 and backbone dynamics via 15 N rotating-frame NMR-relaxation measurements. Biological implications. Eur J Biochem 1999;260:347–54.
[41] Falzone CJ, Wang Y, Vu BC, Scott NL, Bhattacharya S, Lecomte JT. Structural and dynamic perturbations induced by heme binding in cytochrome b_5. Biochemistry 2001;40:4879–91.
[42] Frei E, Bieler CA, Arlt VM, Wiessler M, Stiborová M. Covalent binding of the anticancer drug ellipticine to DNA in V79 cells transfected with human cytochrome P450 enzymes. Biochem Pharmacol 2002;64:289–95.
[43] Moserová M, Kotrbová V, Rupertová M, Naiman K, Hudeček J, Hodek P, et al. Isolation and partial characterization of the adduct formed by 13-hydroxyellipticine with deoxyguanosine in DNA. Neuro Endocrinol Lett 2008;29:728–32.
[44] Zhang H, Im SC, Waskell L. Cytochrome b_5 increases the rate of product formation by cytochrome P450 2B4 and competes with cytochrome P450 reductase for a binding site on cytochrome P450 2B4. J Biol Chem 2007; 282:29766–7.
[45] Gasiewicz TA, Kende RS, Rucci G, Whitney B, Willey JJ. Analysis of structural requirements for Ah receptor antagonist activity: ellipticines, flavones, and related compounds. Biochem Pharmacol 1996;52:787–830.
[46] Stiborová M, Moserová M, Mrázová B, Kotrbová V, Frei E. Role of cytochromes P450 and peroxidases in metabolism of the anticancer drug ellipticine: additional evidence of their contribution to ellipticine activation in rat liver, lung and kidney. Neuro Endocrinol Lett 2010;31(Suppl. 2):26–35.

Please cite this article in press as: Kotrbová V, et al. Cytochrome b_5 shifts oxidation of the anticancer drug ellipticine by cytochromes P450 1A1 and 1A2 from its detoxication to activation, thereby modulating its pharmacological efficacy. Biochem Pharmacol (2011), doi:10.1016/j.bcp.2011.06.003

[47] Finn RD, McLaughlin LA, Ronseaux S, Rosewell I, Houston JB, Henderson CJ, et al. Defining the *in vivo* role for cytochrome b_5 in cytochrome P450 function through the conditional hepatic deletion of microsomal cytochrome b_5. J Biol Chem 2008;283:31385–93.
[48] McLaughin LA, Ronseaux S, Finn RD, Henderson CJ, Wolf CR. Deletion of microsomal cytochrome b_5 profoundly affects hepatic and extrahepatic drug metabolism. Mol Pharmacol 2010;75:269–78.
[49] Perera FP. Environment and cancer: who are susceptible? Science 1997;278: 1068–73.
[50] Hukkanen J, Pelkonen O, Hakkola J, Raunio H. Expression and regulation of xenobiotic-metabolizing cytochrome P450 (CYP) enzymes in human lung. Crit Rev Toxicol 2002;32:391–411.
[51] Dickins M. Induction of cytochromes P450. Curr Top Med Chem 2004;4: 1745–66.
[52] Bae SY, Choi SK, Kim KR, Park CS, Lee SK, Roh HK, et al. Effects of genetic polymorphisms of MDR1, FMO3 and CYP1A2 on susceptibility to colorectal cancer in Koreans. Cancer Sci 2006;97:774–9.
[53] Yoshida K, Osawa K, Kasahara M, Miyaishi A, Nakanishi K, Hayamizu S, et al. Association of CYP1A1, CYP1A2, GSTM1 and NAT2 gene polymorphisms with colorectal cancer and smoking. Asian Pac J Cancer Prev 2007;8:438–44.
[54] D'Alo A, Voso M, Guidy F, Kaseiny G, Sica S, Pagano L, et al. Polymorphisms of CYP1A1 and glutathione S-transferase and susceptibility to adult acute myeloid leukaemia. Haematologica 2004;89:664–70.
[55] Yang CX, Matsuo K, Wang Z, Tajima K. Phase I/II enzyme gene polymorphisms and esophageal cancer risk: a meta-analysis of the literature. World J Gastroenterol 2005;11:2534–8.
[56] Li Y, Millikan R, Bell D, Cui L, Tse C, Newman B, et al. Cigarette smoking, cytochrome P450 1A1 polymorphisms, and breast cancer among African-American and white women. Breast Cancer Res 2004;6:R460–73.
[57] Li Y, Millikan R, Bell D, Cui L, Tse C, Newman B, et al. Polychlorinated biphenyls, cytochrome P450 1A1 (CYP1A1) polymorphisms, and breast cancer risk among African American women and white women in North Carolina: a population-based case-control study. Breast Cancer Res 2005;7:R12–8.
[58] Nakajima M, Yokoi T, Mizutani M, Kinoshita M, Funayama M, Kamataki T. Genetic polymorphism in the 5'-flanking region of human CYP1A2 gene: effect on the CYP1A2 inducibility in humans. J Biochem 1999;125:803–8.
[59] Sachse C, Brockmoller J, Bauer S, Roots I. Functional significance of a C → A polymorphism in intron 1 of the cytochrome P450 CYP1A2 gene tested with caffeine. Br J Clin Pharmacol 1999;47:445–9.
[60] Ghotbi R, Christensen M, Roh HK, Ingelman-Sundberg M, Aklillu E, Bertilsson L. Comparisons of CYP1A2 genetic polymorphisms, enzyme activity and the genotype–phenotype relationship in Swedes and Koreans. Eur J Clin Pharmacol 2007;63:537–46.
[61] Han XM, Ouyang DS, Chen XP, Shu Y, Jiang CH, Tan ZR, et al. Inducibility of CYP1A2 by omeprazole in vivo related to the genetic polymorphism of CYP1A2. Br J Clin Pharmacol 2002;54:540–3.
[62] Ingelman-Sundberg M, Sim SC, Gomez A, Rodriguez-Antona C. Influence of cytochrome P450 polymorphisms on drug therapies: pharmacogenetic, pharmacoepigenetic and clinical aspects. Pharmacol Ther 2007;116:496–526.
[63] Sata F, Sapone A, Elizondo G, Stocker P, Miller VP, Zheng W, et al. CYP3A4 allelic variants with amino acid substitutions in exons 7 and 12: evidence for an allelic variant with altered catalytic activity. Clin Pharmacol Ther 2000;67:48–56.
[64] Schirmer M, Rosenberger A, Klein K, Kulle B, Toliat MR, Nurnberg P, et al. Sex-dependent genetic markers of CYP3A4 expression and activity in human liver microsomes. Pharmacogenomics 2007;8:443–53.
[65] Zanger UM, Turpeinen M, Klein K, Schwab M. Functional pharmacogenetics/genomics of human cytochromes P450 involved in drug biotransformation. Anal Bioanal Chem 2008;392:1093–108.
[66] Morgan ET, Coon MJ. Effects of cytochrome b_5 on cytochrome P-450-catalyzed reactions. Studies with manganese-substituted cytochrome b_5. Drug Metab Dispos 1984;12:358–64.
[67] Porter TD. The roles of cytochrome b_5 in cytochrome P450 reactions. J Biochem Mol Toxicol 2002;16:311–6.
[68] Loughran PA, Roman LJ, Miller RT, Masters BS. The kinetic and spectral characterization of the *E. coli*-expressed mammalian CYP4A7: cytochrome b_5 effects vary with substrate. Arch Biochem Biophys 2001;385:311–21.

Please cite this article in press as: Kotrbová V, et al. Cytochrome b_5 shifts oxidation of the anticancer drug ellipticine by cytochromes P450 1A1 and 1A2 from its detoxication to activation, thereby modulating its pharmacological efficacy. Biochem Pharmacol (2011), doi:10.1016/j.bcp.2011.06.003